Biologically active terpenoids from Bolivian medicinal plants

Lozano Palacios, Maribel

2021

Document Version:
Publisher's PDF, also known as Version of record

Biologically active terpenoids from Bolivian medicinal plants

MARIBEL LOZANO PALACIOS | CENTRE FOR ANALYSIS AND SYNTHESIS | LUND UNIVERSITY

Printed by Media-Tryck, Lund 2021 NORDIC SWAN ECOLABEL 3041 0903

Nothing in life is to be feared
it is only to be understood
now is the time to understand more
and fear less

Marie Curie

ISBN 978-91-7422-812-0

Centre for Analysis and Synthesis
Department of Chemistry
Faculty of Science
Lund University

Biologically active terpenoids from Bolivian medicinal plants

Biologically active terpenoids from Bolivian medicinal plants

Maribel Lozano Palacios

LUND
UNIVERSITY

DOCTORAL DISSERTATION
By due permission of the Faculty of Science, Lund University, Sweden.
To be defended at the Centre of chemistry on 11th June at 14.00, lecture Hall C

Faculty opponent
professor Thomas Ostenfeld Larsen
Department of Biotechnology and Biomedicine, DTU, Denmark

Organization LUND UNIVERSITY Centre of Analysis and Synthesis Department of Chemistry Author(s): Maribel Lozano Palacios	**Document name** DOCTORAL DISSERTATION **Date of issue:** 06.11.2021 **Sponsoring organization** Swedish International Development Cooperation Agency (SIDA)

Title and subtitle:
Biologically active terpenoids from Bolivian medicinal plants

Abstract

Pseudo-guaianolides represent a large group of sesquiterpene lactones exhibiting significant cytotoxic and anti-inflammatory activities. Their biological activities are due to a α-methylene-γ-lactone unit in their chemical structure, which reacts with free sulfhydryl groups of free cysteine *via* a Michael-addition. Damsin is a major pseudo guaianolide found in *Ambrosia arborescens* Mill., a plant distributed in Andes of Bolivia, Peru, Ecuador and Colombia. The aerial parts of this plant are used in traditional medicine against Abortion, menstrual retardation, rheumatic pain.

The overall aim of this thesis was to obtain biological active semi-synthetic pseudo guaianolides from *Ambrosia arborescens* Mill and triterpenes from Bolivian Highlands plants based on Claisen Schmidt condensation conditions.

Paper I Outlines the HPLC evaluation of damsin and coronopilin isolated from *Ambrosia arborescens* Mill in the plant, and their effects of inhibition of pro-inflammatory IL-6 and MCP-1expression in human skin cells though of NF-κB inhibition.

Paper II describes the evaluation of selective cytotoxicity of 23-α-methylene-γ-lactones based on damsin in normal breast epithelial MCF-10A cells and breast cancer JIMT-1 cells, where the IC_{50} values were found to depend strongly on the overall structure.

Paper III refers to semi-synthesis of new derivatives preserving the α-methylene-γ-lactone unit in which Claisen Schmidt condensation products such as (*E*)-3-benzylidendamsin derivatives were found to be more potent in the JIMT-1 cancer cells compared to the MCF-10A normal like cells.

Paper IV describes the oleanolic acid determination in Bolivian highland plants such as *Tetraglochin cristatum*, *Lampaya castellani*, *Junellia seriphioides*, *Baccharis tola*, *Polylepis tomentella*, *P. hieronyni*, *P. besseri* and *Satureja boliviana,* according of our results these plants can be a potential natural source of oleanolic acid since this compound has several applications.

Paper V present the obtention of oleanolic acid derivatives *via* Claisen Schmidt condensation and the evaluation of cytotoxicity of four sapogenins from *Chenopodium quinoa*.

Paper VI refer to acute anti-inflammatory activity evaluation of oleanolic acid **1**, methyl oleanate **2**, hederagenin **3** and phytolaccagenic acid **4** sapogenins from *Chenopodium quinoa* in two murine models: The carrageenan-induced paw edema, and the croton-induced ear edema. the extract shows anti-inflammatory activity significant in ear edema model than the compounds, while in the paw edema model the isolated compounds show a significant anti-inflammatory activity than the extract.

Key words
Bolivian plants, cytotoxicity, triterpenes, damsin, breast cancer

Classification system and/or index terms (if any)

Supplementary bibliographical information		**Language**: English
ISSN and key title		**ISBN** printed version: 978-91-7422-812-0 digital version: 978-91-7422-813-7
Recipient's notes	Number of pages 202	Price
	Security classification	

Signature 

Date2021-04-29

Biologically active terpenoids from Bolivian medicinal plants

Maribel Lozano Palacios

LUND
UNIVERSITY

Coverphoto by

Faculty of science
Department of chemistry
Centre for Analysis and Synthesis

ISBN 978-91-7422-812-0 (print)
ISBN 978-91-7422-813-7 (PDF)

Printed in Sweden by Media-Tryck, Lund University, Lund 2021

Media-Tryck is an environmentally certified and ISO 14001 certified provider of printed material. Read more about our environmental work at www.mediatryck.lu.se

To my loving family

Table of Contents

Abstract

Pseudo-guaianolides represent a large group of sesquiterpene lactones exhibiting significant cytotoxic and anti-inflammatory activities. Their biological activities are due to α-methylene-γ-lactone unit in their chemical structure which reacts with free sulfhydryl groups of free cysteine *via* a Michael-addition. Damsin is a major pseudoguaianolide found in *Ambrosia arborescens* Mill., a plant distributed in Andes of Bolivia, Peru, Ecuador and Colombia. The aerial parts of this plant are used in traditional medicines for abortion, menstrual retardation, and against rheumatic pain.

The overall aim of this thesis was to obtain biological active semi-synthetic pseudo guaianolides from *Ambrosia arborescens* Mill and triterpenes from Bolivian Highlands plants based on Claisen Schmidt condensation conditions.

Paper I Outlines the HPLC evaluation of damsin and coronopilin isolated from *Ambrosia arborescens* Mill in the plant, and their effects of inhibition of pro-inflammatory IL-6 and MCP-1expression in human skin cells though of NF-κB inhibition.

Paper II describes the evaluation of selective cytotoxicity of 23-α-methylene-γ-lactones based on damsin in normal breast epithelial MCF-10A cells and breast cancer JIMT-1 cells, where the IC_{50} values were found to depend strongly on the overall structure.

PaperIII refers to semi synthesis of new derivatives preserving the α-methylene-γ-lactone unit in which Claisen Schmidt condensation products such as (*E*)-3-benzylidendamsin derivatives were found to be more potent in the JIMT-1 cancer cells compared to the MCF-10A normal like cells.

Paper IV describes the oleanolic acid determination in Bolivian highland plants such as *Tetraglochin cristatum*, *Lampaya castellani, Junellia seriphioides, Baccharis tola, Polylepis tomentella, P. hieronyni, P. besseri and Satureja boliviana*, according of our results these plants can be a potential natural source of oleanolic acid since this compound has several applications in medicine.

Paper V present the obtention of oleanolic acid derivatives *via* Claisen Schmidt condensation and the evaluation of their cytotoxicity of four sapogenins from *Chenopodium quinoa*. Our results show that the most active compound was

hederagenin, which is more toxic in JIMT-1 cells (IC50 27.3 μM) thanin MCF-10A cells (IC50 39.6 μM).

Paper VI refer to acute anti-inflammatory activity evaluation of oleanolic acid **1**, methyl oleanate **2**, hederagenin **3** and phytolaccagenic acid **4** sapogenins from *Chenopodium quinoa* in two murine models: The carrageenan-induced paw edema, and the croton-induced ear edema. the extract shows anti-inflammatory activity significant in ear edema model than the compounds, while in the paw edema model the isolated compounds show a significant anti-inflammatory activity than the extract.

Popular summary

Natural products are organic compounds which are products of biosynthesis of living organism such as plants, animals and microorganism. Secondary metabolites (or natural products) are still being the principal source of inspiration of numerous novel medicinal agents. However, the low amounts of these compounds in the plants do not permit us to make a complete study, so, the semi synthesis of compounds from natural products can be solve this problem.

In this thesis we focus on the study of *Ambrosia arborescens* Mill a medicinal plant which grows in Bolivian urban places. It has been isolated two major active compounds damsin and coronopilin from the aerial parts of this plant and evaluated inhibitory effect against inflammatory processes.

Nowadays breast cancer is still being de second cause of women death around the world. New compounds from natural products or semi-synthetized derivatives are urgently needed to assay in order to alleviate this pain. Damsin from *A. arborescens* shows interesting cytotoxicity results and its derivatives demonstrate to have selective cytotoxicity in normal breast epithelial MCF-10A cells and breast cancer JIMT-1 cells. However, some studies such as accesses the solubility are still needed

On the other hand, Bolivian highlands comprises diverse species of plants used in medicine traditional to alleviate different pains such as headache, stomachache and inflammatory pains. These plants are characterized to have high content of oleanolic acid. This compound has a lot of scientific reports about its pharmacological uses. *Chenopodium quinoa* a cropping plant from Bolivian altiplane contents high amounts of bioactive sapogenins and the extract of these sapogenins shows an inhibitory effect of topic inflammation, so, this extract can be use as alternative of phytotherapeutic remedy to control inflammatory pain.

List of papers

The dissertation of this PhD thesis is based on the following papers and manuscript:

Paper I
Daniel Svensson[a], **Maribel Lozano**[b,c], Giovanna R. Almanza[c], Bengt-Olof Nilsson[a], Olov Sterner[b], Rodrigo Villagomez[b,*]. "Sesquiterpene lactones from *Ambrosia arborescens* Mill. inhibit pro-imflammatory cytokine expression and modulate NF-κB signaling in human skin cells"

Published on Phytomedicine 50 (2018) 118–126.

Paper II
Maribel Lozano[1,3], Wendy Soria[2,4], Giovanna R. Almanza[3], Sophie Manner[1], Stina Oredsson[2], Rodrigo Villagomez[3], Olov Sterner[1,*]. "Selective Cytotoxicity of damsin derivatives in breast cancer cells".

Published on Journal of advanced pharmaceutical science and technology ISSN NO: 2328-0182.

Paper III
Maribel Lozano[1,3], Wendy Soria[2,4], Giovanna R. Almanza[3], Sophie Manner[1], Stina Oredsson[2], Rodrigo Villagomez[3] and Olov Sterner[1]*. "Cytotoxicity of new damsin derivatives in breast cancer cells".

Journal of Pharmacy and Drug Development Volume 1 Issue 2 2019

Manuscript I

Soria-Sotillo W[1,2], **Lozano M**[3,4], Huang X[1], Malakpour A[1], Almanza GR[4], Sterner O[2], and Oredsson S.[1*]. "Molecular mechanisms of breast cancer cell active chemically synthesized damsin derivatives"

Paper IV
Maribel Lozano, Yonny R. Flores, Giovanna R. Almanza*. "High contents of Oleanolic Acid in highland Bolivian plants"

Published on Journal of Bolivian Chemistry Vol. 34, No.1, pp. 28-32, 2017.

Paper V
Yaquelin Suxo[1], **Maribel Lozano[1,2]**, Wendy Soria[3,4], Stina Oredsson[4], Giovanna R. Almanza[1],*

Sapogenins from the husk of Chenopodium quinoa, the obtaining of their derivatives, and the evaluation of their cytotoxic activity. Published on Journal of Bolivian Chemistry Vol. vol. 35, no. 3, 2018

Paper VI
Maribel Lozano[a,b], Eduardo Gonzales[b], Yonny Flores[a], Giovanna R. Almanza[a,*]. "Effect in acute inflammation of sapogenin extract and isolated sapogenins from quinoa waste (*Chenopodium quinoa* Willd)

Published on Journal of Bolivian Chemistry Vol. 30, No.2, pp. 115-121.

The author's contribution to the papers

Paper I.
I performed part of the experimental work such as the isolation of compounds and HPLC analysis and wrote part of the manuscript

Paper II
I performed the experimental work, synthetized all the semi-synthetic compounds and wrote part of manuscript

Paper III
I performed the experimental work, obtaining all the semi-synthetic compounds in base of previous results and wrote part of manuscript

Manuscript I
I have participated in preparing all the semi-synthetic compounds according of previous results

Paper IV
I performed all the experimental work, HPLC analysis, sample collection and wrote the manuscript.

Paper V
The author performed the experimental work in collaboration with Yaquelin Suxo and, isolation and obtaining all the semi-synthetic compounds and participated in the writing of the manuscript

Paper VI
I performed the experimental work, Analyzed the results and wrote the first draft of the paper in collaboration with Eduardo Gonzales**.**

List of figures

Abbreviations

CAN	Acetonitrile
αMgL	α-methylene-γ-lactone
DCIS	Ductal carcinoma in situ
DIMCARB	Dimethylammonium dimethyl carbamate
DPA-6S	Discovery solid phase cartridges
HER2	Human epidermal growth factor receptor 2
JIMT-1	Human breast cancer cell line
LCIS	Lobular carcinoma in situ
mCPBA	3-Chloroperoxybenzoic acid,
MECys	Methyl-L-cysteine ester
MOMBr	Methoxymethylbromide
p-TSA	p-toluene sulphonic acid
SERCA	Sarcoplasmic/endoplasmic reticulum calcium adenosine triphosphate
STLs	Sesquiterpene lactones
TBAH	Tetrabutylammonium hydroxide
TNBC	Triple negative breast cancer
TPA	12-O-tetradecanoylphorbol-13-acetate
WHO	World Health Organization

Chapter 1. Introduction

1.1. Terpenes

Plants produce a wide variety of secondary metabolites in order to manage physiological tasks to response to stress, for example some of them are capable to attract pollinators, establish symbiosis, and provide structural components to lignified cell walls of vascular tissues[1,2]. Among these natural products, terpenes comprise the most significant types of structurally different products found in many plants, followed by the alkaloids and phenolics[3] (Figure 1). Historically, the name "terpene" comes from the German “Terpentin”, because the first members of this class were isolated from turpentine (Latin *balsamum terebinthinae*)[4]. In the past, terpenes were used for Egyptians for many religious rituals and cultural purposes[5]. The investigation of terpenes goes back centuries and even millennia, but there is still much to learn about their health benefits. Thus, new types of terpenes with potential benefits and applications in human societies are constantly being discovered[6].

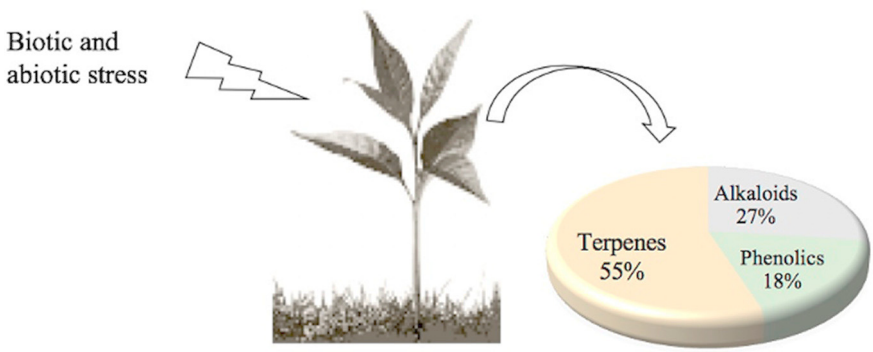

Figure 1. The major groups of plant secondary metabolites according to Croteau *et al.* (2000)

Chemically, terpenes are based on the C_5-isoprene unit, and their carbon skeletons are built up by the union of two or more such units[7]. They are classified by the number of isoprene units, as monoterpenes (C_{10}, two isoprene units), sesquiterpenes (C_{15}, three isoprene units), diterpenes (C_{20}, four isoprene units), sesterterpenes (C_{25}, five isoprene units), triterpenes (C_{30}, six isoprene units), tetraterpenes (C_{40}, eight

isoprene units) and polyterpenes ($C_{[n>40]}$, more than eight isoprene units). They may be subclassified according of the number of rings as "acyclic", "monocyclic, bicyclic", etc[8]. Terpenes can have a varying degree of unsaturation, be oxidized or reduced, possess functional groups, and have various rings (size as well as type). An example that is important for this thesis is sesquiterpene lactones, formed by three isoprene units and in which a part is oxidized and cyclized to a lactone. In this investigation, we have focused in sesquiterpene lactones and triterpenes. Terpenoids are compounds based on a terpene but structurally modified by the attachment of a non-terpene unit, such as a sugar.

1.1.1. Sesquiterpene lactones

Sesquiterpene lactones (STLs) are a wide group of naturally occurring bioactive compounds, which are present in almost 100 families of plants such as; *Acanthaceae*, *Anacardiaceae*, *Apiaceae*, *Euphorbiaceae, Lauraceae, Magnoliacea, Menispermaceae*, *Rutaceae, Winteraceae* and *Hepatidaceae*[9, 10]. However, the greatest number of STLs are present in the *Asteraceae* family, in the majority of its genera such as: *Ambrosia, Artemisia*, *Arnica*, *Ambrosia, Helenium, Tanacetum,* and *Vernonia,* and STLs can be found at concentration between 0.001 and 8% of the dry plant weight[11]. The *Asteraceae* species produce the most diverse group of STLs, from which almost 4000 structures with approximately 30 different skeletal subtypes have been reported so far[12, 13]. The genus *Ambrosia* is a principal representative of this family, with around 30 species which are distributed all over South America.

1.1.2. Chemistry of sesquiterpene lactones

STLs are characterized by being colorless, bitter, stable and predominantly lipophilic compounds, biogenetically derived from the acyclic sesquiterpenoid precursor *E*-farnesyl pyrophosphate (FPP, or *E*-farnesyl diphosphate FDP) that undergoes cyclization(s) and oxidative modifications (see Figure 2)[14]. Many products of this biosynthetical pathway contain a α-methylene γ-lactone unit ("olide"), which can be lactonized towards **C-6/C-7** or **C-7/C-8** positions and that can possess a *cis* or a *trans* configuration (see Figure 2)[15, 16]. According to the carbocyclic skeletons attached to the lactone ring, the main classes of the α-methylene γ-lactone sesquiterpenes are the germacranolides, considered to be the biogenetic precursors, the eudesmanolides, the guaianolides, the pseudo-guaianolides and the less frequent classes the elemanolides, the eremophilanolides and the xanthanolides (see Figure 2)[16-18]. Most of the STLs possess a fused 5-membered lactone group (a γ-lactone) and a methylene group next to the carbonyl group (α-methylene). The final product may also contain substituents such as

hydroxyl groups, esterified hydroxyls, or epoxide rings, and STLs may also occur in a glycosylated form[11].

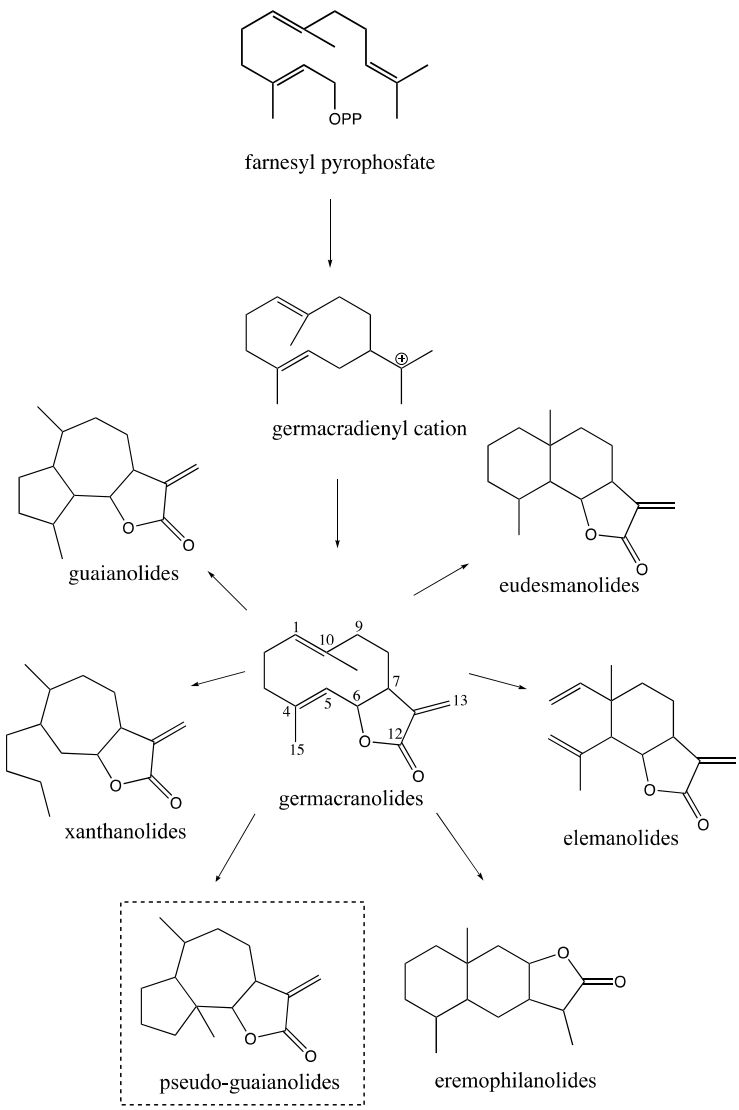

Figure 2. Chemical structure of different subgroups of α-methylene γ-lactone sesquiterpenes

1.1.3. Chemistry of Pseudoguaianolides

Among such sesquiterpenes lactones, pseudoguaianolides possess a 5,7,5-ring system, with a *cis* or a *trans* configuration, and a methylene group at C-11. They can be sub-categorized as 6,12-and 8,12-pseudoguaianolide based on the position of their lactone ring. Furthermore, pseudoguaianolides include the two groups helenanolides, with a 10α-methyl substituent, and ambrosanolides, with a 10β-methyl substituent[19]. The most abundant pseudoguaianoldes are ambrosanolides, and their structures show in Figure 3.

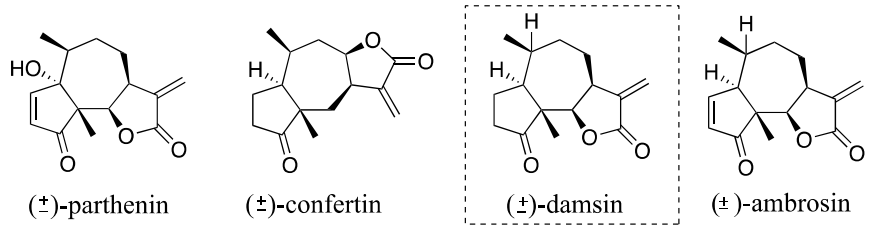

Figure 3. The most abundant ambrosanolides

1.1.4. Biological aspects of sesquiterpene lactones

Several studies have demonstrated that STLs from a diverse of plants show important biological activity in diverse assays, and their anti-tumor, cytotoxic, allergenic, anti-inflammatory, anti-microbial, anti-ulcer, insect antifeedant, as well as plant growth regulatory effects can be regarded as being of particular interest[20]. Studies of structure-activity relationship have shown that the broad range of biological properties of STLs are in general associated with the presence of α-methylene-γ-lactone (αMγL) group, since this group may act as a Michael acceptor and reacts covalently with sulfhydryl (-SH) groups in cysteine residues of enzymes, proteins and glutathione, forming more or less stable adducts. As a consequence of this reaction, they may produce an alteration of gene expression, by the inhibition of a number of enzymes implicated in key biological processes such as DNA and RNA synthesis. The Michael reaction is mediated chemically by an α,β-unsaturated carbonyl moiety present in the αMγL-STLs (Figure 4). Other aspects, such as lipophilicity, molecular geometry, and chemical environment, can also impart to the biological activities of the STLs. It is therefore not clearly understood how STLs may affect cellular targets, because the targets and STLs are three-dimensional structures and interact under in specific environments[21,22,23,24, 25].

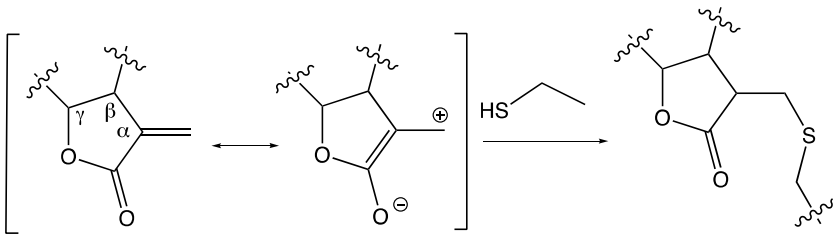

Figure 4. A Michael addition reaction of a thiol to the α-methylene-γ-lactone moiety of a αMγL-STL.

1.1.5. Sesquiterpene lactones and Cancer

Cancer is becoming one of the most common cause of death in the world, with an approximation of 9.6 million death in 2018[26, 27]. The most common types of treatment for cancer include radiation, surgery and chemotherapy or the combination of one of them. Currently, the chemotherapy is still being a good option for cancer treatment. However, the available cancer chemotherapy may lead in critical problems, due to low effectiveness, adverse effects, multidrug resistance development and the low efficacy *in vivo* systems [28,29]. Thus, new anticancer agents to face these problems are highly required. Secondary metabolites derived from natural sources have been proven to be effective for cancer treatment either preventing the proliferation of cancerous cells in humans[30]. Additionally, the anticancer properties of STLs have attracted a great interest for many researchers. The large investigation of the anticancer effects of STLs are mediate by different molecular mechanism such as they may induce apoptosis, inhibits cell proliferation, supresses angiogenesis, and metastasis[31].

On the other hand, there are some STLs drugs in ongoing trials are used for cancer therapies, among these is artemisinin a sesquiterpene lactone isolated from *Artemisia annua*. which was even recommended by World Health Organization (WHO) as the best treatment for malaria disease, and it is available on the drug market, originally the pure compound was extracted for this use in the 1970`s by Youyou Tu. Furthermore, artemisinin and its derivatives has also shown potent anticancer activity against breast cancer and colorectal cancer cells[32]. Another STLs used for cancer therapies is parthenolide from *Tanacetum parthenium,* which is the main responsible to induce apoptosis in cancer cell and it has demonstrated to have potent *in vitro* anti-cancer and antiangiogenic properties[33]. Finally, thapsigargin a sesquiterpene lactone isolated from *Thapsia garnanica* is in clinical trial for cancer treatment, it is a potent sarcoplasmic/endoplasmic reticulum calcium adenosine triphosphate (SERCA) inhibitor which leads to apoptosis[34 35] (Figure 5).

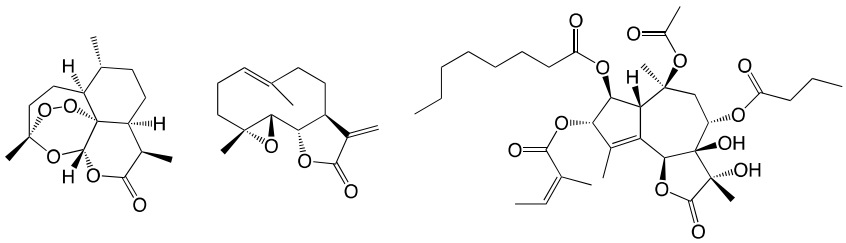

Figure 5. Common sesquiterpene lactones drugs in clinical trials

1.1.6. Sesquiterpene lactones cytotoxicity

The cytotoxicity of sesquiterpene lactones have been studied since the 1970s, and it is the largest group of cytotoxic compounds isolated from natural sources. The essential group for cytotoxic activity of SLTs is the presence of the exo-methylene unit, conjugated with the carbonyl in the γ-lactone ring. However, other factors, such as the lipophilicity and the molecular geometry, as well as the presence of two alkylating centers, are more potent inhibitors of tumor cell proliferation. This is all linked to the general toxicity of the compounds[36, 37], and the balance needs to be controlled.

1.2. Breast cancer

Among all the types of cancer in the world breast cancer is the second most common cancer overall, it is the most commonly occurring cancer in women worldwide with an estimated 2 million new cases reported in 2018[38], and over 625,000 died from it before the age of 70. In Bolivia an estimated 1458 cases of breast cancer were reported in 2018[39].

Breast cancer is heterogeneous malignant tumour arising from epithelial cells of glandular milk ducts or lobules of the breast, carcinomas represent the vast majority of all breast cancer [40]. The normal breast epithelial organ is composed by glandular and adipose hormones where its growth factor such as epidermal growth (EGF), fibroblast growth (FGF) and insulin-like growth (IGF) which up and down regulate a variety of genetic pathways[41]. Breast cancer occur as result of mutations, or abnormal changes in the genes which are responsible for regulating the growth factor of the cells (Figure 6).

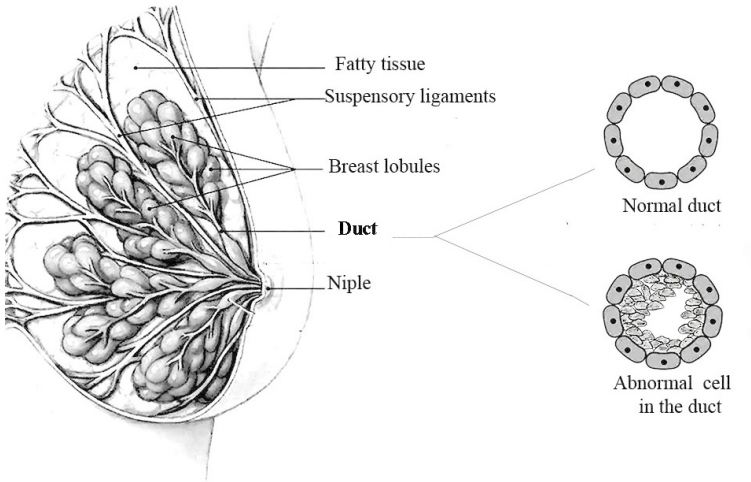

Figure 6. Schematic illustration normal breast and their normal duct compared with abnormal cell in the duct

1.2.1. Histological base classification of breast cancer

For a long time, the breast cancer classification system were only based on the histological appearances of breast cancer as either non-invasive (carcinoma *in situ*) or invasive (Figure 7)[42]. In non-invasive carcinoma *in situ* the cancer cells are developed inside the milk ducts of the breast and do not extend to the lobules into the breast tissue[43,44]. Breast carcinoma *in situ* can be sub-classified based on the location of aggressiveness of the disease as either ductal or lobular in which ductal carcinoma *in situ* (DCIS) is considered more common than lobular carcinoma *in situ* (LCIS)[40]. Furthermore, the DCIS has been sub-classified in five well recognized architectural subtypes: comedo, cribiform, micropapillary, papillary and solid[45]. Invasive carcinoma is the type of cancer that spreads outside the membrane of the lobule or duct into the breast tissue, and the cancer cells can produce to metastatic breast cancer. Invasive carcinomas are classified into histological sub-types named as infiltrating ductal carcinoma (IDC), invasive lobular carcinoma, (ILC), musinous (colloid), medullary and papillary carcinomas. Almost about 80% of breast cancer are invasive ductal carcinomas (IDC) spreading through lobules[46].

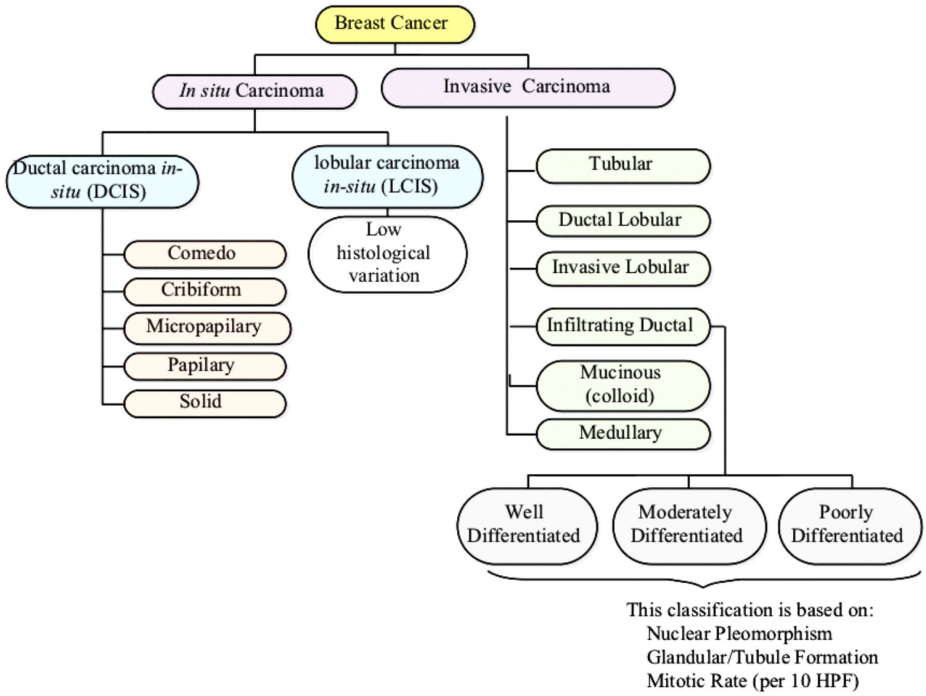

Figure 7. Histological classification of breast cancer sub-types

1.2.2. Molecular classification of breast cancer

Early studies of transcription factor profiles using DNA microarrays or RT-PCR have had a considerable impact on the understanding of breast cancer biology identifying five molecular subtypes of breast cancer[47] (Figure 8). These molecular subtype classifications are often key references for predicting prognosis as well as a potential response to endocrine treatment, and the humanized monoclonal antibody trastuzumab[48]. They include luminal A and luminal B (expressing the oestrogen and progesterone receptor ER, PR), human epidermal growth factor receptor 2 (HER2)-enriched (without ER expression), and basal-like according to the gene expression patterns[49]. Molecular luminal A type includes tumors that are positive for ER and PR, but they are negative for HER2, which does not benefit from Chemotherapy. While molecular luminal B includes tumors that are ER positive and can be PR negative and/or HER2 positive, which is beneficial for chemotherapy[50]. On the other hand, triple negative breast cancer (TNBC) include tumour that is negative for ER and PR.

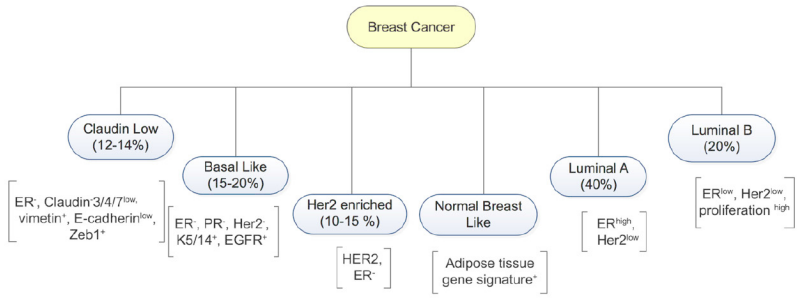

Figure 8. Molecular classification of breast cancer sub-types

1.2.3. Risk factors

Several risk factors were identified that increase breast cancer incidence. The main factors are related to exposure to the hormone oestrogen, which plays an important role in the progression of cancer. The risk of developing breast cancer increases with a long time of fertility, the use of preventive pregnancy hormones, and having no children or having the first child after the age of 35. The risk increases by four and six times if two first degree relatives develop the disease[51, 52]. Furthermore, the incidence of breast cancer increases exponentially with age, as in the case of ductal carcinoma the risk increases gradually starting at the age of 40 and reaches a plateau after the age of 60[53]. Additionally, alcohol consumption also may increase breast cancer risk[54]. However, early detection through mammography has been demonstrated to provide treatment options and to save lives. Regular exercise can also protect the development of breast cancer[55].

1.2.4. Current drug therapy for breast cancer

Treatment options for breast cancer includes surgery with or without radiation, hormone therapy and chemotherapy, or the combination of more than one treatment. Depending of the stage of disease, surgery can be the first option for early stage breast cancer, with consideration of postoperative radiation[56]. However, chemotherapy is the only treatment option for the highly aggressive triple negative breast cancer. There are three types of chemotherapy regimens: neoadjuvant, adjuvant and palliative. Neo-adjuvant chemotherapy is recommended for patients who have inoperable or inflammatory breast cancer at diagnosis, while adjuvant chemotherapy is associated with severe physical symptoms, such as musculo-skeletal pain, nausea and weight problems[57]. The cytotoxic chemotherapy options have expanded quickly, novel agents have been proven to treat metastatic breast

cancer, include eribulin, nanoparticle albumin-bound-paclitaxel, ixabelipone [58]. On the other hand, almost 25% of all breast cancers are characterized by the overexpression of the HER2 protein. Trastuzumab is a recombinant monoclonal antibody to HER2+ breast cancer, and can be used to treat both early-stage and advanced breast cancer[59]

1.2.5. Targest for chemotherapy

Breast cancer tergeted therapies use drugs which may block on a specific molecular target. Actually, the understanding of the molecular patways dysregulated in cancer cells has increased rapidly, promoting the development of drugs with more specific targets. Examples are cell-cycle proteins, modulator of apoptosis, growth factor, signalling molecules and angiogénesis now became potential anti-cancer targets. Reports have demostrated that phytochemicals have the ability to target multiple patways in breast cancer cells such as signalling[60]. Previous investigations have demonstrated HER2 as an effective therapeutic target in breast cancer treatment.

Several suidies have confirmed that sesquiterpene lactones interact with multiple targets in cancer, they show capability to inhibit trasncription factors such as NF-κB, STAT3, and AP-1, up- or downregulate the protein kinase MAPK and c-N-terminal kinase JNK, and increse the expresion of the p53 protein. Some STLs can also affect cell-cyclo arrest[31].

In this thesis, based on previous reports, the human breast cancer cell lines JIMT-1 were selected for testing the compounds, and human breast-derived MCF-10A cell line was used as a normal-like cell model for comparison. JIMT-1 is a ductal carcinoma breast cancer cell line derived from a HER2 positive clinically resistant to trastuzumab, which contitute a good model to test the cytotoxic activity of new drugs[61].

1.3. Triterpenes

Triterpenes are a large and structurally diverse C_{30} natural secondary metabolites, and more than 20,000 triterpene structures have been reported up to now. The majority of triterpenes are widely distributed in numerous classes of natural products, especially in the plant kingdom, although other organism such as fungi, lichens, and bryophytes also produce triterpenes[62]. The triterpenes in plants possess defense activities since they are capable of preventing various pathogen infections, and provide a repair mechanism for wounds and injuries[63]. Additionally, plants usually accumulate triterpenes in their glycosylated forms (saponin), which is considered as part of plant defense systems against pathogens and herbivores[64].

1.3.1. Chemistry of triterpenes

The majority of triterpenes possess the conventional carbon skeleton, arising from the cyclization of squalene-2,3-oxidosqualene which result in the formation the typical skeletons. Thus, in nature triterpenes are represented by different types of compounds divided into more common chemical structure groups, and classified into main group as; tetracyclic and pentacyclic triterpenes[65]. The tetracyclic triterpenes consist of dammarane and tirucallane among others, while the pentacyclic triterpenes are divided in tree groups, lupane, oleanane and ursane (see Figure 9), that regularly are isolated as active substances from plants[66]. Chemically, oleanane and ursane groups have three active sites, the hydroxy group at position C-3, the C-12/C-13 double bound, and the carboxylic acid at position C-28, and some modifications were made in these positions. This investigation is focused on triterpene of oleanane type.

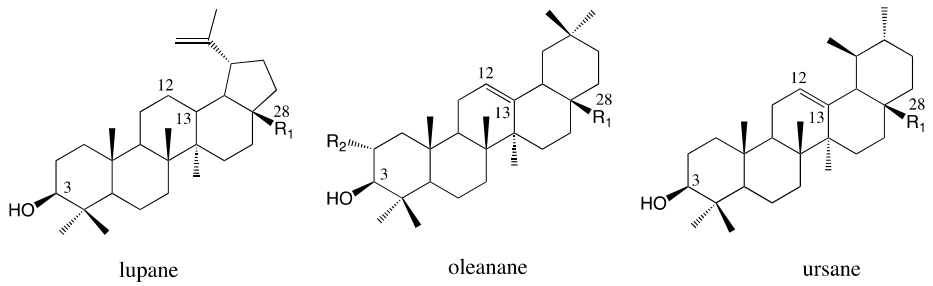

Figure 9. Molecule structures of lupane, oleanane, and ursane

Table 1. Triterpene characterization

Triterpene family	Triterpene	R_1	R_2
lupane	lupeol	CH_3	-
	betulin	CH_2OH	-
	betulinic acid	COOH	
oleanane	β-amirin	CH_3	H
	erythrodiol	CH_2OH	H
	oleanolic acid	COOH	H
	maslinic acid	COOH	OH
ursane	α-amirin	CH_3	-
	uvaol	CH_2OH	-
	ursolic acid	COOH	-

1.3.2. Biological aspects of triterpenes

Triterpenes from plants are characterized by the hydrophobic scaffolds and have shown a broad range of pharmacological effects and biological activity. In particular for anti-inflammatory, analgesic, hepatoprotective, cardiotonic, anti-tumor, immune regulation, sedative, antimicrobial, antioxidant, and spasmolytic activity, among

others[67, 68,69]. Among these, lupane, oleanane and ursane triterpenes have demonstrated to have cytotoxic effects against various cancer cell lines, and are considered as promising anticancer drugs[70]. Currently, a variety of natural triterpenoids and their derivatives, such as oleanolic acid, ursolic acid, botulinic acid, boswellic acid and cucurbitacin B (see Figure 10), are in clinical trials for cancer treatment[71]. Chemically modified oleanolic acid is one of the most interesting groups of new lead compound sources with anti-inflammatory, anti-ulcer and anti-tumoral effects[72].

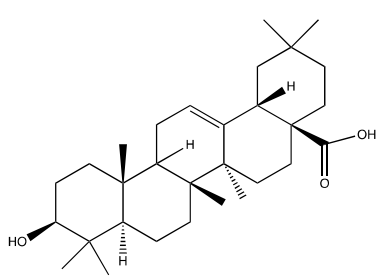

oleanolic Acid

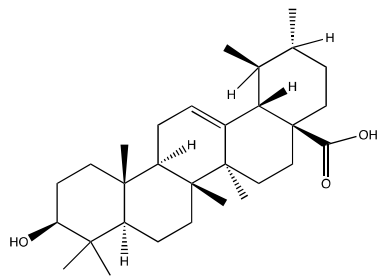

ursolic acid

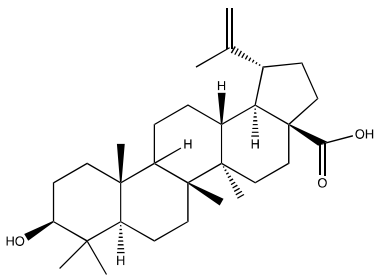

betulinic acid

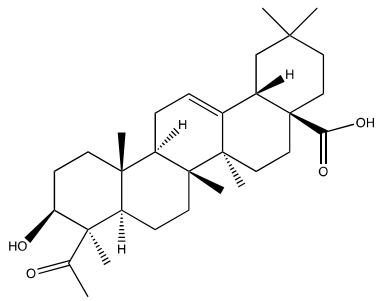

boswellic acid

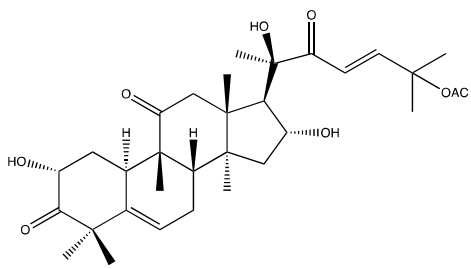

cucurbitacin B

Figure 10. Triterpenoids with specific anticancer activity

1.4. Terpene-rich Medicinal Plants

Terpenoids play an important physiological and ecological function in higher plants[73], and in plant-insect, plant-pathogen, and plant-plant interaction. Terpenoids are primarily produced in the vegetative tissues, the flowers, and, occasionally, in the roots[74].

Pentacyclic triterpenes such as β-amirin oleanane, are accumulated in fruits, leaves and bark of various medicinal plants such as *Lantana camara* roots, *Salvia officinalis*, *Satureja montana* and *Olive europea*. They may be present in cuticular waxes of leaves and fruit of various species, affecting their cuticular structure and the water permeability[75,76]. For instance, high amounts of pentacyclic triterpenes are found in the surface waxes of the olive skin[77].

1.4.1. Bolivian plants terpenes production

In Bolivia there are 31 indigenous groups and many mestizo communities living in different natural areas of de country, as Altiplano, Yungas, Chaco or lowlands[78]. Among these groups, a high percent of the indigenous population lives in the Altiplano. The Southern Altiplano region of Bolivia is an extensive area characterized by an average elevation of 4000 meters above sea level, an arid climate, extreme temperature that range from -11°C to 30°C, poor soil and high salinity. These ecological aspects are defined by an extensive surface of Uyuni Salt Flat[79]. Most surface is covered by crops that can tolerate these extremely growing conditions, such as white and bitter potato species (*Solanum tuberosum, S. juszepczukii, S. andigenum* and *S. ajanhiri*), quinoa (*Chenopodium quinoa*, cañiwa (*Chenopodium pallidicaule*), *etc.*, being the major agricultural economic output and export[80, 81]. On the other hand, the dominant plants biodiversity present in the south of the Bolivian altiplano were identified as Asteraceae family; *Parastrephia, Baccharis,* Verbenaceae family; *Lampaya, Junellia* and species of the genus *Polylepis*[82, 83]. Phytochemical studies of these plants have confirmed the presence of high amounts of pentacyclic triterpenes[84, 85, 86]. Thus, the evaluation of pentacyclic triterpenes in selected plants from Southern Altiplano of Bolivia, was investigated, and the results reported in this thesis.

Chapter 2. (Paper I) Sesquiterpene lactones from *A. arborencens* and anti-inflammatory activity

2.1. Background

Among the medicinal plants studied in South America are *Ambrosia arborescens* Mill., a specie from Asteraceae family, tribe Heliantheae, and subtribe Ambrosinae[87]. It is an aromatic plant distributed around western South America (Ecuador, Bolivia and Peru), native to Ecuador, growing between 2000 and 3500 m.a.s.l. commonly know as "marco", "marku", "Altamisa", or "artemisia". Its aereal parts has been traditionally used in folk medicine to brush away insects, rheumatism, muscle pains, for the treatment of infections and skin disorders[78, 87-89]. In Bolivia indigenous populations use the aerial part of "Marku" as topical agent to alleviate pain, as a treatment amebic dysentery and to treatment imflammation disease. It is also employed as a flea repellent, because the plant possess a bitter sensory quialities, which believed to conribute to the plants defense against hervivores [90].

As metion in the previous chapter all *Ambrosia* species are chemically characterized by the presence of high content of sesquiterpene lactones, wich is also used as chemotaxonomic marker. Among these species, it has been isolated four sesquiterpene lactones from *Ambrosia arborescens* M, where the major constituents of this plant are; damsin (**1**), coronopilin (**2**), psilostachyin, psilostachyin C and small amount of 11-epidihydropsilostachyin[91] (Figure 11). Damsin **1** and coronopilin **2** were reported as the major compounds studied in this specie, since these compounds show inhibitory effect against inflammatory processes[92]. However, the underlying mechanisms are not fully understood

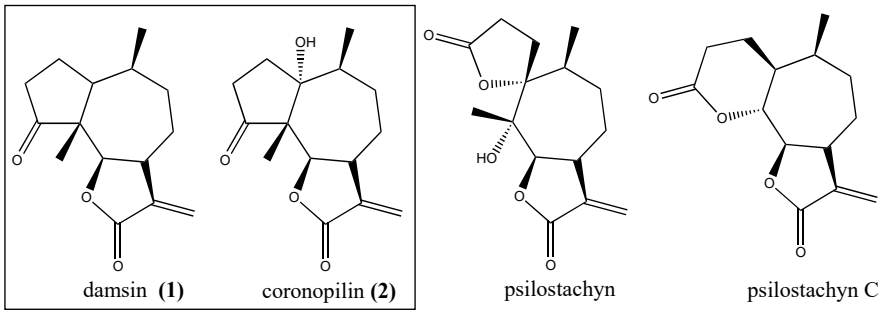

Figure 11. Sesquiterpene lactones from *Ambrosia arborescens* Mill.

2.2. Sesquiterpene lactones antiinflammatory agent

The potent antiinflammatory activitity of STLs have been widely reported since 1979. Early report of antiinflammatory activity of STLs in rodents by carrageenan-induced-paw have demosntrated that the α-methylene-γ-lactone of cyclopentenone moiety plays an important role in *in vivo* antiinflammatory activity[93]. The mode of action of STLs as antiinflamatory agents were shown to be potent inhibitor of many inflammatory processes, such as oxidative phosphorylation in neutrophils, platelet aggregation, chemotaxis, histamine and serotonin release and pro-inflammatory cytokines[94, 95]. Chemically, the anti-inflammatory activity of STLs is mediated by α-methylene-γ-lactone moiety which may alkylate biological nucleophiles such as, L-cysteine, glutathionine *via* a Michael type addition [95, 96,97]. Thus, proteins with cysteine residues, seems to be the principal targets of STLs. STLs involves specifically transcription nuclear factors such as NF-κB, STAT3, and Nrf2 as molecular targets, these have been descrived to play an important role in regulating genes expression in inflammation patways[93, 98]. However, other factors such as the conformation of the basic carbocyclic skeleton may also influence the antiinflammatory activity and selectivity of sesquiterpene lactones[99].

NF-κB family are composed of five structurally well known members, which include, p50 (NF-κB1), p52 (NF-κB2), p65 (ReIA), ReIB and c-ReI. Chemically, these members of the family may share an N-terminal Rel homology domain (RHD), which is respomsable for DNA binding, homo-and heterodimerization. The p65 and p50 menbers are ubiquitously expressed, while the others members are tissue specific[100]. The most predominant form of NF-κB is a dimer conformed by p65 and p50 proteins, which is inactive complex and sequestered in the cytoplasm by interacting with the inhibitor of NF-κB (IκB) proteins, most commonly IκBα under unstimulated basal conditions[101]. The exposition of the cell to a wide range of

stimuli, such as cytokines; interleukin-1(IL-1), tumor necrosis factor-α (TNF-α) and bacterial lipopolysaccharide (LPS) leads to phosphorylation and activation of the kinase complex by IKKα, IKKβ and NEMO (NF-κB essential modifier)[102]

Figure 12. Members of the A) NF-κB (Rel family), B) IκB family and C) IKK complex. The numbers of amino acids in each the human protein is indicated on the *right*. All members of NF-κB may share a rel homology domain (RHD) which is required for their dimerisation.

2.2.1. The NF-κB signaling pathways

Nuclear factor kappa B (NF-κB) is a transcription factor which is found in the majority of cells as inactive complex (IκB-bound). Therefore, it has been discovered two important patways to lead the activation of NF-κB[103]. These two more descrived patways are named either the canonical and non-canonical patways or the classical and alternative patways, respectivetely. The canonical NF-κB patways regulate the activation of NF-κBl p50, RELA and c-REL and it is mediated principally by degradation of inhibitors present in the cytoplasm. Whilst, activation of non-canonical pathways NF-κB (NF-κB2) commonly take place after activation of canonical patway and principally activates p100-sequestred NF-κB members and RELB aditionally this pathway, may require new protein synthesis in contrast of canonical pathway[104, 105].

The canonical NF-κB patway begins through the xposure to inflammatory stimuli, including ligands of various cytokine receptors such as tumor necrosis factor (TNF) and interleukin-1 (IL-1), which lead to activation of the β subunit of the IκB kinase (IIK) complex, then phosphoprylates IκBα proteins on two N-terminal serine residues, which leads to ubiquitinination and degradation of IκBα, which then allows the unbound NF-κB dimers able to translocate to the nucleous where it becomes phosphorylated, binds to specific DNA secuences and induces the expression of genes involved in inflamation such as IL-8 and IL-6, as well as anti-apoptotic genes including cIAP2, Bcl-2 and Bcl-xL[106].

The non-canonical pathway of NF-κB activation begins from different of type of receptors such as B-cell activation factor (BAFFR), lymphotoxin β-receptor (LTβP), CD40, receptor activator for nuclear kappa B (RANK), TNFR2 and Fn14. However, the p100 IκB family member are the specifically targets, because these menbers principally inyteracts with RelB in the cytoplasm. Once stimulated, p100 is partially degraded to generate p52[105] (Figure 13)

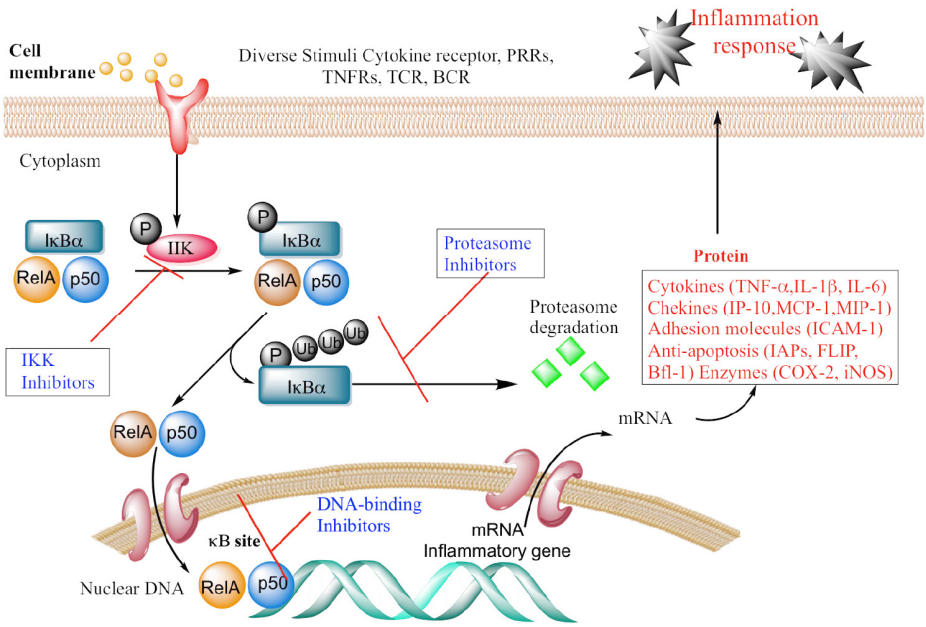

Figure 13. NF-κB signaling in inflammation[107]

2.2.2. Lipopolysaccharide-induced MCP-1 gene expression

Monocyte chemoattractant protein-1 (MCP-1) is one of the principal chemokines synthesized by several cell types and various non-leukocytic cells, including endothelial, epithelial, smoot muscle, mesangial, astrocytic, monocytic, microglial and fibroblastic[108]. It can be induced by lipopolysaccharide (LPS) of murine peritoneal macrophages and human endothelial cells and may contribute to renal inflammation. LPS is a potent stimulus of cytokine production and has been shown to increase MCP-1 expression in mesangial cells and renal cortical cells, which can induce a strong inflammatory response by the human immune system.

Aim of this section

The main purpose of this section was to isolate two major sesquiterpene lactones from *A. arborescens*. and develop a novel, rapid and precise HPLC method for sinultaneous determination of damsin **1** and coronopilin **2**, because the quantification of these compounds in the plant will be very important for the establishment of quality control procedure of STLs in the extracts and plants and for the rapid isolation of active compounds. Aditionally, we are going to investigate the effects of damsin and coronopilin in attenuation of IL-6 and MCP-1 expression

and inhibition of NF-κB in human dermal fibroblasts (HDFa) and human keratinocytes (HaCaT).

2.3. Result and discussion

2.3.1. Chemistry evaluation

A. arborescens have been charaterized to contain high levels of pseudoguaianolides concentrated principally in the aereal parts of the plan, where the range of STLs contentnt may vary from 0.01 % to 8 %, and STLs can be also found within the vacuoles of cell in the plant in response of biotic stresses[10]. Chemically, the type of STLs present in *A. arborescens* are pseudoguaianolides which possess a lactone ring with exocyclic double bond conjugated with a cabonyl group. Especially, for these particular characteristic STLs have gained increasing attention in the medicinal chemistry and chemical synthesis.

HPLC analysis

A precise and rapid HPLC method was developed for simultaneous quantification of major STLs from *A. arborescens,* a detalied procedure is described in **paper I**. For this purpose, the aerial parts of the plant were collected in June 2014 and 2015 in La Paz city from Bolivia country at (16° 30′ 01″ S, 68° 06′ 23″ W, 3804 m.a.s.l). The dried leaves (0.5 g) were subjected for extraction with 15 ml of EtOAc for 24 h, then the liquid extract was filtered and concentrated *in vacuo.* Previous to HPLC injection the sample was dissolved in 5 ml of MeOH (HPLC grade) and filtered through Discovery DPA-6S solid phase cartridges and then dilute to 25 ml in volimetrics flask to inject 25 µl into the HPLC using an isocratic elution with a mixture of solvents of 60% of ACN and 40% of formic acid at 0.15 % in water with a running time of 15 minutes and post time 5 minutes. The detector wavelenged was fixed at 215 nm.

Preparation of standar solutions

Reference sesquiterpene lactones (Standar) damsin **1** and coronopilin **2,** were isolated from *A. arborescens.* by chromatographic methods. Then, the structures and relative configuration of dansin and coronopilin were confirmed from 2D NMR analysis (including COSY, HMBC, and NOESY) and comparison with literature spectroscopic data from previous studies (spectroscopic data, **appended 1**). These pure sesquiterpene lactones were used as external standar for quantification the major STLs in the plant. The standard solutions were prepared by dissolving each

compounds in methanol (HPLC grade) and diluted to four concentration points (75, 150, 225 and 300 µg/ml) for establishing calibration curve.

The two STLs, damsin **1** and coronopilin **2** have shown good chromatographic separation and resolved with relatively differences in their retention times (3.30 min and 6.28 min) at 210 nm and have also shown a good resolution between the peaks (Figure 14). The HPLC method was aplied to determine the amount of damsin **1** and coronopilin **2** in the leaves of the plant, which gave 13.4 mg/g of compound **1** and 12.3 mg/g of compound **2**.

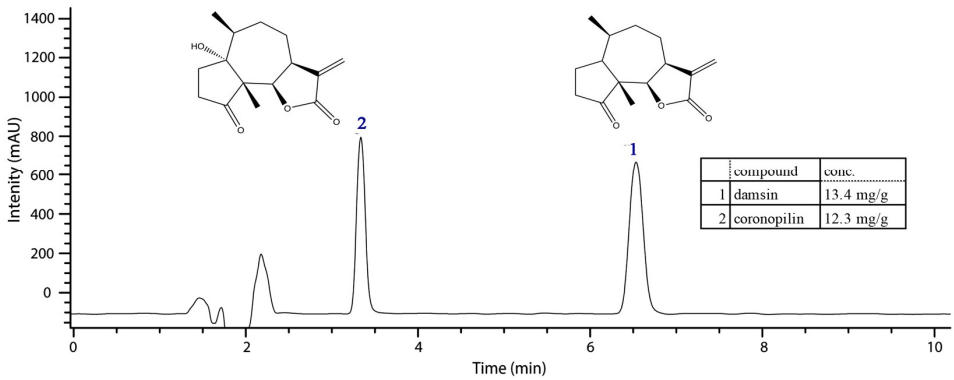

Figure 14. HPLC chromatogram of pseudoguaianolides from *A. arborescens*.

The HPLC analysis demostrated that the calibration curve have shown linear regressions with the determination coefficient (R^2) between 0.9965 and 0.9925, the LODs and LOQs of two compounds were 28.3 µg/ml and 85.8 µg/ml for compound **1** and for compound **2** 41.7 µg/ml and 126.5 µg/ml. The contents of damsin and coronopilin in the dry leaves were 13.4 ± 0.02 and 12.3 ± 0.3 mg/g respectively (Table 2)

Table 2. HPLC-DAD Calibtation curve result from quantification of damsin 1 and coronopilin 2 in *A. arborescens*

Compounds	Retention time (min)	Concentration (mg/g)	CV (%)	R^2 µg/ml	LOD[a] µg/ml	LOQ[b] µg/ml
1	6.28	13.4 ± 0.02	0.18	0.9965	28.3	85.8
2	3.30	12.3 ± 0.3	2.12	0.9925	41.7	126.5

[a]limit of detection
[b]limit of quantification

The HPLC-DAD three-dimentional spectrum of *A. arborescens* of EtOAc extract (25 µl injection) containing 13.4 ± 0.02 mg/g of damsin **1** and 12.3 ± 0.3 mg/g of coronopilin **2**. These two compounds have shown good absoption at 215 nm for the quantification of the compounds of interest, and their retention time were 3.30 min

for coronopilin and 6.28 min for damsin no other type of sesquiterne lactone were detected in the extract at this retention time. In addition unkown peaks did not match with any our standar (Figure 15 and Table 2).

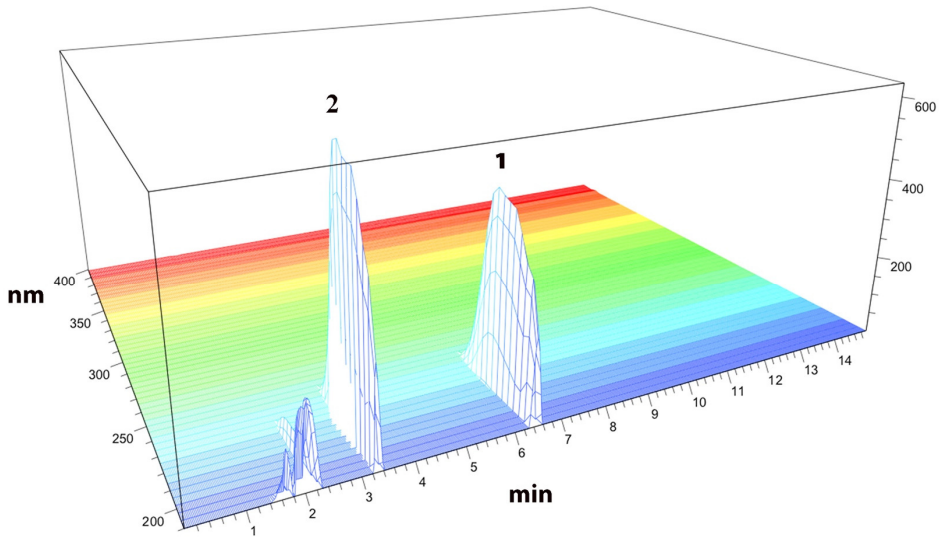

Figure 15. HPLC-DAD three- dimentional spectrum of *A. arborescens* EtOAc "2" coronopilin and "1" damsin

2.3.2. Biological evaluation

Medicinal plants with high contents in STLs have become an important source of compounds for studies on nonsteroidal anti-inflammatory drug (NSAID). Thus, we have demostrate that the SLTs damsin **1** and coronopilin **2**, isolated from *A. arborescens*, down-regulates proinflammatory cytokine production in human dermal fibroblasts, adult (HDfa). Reduce phosphorylated p65 and p105 subunits in HDFa cells and the detailed precedures are described in **paper 1**. However, the positive control (Dexamethasone) atenuate monocyte chemoattractant protein-1 (MCP-1) expression in human THP-1 monocytes. The compounds and positive control principally prevented the LSP-induced MCP-1 expression. Therefore, the compounds **1** and **2** demostrate a major consistent action on LPS-induced cytokine expression in different cell types than Dexametasone a commercial steroidal drug (Figure 16). Damsin and coronopilin did not affect the HDFa cell morphology and viability at concentration range (1-10 µM). Also, in HaCaT cells, treatment with

damsin (1–10 μM) for 24 h inhibited the MCP-1 expression, and damsin thereby attenuated cytokine expression both in HDFa and HaCaT cells**.**

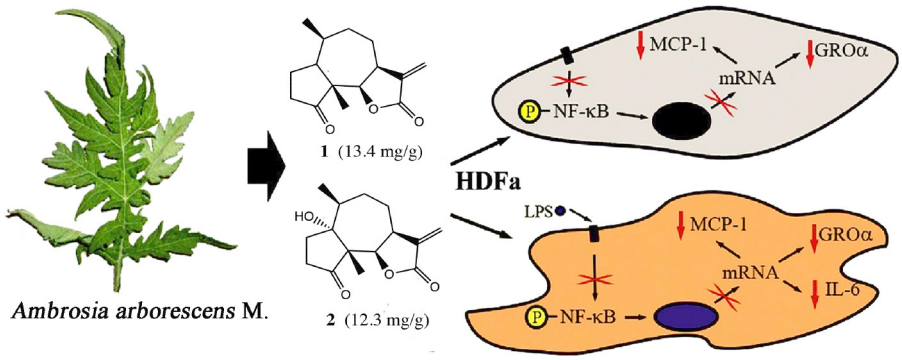

Figure 16. Damsin **1** and coronopilin **2** from *A. arborescens* 2, NF-κB target genes involved in inflammation development

Chapter 3. (Paper II and III) Semi-synthetic derivatives of damsin

3.1. Background

Among the STLs, the pseudoguaianolides are composed by the two groups ambrosanolides and helenanolides, which differ only in their stereochemistry at C-10. Damsin has its C-10 methyl group in a β-position,and is a representative of the ambrosanolide group[109]. Recently, damsin and other pseudoguaianolides have gained attention in the medicinal chemistry and chemical synthesis fields, due to numerous studies of their biological properties reported. Studies of damsin have suggested that it is a promising starting material for the semis-synthesis of active derivatives, since it has been shown to possess important cytotoxic effects on the colon cancer cell line Caco-2 (epithelial colorectal adenocarcinoma). In addition, it has significaticative inhibitory effects on the NF-κB and STAT3 transcriptional pathways in Jurkat cells and HeLa cells[110]. In addition, damsin has also been shown to be cytoxic towards breast cancer cell lines (MCF-7, JIMT-1, and HCC1937)[111]. In order to improve the biological properties of damsin (potency and selectivity), some structural modification in positions C-3, C-4, and between C-11 and C-13 have been reported. For example, the bromination of the C-11/C-13 double bond with trimethylammonium perbromide to give 11α,13- dibromodamsin and 11β,13-dibromodamsin, resulted in the loss of its biological activity. This reaction therefore demostrated the importance to maintain the exocylic double bound between C-11 and C-13 of damsin, as well as the carbonyl group at C-4. Therefore, some structural modification at C-3 could improve the biological activity of damsin[110]

The principal aim in this section was to prepare derivatives of damsin with modifications at C-3 through Claisen Schmidt condensations between mono- and bi-substituted benzaldehydes. This is an important transformation in organic synthesis, because it provides a good way to generate carbon-carbon double bonds next to a carbonyl group, and thereby a Michael acceptor which theoretically could interact with a biological receptor. We also prepared the thiol adducts for kinetics studies.

Tabla 3. Structural modification of damsin and its biological activities[110, 112]

Compound	Biological activity	Compound	Biological activity
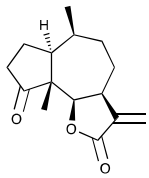 damsin	The cytotoxicity against normal human fibroblasts, human laryngeal carcinoma and human with simian virus 40[37]. Has shown antiproliferative activity against colon carcinoma (Caco-2 cells)[110]. The cytotoxicity effect on A549 (non-small cell lung cancer), HeLa (cervical cancer) and Panc-1 (pancreatic cancer)[114] Anti-arthritic effect[115]	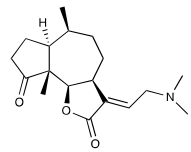 (E)-13-(N,N-dimethylaminomethyl) damsin	NF-κB inhibitory activity[113]
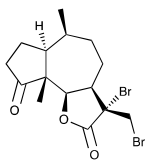 11α, 13-dibromodamsin	Has shown antiproliferative activity against colon carcinoma (Caco-2 cells)[110]	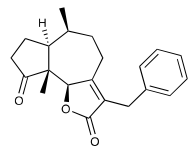 13-phenylisodamsin	NF-κB inhibitory activity[113]
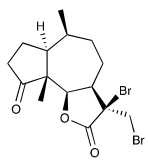 11β, 13-dibromodamsin	Antiproliferative activity against colon carcinoma (Caco-2 cells)[110]	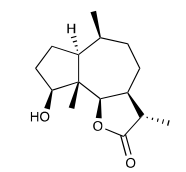 11α,13-dihydro-4α-hydroxy-4-deoxydamsin	NF-κB inhibitory activity[113]
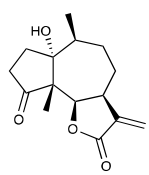 coronopilin	NF-κB inhibitory activity[113] Effects against leukaemia cells (Jurkat and U937 cells)[116] Cytotoxicity on human cancer cell lines including PC-3 (prostrate), HCT-15 (colon), THP-1 (leukaemia), HeLa (cervix), A549 (lung) and MCF-7 (breast)[117]	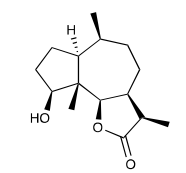 11β,13-dihydro-4β-hydroxy-4-deoxydamsin	NF-κB inhibitory activity[113]

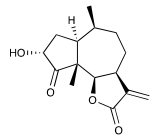 3α-hydroxydamsin	NF-κB inhibitory activity[113]	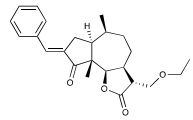 (E)-11β,13-dihydro-13-ethoxy-3-(phenylmethylene)-damsin	NF-κB inhibitory activity[113]
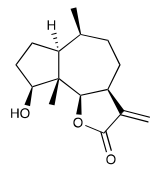 4β-hydroxydamsin	NF-κB inhibitory activity[113]	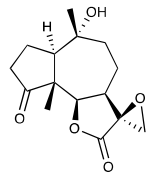 11β,13-epoxy-10-hydroxydamsin	NF-κB inhibitory activity[113]
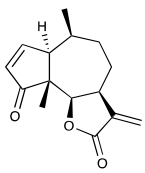 ambrosin	NF-κB inhibitory activity[113] Cytotoxic activity against lung (NCI-H522), colon (HCT-116), melanoma (LOX-IMVI), ovarian (OVCAR-5), renal (SN12C), prostate (PC-3), breast (MCF-7)[118]	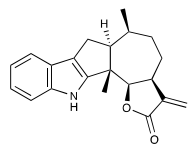 Dindol-01	NF-κB inhibitory activity[113] Cytotoxicity on human cancer cell lines including PC-3 (prostrate), HCT-15 (colon), THP-1 (leukaemia), HeLa (cervix), A549 (lung) and MCF-7 (breast)[117]
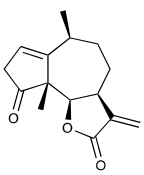 neoambrosin	NF-κB inhibitory activity[113] C ytotoxicity against different drug-resistant tumor cell lines[119]	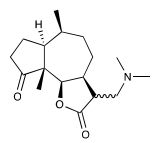 *epi*-11,13-dihydro-13-(N,N-dimethylamino)damsin	NF-κB inhibitory activity[113]

3.2. Damsin synthetic analogs

3.2.1. The Claisen-Schmidt condensation reaction

The Claisen-Schmidt or crossed-aldol condensation has gained attention in natural product science, since it is involved in the biosynthesis of many significant natural products. It results in the important carbon-carbon bond creation and the formation of α,unsaturated carbonyl compounds. Derivatives of damsin subjected to this reaction would possess two Michael acceptor units a functionalityl responsible for the biological activity of many natural products.

Claisen-Schmidt condensation is typically carried out between benzaldehydes and cyclic ketones, catalyzed by acids ($AlCl_3$ or HCl), strong bases (NaOH, KOH and $Ca(OH)_2$, metal ions such as Zn (II) and Ni(II) under homogenous, heterogenous or solvent-free conditions. In the case of base catalysis, the desired product is generated by an initial aldol condensation followed by dehydration via an enolate mechanism (see Figure 17), while in the case of acid catalysis the desired product is generated via an enol mechanism. However, these conditions suffer from side reactions, such as self-condensation of the ketone, and the formation of by-products will directly affect the yields of the desired product[120, 121].

Claisen-Schmidt, base-catalyzed

The classical Claisen-Schmidt reaction involves the reaction between benzaldehydes and cyclic ketones such as damsin **I**, with base-catalysis in a polar solvent. Strong bases such as potassium hydroxide, sodium hydroxide and potassium *tert*-butoxide are often used[122]. However, the basic conditions require some modifications, e.g. temperature adjustment and time of reaction. A strong base can extract the weakly acidic α-proton of the ketone moiety of damsin **I**, to form an enolate anion **II**. Next, the enolate anion will attacks the carbonyl carbon of the benzaldehyde to form the β-hydroxy carbonyl intermediate **III**. Then, the base B: pulls off the remaining α-hydrogen to give the new enolate anion **IV**, followed by the loss of water to give the desired α–benzylidendamsin product **V.** There is a higher preference for the formation a *trans* double bound product which is defined in the dehydration step, presumably due to steric reasons (see Figure 17).

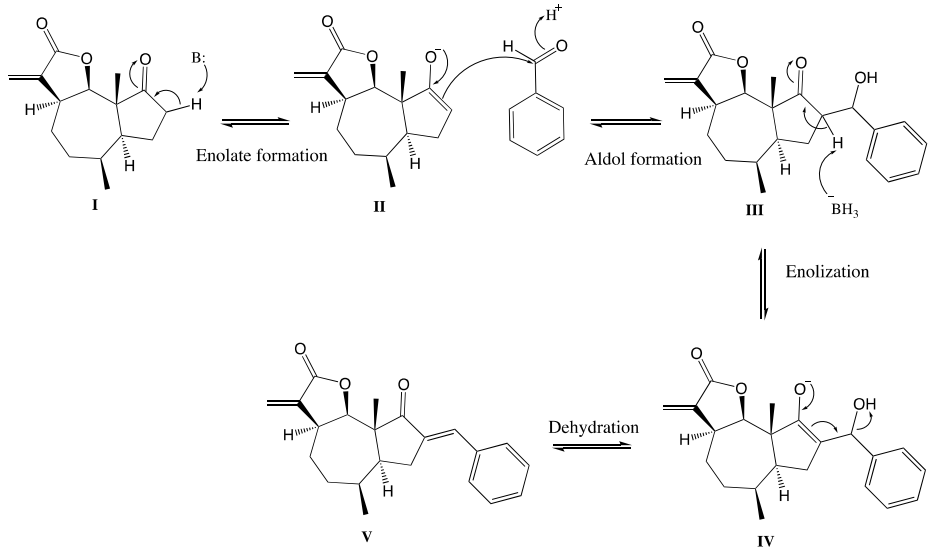

Figure 17. Mechanism of the Claisen-Schmidt base-catalyzed condensation between damsin and benzaldehyde.

The *trans* stereochemistry of the double bond in all derivatives from Claisen Schmidt condensation were confirmed by NOESY experiments.

Claisen-Schmidt, acid-catalyzed

Claisen-Schmidt condensation can be carried out with acidic catalysis as well, including Lewis acids and Brønsted acids in a polar solvent. Among the common acid catalysts used are B_2O_3, $RuCl_3$, BF_3, and dry HCl. However, these reactions sometimes require more severe conditions (high temperature, longer reaction times, and tedious purification times)[123]. Recently, *p*-toluene sulphonic acid (*p*-TSA) has been employed in the procedure of a variety of synthetic metodologies with good results[124].

The classic mechanism of an acid-catalyzed Claisen-Schmidt condensation is similar to that of the base-catalyzed condensation. It which procedeeds through the tautomerization of the ketone to form enol intermediate **II**, which will add to the carbonyl carbon of benzaldehyde to yield **III**, followed by the acid catalysed dehydration to produce the desired condensation product **V** (see Figure 18).

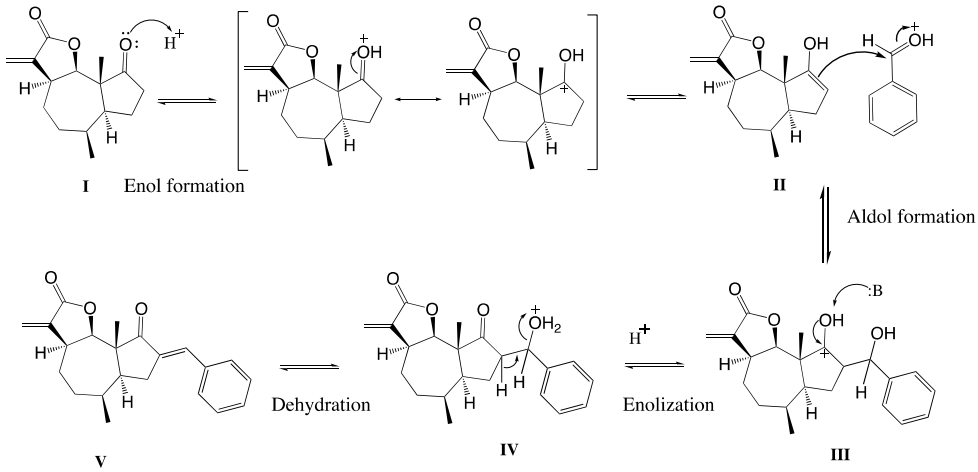

Figure 18. Mechanism of an acid-catalyzed Claisen-Schmidt condensation of damsin with benzaldehyde.

3.3. Results and discussion

3.3.1. Group one of damsin derivatives (Paper I)

The synthetic analogs from damsin **1** were previously prepared by a Claisen-Schmidt condensation, with both acid and base catalysts and solvents described in Table 4, to establish the optimal reaction conditions. The yields of reactions obtained for each catalyst and solvent are show in Table **4**. In this two first cases, neither (S)-N-(2,2,2-trifluoroacetyl)pyrrolidine-2-carboxamide nor dimethylammonium dimethyl carbamate (DIMCARB) catalysts yielded the desired product **V**. However, using TBAH, an organic-soluble hydroxide source in the form of tetrabutylammonium hydroxide as the base catalyst in toluene: H2O gave better yields, but the most efficient reaction was obtained using an organic acid catalyst, such as *p*-toluene sulfonic acid (*p*TSA).

Table 4. Effect of catalyst and solvent on Claisen Schmidt condensation of damsin **I** and benzaldehyde **II**

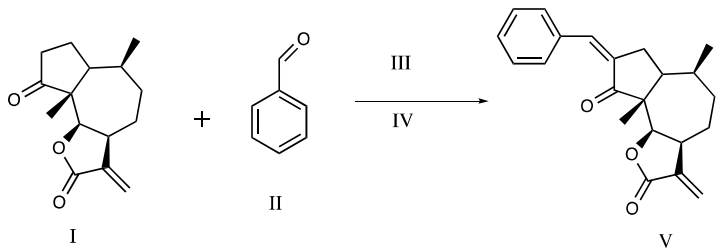

Entry	Catalyst III	Solvent IV	Time	Yields V (%)
1	(S)-N-(2,2,2-Trifluoroacetyl)pyrrolidine-2-carboxamide; r.t.	DMSO	42 h 30 min	0
2	Dimethylammonium dimethyl carbamate (DIMCARB); r.t	Free	3h	0
3	Tetrabutylammonium hydroxide (TBAH); r.t.	PhMe; H20 (80:20)	1h	11
4	Tetrabutylammonium hydroxide (TBAH); r.t.	THF; *t*-BuOH	2h 20 min	12
5	Tetrabutylammonium hydroxide (TBAH); r.t.	PhMe; H20 (50:50)	23 h 15 min	35
6	Tetrabutylammonium hydroxide (TBAH); r.t.	DMSO	26 min	0
7	Tetrabutylammonium hydroxide (TBAH); Na OH, r.t:	PhMe	10 min	6
8	*p*-Toluene sulfonic acid (PTSA) ; 80°C	Bz	23 h 15 min	72
9	*p*-Toluene sulfonic acid (PTSA) ; m.w. 180°C	Bz	2h	89

The Claisen Schmidt condensation between damsin and substituted benzaldehydes **4a-4n** were subjected under acid and basic optimized conditions (see Table 4) to obtain benzylidendamsin adducts **3a – 3u,** prepared as described in the **paper I**. These two different condensation procedures selected as optimized conditions from Table **4** such as: *i)* acidic catalysis with an excess of *p*-toluenesulfonic acid (*p*TSA) in benzene (entry 8 and 9), and *ii)* basic catalysis by treatment with tetrabutylammonium hydroxide (TBAH) in a heterogeneous mixture of solvent such as (50:50) toluene/water (entry 5). The results of optimization condition show the acidic conditions gave the higher yields than basic conditions (Table **1** and Figure **19**), although the condensation of damsin **1** with the protected hydroxybenzaldehydes to give the phenolic derivatives **3l** – **3n** were only performed under basic conditions, however, the yields were modest. (Figure 20)

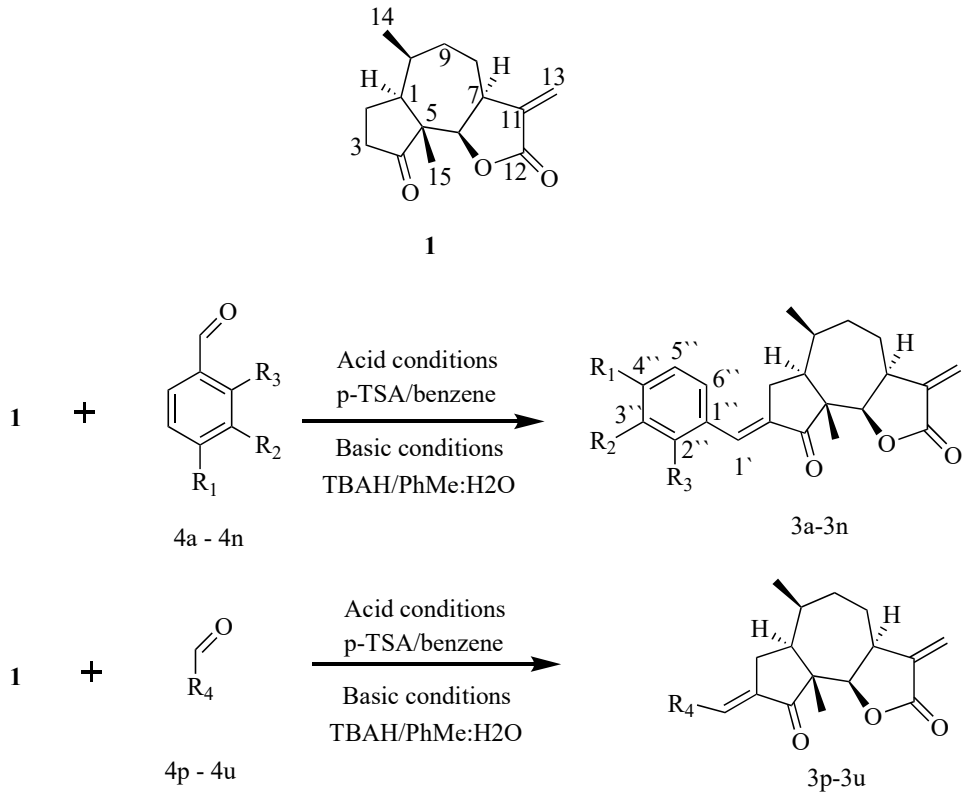

Figure 19 Damsin derivatives *via* Claisen-Schmidt condensation carried out in basic or acidic media under heterogeneous conditions.

The group of compounds, **3p–3u**, are the Claisen Schmidt condensation adducts between **1** and alkyl aldehydes and cyclohexyl aldehyde. Both acidic and basic catalysis for the condensation were tested. The condensation under basic conditions gave a better result for compounds **3s**-**3u**, while the yields for compounds **3p** and **3q** were higher under acidic conditions (Table 5).

Table 5. Synthesis of Claisen-Schmidt condensation derivatives **1**

				Yields (%)	
				Basic condensation	**Acidic condensation**
Compound	**R_1**	**R_2**	**R_3**		
3a	H	H	H	40	72
3b	CH_3	H	H	28	70
3c	H	CH_3	H	34	80
3d	H	H	CH_3	25	90
3e	CH_3	H	CH_3	x	46
3f	CF_3	H	H	84	88
3g	H	CF_3	H	56	34
3h	H	H	CF_3	27	71
3i	OCH_3	H	H	21	87
3j	H	OCH_3	H	3	73
3k	H	H	OCH_3	1	100
3l	OH	H	H	23 (from 1)	0
3m	H	OH	H	43 (from 1)	0
3n	H	H	OH	27 (from 1)	0
3p	R4 = (E)-cyclohexyl			x	41,5
3q	R4 = (Z)-cyclohexyl			x	20
3r	R4 = ethyl			9	20
3s	R4 = propyl			42	0
3t	R4 = 2-methyl propyl			42	0
3u	R4 = 3-butenyl			36	0

Generally, in the Claisen Schmidt condensation the mechanism involves a nuclephilic addition of an enolate anion under basic conditions or an enol intermediate under acid conditions, to the carbonyl carbon of a benzaldehyde. The benzaldehyde substituents, such as electron withdrawing group(s) in the aromatic ring, should increase the reactivity of the benzaldehyde. Benzaldehydes with electron-donating substituent(s) are consequently expected to be less reactive[125]. However, we observed that the electron-donating substituents in the benzaldehydes, such as -CH_3 and -OCH_3 makes the carbonyl carbon of aldehyde more reactive for nucleophilic reaction with enol intermediate (acid conditions), with the exeption of -OH which is unsuitable both in basic as well as acid conditions.

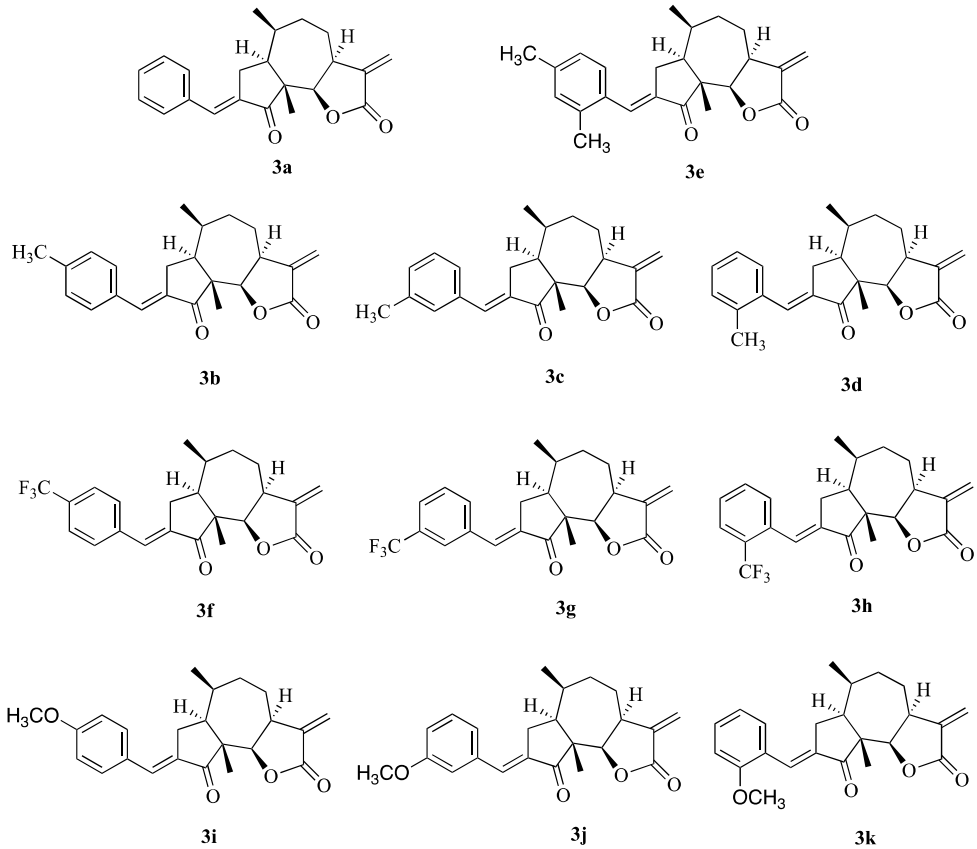

Figure 20. (*E*)-3-(Benzyliden)damsin adducts from Claisen Schmidt condensation

To prepare the phenolic adducts **3l-3n**, the hydroxy subtituents groups of the corresponding benzaldehydes were protected by treatment with methoxymethylbromide (MOMBr). The methoxymethyl (MOM) is extensively used as as a hydroxy-protecting group, because it can easily be introduced and it is stable under the reaction conditions used here. The protected benzaldehydes were then condensated under basic conditions, and deprotected, resulting in reasonable yields of **3l-3n**. The MOM deprotection was carried out by treatment with HCl (Figure 21).

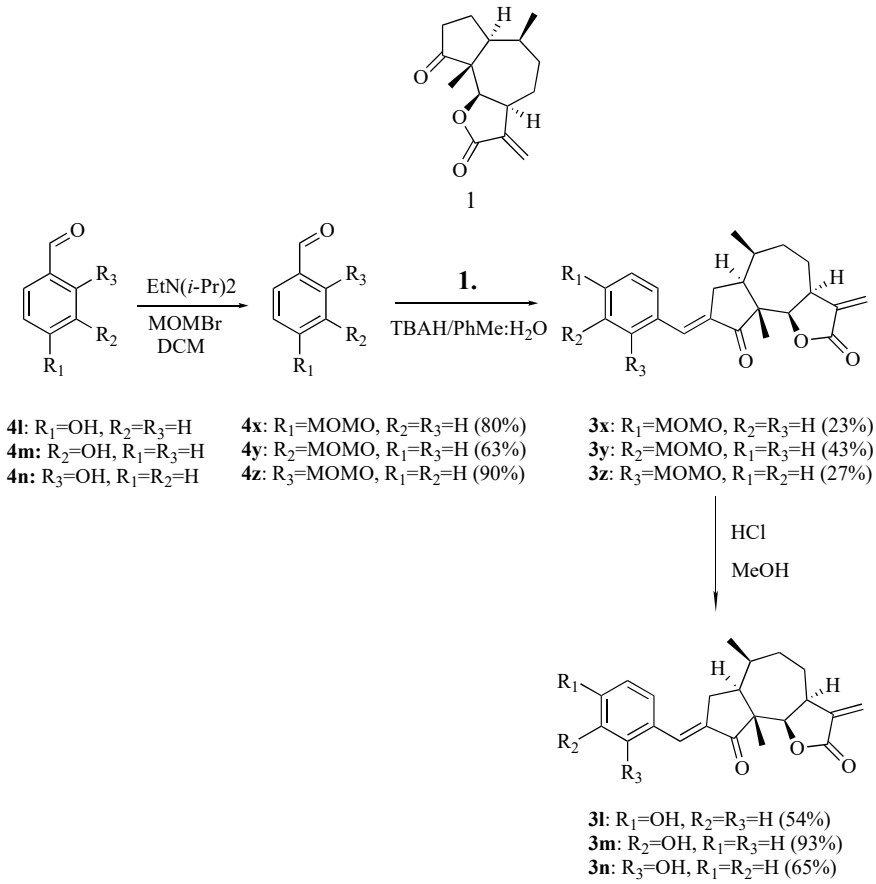

Figure 21. Hydroxyl-protection **(4x-4z)**, Claisen Schmidt condensation **(3x-3z),** Hydroxyl deprotection **(3l-3n)**

The formation of an isomeric mixture of adducts **3p** and **3q** were obtained only with cyclohexyl aldehydes and the formation of *E* (*trans*) isomer was more favoured than Z *(cis*) (Figure 22).

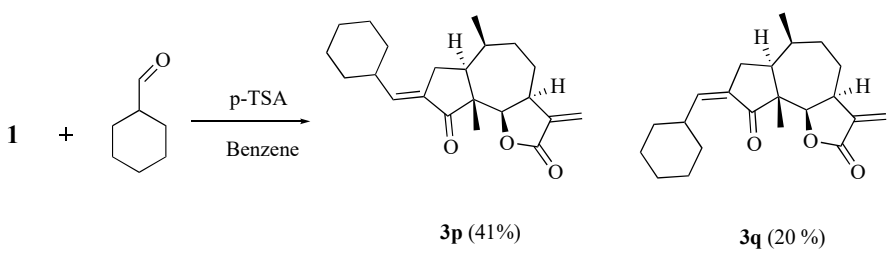

Figure 22. Mixture of E /Z isomers from Claisen Schmidt condensation

3.3.2. Group two of damsin derivatives (Paper III)

Influence of the nature of aldehydes

The new derivatives **2a** to **2i** were prepared by Claisen-Schmidt condensations between various benzaldehydes with electronwithdrawing substituents in the *para, meta* and *orto* positions, with damsin **1a** (or **1**?) according to the procedures described in **paper III**. The results showed that the yields of the reaction products depended on the position of the substituent, *orto>meta>para*. However, the reaction times with *meta* and *para*-substituted benzaldehydes were shorter compared to the corresponding *orto*-substituted benzaldehyde, presumabl because electron-withdrawing group in the *para* position decreases the electron density at the carbonyl carbon of the aldehyde, making the aldehyde more sensitive to nucleophilic addition (Table 6).

Table 6. Influence of withdrawing group in Claisen Schmidt condensation

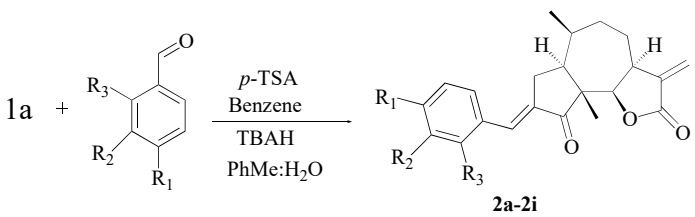

2a-2i

compound	R_1	R_2	R_3	time	yields
2a	F	H	H	4h	21,9
2b	H	F	H	4h	59
2c	H	H	F	6h	71
2d	H	Cl	H	3h45min	51
2e	Br	H	H	1h	8,4
2f	H	Br	H	1h	35
2g	H	H	Br	1h	51
2h	Et,	H	H	2h	30
2i	i-Pr	H	H	2h	29

The new derivatives **1c** and **1f** were prepared by Rubottom oxidation of the corresponding silyl enol ether intermediate, according of procedures described in paper **III** and **Figure 23**. Where damsin **1a** was treated with trimethylsilyl trifluoromethanesulphonate to give 100 % yield from regioselective formation of enol silyl ether intermediate by silylation of enolate anion of **1a**. The Rubottom oxidation process involves the reaction of *m*-MCPB react with the enol silyl intermediate through a cycloaddition, followed by a rearrangement yielding the derivatives **1c** (33 %) and 1f (19 %). The acylation of Rubottom oxidation product **1c** by the treatment with acetic anhydride and benzoyl chloride gave **1d** and **1e** (Figure 23).

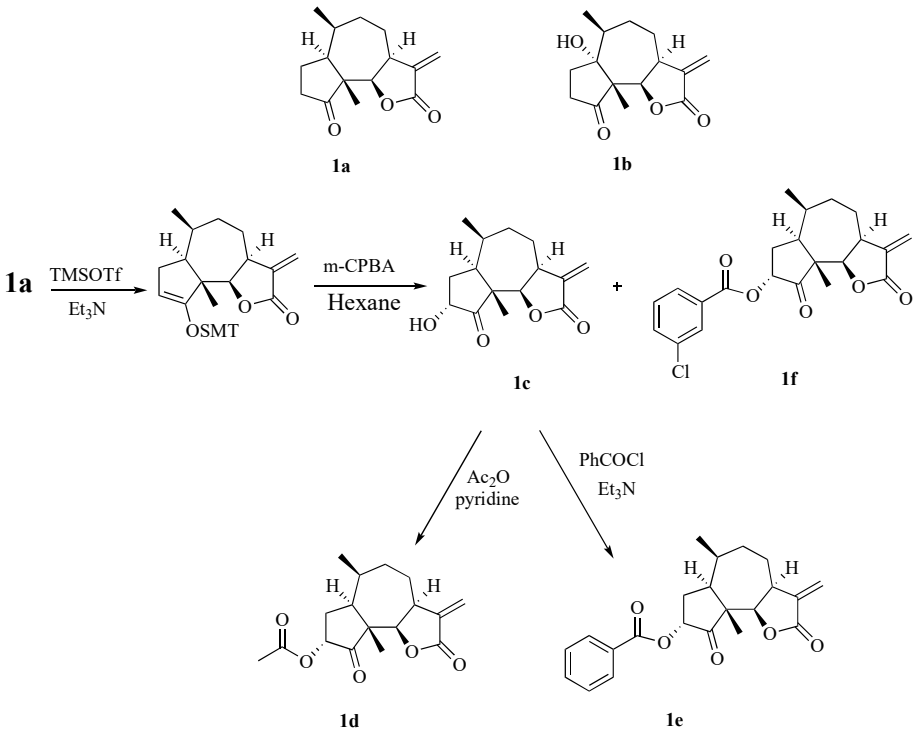

Figure 23. Rubottom oxidation of **1a** to give **1c** and **1f**; Acylation of **1c** to prepare **1d** and **1e**

Double bond reduction

In order to investigate the influence on the cytotoxicity on the presence of a second Michael acceptor, formed by the Claisen-Schmidt condensation, the compound **3o** was prepared by the reduction of the double bond between C3 and C1´ of **2a** or **6.** Several catalyst and solvents were tested to achieve this double bond reduction (Table 7). Among the catalysts tested, the hydrogenation using PdC and solvents such as EtOH:DCM gave better results than others catalysts, affording **3o** in 18 %. No product was observed for the entries 2, 3, 4, 6, 8 and 9, because double bond isomerization between C-11/C-13 was observed to give compound 9.

Table 7. Initial testing of catalyst and solvents for the hydrogenation of derivatives **3a** or **6**

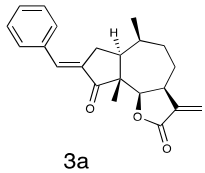

3a

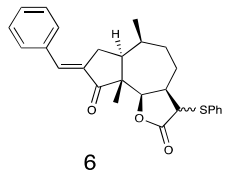

6

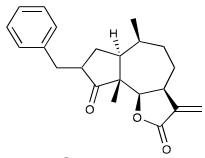

3o

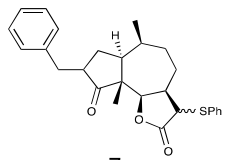

7

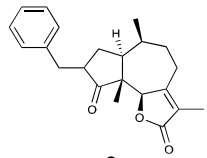

9

Entry	sustrate	reduction reaction conditions		Product
1	3a	$Co(CO)_8$	DME:H_2O	9
2	6	$Co(CO)_8$	DME:H_2O	6
3	6	H_2/s-Proline, PdC	MeOH	6
4	3a	Bu_3SnH/AIBN	PhH	3a
5	3a	$RuCl_2(P(Ph3))_3$	BnOH	9
6	6	$RuCl_2(P(Ph3))_4$	BnOH	6
7	3a	H_2/PdC	MeOH	9
8	6	H_2/PdC	EtOAc	6
9	6	H_2/PdC 4MP	EtOH	6
10	6	H_2/PdC	EtOH:DCM	7

The compound **3o** was prepared according of procedure described in **paper II**. Damsin **1** was subjected to protection of the exocyclic double bond *via* the Michael addition of thiophenol in EtOH to afford 14 % yield of intermediate **5**. A subsequent Claisen Schmidt condensation of **5** with benzaldehyde under acidic conditions to give 82 % yield of compound **6**. Hydrogenation of **6** was carried out by using PdC catalyst in EtOH:DCM under hydrogen atmosphere to give the reduced product **7** in 18 % yield, while the removal of the sulphur moiety in the double bound protection by treatment of **7** with $NaIO_4$ and MeOH yielded the desired product **3o** in 53 % yield (Figure 24).

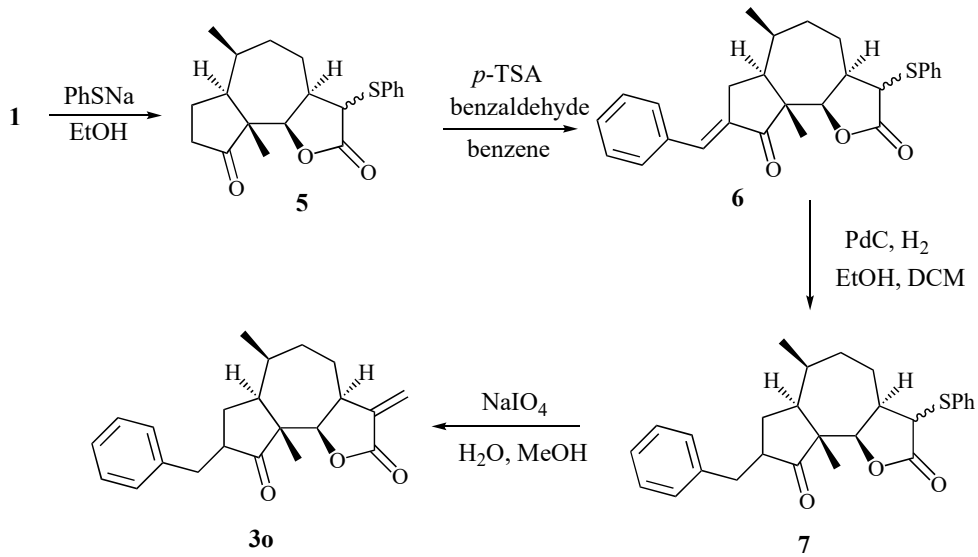

Figure 24. Hydrogenation of Claisen-Schmidt condensation product **6.**

3.3.3. Michael addition adducts (paper II)

As mention before the biological effects of damsin have been attributed to their capability to form covalent bonds with free cysteine *via* Michael addition of α,β□unsaturated carbonyl. The thiol adducts **5a** and **5b** from damsin **1a** and **4a** and **4b** from **3n** were prepared according of the procedures described in **paper II** by addition of L-cysteine methyl ester in MeOH to damsin **1a** and derivative **3n**. The results show that the damsin **1a** and derivative **3n** treated with L-cysteine methyl ester to give an isomeric mixture of thiol adducts **5a** and **5b**, **4a** and **4b** (Figure 25). The Michael addition reaction was observed only with the exocyclic double bond between C-11 and C13.

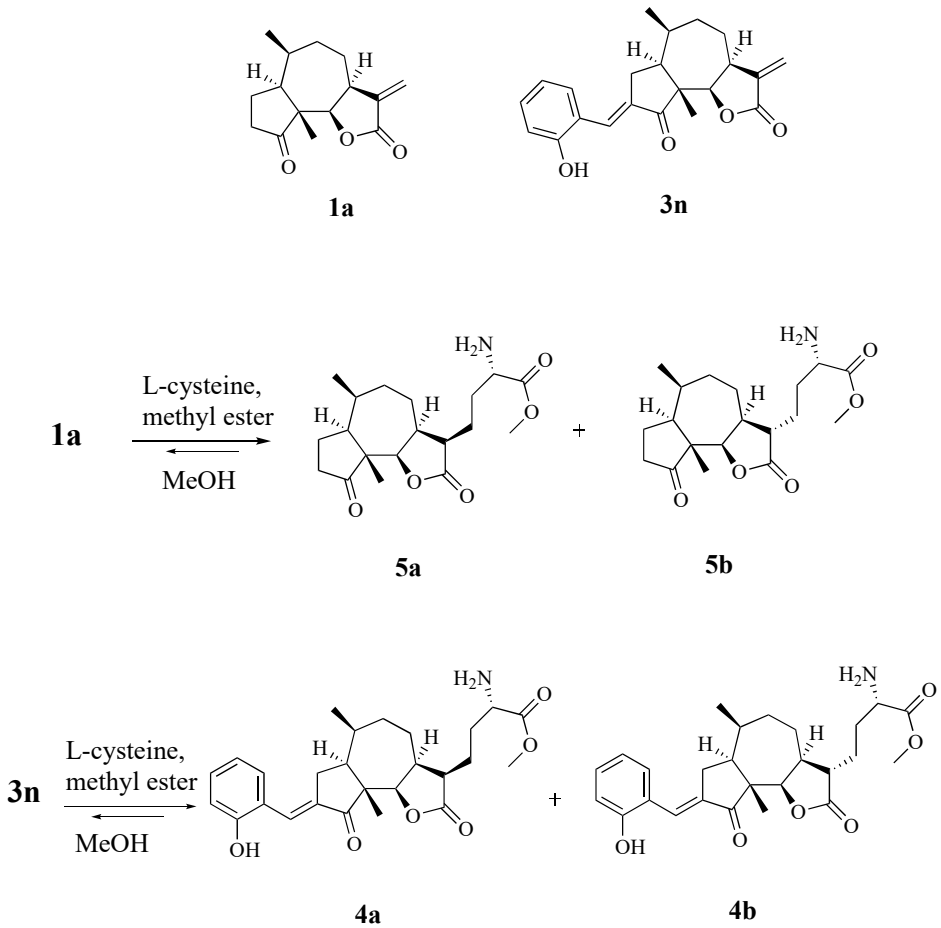

Figure 25. Michael addition adducts from **1a** (damsin) and **3n** (o-hydroxy phenyl methylene damsin

Kinetic of Michael addition

The reactivity of damsin **1a** with thiols is important for the understanding of the toxicity of α,β-unsaturated carbonyl derivatives. Our results, plotted in Figure 26-a), show the kinetic of the reaction between damsin **1a** and methyl-L-cysteine ester (MECys), to form isomers **5a** and **5b**, where the progress of reaction was monitored by ^{1}H NMR spectroscopy. The Michael addition of the thiol methyl-L-cysteine ester (MECys), to damsin **1a** was found to be relatively slow (see Figure 26 a)). The linearization of the reaction between **1a** and L-cysteine methyl ester (MECys), was possible to fit by a second-order (ec-1) with a slope k 0.345 mol/l*min and the corresponding coefficient of correlation R^2 0.994. However, the reaction of 3d with methyl-L-cysteine ester (MECys) to give a mixture of isomers 4a and 4b. The results plotted in the Figure 26-b) shows the kinetic of reaction between compound 3d and

methyl-L-cysteine ester (MECys), where the formation of products 4a and 4b were slowly than reaction with **1a**.

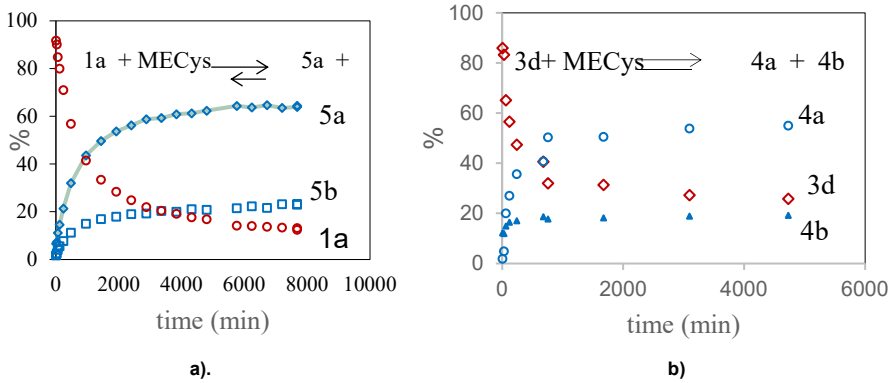

Figure 26. Kinetics of the Michael addition of a thiol to a) damsin **1a** and b) benzylidene damsin derivative **3d**

The rate of the reversible Michael reaction of adducts **5a** and **5b** were slower than the formation of the products. These values are very important for pharmacokinetic studies. We can suggest that the dissociation is also fit by second order whit some considerations.

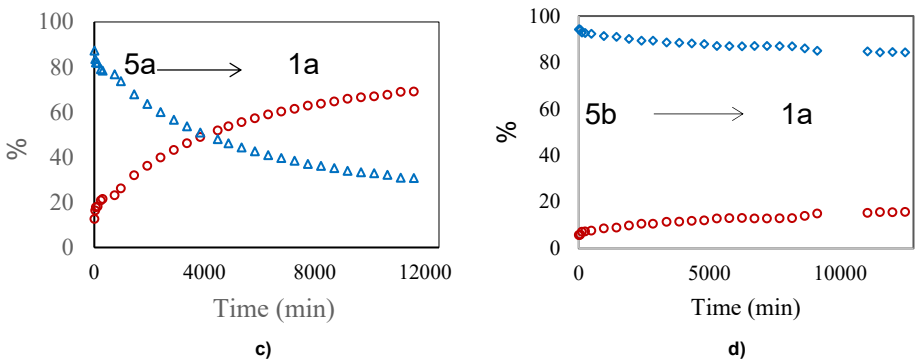

Figure 27. The stability of the thiol adducts c) thiol-damsin adduct isomer **5a** and d) thiol-damsin adduct isomer **5b**

Chapter 4. (Paper II, III and manuscript 1) Semi-synthetic derivatives of damsin and their cytotoxicity towards breast cancer cell lines

4.1. Background

Cytotoxicity plays an important role in investigations of carcinogenic processes, and the determination of cytotoxic effects on cancer cells is an initial step for the evaluation of the potential usefulness of test substances. Evidently, the lack of cytotoxicity towards normal cells is equally important, and the selectivity ratio is important to determine for promising bioactive substances.

Breast cancer is one of most common cancer in women worlwide, and it is the major cause of mortality. Therefore, new alternative therapies to control this desease have been reported, such as therapeutic drugs derived from natural compounds. Sesquiterpene lactones have been shown to possess a significant cytotoxic activity due to the presence of an α-methylene-γ-lactone moiety, which *via* a Michael addition can react with free thiols of the amino acid cysteine in proteins. Previous studies suggest that the cysteine 38 in the p65 subunit of the transcription factor NF-κB is the target for the inhibitory action of STLs[126]. Based on our previous works, damsin and its derivatives showed a significant effect on the growth of Caco-2 cells, a colorectal cancer cell line, and inhibitory effects were showed in NF-κB and STAT 3 transcriptional activities in Jurkat and HeLa cells[110]. The theory was therefore that structure modifications at position C-3 in damsin might result in analogues with improved cytotoxicity and selectivity against breast cancer cells.

4.1.1. The pricipal aim of this section

The principal aim of this section was to evaluate de cytotoxicity and selective cytotoxicity of two groups of benzyliden damsin derivatives as well as oxidized damsin derivatives. Aditionally, we report the molecular mechanistics aspects of selected benzyliden damsin derivatives in **manuscrip I**

4.2. Results and discussion

4.2.1. Selective cytotoxicity of damsin derivatives (Paper II)

Pseudoguaianolides damsin **1** and coronopilin **2** were isolated from *A. arborescens*, and the semi-synthetic (*E*)-3-benzylidendamsin derivatives **3a-3u** were prepared from **1** *via* Claisen Schmidt condensations as described in the chapter **3**. All these compounds were tested for their *in vitro* cytotoxicity against the selected breast cancer JIMT-1 cells, and against normal breast epithelial MCF-10A cells. The selectivity of cytotoxicity in cancer/normal cells were expresed as the ratio of IC_{50} (μM) values between MCF-10A and JIMT-1 cells. According to preliminary studies, a benzylidene substituent at position C-3 of **1** may improve the potency as well as the selectivity. Based of these result, we prepared **3a-3u** from **1** *via* Claisen Schmidt condensations, and the methodologies for this evaluation are described in the **paper II**. Our results are shown in Table 8, and demonstrate that the derivatives **1** and **2** show similar cytotoxic actitivity. **3a** is both more potent and selective compared with **1**. It therefore appears that a benzylidene substituent at position 3 of **1** is beneficial. It was consequently decided to study the influence of electron-withdrawing and electron-donating substituent in the aromatic ring of derivatives **3b- 3n**, for the cytotoxicity. The results show that JIMT-1 cells were more sensitive than normal (MCF-10A) cells with derivatives **3b-3n**.

Table 8. Cytotoxic activity (IC_{50}, μM) of compounds 1,2 and 3a – 3u against breast cancer and normal breast cell line.

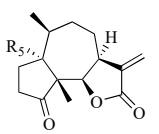

1-2

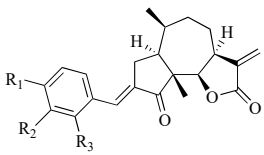

3a-3n

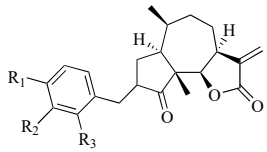

3o

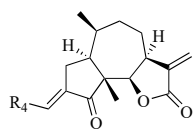

3p-3u

compound	R_1	R_2	R_3	MCF-10A (mM)	JIMT-1 (mM)	Ratio MCF-10A: JIMT-1
1		R_5 = H		8.1 ± 0.4[2]	3.3 ± 0.6[2]	2.5
2		R_5 = OH		15.3 ± 0.9[2]	5.6 ± 0.8[2]	2.7
3a	H	H	H	8.2 ± 1.6[2]	1.7 ± 0.4[1]	4.8
3b	CH_3	H	H	3.7 ± 0.4[2]	2.1 ± 0.3[2]	1.8
3c	H	CH_3	H	12.6 ± 1.6[2]	4.8 ± 0.3[2]	2.6
3d	H	H	CH_3	11.1 ± 1.8[2]	4.7 ± 0.1[1]	2.4
3e	CH_3	H	CH_3	5.2 ± 1.5[2]	3.5 ± 0.7[2]	1.5
3f	CF_3	H	H	3.1 ± 0.3[2]	1.8 ± 0.2[2]	1.7
3g	H	CF_3	H	11.9 ± 0.4[1]	4.4 ± 0.7[1]	2.7
3h	H	H	CF_3	13.0 ± 0.8[1]	8.1 ± 0.6[1]	1.6
3i	OCH_3	H	H	7.9 ± 1.2[2]	1.6 ± 0.1[2]	4.9
3j	H	OCH_3	H	> 20[1]	9.0 ± 1.0[1]	na
3k	H	H	OCH_3	> 20[1]	7.1 ± 0.2[1]	na
3l	OH	H	H	13.6 ± 0.6[2]	2.9 ± 0.2[1]	4.7
3m	H	OH	H	10.6 ± 1.3[2]	2.4 ± 0.1[2]	4.4
3n	H	H	OH	6.7 ± 0.9[2]	2.1 ± 0.2[1]	3.2
3o	H	H	H	7.1 ± 0.6[2]	2.0 ± 0.6[2]	3.6
3p	R_4 = (E)-cyclohexyl			11.7 ± 1.9[2]	8.1 ± 3.1[2]	1.4
3q	R_4 = (Z)-cyclohexyl			> 20[2]	12.3 ± 1.3[2]	na
3r	R4 = ethyl			5.5 ± 1.1[1]	1.4 ± 0.1[1]	3.9
3s	R4 = propyl			12.6 ± 0.8[1]	3.7 ± 0.1[2]	3.4
3t	R_4 = 2-methyl propyl			20.3 ± 0.3[1]	8.1 ± 0.1[1]	2.5
3u	R_4 = 3-butenyl			17.5 ± 5.1[1]	1.7 ± 0.0[1]	10.3

Among the **3a-3n** derivatives, *para*-benzyl substituent were more active and selective, although electron-withdrawing or electron-donating substituents did not influence the cytotoxicity a lot. The derivatives **3r** and **3u** were most potent towards cancer cells in the group **3p-3u**, suggesting that a linear alkyl or alkyliden substituent at C-3 position of **1** is benificial for the potency (Figure 28).

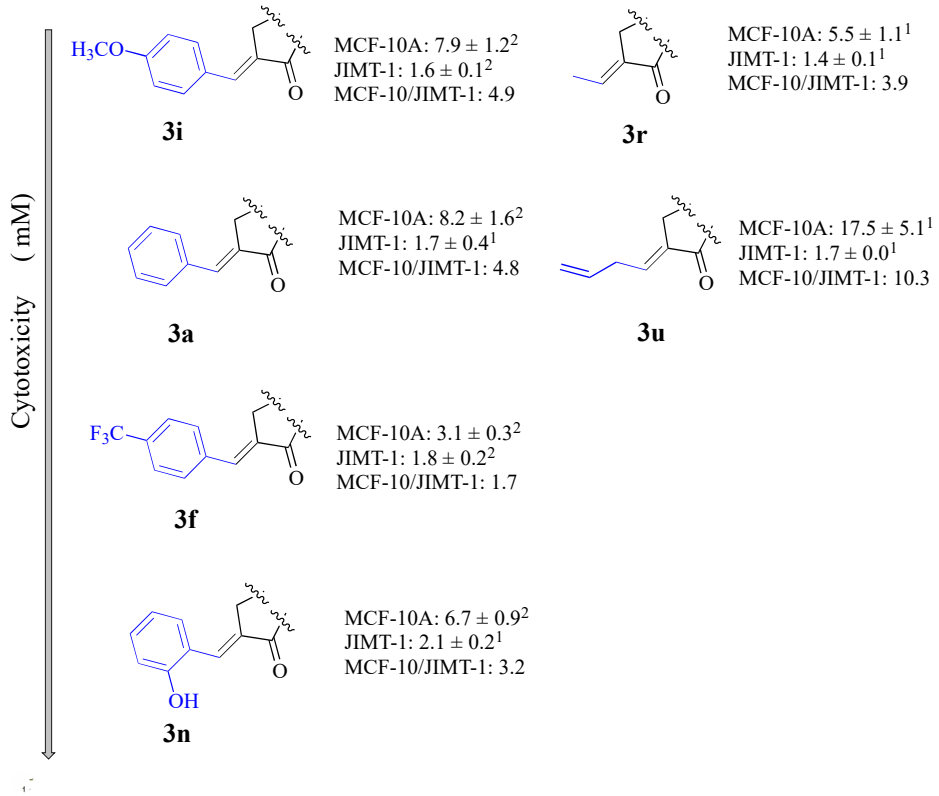

Figure 28. Selected analogues sorted according to potency and selectivity.

4.2.2. Second group of damsin derivatives (Paper III)

Based on the positive effects on potency and selectivity of Claisen Schmidt condensation products from **1a**, new groups of derivatives were prepared *via* Claisen Schmidt condensation and Rubottom oxidation. The subsequent C-3 acetylation of damsin **1a** was carried out according to the methodologies described in **paper III**. Our results, expressed as IC_{50} values for breast cancer JIMT-1 cells and normal breast epithelial MCF-10A cells, and the selectivity measured as the ratio of the IC_{50} values between MCF-10A and JIMT-1 cells, are shown in Table 9. The results reveale that oxidized derivatives (**1b-1c**) are less cytotoxic than damsin **1a** and (*E*)-3-benzylidendansin derivatives **(2a-2i, 3a-3d)** with an IC_{50} values ranging from 0.7 to 3.8 µM against breast cancer JIMT-1cells, and the derivatives (**1d-1f)** from Rubottom oxidation also resulted in loss of cytotoxic activity compared with **1a.** According to the IC_{50} values, JIMT-1 cells were more sensitive to the assayed derivatives (**2a-2i** and **3a-3d)** than the MCF-10A cells, which is in agreement with our previous study (**paper II)**. In general, analogues with electron-

withdrawing substituents such as F, Cl, Br in the *para* position of the benzylidene moiety were more potent and selective, compared to **1a** and previous derivatives assayed in **paper II**. However, derivative **3d**, with two substituent groups in the benzyliden-damsin (OH and Cl) was found to be the most potent and selective to breast (JIMT-1) cancer cells with an IC_{50} value 0.7 ± 0.1 μM. This indicate that the substituents -Cl and -OH in the aromatic ring of (*E*)-3-benzylidendamsin are beneficial, and should be considered for further studies.

Table 9. Cytotoxic activity of second group of benzylidendamsin derivatives

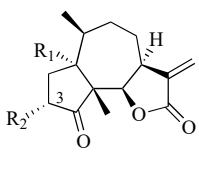

1a-1f

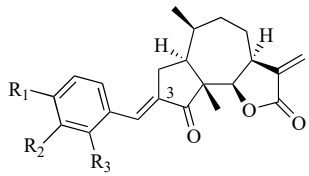

2a-2i

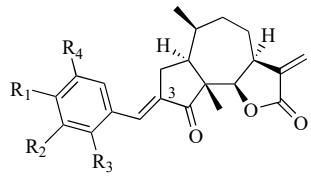

3a-3d

Compound	R_1	R_2	R_3	R_4	MCF-10A (μM)	JIMT-1 (μM)	Ratio MCF-10A : JIMT-1
1a	H	H	-	-	8.1 ± 0.4[2]	3.3 ± 0.6[2]	2.5
1b	OH	H	-	-	15.3 ± 0.9	5.6 ± 0.8	2.7
1c	H	OH	-	-	12.8 ± 1.1[2]	6.3 ± 0.2[2]	2.0
1d	H	OAc	-	-	> 20 [1]	> 20 [1]	na
1e	H	OBz	-	-	> 20 [1]	> 20 [1]	na
1f	H	*m*-Cl-OBz	-	-	> 20 [1]	> 20 [1]	na
2a	F	H	H	H	4.4 ± 1.6[2]	2.3 ± 0.4[3]	1.9
2b	H	F	H	H	2.5 ± 0.3[2]	1.1 ± 0.1[3]	2.3
2c	H	H	F	H	2.2 ± 0.4[2]	1.1 ± 0.3[3]	2.0
2d	H	Cl	H	H	3.8 ± 0.6[2]	1.4 ± 0.3[2]	2.6
2e	Br	H	H	H	6.2 ± 1.3[3]	1.8 ± 0.7[3]	3.5
2f	H	Br	H	H	6.1 ± 0.4[3]	1.8 ± 0.9[3]	3.4
2g	H	H	Br	H	2.0 ± 0.4[3]	1.2 ± 0.3[3]	1.6
2h	Et	H	H	H	2.5 ± 0.4[2]	1.9 ± 0.8[2]	1.3
2i	*i*-Pr	H	H	H	6.2 ± 1.4[2]	3.8 ± 1.0[2]	1.6
3a	CF_3	H	F	H	2.3 ± 0.9[2]	1.2 ± 0.1[3]	2.0
3b	CH_3	H	OH	H	4.7 ± 0.7[2]	1.9 ± 0.1[3]	2.4
3c	OH	CF_3	H	H	5.4 ± 1.4[3]	1.8 ± 0.2[3]	3.0
3d	H	H	OH	Cl	2.1 ± 0.7[2]	0.7 ± 0.1[2]	2.6

[1]two dose-response curves, [2]three dose-response curves, or [3]four dose-response curves.

4.2.3. Molecular mechanisms of breast cancer cells in selected damsin derivatives (manuscript I)

It has been reported that the cytotoxicity of STLs depends mainly of their alkylating ability, due to the interaction with nucleophilic structures of proteins such as the transcription factor Nuclear Factor-κB (NF-κB). However, the lipophilicity of the side chain of the STLs may also affect their cytotoxicity since it facilitate the entering into the cell. Thus, investigations demonstrated that the anti-cancer properties of STLs is due to the inhibition of the signaling pathway of NF-κB. NF-κB has in cancer cells a major role to inhibit apoptosis, inducion of metastasis, resistance to chemotherapy, and resistance to radiotherapy[32] . Based on such previous report, and the results of selective cytotoxicity reported in the paper **II**, we selected twelve derivatives from group one of benzylidendamsin derivatives for molecular mechanistic studies (Figure 29), the metodologies used are described in **Manuscript I.** Our result show that TNF-α induced translocation of NF-κB is blocked by treatment with STLs. Additionally, it was observed that STAT3 can binds to the p65/NF-κB transactivation domain and that STAT3 is located in the DNA binding complex.

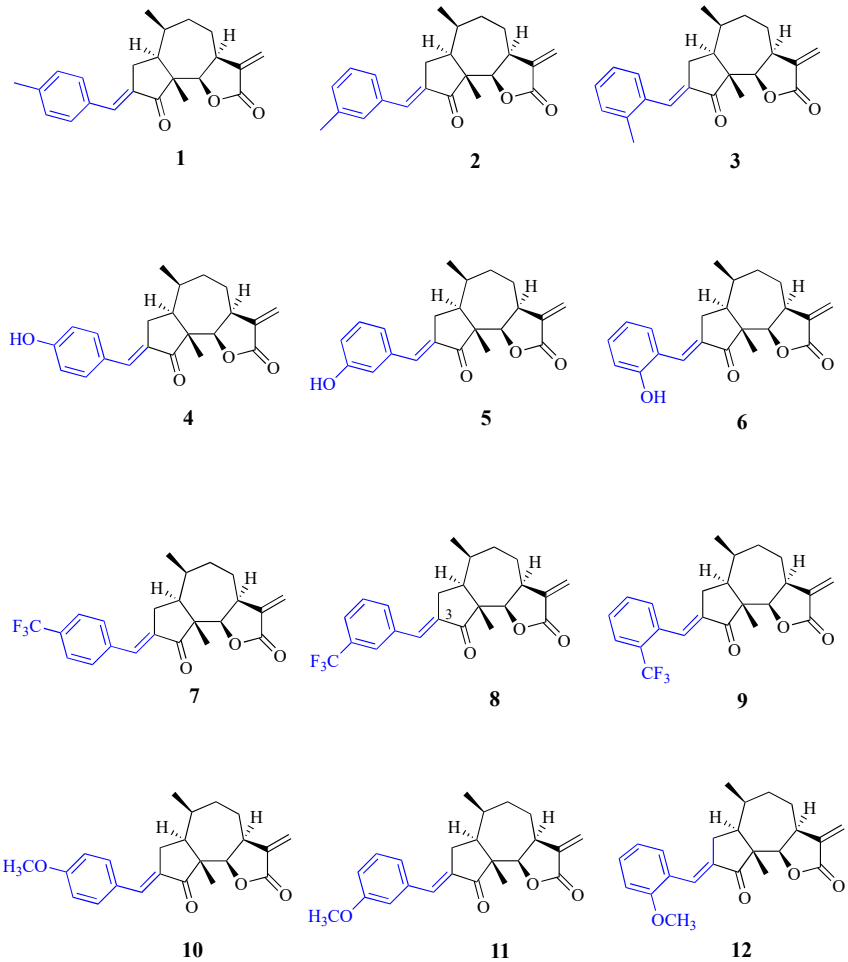

Figure 29. Selected benzylidendansin for molecular mechanistic studies.

Chapter 5. (Paper IV, V) Triterpenes from Bolivian plants, and the preparation of semi-synthetic derivatives

5.1. Background

Medicinal plants play a considerable role for the development of potentially useful bioactive compounds. A special class are the triterpenes, especially with oleanane, lupane and ursane-type skeletons. Pentacyclic triterpenes have attracted attention due to their numerous biological activities reported, such as anticancer, antifungal, antiviral, cytotoxic, analgesic, antiinflammatory, antiulcer, antibacterial, hepatoprotective, *etc*[66,127]. Triterpenes in plants can be in their free form with low water solubility, or as aglycone of saponins. They are present in abundance in different organs such as surface cuticle waxes and steam barks[128]. Thus, the screening of medicinal plants in the search for triterpenoids is continuously needed for therapeutic studies. Species belonging to the genera *Tetraglochin. Baccharis*, *Junellia* and *Lampaya* are used in local traditional medicine to treat digestive disorders, fever, coughs and colds. Previous studies have reported the presence of significant concentration of oleanolic acid (AO) in these species[129]. Additionally, a study about the antiproliferative evaluation of extracts from *Tetraglochin cristatun, Junellia seriphioides* and *Lampaya castellani* have demonstrated that these species possess inhibitory effects on the proliferation of colon cancer cells (Caco-2)[83] (Figure 30). Several structural modifications in oleanolic acid at positions C-3, C-28, and C-12 have been reported to improve the anticancer activity compared to OA, also the esterification of the hydroxyl substituent at position C-3 of OA seems to affect their cytotoxicity. However, the modification of the carboxylic group at C-27 seems to reduce the cytotoxicity[130]. Additionally, the introduction of a benzylidene substituent at position C-2 of triterpene natural products such as β–boswellic acid

and ursolic acid to produce 2-benzylidene derivatives, have been reported to improve anticancer activity[131,132].

Moreover, oleanolic acid and similar triterpenes are present as aglycones of a variety of saponins. Previous reports have described the high concentration of triterpenoid saponins in *Chenopodium quinoa*, mostly derived from oleanolic acid, hederagenin, phytolaccagenic acid, and serjanic acid[87]. Our previous report showed that triterpene saponins with a hydroxyl group at C-3 and a carboxylate group at C-28, are accumulated in high concentration in the seed pericarp [133,134].

5.1.1. The principal aim of this section

The principal aim of this section was to evaluate the contents of oleanolic acid among eight species found in the Bolivian altiplano, since this compound and its derivatives possess anticancer and anti-inflammatory activities.

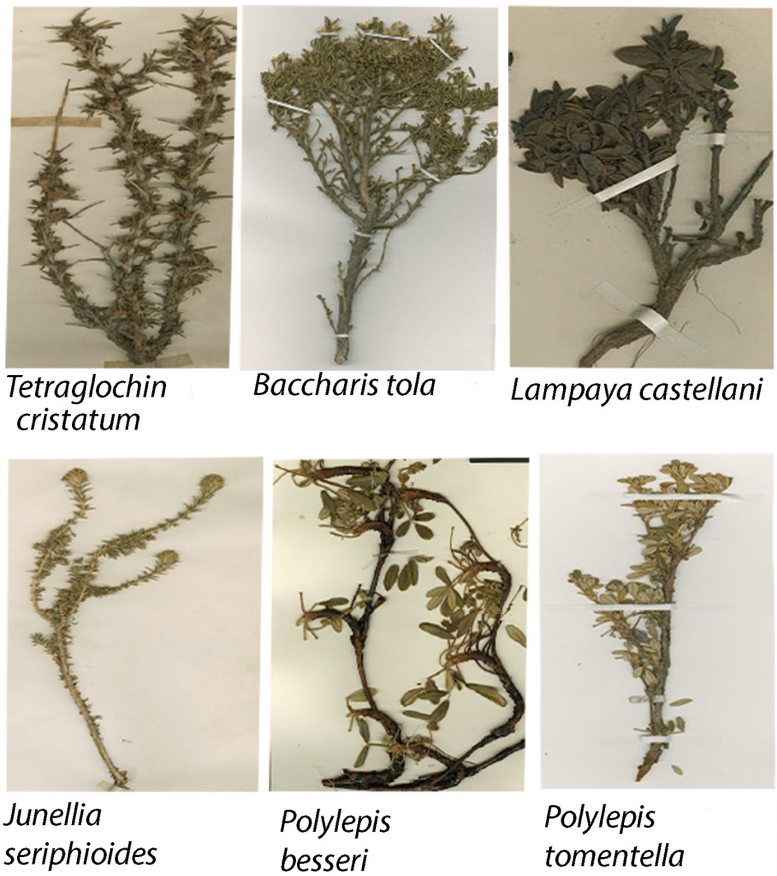

Figure 30. Medicinal plants of Bolivian highlands (3500 to 4200 m.a.s.l.).

5.2. Results and discussion

5.2.1. Oleanolic acid evaluation in plants (paper IV)

Comparative evaluation of the contents of oleanolic acid (OA) by rapid and precise high-performance liquid chromatography (HPLC) method were carried out in eight extracts of plants of Bolivian altiplano (Table 10). These plants were selected according to our previous reported preliminary TLC analysis study. The separation was carried out on RP-C18 (4.6×250 mm×5µm) with a 0.5 µm pre-column filter (Agilent Technologies), with a mobile phase composed of acetonitrile/water with

isocratic elution. The method was carried out to get a good separation of OA for the quantification in crude extracts of the eight plants, and the detection wavelength was 210 nm for OA because it has good absorption and sensitivity at this wavelength. The retention time (RT) for OA in the extracts compared with the external standard was 8.305 min. The peak identity was confirmed by comparison of retention time and their UV spectrum of each peaks in the chromatogram. HPLC chromatogram of OA are shown in Figure 31.

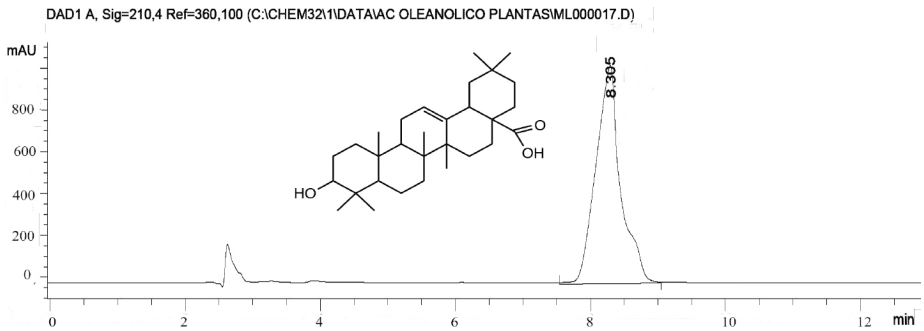

Figure 31. HPLC chromatogram of OA standard.

Linearity

The calibration curve was constructed using standard solutions of OA as external standard in the range of 400, 800, 1500, 2000, 2500 µg/mL each concentration was injected into the HPLC by triplicate. The regression equation and correlation coefficient (R) was: 12,957x + 735,69 and 0.9983 indicated good linearity.

Limit of detection and limit of quantification

The limit of detection (LOD) and limit of quantification (LOQ) of OA in this method were 138.96 µg/ml and 421,11 µg/ml respectively these values permit the detection and quantification of OA at low concentrations.

The HPLC quantification of OA showed in Table 10 indicated that the highest concentration of AO was found in *Junellia seriphioide, Lampaya catellani, Baccharis tola, Satureja boliviana* and *Polylepis besseri bark.* However, all species show high contents of OA compared with other species such as those found in the olive fruit (0,17-0,56 mg/g) and similar than the reported for olive leaf (31,0 mg/g) which is still used as main source of commercial oleanolic acid. Among these plants, *Baccharis tola* commonly known as "tola", is widely distributed in the Bolivian altiplano, so it could be used as new natural source for obtaining this bioactive compound. It is also interesting to highlight that the bark of *Polylepis besseri* has a good content of oleanolic acid, because the shredding bark of *Polylepis* is constantly peeling.

Table 10. Oleanolic acid in Bolivian highland plants

Code	Plant	RT (min)	AO		CV (%)
			(Mean ± SD)	mg/g	
June.	*J. seriphioide*	8.323	22,7	±0,41	1,8
Tetra.	*T. cristatum*	8.309	4,2	±0,04	1,2
Lamp.	*L. castellani*	8.315	13,9	±0,08	0,6
B.to.	*B. tola*	8.303	11,9	±0,32	2,7
P.tom. **	*P. tomentella (leaves)*	8.294	4,5	±0,15	3,5
Sat.b.	*S. boliviana*	8.291	8,7	±0,08	1
P.tom *	*P. tomentella (bark)*	8.327	2,9	±0,04	1,4
P.hie	*P. hieronyni*	8.323	3,6	±0,04	1,1
P.bess *	*P. besseri bark*	8.294	11,1	±0,03	0,3
P.bess **	*P. besseri (leaves)*	8.325	2,9	±0,16	5,8

5.2.2. Triterpenes and their synthetic derivatives (Paper V)

Acid hydrolysis of triterpenic saponins from quinoa husk

To obtain the triterpenoids**1-4** from quinoa husk, which is widely produced in Bolivia, the hydroalcoholic extract was obtained from quinoa residues by extraction with a mixture EtOH: H_2O (50:50), then the crude extract was subjected to acidic hydrolysis with HCl (10 ml, 2M). The hydrolysis reaction was carried out by microwave and conventional methods according of the procedures described in **paper V**. The results showed in Table 11 show that the oleanolic acid and hederagenin were found as the aglycone present in highest amount in quinoa husk. These values are in accordance with reported in other investigation[135]. In general, the procedure gave higher concentration of compound **1-4** than microwave method, but the conventional method was improved in several assays and this was the first assay using this microwave method, which maybe could be improved.

Table 11. Acid hydrolysis of quinoa husks saponins to give triterpenoids **1-4**

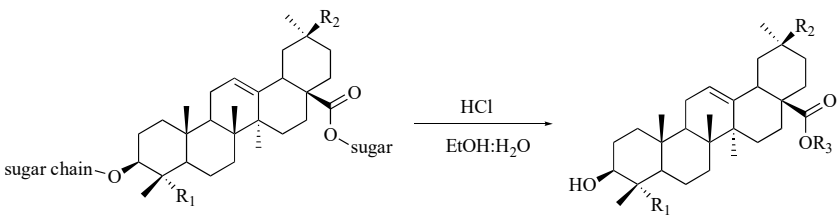

1-4

Compound	substituent	Concentration (mg/g)[a]

	R_1	R_2	R_3	microwave	conventional
1	CH_3	CH_3	H	98	317
2	CH_3	CH_3	CH_3	21.2	66
3	CH_2OH	CH_3	H	21.6	279
4	CH_2OH	$COOCH_3$	H	116	104

[a]mg of sapogenin per g of hydro-alcoholic extract

Semi-synthesis of oleanolic acid derivatives

The oleanolic acid derivatives **(6a-6d)** were prepared in two steps, including Jones oxidation and subsequent Claisen Schmidt condensations with substituted benzaldehydes under acid catalysis, the detailed description of the procedure is found in the **paper V.** The OA was treated with Jones reagent to get the C-3 oxidized derivative **5** in 70.1% yield. The 2-arylidene-3-oxoolean-12-hydroxy-28-oic acids derivatives (**6a-6d)** were prepared *via* Claisen Schmidt condensations of derivative **5** with substituted benzaldehydes under acid catalysis to give the desired product in moderate yields (Table 12). The structures of the derivatives were identified by spectroscopy methods (^{1}H NMR and ^{13}C NMR).

Table 12. Semi synthesis of benzylidene derivatives from oleanolic acid

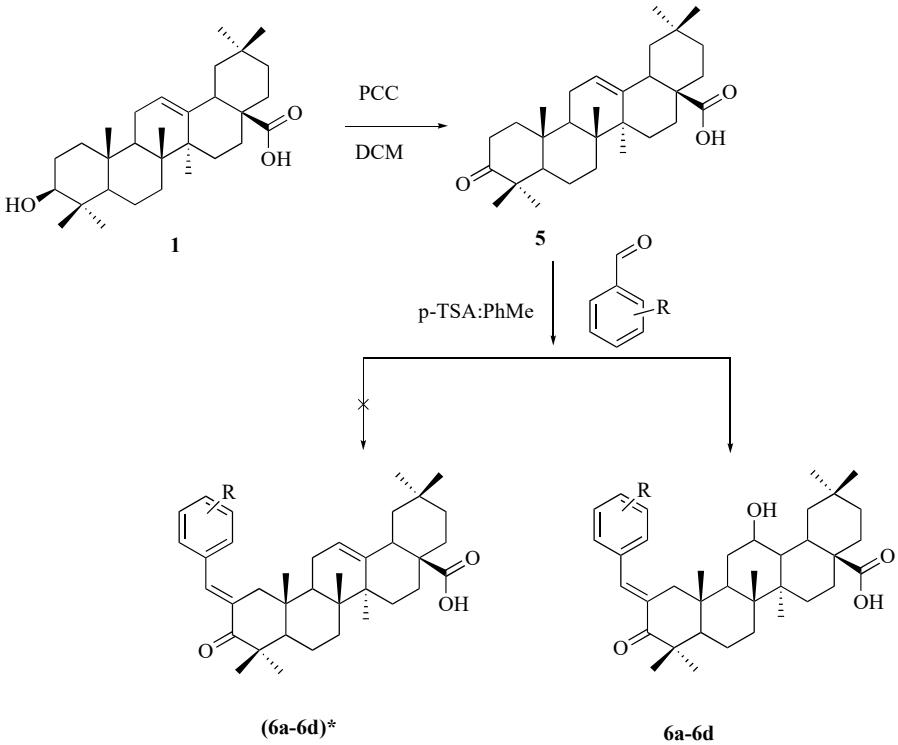

Compound	R	Yield(%)
6a	H	48.9
6b	CH3 (*para*)	41.8
6c	CH3 (*meta*)	9.3
6d	CH3 (*orto)*	10.3

The OA derivatives (**6a-6d**) were obtained with the objective to evaluate the effect of the new substituents in the anticancer or anti-inflammatory activities, aspects discussed in the forward section.

Chapter 6. (Paper V, VI) Triterpenes and their cytotoxicity towards breast cancer cell lines and anti-inflammatory activity

6.1. Background

Natural pentacyclic triterpenes have shown a wide spectrum of biological activity, among them highlights their cytotoxic and anti-inflammatory activity. Oleanolic acid has been reported to have potential effects in the chemoprevention of breast carcinoma. Additionally, it has been reported that oleanolic acid can suppress TPA-induced tumor promotion and exhibit direct antiproliferative effects in many cancer cells lines such as HCT15, A547, H460, HepG2, Hep3B, Huh7, and HA22T, *etc*[136]. On the other hand, oleanolic acid and similar triterpenes are also considered to have potent antiinflammatory activity, because it shows antiinflammatory activity in carrageenan-induced paw oedema [137,138].

6.1.1. The aim of this section

The principal aim of this section was to evaluate the cytotoxicity and antiinflammatory activity of pentacyclic triterpenes isolated from quinoa husk.

6.2. Results and discussions

6.2.1. Cytotoxic activity of triterpenes

The isolated sapogenins **(1-4)** from crude sapogenins extract were subjected to cytotoxic evaluation against normal-like human breast epithelial cell line (MCF-10A) and breast cancer cell line (JIMT-1) using an MTT dose response assay, where the cells were incubated with each compound for 72 h according of procedure

described in **paper V**. Results are show in **Table 13** and the values given represents the IC_{50} in μM obtained from dose response curves. Compound **3** was found to be the most active and it is more toxic in JIMT-1 cells than in MCF-10A cells. Methyl oleanate also shows toxicity in both cell lines, however, for this compound the MCF-10A cells were more sensitive than the JIMT-1 cells. Oleanolic acid itself and phytolaccagenic acid where less toxic than hederaginin and methyl oleanate. In general, all the compounds are notno compound is selectively cytotoxic. Although moderate cytotoxicity of hederaginin can be used as starting material for further synthetic modification to increase the bioactivity preferentially towards breast cancer cells. In addition, it is recommend evaluating these derivatives against other cancer cell lines. Moreover, the obtained OA derivatives (**6a-6d**) should be evaluated against cancer cell lines to know the effect of the new substituents in the structure.

Table 13. Sapogenins from quinoa, cytotoxic values

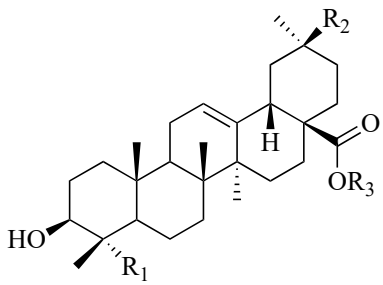

1-4

Compound	substituent			IC_{50} (μM)[a]		
	R_1	R_2	R_3	MCF-10A	JIMT-1	Ratio MCF-10A : JIMT-1
1	CH_3	CH_3	H	101.5 ± 16.1	90.9[b]	1,12
2	CH_3	CH_3	CH_3	51.8 ± 2.8	80.3 ± 10.7	0,65
3	CH_2OH	CH_3	H	39.6 ± 0.6	27.3 ± 7.1	1,45
4	CH_2OH	$COOCH_3$	H	73.0 ± 0.6	105.1 ± 3.8	0,69

a Each value represents the mean of two determinations ± gives the highest and lowest value.
[b]This result represents just one determination

6.2.2. Anti-inflammatory activity of triterpenes

Mouse ear edema induced by TPA

The model of edema induced by croton oil/12-O-tetradecanoylphorbol-13-acetate (TPA) has been used for evaluating the anti-inflammatory activity of steroidal and non-steroidal anti-inflammatory drugs. Where topical administration of TPA causes vasodilatation, promote vascular permeability, neutrophil influx, synthesis of

eicosanoids, and liberation of serotonin and histamine[139]. Previous reports have demonstrated that OA (compound **1**) shows inhibition of the synthesis of several cytokines, prostaglandin E_2 and nitric oxide[140]. In our investigation the compounds (**1-4**) and sapogenin extract from *C. quinoa* were submitted to the croton oil ear test, at the dose of 2 mg/ear for compounds and 56 mg/ear for sapogenin extract, to evaluate the topical anti-inflammatory effect. The result shows (Figure 32) that the sapogenins extract induce 68,2% edema inhibition at the highest administered dose (56 mg/ear) more active than the pure compounds which induced from 12.7% to 30.61% edema inhibition. The sapogenin extract was more active than the dexamethasone NSAID, which induce 47.9 % edema inhibition, whereas the compounds were less active than the dexamethasone NSAID. Thus, the sapogenin extract could be very interesting for new pharmaceutical formulations by topical application.

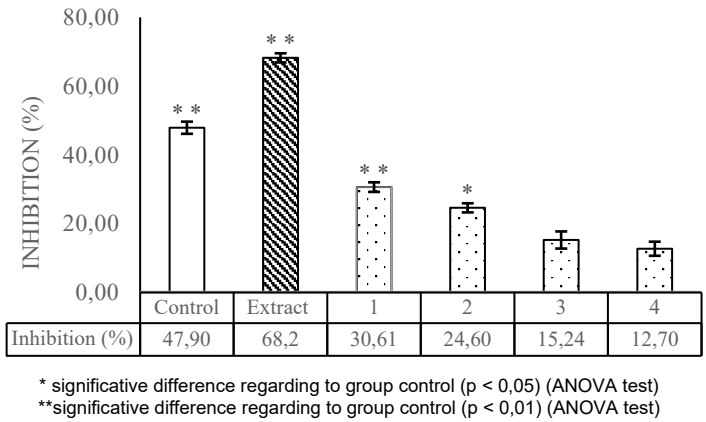

Figure 32. Effects of compounds **(1-4)** and sapogenin extract from *Ch. quinoa* on acute inflammation induced by croton oil/ TPA in mouse ear. All values were significantly different from the negative control (dexamethasone) considered as 100% inflammation

Mouse paw edema induced by Carrageenan

The development of edema induced by carrageenan corresponded to the events in the acute phase of inflammation mediated by histamine and serotonin released during first 1.5 h after carrageenan injection and after 5 h kinin and prostaglandins produced under an effect of cyclooxygenase[141]. The results of the inflammatory inhibition induced by intraperitoneal administration of the assayed compound (**1-4**) and sapogenin extract are shown in Table 14. All the compound and extract show progressive inhibition from 3 h to 7 h. The compounds **1** and **2** show more significant inhibition than sapogenin extract and compounds **1-4** had an anti-inflammatory effect at 636 mg/kg po and 100 mg/po respectively, observable to 3

(p< 0,05), 5 (p< 0,01). Thus, the compounds **1** and **4** reduce the edema with 84.3 and 84.6 %

Table 14. Effects of intraperitoneal administration of compounds **(1-4)** and sapogenins extract from *C. quinoa* on the carrageenan-induced paw edema

Product	Number of animals	Inhibition (%) of carrageenan edema (acute test)		
		3 h	5 h	7 h
1(100 mg)	6	54.4*	75.7**	84.3**
2(100 mg)	6	32.5*	47.6**	57.6**
3(100 mg)	6	29.5	59.8**	70.3**
4(100 mg)	6	62.5**	73.4**	84.6**
Extract(636 mg)	6	37.1*	37.8**	55.3**
Indomethacine (10mg)	6	45.5**	61.2**	71.9**

* significative difference regarding to group control (p < 0,05) (ANOVA test)
** significative difference regarding to group control (p < 0,01) (ANOVA test)

Conclusions

Several investigations have reported the high content of STLs in *Asteraceae* family. Our result confirmed the high concentrations of STLs in *A. arborescens* with values 13.4 mg/g for damsin, and 12.3 mg/g coronopilin. Additionally, we demonstrate that damsin and coronopilin show an inhibitory effect against pro-inflammatory IL-6 and MCP-1 expression in human skin cells (HDFa and HaCaT) *via* NF-□B inhibition. Thus, this study suggests that these compounds can be a potential therapeutic candidate for treatment skin inflammatory diseases.

Two groups of benzylidene derivatives were synthesized *via* Claisen Schmidt condensation from damsin **1** which then were tested their cytotoxicity against JIMT-1 cells. The most cytotoxic were **3a** and **3i**, both with ratios between the IC_{50} values for MCF-10A and JIMT-1 cells of approximately 5. On the other hand, the condensation products with acyclic aldehydes, such as **3r** and **3u**, were equally potent, and show selective cytotoxicity. In general, the cytotoxicity results in both groups of derivatives have shown a dependency on the overall structure, although less in this subset of compounds compared to a previous investigation.

The study of triterpenes in Bolivian highland plants demonstrated a high concentration of oleanolic acid (OA) in several of them, like: *Junellia seriphioide, Lampaya catellani, Baccharis tola, Satureja boliviana* and *Polylepis besseri.* All of them show higher contents of OA than those found in the olive fruit (0,17-0,56 mg/g) and similar than the olive leaf (31,0 mg/g) which is still used as main source of commercial oleanolic acid, a bioactive compound with anticancer and anti-inflammatory activities. In addition, the quinoa husk is a good font to obtain a sapogenins extract constituted by 4 triterpenes (1-4) were the OA (1) and hederagenin (3) were found as the triterpenes present in highest amount in quinoa husk. Those compounds and the sapogenins extract were evaluated against breast cancer cell lines and anti-inflammatory assays against edemas induced by croton and carrageenan founding as the highlighted result the high inhibition of the sapogenins extract which show a higher inhibition than the the dexamethasone NSAID, used as control, in the model of edema induced by croton oil. Then this extract, which could be obtained in good quantities from quinoa husk, have a potential use in the formulation of new anti-inflammatory phytotherapeutical product of topical application.

Acknowledgments

My greatfully to the next persons:

I would like to thank my supervisor professor Olov Sterner, for accepting me to work in his research group during my PhD studies. I would also like to thank you for sharing me your experience and knowledge about natural products, synthetic chemistry. My gratefully for always take the time to discuss all my experimental results

I would also like to thank my supervisor and coordinator of project from Bolivia Giovanna Almanza for introducing me to the research field and for giving me all the opportunities during all the time of my studies

I would also like to thank Rodrigo Villagomez I would say it has been a privileged to work with you. Thank you for sharing me all your skills and knowledge in the lab.

To the Co-authors and authors specially Wendy Soria, Stina Oredsson, Daniel, Svensson for conducing anti-inflammatory and cytotoxicity assays

To my assistant supervisor Sophie Manner and Ulf Ellervik for help me in the academic tasks

To my research group; Zilma thank you for being always my friends, my syster and my inspiration for doing this work, Ivan, Paola, Mariela, Narda and Juliao thank so much for creating good environment to work and for sharing me funny moments.

I would also like to thank Maria, Bodil and Katarina for excellent technical and administrative support, for all the help when something needs to be fixed.

I would also like to thank Karl-Erik Bergquist for theaching me about NMR spectroscopy and Sofia Essén for help me with high-resolution mass spectrometry and for theaching MS in analytical course

To all members of Bioorganic research group in La Paz Bolivia thank you for creating good enviroment and fanny moments. I would also like to thank Yonny Flores, Santiago, Yaquelin for help me with the collection all the samples from Bolivian Highlands.

To my friends in Bolivia Lizangela, Shirley, Fatima, Esther, Pamela, Roxana, Karen and Ebbe Luz thank you for all the moments we have shared.

My special thanks to my parents, Adela y Julian for their unconditional love. Thanks to my Husband for his support and constant encouragement to achieve my goals.

I would also like to thank to the financial support of the Swedish International Development Agency (SIDA) through a bilateral collaboration between Lund University (Sweden) and Mayor de San Andres University (Bolivia)

Appendix

Spectroscopic data

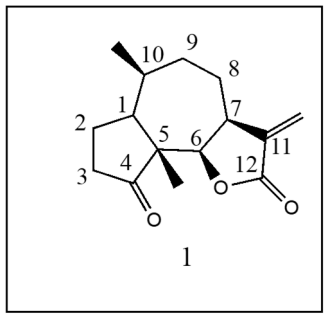

1

Compound 1: (Damsin) was isolated as white powder ^{1}H NMR (300 MHz, $CDCl_3$) δ 6.13 (1H, *s*, H-13b), 5.46 (1H, *s*, H-13b), 4.44 (1H, *d*, *J* 6.9 Hz, H-6), 3.24 (1H, *m*, H-7), 2.38 (2H, *m*, H-3),2,15(1H, *m*, H-10) 2,01 (1H, *m*, H-1) 1,95 (1H, *m*, H-8b) 1,81 (2H,*m*, H-9 a,b) 1,79 (1H, *m*, H-8a) 1,69 (2H, *m*, H-2) 1,01 (3H, *m*, H-14) 1,0 (3H, *m*, H-15) δ_C (75 MHz, $CDCl_3$) 218.9 (C-4), 170.1 (C-12), 139.5 (C-11), 120.6 (C-13), 81.6 (C-6), 54.7 (C-5), 45.8 (C-1), 44.2 (C-7), 36.0 (C-3), 34.1 (C-10), 33.2 (C-9), 25.5 (C-2), 23.8 (C-8), 15.7 (C-14), 13.6 (C-15).

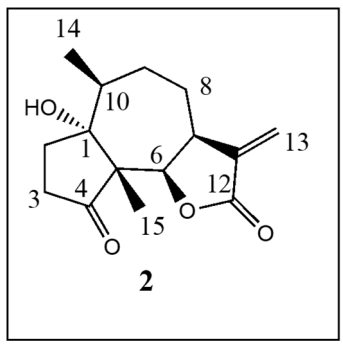

2

Compound 2: (Coronopilin) ^{1}H NMR (300 MHz, $CDCl_3$) δ 6.26 (1H,*s*, H-13b), 5.58 (1H,s, H-13a), 4.92 (1H,d, *J* = 8.2 Hz, H-6), 3.34 (1H,*m*, H-7), 2.65 (1H, *dd*, *J* = 23.2, 10.5 Hz, H-3b), 2.47 (2H, *m*, H-2), 2,40 (1H, *m*, H-9b), 2,19 (1H,*m*, H-10) 2,08(1H, *m*, H-8b) 1,71(1H, *m*, H-8a) 1,61 (1H,*m*, H-3a), 1,60 (1H, *m*, H-9a), 1.20 (3H, *d*, *J* = 7.5 Hz, H-14), 1.15 (3H, *s*, H-15). δ_C (75 MHz, $CDCl_3$) 216.4 (C-4), 169.4 (C-12), 140.0 (C-11), 120.7 (C-13), 84.2 (C-1), 78.4 (C-6), 57.9 (C-5), 43.9 (C-7), 42.1 (C-10), 32.3 (C-2), 31.0 (C-3), 29.4 (C-9), 26.8 (C-8), 16.5 (C-14), 13.9 (C-15).

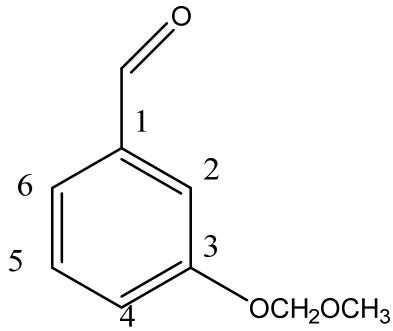

3-(Methoxymethyl)benzaldehyde: ^{1}H NMR (400 MHz, $CDCl_3$) δ 9.95 (1H, s, H-CO), δ 7.52 (1H, *J* 4.3 H-4), δ 7.50 (1H, *s*, H-2), δ 7.43 (1H, *t, J* 7.8 Hz, H-5), δ 7.28 (1H, *ddd, J* = 8.1, 2.5, 1.1 Hz, H-6), δ 5,21 (2H, *s*, -H2C-OAr), δ 3.47 (3H, *s*, H3C-OH2COAr) δ $_C$ (101 MHz, $CDCl_3$). 170.5 (CO-Ar), 157.2 (C-3), 130.5 (C-4), 123,3 (C-5), 121.8 (C-2), 117.5 (C-6), 114.7 (C-1), 94.4 (-H2C-OAr), 56,1 (H3C-OH2COAr)

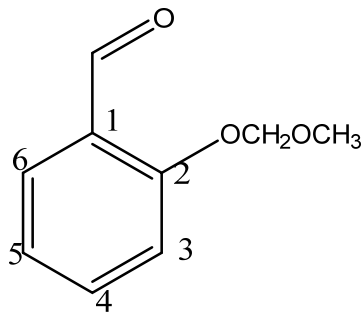

2-(Methoxymethyl)benzaldehyde: ^{1}H NMR (400 MHz, $CDCl_3$) δ 10.46 (1H, s, H-CO), 7.79 (1H, d, *J* 7.7 Hz, H-6), 7.47 (1H, m, H-4), 7.17 (1H, d, *J* 8.5 Hz, H-3), 7.02 (1H, m, H-5), 5.26 (2H, s, -H2C-OAr), 3.47 (3H, s, H3C-H2COAr).δ $_C$ (101 MHz, $CDCl_3$) 189.6 (CO-Ar), 159.6 (C-2), 135.8 (C-4), 128.2 (C-6), 125.4 (C-1), 121.7 (C-5), 115.0 (C-3), 94.5 (-H2C-OAr), 56.4 (H3C-H2COAr) .

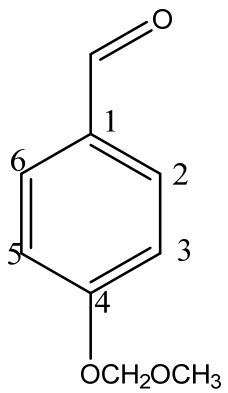

4-(Methoxymethyl)benzaldehyde: ^{1}H NMR (400 MHz, $CDCl_3$) δ 9.83 (1H, *s*, H-CO), δ 7.77 (2H, *d*, *J* 8.7 Hz, H-2/6), δ 7.09 (2H, *d*, *J* 8.7 Hz, H-3/5), δ 5.19 (2H, *s*, -H_2C-OAr), δ 3.43 (3H, *s*, H_3C-OH_2OAr). δ $_C$ (101 MHz, $CDCl_3$) 190.8 (CO-Ar) 162.1 (C-4), 131.8 (C-2/6), 130.6 (C-1), 116.2 (C-3/5), 94.0 (-H_2C-OAr), 56.2 (H_3C-OH_2COAr).

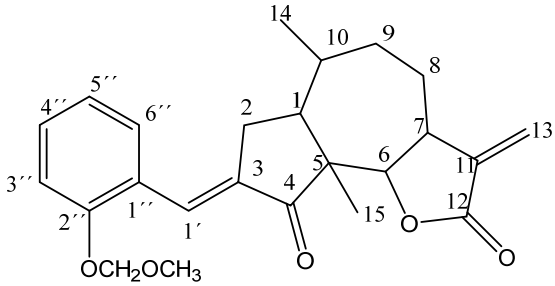

(*E*)-3-(*o*-Methoxymethoxyphenyl)methylene)damsin**:** ^{1}H NMR (400 MHz, $CDCl_3$) δ 7.88 (1H, *dd*, *J* 3.0; 2.0 Hz, H-1´), 7.52 (1H, *dd*, *J* 7.8; 1.5 Hz, H-6´´), 7.33 (1H, *ddd, J* 8.9, 7.5, 1.7 Hz, H-4´´), 7.17 (1H, *dd*, *J* 8.4, 1.0 Hz, H-3´´), 7.05 (1H, *t*, *J* 7.8 Hz, H-5´´), 6.29 (1H, d, *J* 3.0 Hz, H-13b), 5.57 (1H, d, *J* 2.6 Hz, H-13a), 5.23 (2H, *d*, *J* 2.3 Hz,-CH_2O-Ar), 4.65 (1H, *d*, *J* 8.5 Hz, H-6), 3.49 (3H, *s*, H_3COH_2CO-Ar), 3.28 (1H, m, H-7), 2.96 (1H, *ddd*, *J* 16.1, 10.0, 3.3 Hz, H-2b), 2.80 (1H, *ddd*, *J* 16.7, 7.1, 1.9 Hz, H-2a), 2.25 (1H, m, H-10), 2.09 (1H, m, H-8b), 2.06 (1H, m, H-1), 1.87 (1H, m, H-9b), 1.80 (1H, m, H-8a), 1.72 (1H, m, H-9a), 1.19 (1H, s, H-15), 1.17 (3H, d, 7.5 Hz, H-14)

δ_C (101 MHz, $CDCl_3$) 208.0 (C-4), 170.4 (C-12), 156.9 (C-2´´), 140.2 (C-11), 133.5 (C-3), 131.1 (C-4´´), 129.7 (C-6´´), 128.7 (C-1´), 125.3 (C-1´´), 121.6 (C-5´´), 121.3 (C-12), 114.8 (C-3´´), 94.8 (-H2CO-Ar), 82.0 (C-6), 56.5 (H3COH2CO-Ar), 54.9 (C-5), 45.0 (C-7), 43.8 (C-1), 34.3 (C-9), 34.2 (C-10), 31.5 (C-2) 26.6 (C-8), 15.9 (C-14), 14.6 (C-15).

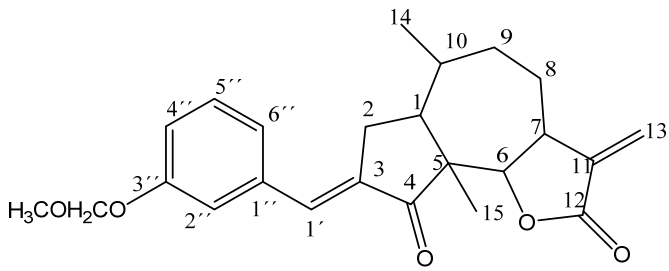

(*E*)-3-(*m*-Methoxymethoxyphenyl)methylene)damsin**:**^{1}H NMR (400 MHz, $CDCl_3$) δ 7.38 (1H, m, H-1´), 7.33 (1H, t, *J* 7.9 Hz, H-5´´), 7.21 (1H, s, H-2´´), 7.18 (1H, d, *J* 7.8 Hz, H-6´´), 7.06 (1H, dd, *J* 7.9, 2.0 Hz, H-4´´), 6.27 (1H, d, *J* 3.0 Hz, H-13b), 5.56 (d, *J* 2.6 Hz, H-13a), 5.19 (2H, s, -H2CO-Ar), 4.64 (1H, d, *J* 8.5 Hz, H-6), 3.48 (3H, s, *J* 3.6 Hz, H_3COH_2CO-Ar), 3.28 (1H, m, H-7), 2.95 (1H, *ddd*, *J* 16.1, 10.0, 3.3 Hz, H-2b) 2.86 (1H, ddd, *J* 16.9, 7.4, 1.9 Hz, H-2a), 2.27 (1H, *m,* H-10), 2.07 (1H, m, H-8b), 2.06 (1H, m, H-1), 1.90 (1H, m, H-9b), 1.81 (1H, m, H-8a), 1.73 (1H, m, H-9a), 1.17 (3H, d, H-14), 1.15 (3H, s, H-15)

δ_C (101 MHz, $CDCl_3$) 207.9 (C-4), 170.3 (C-12), 157.5 (C-3´´), 140.1 (C-11), 136.8 (C-1´´), 133.8 (C-3), 133.6 (C-1´), 129.8 (C-5´´), 124.3 (C-6´´), 121.3 (C-13), 118.3 (C-2´´), 117.4 (C-4´´), 94.6 (-H_2CO-Ar), 81.8 (C-6), 56.1 (H_3COH_2CO-Ar), 54.8 (C-5), 44.8 (C-7), 43.6 (C-1), 34.2 (C-9), 34.1 (C-10), 31.4 (C-2), 26.5 (C-8), 15.8 (C-14), 14.5 (C-15).

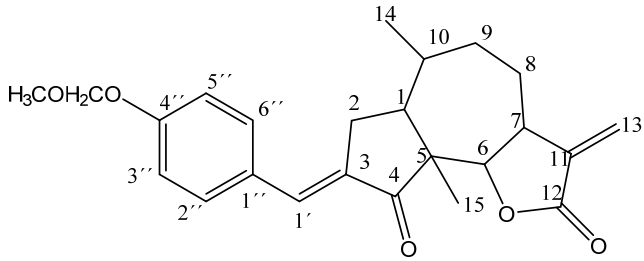

(*E*)-3-(*p*-Methoxymethoxyphenyl)methylene)damsin:[1]H NMR (400 MHz, $CDCl_3$) δ 7.51 (2H, d, *J* 8.8 Hz, H-2´´/6´´), 7.40 (1H, s, H-1´), 7.08 (2H, *d*, *J* 8.8 Hz, H-3´´/5´´), 6.29 (1H, d, *J* 2.9 Hz, H-13b), 5.57 (1H, d, *J* 2.6 Hz, H-13b), 5.21 (2H, s, -H_2CO-ArH), 4.65 (1H, d, *J* 8.5 Hz, H-6), 3.48 (3H, s, H3COH2CO-Ar), 3.28 (1H, m, H-7), 2.94 (1H, *ddd*, *J* 16.1, 10.0, 3.3 Hz, H-2b), 2.84 (1H, ddd, *J* 16.7, 7.4, 1.9 Hz, H-2a), 2.29 (1H, m, H-10), 2.09 (1H, m, H-8b), 2.08 (1H, m, H-1), 1.89 (1H, m, H-9b), 1.81 (1H, m, H-8a), 1.73 (1H, m, H-9a), 1.18 (3H, d, H-14), 1.16 (3H, s, H-15)

δ $_C$ (101 MHz, $CDCl_3$) 208.1 (C-4), 170.4 (C-12), 158.3 (C-4´´), 140.2 (C-11), 133.7 (C-1´), 132.4 (-2´´/6´´), 131.4 (C-1´´), 129.2 (C-3) 121.3 (C-2), 116.4 (C-3´´/5´´), 94.3 (-H2CO-Ar), 81.9 (C-6), 56.3 (H3COH2CO-Ar), 54.8 (C-5), 44.9 (C-7), 43.7 (C-1), 34.4 (C-9), 34.2 (C-10), 31.4 (C-2), 26.6 (C-8), 15.9 (C-14), 14.7 (C-15).

ML-A158a

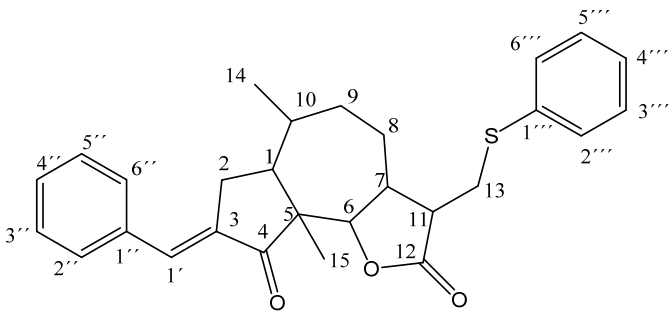

[1]H NMR (400 MHz, $CDCl_3$) δ 7.56 (2H, d, *J* 6.9 Hz, H-2´´/6´´), 7.47 (1H, m, H-4´´), 7.45 (1H, d, *J* 2.0 Hz, H-1´), 7.43 (2H, m, H-3´´/5´´), 7.39 (2H, d, *J* 1.1 Hz, H-2´´´/6´´´), 7.31 (2H, m, H-3´´´/5´´´), 7.23 (1H, ddd, *J* 7.2, 3.8, 1.3 Hz, H-4´´´), 4.66 (1H, d, *J* 8.2 Hz, H-6), 3.49 (1H, dd, *J* 13.5, 3.9 Hz, H-13b), 3.04 (1H, dd, *J* 13.5, 9.6 Hz, H-13a), 2.96 (1H, m, H-2b), 2.87 (1H, ddd, *J* 16.8, 7.4, 1.9 Hz, H-2a), 2.75 (1H, m, H-7), 2.59 (1H, ddd, *J* 9.9, 6.2, 3.9 Hz, H-11), 2.26 (1H, dd, *J* 7.9, 4.2 Hz, H-10), 2.06 (1H, m, H-1), 1.95 (1H, m, H-8b), 1.81 (1H, m, H-9a), 1.67 (1H, m, H-8a), 1.63 (1H, m, H-9a), 1.20 (3H, s, H-15), 1.17 (3H, d, *J* 7.5 Hz, H-14).

δ $_C$ (101 MHz, $CDCl_3$) 208.5 (C-4), 177.0 (C-12), 135.5 (C-1´´), 134.8 (C-1´´´), 134.2 (C-1´), 130.7 (C-2´´/6´´), 130.3 (C-2´´´/6´´´), 129.7 (C-3´´/5´´), 129.4 (C-3´´´/5´´´) 127.0 (C-4´´´), 82.4 (C-6), 47.7 (C-11), 46.1 (C-7), 43.6 (C-1), 35.3 (C-13), 34.7 (C-9), 34.1 (C-10), 31.4 (C-2), 26.1 (C-8), 16.1 (C-14), 15.1 8 (C-15).

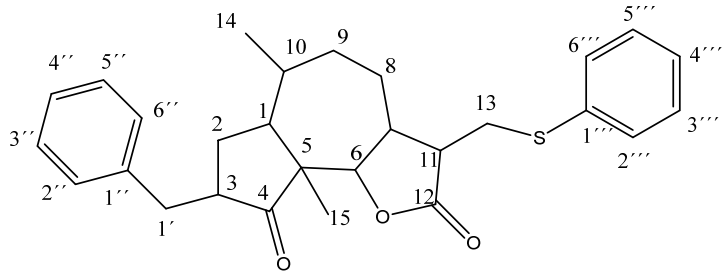

^{1}H NMR (400 MHz, $CDCl_3$) δ 7.37 (2H, dt, *J* 3.3, 1.9 Hz, H-2´´´/6´´´), 7.31 (2H, dd, *J* 7.0, 1.7 Hz, H-3´´´/5´´´), 7.28 (2H, dd, *J* 3.9, 1.5 Hz, H-3´´/5´´), 7.23 (1H, dd, *J* 4.9, 3.6 Hz, H-4´´´), 7.20 (1H, t, *J* 2.2 Hz, H-4´´), 7.16 (2H, dd, *J* 8.2, 6.7 Hz, H-2´´/6´´), 4.42 (1H, d, *J* 8.5 Hz, H-6), 3.46 (1H, dd, *J* 13.6, 3.9 Hz, H-13b), 3.16 (1H, dd, *J* 13.8, 4.0 Hz, H-1´b), 3.03 (1H, dd, *J* 13.6, 8.6 Hz, H-13a), 2.76 (1H, ddd, *J* 18.2, 8.8, 3.5 Hz, H-7), 2.65 (1H, d, *J* 8.9 Hz, H-1´a), 2.60 (1H, m, H-11), 2.51 (1H, ddd, *J* 16.9, 8.4, 4.2 Hz, H-3), 2.11 (1H, m, H-10), 1.95 (1H, m, H-1/8b), 1.85 (1H, m, H-2b), 1.69 (1H, m, H-2a), 1.69 (1H, m, H-9b), 1.66 (1H, m, H-8a), 1.63 (1H, m, H-9a), 0.96 (3H, d, *J* 7.5 Hz, H-14), 0.91 (3H, s, H-15).

δ_C (101 MHz, $CDCl_3$) 218.8 (C-4), 176.9 (C-12), 139.5 (C-1´´), 135.0 (C-1´´´), 130.1 (C-6´´´/2´´´), 129.3 (C-3´´´/5´´´), 129.2 (C-2´´/6´´), 128.5 (C-5´´/3´´), 127.0 (C-4´´´), 126.4 (C-4´´), 82.4 (C-6), 55.0 (C-5), 50.2 (C-3), 46.2 (C-11), 45.8 (C-7), 43.9 (C-1), 36.3 (C-1´), 35.1 (C-13), 34.1 (C-10), 33.3 (C-9), 30.5 (C-2), 25.3 (C-8), 16.4 (C-14), 14.3 (C-15).

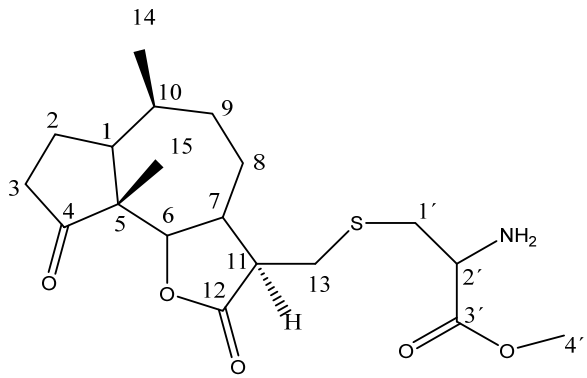

^{1}H NMR (500 MHz, CD_2Cl_2) δ 4.45 (1H, d, *J* 5.5 Hz, H-6), 3.70 (1H, s, H-4´), 3.65 (1H, dd, *J* 7.1, 4.9 Hz, H-2´), 3.00 (1H, dd, *J* 13.0, 4.5 Hz, H-13b), 2.93 (2H, m, H-11/1´), 2.78 (1H, ddd, *J* 13.5, 7.2, 0.7 Hz, H-1´), 2.59 (2H, m, H-7/13a), 2.43 (1H, dd, *J* 19.2, 8.6 Hz, H-3), 2.21 (1H, m, H-10), 2.16 (1H, m, H-3a), 2.08 (1H, m, H-1), 2.03 (1H, m, H-2),1.85 (1H, m, H-9b), 1.81 (1H, m, H-2a), 1.60 (1H, tdd, *J* 13.3, 8.7, 4.8 Hz, H-9a), 1.52 (2H, dd, *J* 9.5, 5.8 Hz, H-8a/8b), 1.11 (3H, s, H-15), 1.06 (3H, d, *J* 7.6 Hz, H-14).

δ_C (126 MHz, CD_2Cl_2) 221.7 (C-4), 176.4 (C-3´), 174.8 (C-12), 82.3 (C-6), 55.0 (C-5), 54.8 (C-2´), 52.5 (C-4´), 46.2 (C-1), 45.9(C-7), 45.8 (C-11), 38.3 (C-1´), 37.4 (C-9), 35.4 (C-10), 35.3 (C-3), 28.6 (C-13), 24.6 (C-2), 18.4 (C-8), 16.9 (C-14), 16.1 (C-15).

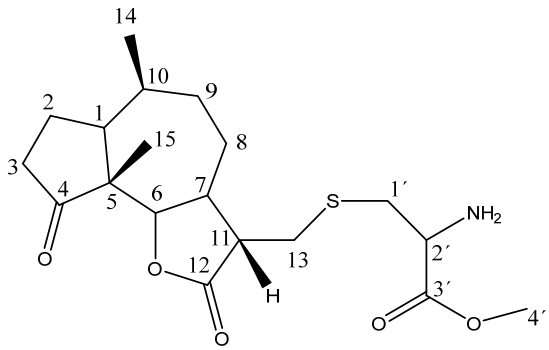

^{1}H NMR (500 MHz, CD_2Cl_2) δ 4.41 (1H, dd, *J*, 8.8, 2.8 Hz, H-6),3.74 (1H, m, H-2´), 3.73 (3H, s, H-4´), 2.98 (1H, td, *J* 13.3, 4.8 Hz, H-1´b),2.96 (1H, m, H-13b), 2.87 (1H, ddd, *J* 13.6, 6.6, 3.8 Hz, H-13a), 2.86 (1H, m, H-1b), 2.79 (1H, m, H-7) 2.78 (1H, ddd, *J* 18.7, 9.3, 4.5 Hz, H-7), 2.64 (1H, ddd, *J* 9.3, 6.3, 4.6 Hz, H-11), 2.40 (1H, m, H-3b), 2.22 (1H, m, H-3a), 2.18 (1H, m, H-10),2.05 (1H, m, H-1) 1.98 (1H, m, H-2b), 1.87 (1H, m, H-8b) 1.83 (1H, m, H-2a), 1.78 (1H, m, H-8a) 1.74 (1H, m, H-9b), 1.66 (1H, m, H-9a), 1.08 (3H, m, H-15), 1.07 (3H, m, H-14).

δ_C (126 MHz, CD_2Cl_2) 219.3 (C-4), 177.6 (C-12), 174.2 (C-3´), 83.1 (C-6), 55.1 (C-5), 54.8 (C-2´), 52.7 (C-4´), 47.2 (C-11), 46.8 (C-1), 45.2 (C-7), 38.2 (C-1´), 36.9 (C-3), 34.8 (C-10), 33.5 8C-9), 33.3 (C-13), 25.3 (C-8), 24.3 (C-2), 16.2 (C-14), 14.3 (C-15)

References

(1) Liu, T.; Zhang, L.; Joo, D.; Sun, S.-C. J.
(2) Ncube, B.; Van Staden, J. J. M. **2015**, *20*, 12698.
(3) Singh, B.; Sharma, R. A. J. B. **2015**, *5*, 129.
(4) Huang, A. C.; Osbourn, A. J. P. m. s. **2019**.
(5) Croteau, R.; Kutchan, T. M.; Lewis, N. G. J. B.; plants, m. b. o. **2000**, *24*, 1250.
(6) Brahmkshatriya, P. P.; Brahmkshatriya, P. S. J. N. p. p., botany; metabolism of alkaloids, p.; terpenes **2013**, 2665.
(7) Richardson, P. J. A. i. L. S. H. R.; Reynolds T, e. U. R. B. G. U. **1992**.
(8) Zwenger, S.; Basu, C. J. B.; Reviews, M. B. **2008**, *3*, 1.
(9) Perveen, S.; Al-Taweel, A. In *Terpenes and Terpenoids*; IntechOpen: 2018.
(10) Chadwick, M.; Trewin, H.; Gawthrop, F.; Wagstaff, C. J. I. j. o. m. s. **2013**, *14*, 12780.
(11) Chaturvedi, D. J. I.-.-.-.-., Research Signpost, Trivandrum **2011**, 313.
(12) Ivanescu, B.; Miron, A.; Corciova, A. J. J. o. a. m. i. c. **2015**, *2015*.
(13) Zhang, S.; Won, Y.-K.; Ong, C.-N.; Shen, H.-M. J. C. M. C.-A.-C. A. **2005**, *5*, 239.
(14) Da Costa, F. B.; Terfloth, L.; Gasteiger, J. J. P. **2005**, *66*, 345.
(15) Neerman, M. F. J. I. J. o. A. **2003**, *13*, 114.
(16) Sülsen, V. P.; Martino, V. S. *Sesquiterpene Lactones: Advances in their Chemistry and Biological Aspects*; Springer, 2018.
(17) Amorim, M. H. R.; Gil da Costa, R. M.; Lopes, C.; Bastos, M. M. J. C. r. i. t. **2013**, *43*, 559.
(18) Guerra, F. M.; Moreno-Dorado, F. J.; Jorge, Z. D.; Massanet, G. M. J. N. p. c. **2011**, *6*, 1934578X1100600409.
(19) Fischer, N. H. In *Biochemistry of the mevalonic acid pathway to terpenoids*; Springer: 1990, p 161.
(20) Barbero, M.; Prandi, C. J. N. P. C. **2018**, *13*, 1934578X1801300303.
(21) Padilla-Gonzalez, G. F.; dos Santos, F. A.; Da Costa, F. B. J. C. R. i. P. S. **2016**, *35*, 18.
(22) Arakawa, N. S.; Schorr, K.; Ambrosio, S. R.; Merfort, I.; Da Costa, F. B. J. Z. f. N. C. **2008**, *63*, 533.
(23) Kupchan, S. M.; Eakin, M.; Thomas, A. J. J. o. M. C. **1971**, *14*, 1147.
(24) Beekman, A. C.; Woerdenbag, H. J.; van Uden, W.; Pras, N.; Konings, A. W.; Wikström, H. V.; Schmidt, T. J. J. J. o. N. P. **1997**, *60*, 252.
(25) Rodriguez, E.; Towers, G.; Mitchell, J. J. P. **1976**, *15*, 1573.
(26) Sun, C.-M.; Syu, W.-J.; Don, M.-J.; Lu, J.-J.; Lee, G.-H. J. J. o. n. p. **2003**, *66*, 1175.

(27) Ferlay, J.; Colombet, M.; Soerjomataram, I.; Mathers, C.; Parkin, D.; Piñeros, M.; Znaor, A.; Bray, F. J. I. j. o. c. **2019**, *144*, 1941.
(28) Bray, F.; Ferlay, J.; Soerjomataram, I.; Siegel, R. L.; Torre, L. A.; Jemal, A. J. C. a. c. j. f. c. **2018**, *68*, 394.
(29) Schirrmacher, V. J. I. j. o. o. **2019**, *54*, 407.
(30) Johnstone, R. W.; Ruefli, A. A.; Lowe, S. W. J. C. **2002**, *108*, 153.
(31) Aung, T. N.; Qu, Z.; Kortschak, R. D.; Adelson, D. L. J. I. j. o. m. s. **2017**, *18*, 656.
(32) Kreuger, M. R. O.; Grootjans, S.; Biavatti, M. W.; Vandenabeele, P.; D'Herde, K. J. A.-c. d. **2012**, *23*, 883.
(33) Chaturvedi, D.; Goswami, A.; Saikia, P. P.; Barua, N. C.; Rao, P. G. J. C. S. R. **2010**, *39*, 435.
(34) Liu, Z.; Liu, S.; Xie, Z.; Pavlovicz, R. E.; Wu, J.; Chen, P.; Aimiuwu, J.; Pang, J.; Bhasin, D.; Neviani, P. J. J. o. P.; Therapeutics, E. **2009**, *329*, 505.
(35) Zhang, S.; Ong, C.-N.; Shen, H.-M. J. C. l. **2004**, *208*, 143.
(36) Wu, L.; Huang, X.; Kuang, Y.; Xing, Z.; Deng, X.; Luo, Z. J. D. d., development; therapy **2019**, *13*, 2787.
(37) Gach, K.; Długosz, A.; Janecka, A. J. N.-S. s. a. o. p. **2015**, *388*, 477.
(38) Lee, K.-H.; Huang, E.-S.; Piantadosi, C.; Pagano, J. S.; Geissman, T. J. C. R. **1971**, *31*, 1649.
(39) Donepudi, M. S.; Kondapalli, K.; Amos, S. J.; Venkanteshan, P. J. J. o. c. r.; therapeutics **2014**, *10*, 506.
(40) **2019**
(41) Makki, J. J. C. M. I. P. **2015**, *8*, CPath. S31563.
(42) Campbell, J. J.; Watson, C. J. J. O. **2009**, *5*, 43.
(43) Sharma, G. N.; Dave, R.; Sanadya, J.; Sharma, P.; Sharma, K. J. J. o. a. p. t.; research **2010**, *1*, 109.
(44) Brown, M.; Koch, T.; Webb, C. J. J. o. C. N. **2000**, *9*, 713.
(45) Cowell, C. F.; Weigelt, B.; Sakr, R. A.; Ng, C. K.; Hicks, J.; King, T. A.; Reis-Filho, J. S. J. M. o. **2013**, *7*, 859.
(46) Malhotra, G. K.; Zhao, X.; Band, H.; Band, V. J. C. b.; therapy **2010**, *10*, 955.
(47) Alanazi, I. O.; Khan, Z. In *Breast Cancer and Surgery*; IntechOpen: 2018.
(48) Oestreicher, N.; Ramsey, S. D.; Linden, H. M.; McCune, J. S.; van't Veer, L. J.; Burke, W.; Veenstra, D. L. J. G. i. M. **2005**, *7*, 380.
(49) Vuong, D.; Simpson, P. T.; Green, B.; Cummings, M. C.; Lakhani, S. R. J. V. A. **2014**, *465*, 1.
(50) Zhao, S.; Liu, X.-Y.; Jin, X.; Ma, D.; Xiao, Y.; Shao, Z.-M.; Jiang, Y.-Z. J. T. **2019**, *9*, 4935.
(51) Al-thoubaity, F. K. J. A. o. M.; Surgery **2020**, *49*, 44.
(52) Ghoncheh, M.; Pournamdar, Z.; Salehiniya, H. J. A. P. J. C. P. **2016**, *17*, 43.
(53) McPherson, K.; Steel, C.; Dixon, J. J. B. **2000**, *321*, 624.
(54) Allegra, C. J.; Aberle, D. R.; Ganschow, P.; Hahn, S.; Lee, C. N.; Millon-Underwood, S.; Pike, M. C.; Reed, S. D.; Saftlas, A. F.; Scarvalone, S. A. J. N. c.; statements, s.-o.-t.-s. **2009**, *26*, 1.

(55) Khushalani, J. S.; Qin, J.; Ekwueme, D. U.; White, A. J. P. M. R. **2020**, *17*, 101029.
(56) Williams, L. A.; Casbas-Hernandez, P.; Nichols, H. B.; Tse, C. K.; Allott, E. H.; Carey, L. A.; Olshan, A. F.; Troester, M. A. J. P. o. **2019**, *14*.
(57) Waks, A. G.; Winer, E. P. J. J. **2019**, *321*, 288.
(58) LEGHA, S. S.; DAVIS, H. L.; MUGGIA, F. M. J. A. o. i. m. **1978**, *88*, 69.
(59) Twelves, C.; Jove, M.; Gombos, A.; Awada, A. J. C. r. i. o. h. **2016**, *100*, 74.
(60) Rampurwala, M. M.; Rocque, G. B.; Burkard, M. E. J. B. c. b.; research, c. **2014**, *8*, BCBCR. S9454.
(61) Dandawate, P. R.; Subramaniam, D.; Jensen, R. A.; Anant, S. In *Seminars in cancer biology*; Elsevier: 2016; Vol. 40, p 192.
(62) Menendez, J. A.; Vazquez-Martin, A.; Colomer, R.; Brunet, J.; Carrasco-Pancorbo, A.; Garcia-Villalba, R.; Fernandez-Gutierrez, A.; Segura-Carretero, A. J. B. c. **2007**, *7*, 80.
(63) Thimmappa, R.; Geisler, K.; Louveau, T.; O'Maille, P.; Osbourn, A. J. A. r. o. p. b. **2014**, *65*, 225.
(64) Levin, D. A. J. A. r. o. E.; Systematics **1976**, *7*, 121.
(65) Ghosh, S. J. P. o. t. I. N. S. A. **2016**, *82*, 1189.
(66) Patocka, J. J. J. A. B. **2003**, *1*, 7.
(67) Jäger, S.; Trojan, H.; Kopp, T.; Laszczyk, M.; Scheffler, A. J. M. **2009**, *14*, 2016.
(68) Xu, F.; Huang, X.; Wu, H.; Wang, X. J. B.; Pharmacotherapy **2018**, *103*, 198.
(69) Jesus, J. A.; Lago, J. H. G.; Laurenti, M. D.; Yamamoto, E. S.; Passero, L. F. D. J. E.-B. C.; Medicine, A. **2015**, *2015*.
(70) Wei, L.; Zhang, W.; Yin, L.; Yan, F.; Xu, Y.; Chen, F. J. E. J. o. B. **2015**, *18*, 88.
(71) Laszczyk, M. N. J. P. m. **2009**, *75*, 1549.
(72) MR Patlolla, J.; V Rao, C. J. C. p. b. **2012**, *13*, 147.
(73) Liu, J. J. J. o. e. **2005**, *100*, 92.
(74) Gershenzon, J. J. J. o. c. e. **1994**, *20*, 1281.
(75) Cheng, A. X.; Lou, Y. G.; Mao, Y. B.; Lu, S.; Wang, L. J.; Chen, X. Y. J. J. o. I. P. B. **2007**, *49*, 179.
(76) Banik, R.; Pandey, D. J. I. c.; products **2008**, *27*, 241.
(77) Jetter, R.; Schäffer, S.; Riederer, M. J. P., Cell; Environment **2000**, *23*, 619.
(78) Stiti, N.; Hartmann, M.-A. J. J. o. l. **2012**, *2012*.
(79) Macía, M. J.; García, E.; Vidaurre, P. J. J. J. o. e. **2005**, *97*, 337.
(80) Jacobsen, S. E. J. J. o. A.; Science, C. **2011**, *197*, 390.
(81) García, M.; Raes, D.; Jacobsen, S.-E.; Michel, T. J. J. o. A. E. **2007**, *71*, 109.
(82) Browman, D. J. E. A. **1984**, 179.
(83) Rodrigo, G. C.; Almanza, G. R.; Akesson, B.; Duan, R.-D. J. J. o. M. P. R. **2010**, *4*, 2204.
(84) Navarro, G.; Molina, J. A.; De la Barra, N. J. P. E. **2005**, *176*, 113.
(85) Caldwell, C. G.; Franzblau, S. G.; Suarez, E.; Timmermann, B. N. J. J. o. n. p. **2000**, *63*, 1611.
(86) De Lampasona, M. E.; Catalán, C. A.; Gedris, T. E.; Herz, W. J. P. **1998**, *49*, 2061.

(87) Alvarez, M. E.; Rotelli, A. E.; Pelzer, L. E.; Saad, J. R.; Giordano, O. J. I. F. **2000**, *55*, 502.
(88) De Leo, M.; Saltos, M. B. V.; Puente, B. F. N.; De Tommasi, N.; Braca, A. J. P. **2010**, *71*, 804.
(89) Morejón, B.; Pilaquinga, F.; Domenech, F.; Ganchala, D.; Debut, A.; Neira, M. J. J. o. N. **2018**, *2018*.
(90) Zapata, B.; Betancur-Galvis, L.; Duran, C.; Stashenko, E. J. J. o. E. O. R. **2014**, *26*, 50.
(91) Abad, M. a. J.; Bermejo, P.; Gonzales, E.; Iglesias, I.; Irurzun, A.; Carrasco, L. J. G. P. T. V. S. **1999**, *32*, 499.
(92) Herz, W.; Anderson, G.; Gibaja, S.; Raulais, D. J. P. **1969**, *8*, 877.
(93) Paniagua-Zambrana, N. Y.; Bussmann, R. W.; Echeverría, J.; Romero, C. J. E. o. t. A. **2020**, 1.
(94) Hall, I.; Lee, K.; Starnes, C.; Sumida, Y.; Wu, R.; Waddell, T.; Cochran, J.; Gerhart, K. J. J. o. P. S. **1979**, *68*, 537.
(95) Bosco, A.; Golsteyn, R. M. J. M. **2017**, *22*, 459.
(96) Hall, I.; Starnes Jr, C.; Lee, K.; Waddell, T. J. J. o. p. s. **1980**, *69*, 537.
(97) Fonseca, L. C.; Dadarkar, S. S.; Lobo, A. S.; Mishra, P. B.; Thakkar, A. D.; Chandrababu, S.; Padigaru, M. J. E. j. o. p. **2011**, *657*, 41.
(98) Tornhamre, S.; Schmidt, T. J.; Näsman-Glaser, B.; Ericsson, I.; Lindgren, J. Å. J. B. p. **2001**, *62*, 903.
(99) Castro, V.; Rüngeler, P.; Murillo, R.; Hernandez, E.; Mora, G.; Pahl, H.; Merfort, I. J. P. **2000**, *53*, 257.
(100) Lyss, G.; Schmidt, T. J.; Merfort, I.; Pahl, H. L. J. B. c. **1997**, *378*, 951.
(101) Bottero, V.; Withoff, S.; Verma, I. J. C. d.; differentiation **2006**, *13*, 785.
(102) McFarland, B. C.; Hong, S. W.; Rajbhandari, R.; Twitty Jr, G. B.; Gray, G. K.; Yu, H.; Benveniste, E. N.; Nozell, S. E. J. P. o. **2013**, *8*, e78728.
(103) Karin, M. J. O. **1999**, *18*, 6867.
(104) Wang, W.; Mani, A. M.; Wu, Z.-H. J. J. o. c. m.; treatment **2017**, *3*, 45.
(105) Hostager, B. S.; Bishop, G. A. J. F. i. i. **2013**, *4*.
(106) Sun, S.-C. J. N. r. i. **2017**, *17*, 545.
(107) Lawrence, T. J. C. S. H. p. i. b. **2009**, *1*, a001651.
(108) Mulholland, B. S.; Forwood, M. R.; Morrison, N. A. J. C. o. r. **2019**, *17*, 538.
(109) Grieco, P. A.; Majetich, G. F.; Ohfune, Y. J. J. o. t. A. C. S. **1982**, *104*, 4226.
(110) Villagomez, R.; Rodrigo, G. C.; Collado, I. G.; Calzado, M. A.; Muñoz, E.; Åkesson, B.; Sterner, O.; Almanza, G. R.; Duan, R.-D. J. A. r. **2013**, *33*, 3799.
(111) Sotillo, W. S.; Villagomez, R.; Smiljanic, S.; Huang, X.; Malakpour, A.; Kempengren, S.; Rodrigo, G.; Almanza, G.; Sterner, O.; Oredsson, S. J. P. o. **2017**, *12*.
(112) Villagomez, R.; Hatti-Kaul, R.; Sterner, O.; Almanza, G.; Linares-Pastén, J. A. J. P. o. **2015**, *10*, e0115819.
(113) Villagomez, R.; Collado, J. A.; Muñoz, E.; Almanza, G.; Sterner, O. J. J. o. B. S.; Engineering **2014**, *2014*.

(114) Iturri, J. P.; Rodrigo, G. D. J. R. B. d. Q. **2018**, *35*.
(115) Abdel-Dayem, S. I.; Khalil, M. N.; Abdelrahman, E. H.; El-Gohary, H. M.; Kamel, A. S. J. J. o. E. **2021**, *266*, 113407.
(116) Cotugno, R.; Fortunato, R.; Santoro, A.; Gallotta, D.; Braca, A.; De Tommasi, N.; Belisario, M. J. C. p. **2012**, *45*, 53.
(117) Khazir, J.; Hyder, I.; Gayatri, J. L.; Yandrati, L. P.; Nalla, N.; Chasoo, G.; Mahajan, A.; Saxena, A.; Alam, M.; Qazi, G. J. E. j. o. m. c. **2014**, *82*, 255.
(118) Hejchman, E.; Haugwitz, R. D.; Cushman, M. J. J. o. m. c. **1995**, *38*, 3407.
(119) Saeed, M.; Jacob, S.; Sandjo, L. P.; Sugimoto, Y.; Khalid, H. E.; Opatz, T.; Thines, E.; Efferth, T. J. F. i. p. **2015**, *6*, 267.
(120) Rayar, A.; Veitía, M. S.-I.; Ferroud, C. J. S. **2015**, *4*, 1.
(121) Hazarkhani, H.; Kumar, P.; Kondiram, K. S.; Shafi Gadwal, I. M. J. S. C. **2010**, *40*, 2887.
(122) Zhuang, C.; Zhang, W.; Sheng, C.; Zhang, W.; Xing, C.; Miao, Z. J. C. r. **2017**, *117*, 7762.
(123) Karimi-Jaberi, Z.; Pooladian, B. J. G. C. L.; Reviews **2012**, *5*, 187.
(124) Adnan, D.; Singh, B.; Mehta, S. K.; Kumar, V.; Kataria, R. J. C. R. i. G.; Chemistry, S. **2020**, *3*, 100041.
(125) Bhagat, S.; Sharma, R.; Chakraborti, A. K. J. J. o. M. C. A. C. **2006**, *260*, 235.
(126) García-Piñeres, A. J.; Castro, V. c.; Mora, G.; Schmidt, T. J.; Strunck, E.; Pahl, H. L.; Merfort, I. J. J. o. B. C. **2001**, *276*, 39713.
(127) Szakiel, A.; Pączkowski, C.; Pensec, F.; Bertsch, C. J. P. R. **2012**, *11*, 263.
(128) Szakiel, A.; Pączkowski, C.; Koivuniemi, H.; Huttunen, S. J. J. o. a.; chemistry, f. **2012**, *60*, 4994.
(129) Flores, Y.; Sterner, O.; Almanza, G. R. J. R. B. d. Q. **2004**, *21*, 31.
(130) Oyedeji, O. O.; Shode, F. O.; Oyedeji, A. O.; Songca, S. P.; Gwebu, E. T.; Hill, G. M.; Setzer, W. N. J. A. r. **2014**, *34*, 4135.
(131) Kumar, A.; Qayum, A.; Sharma, P. R.; Singh, S. K.; Shah, B. A. J. B.; letters, m. c. **2016**, *26*, 76.
(132) Dar, B. A.; Lone, A. M.; Shah, W. A.; Qurishi, M. A. J. E. j. o. m. c. **2016**, *111*, 26.
(133) Kuljanabhagavad, T.; Thongphasuk, P.; Chamulitrat, W.; Wink, M. J. P. **2008**, *69*, 1919.
(134) Prado, F.; Gallardo, M.; González, J. J. B.-M.-. **1996**, *20*, 259.
(135) Koziol, M. J. J. J. o. t. S. o. F.; Agriculture **1991**, *54*, 211.
(136) Zhu, Y. Y.; Huang, H. Y.; Wu, Y. L. J. M. m. r. **2015**, *12*, 5012.
(137) Chudzik, M.; Korzonek-Szlacheta, I.; Król, W. J. M. **2015**, *20*, 1610.
(138) Bishayee, A.; Ahmed, S.; Brankov, N.; Perloff, M. J. F. i. b. a. j.; library, v. **2011**, *16*, 980.
(139) Rao, T. S.; Currie, J. L.; Shaffer, A. F.; Isakson, P. C. J. I. **1993**, *17*, 723.
(140) Ha, C.-L.; Weng, C.-Y.; Wang, L.; Lian, T.-W.; Wu, M.-J. J. J. o. e. **2006**, *107*, 116.
(141) Di Rosa, M.; Giroud, J.; Willoughby, D. J. T. J. o. p. **1971**, *104*, 15.

Paper I

Phytomedicine 50 (2018) 118–126

Contents lists available at ScienceDirect

Phytomedicine

journal homepage: www.elsevier.com/locate/phymed

Sesquiterpene lactones from *Ambrosia arborescens* Mill. inhibit pro-inflammatory cytokine expression and modulate NF-κB signaling in human skin cells

Daniel Svensson[a], Maribel Lozano[b,c], Giovanna R. Almanza[c], Bengt-Olof Nilsson[a], Olov Sterner[b], Rodrigo Villagomez[b,*]

[a] Department of Experimental Medical Science, Lund University, Sölvegatan 19, Lund SE-221 84, Sweden
[b] Centre for Analysis and Synthesis, Lund University, Naturvetarvägen 14 (former Getingev 60)/Sölvegatan 39 A-C, Lund SE-221 00, Sweden
[c] Instituto de Investigaciones Químicas, Universidad Mayor de San Andrés, Calle 27, Cota-Cota, La Paz CP 303, Bolivia

ARTICLE INFO

Keywords:
NSAID
Pseudoguaianolides
NF-κB
Inflammation
Dermal fibroblasts
Andean medicine

ABSTRACT

Background: *Ambrosia arborescens* has been used in Andean traditional medicine to reduce problems associated with various inflammatory diseases and conditions, although the underlying mechanism is unknown.
Hypothesis/purpose: The sesquiterpene lactones (SLs) coronopilin and damsin, which are major secondary metabolites of *A. arborescens*, have anti-inflammatory activity by attenuation of IL-6 and MCP-1 expression and inhibition of NF-κB in human dermal fibroblasts (HDFa) and human keratinocytes (HaCaT).
Study design: In order to confirm a high concentration of damsin and coronopilin in the plant material, a quantitative method was developed. The effect of the pure compounds on cytokine and NF-κB expression was examined, as well as their effects on HDFa and HaCaT cell morphology and viability.
Methods: Coronopilin and damsin were quantified by HPLC-DAD analysis, from EtOAc extracts of the aerial parts of *A. arborescens*. Cell morphology was investigated by phase-contrast microscopy and cell viability by the MTT assay. IL-6 and MCP-1 cytokine gene expression was assessed by quantitative real-time RT-PCR in LPS stimulated cells. The NF-κB pathway was studied through western blotting of the phosphorylated forms of p65 and p50/p105, as well as the non-phosphorylated IκB. Dexamethasone was used as positive control.
Results: Dry aerial parts contained 12.3 mg/g and 13.4 mg/g of coronopilin and damsin, respectively. Treatment with either compound (1–10 μM) for 24 h attenuated LPS-induced mRNA expression of the pro-inflammatory cytokine IL-6 and the chemokine MCP-1 in HDFa cells. The down-regulation of MCP-1 mRNA induced by coronopilin and damsin was confirmed on the protein level. Damsin reduced phosphorylated p65 and p105 subunits in HDFa cells. Neither coronopilin nor damsin affected HDFa cell morphology and viability within the used concentration range (1–10 μM). Also, in HaCaT cells, treatment with damsin (1–10 μM) for 24 h inhibited the MCP-1 expression, and damsin thereby attenuated cytokine expression both in HDFa and HaCaT cells.
Conclusion: We show that coronopilin and damsin from *A. arborescens* inhibit pro-inflammatory IL-6 and MCP-1 expression in human skin cells via NF-κB inhibition, suggesting that they may be useful for antagonizing inflammatory conditions of the human skin.

Introduction

The secondary metabolites isolated from plants used in the indigenous medicine have become a relevant source for drug discovery (Kumar et al., 2012). It is important to identify the mechanism of action of these compounds, in order to understand the efficiency and safety of herbal medicines or galenical preparations, as well as for the discovery and design of new lead compounds (Farnsworth et al., 1985; Schenone

Abbreviations: SL, sesquiterpene lactone; RT-PCR, reverse transcription-polymerase chain reaction; DMSO, dimethyl sulfoxide; NF-κB, nuclear factor kappa-light-chain-enhancer of activated B cells; HPLC, high performance liquid chromatography; DAD, Diode Array Detector; HDFa, human dermal fibroblasts; C.V., coefficient of variation; MTT, 3-(4,5-dimethylthiazol-2-yl)-2,5-diphenyltetrazolium bromide

* Corresponding author.
E-mail address: rodrigo.villagomez@chem.lu.se (R. Villagomez).

https://doi.org/10.1016/j.phymed.2018.04.011
Received 11 August 2017; Received in revised form 14 February 2018; Accepted 4 April 2018

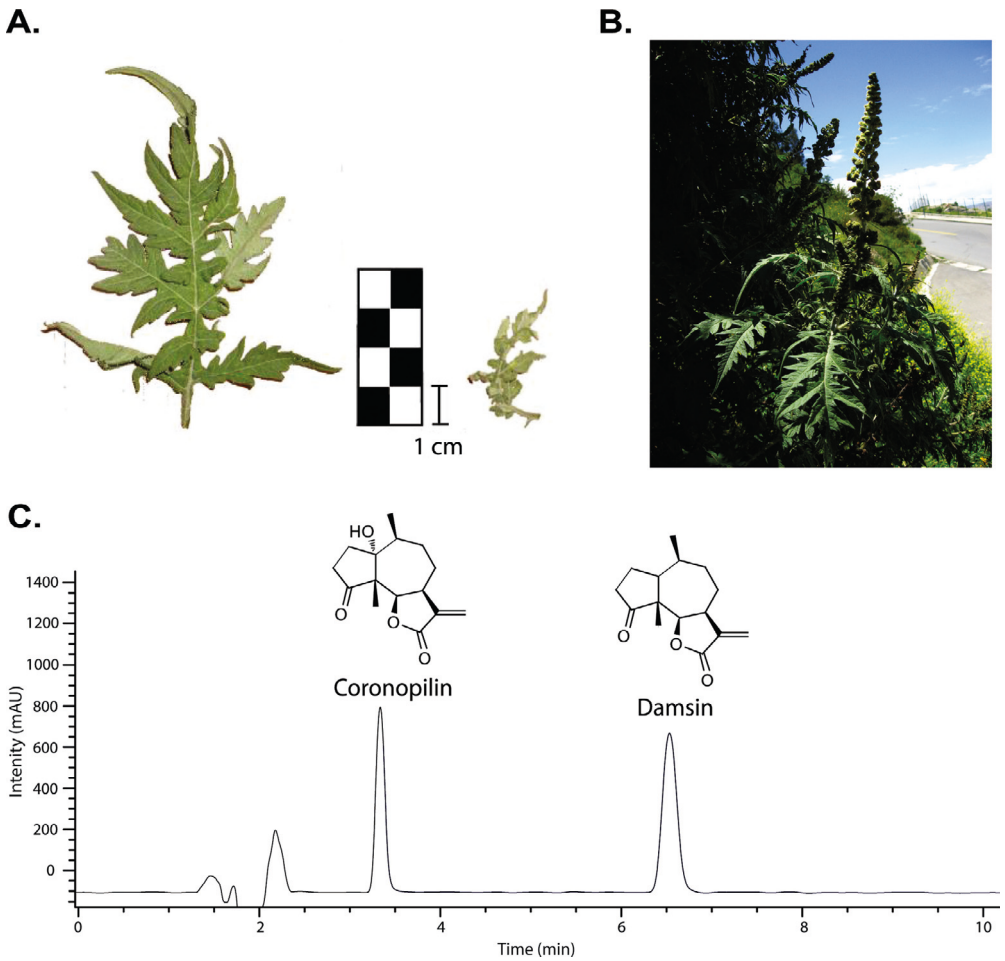

Fig. 1. (A) Leaves of *A. arborescens* Mill. (B) Inflorescence of *A. arborescens* Mill. (C) HPLC-DAD chromatogram at 210 nm of coronopilin (t_r = 3.299 min) and damsin (t_r = 6.288 min).

et al., 2013). Also, it is especially valuable if direct links between scientific results and ethnomedical uses are established (Farnsworth et al., 1985). In that regard, the continent of South America has an important potential as it possesses a major part of the world's biodiversity, which is more or less unexplored from a scientific point of view (Calixto, 2005), and a strong tradition of using plants in the indigenous medicine has developed in this continent (Pedersen and Baruffati, 1985).

Ambrosia arborescens Mill. (syn. *Franseria artemisioides* Willd., *Ambrosia artemisioides* Meyen & Walp) is an erect shrub distributed in the Andean region (Fig. 1A and B), and it can be found from North Colombia to Western Bolivia (Payne, 1964). Depending on the region or ethnic group the plant has different vernacular names, the most common being Altamisa, Marco and Markhu (Cavender and Albán, 2009; De-la-Cruz et al., 2007; Macía et al., 2005; Payne, 1964). This plant has a variety of medicinal uses in the Andean region, such as antispasmodic, emmenagogue, vermifuge, amebic dysentery, stomach ache, tonic for the digestive system, antiseptic, abortive, contraceptive and even for the treatment of "supernaturally caused illnesses" (Abad et al., 1999; Cavender and Albán, 2009; Gonzales de la Cruz et al., 2014; Jerves-Andrade et al., 2014; Lagos-López, 2007; Macía et al., 2005; Rojas et al., 2003). However, among all of the uses, the topical treatment of inflammation is the most frequent (De-la-Cruz et al., 2007; Fernandez et al., 2003; Macía et al., 2005; Rehecho et al., 2011; Rojas et al., 2003; Tene et al., 2007), suggesting that this plant may have anti-inflammatory properties.

Glucocorticoids are the backbone for the treatment of inflammatory diseases, and have for decades been used to combat inflammation. However, they also have limitations due to their many severe side effects (Clark, 2007). The glucocorticoids' anti-inflammatory effects

depend mainly on their inhibition of NF-κB-evoked transcription of pro-inflammatory cytokines such as interleukin-6 (IL-6) and the monocyte chemoattractant protein-1 (MCP-1) (Libermann and Baltimore, 1990; Rovin et al., 1995). On the other hand, the detrimental side effects of glucocorticoid treatment are largely dependent on other mechanisms (Clark, 2007; Rosen and Miner, 2005).

Hence, there is a large interest in the development of alternative anti-inflammatory agents. This search has resulted in a number of leads, including sesquiterpene lactones (SLs) (Ekenas et al., 2008; Emami et al., 2010; Valerio et al., 2007; Villagomez et al., 2013). Most anti-inflammatory SLs act as Michael-acceptors due to the presence of a α-methylene-γ-lactone functional group. This is reactive and may inactivate certain thiol containing proteins, most importantly NF-κB and other pro-inflammatory transcription factors (Kreuger et al., 2012).

Previously, we studied the inhibitory activity of coronopilin and damsin (see Fig. 1C for chemical structures) on NF-κB and STAT3 through the use of luciferase-reporter transfected Jurkat cells, with the aim to find new anticancer lead compounds (Villagomez et al., 2013). The positive results obtained raised the question whether or not the inhibition of NF-κB could be related to inhibition of cytokine production and thereby an anti-inflammatory effect of the plant. The objective of the present study was to determine if coronopilin and damsin may act anti-inflammatory through down-regulation of pro-inflammatory cytokine expression, and if they interact with NF-κB signaling in human skin cells. Here, we show for the first time that both coronopilin and damsin prevent pro-inflammatory cytokine expression in human skin fibroblasts and keratinocytes, at low concentrations relevant for their natural presence in the plant leafs. Furthermore, we demonstrate that the two compounds reduce NF-κB phosphorylation, indicating a mechanism of action. Taken together, our data suggest that coronopilin and damsin may have a beneficial anti-inflammatory effect in the skin through this mechanism.

Material and methods

Chemicals

HPLC grade acetonitrile (Sigma-Aldrich), formic acid > 98% (Merck) and ultrapure water were used as mobile phase. SLs were isolated from *A. arborescens* as previously described with a purity of 99.5% for coronopilin and 99.1% for damsin (Villagomez et al., 2013) and dissolved in dimethyl sulfoxide (DMSO). LPS (*Escherichia coli* 0111:B4 LPS; Sigma Chemicals) was dissolved in PBS. Dexamethasone was purchased from Sigma Chemicals and dissolved in DMSO. Controls received vehicle as appropriate.

HPLC analysis and quantification

Sample preparation

The aerial parts of *A. arborescens* were collected in June 2015 at La Paz City, Bolivia (16° 30′ 01″ S, 68° 06′ 23″ W, 3804 m.a.s.l) and the voucher specimen was deposited at Herbario Nacional de Bolivia, Universidad Mayor de San Andrés (voucher specimen code: MLP No.1). The collected material was dried at room temperature for 2 weeks. The leaves, 0.5 g, were extracted in 15 ml of EtOAc for 24 h. The extract was filtered and the solvent was completely evaporated *in vacuo*. Before analysis, the dry extract was dissolved in 5 ml of MeOH (HPLC grade) and passed through Discovery DPA-6S solid phase extraction cartridges (Supelco) followed by MeOH washing (3 × 5 ml). All eluates were pooled and diluted to 25 ml in a volumetric flask.

HPLC-DAD

The HPLC system was an Agilent Technologies 1100 Series consisting of a quaternary pump, continuous vacuum degasser, thermostated autosampler and column compartment coupled to a variable wavelength diode-array detector. The column was an Agilent Technologies EclipsePlus C-18 (4.6 × 250 mm × 5 µm) with a 0.5 µm pre-column filter (Agilent Technologies), and the column compartment was heated at 45 °C. The injection volume was 25 µl (standards and samples) and the chromatographic separation was done with an isocratic solvent mixture of 60% ACN in 0.15% (v/v) formic acid in water at a flow rate of 1.0 ml/min. The standards solutions of coronopilin and damsin were prepared in MeOH at four different concentrations. The analytes were detected at 210 nm (DAD) with a bandwidth of 4 nm. Fig. 1C shows the DAD chromatogram of coronopilin and damsin standard mixture.

Cells and cell viability and gene expression assays

Cells and cell culture

Primary human dermal fibroblasts (HDFa), human HaCaT keratinocytes and human THP-1 monocytes were purchased from Cascade Biologics, CLS Cell Line Service GmbH and ATCC, respectively. HDFa and HaCaT cells were cultured in DMEM/Ham´s F12 (1:1) (Life Technologies) and THP-1 cells in RPMI-1640 medium (Thermo Fisher Scientific), both supplemented with antibiotics (penicillin 50 U/ml, streptomycin 50 µg/ml, Biochrom GmbH) and 10% fetal bovine serum (FBS, Biochrom GmbH). The cells were kept at 37 °C under 5% CO_2 in a water-jacketed cell incubator. Adherent cells were trypsinized (0.25% trypsin/EDTA), counted using the Luna™ Automated Cell Counter system (Logos Biosystem) and then re-seeded. The primary HDFa cells were used up to passage 10.

Cell morphology

For assessment of cell morphology, the cells were cultured in 6-well plates. At 80% cell confluence culture medium was replaced with DMEM supplemented with 2% FBS and SLs were added. Control cells received DMSO (0.1%) as vehicle. After 24 h incubation cell morphology was evaluated in photographs obtained by a Nikon TMS phase-contrast microscope equipped with a digital camera (Pixelink, Nikon).

Cell viability

Cell viability was assessed using the 3-(4,5-dimethylthiazol-2-yl)-2,5-diphenyl tetrazolium bromide (MTT) assay as previously described (Svensson et al., 2016). Briefly, HDFa and HaCaT cells were seeded at a density of 7000 and 20,000 cells/well, respectively, in 96-well plates. At 24 h after seeding, the culture medium was replaced with DMEM medium supplemented with 2% FBS, and the cells were treated with SLs or DMSO as vehicle for 24 h. After the 24 h of incubation, MTT (0.5 mg/ml) was added, and the plate was returned to the incubator for 1 h. The MTT-containing medium was removed and the blue formazan product dissolved by adding 100 µl of DMSO per well. Absorbance was monitored at 540 nm in a Multiskan GO Microplate Spectrophotometer (Thermo Fisher Scientific).

Cytokine gene expression analysis

Cells were pre-treated with SLs, dexamethasone or vehicle for 30 min in culture medium (2% FBS) before lipopolysaccharide (LPS, 0.5 µg/ml, *E. coli* 0111:B4, Sigma Chemicals) was added. Cells were incubated for 24 h in the presence or absence of SLs, dexamethasone and LPS before total RNA was extracted and purified from cells using the miRNeasy kit (Qiagen). Concentration and quality of RNA was assessed using a NanoDrop 2000C spectrophotometer (Thermo Fisher Scientific). The RNA samples were subjected to one-step quantitative real-time RT-PCR measurements using the QuantiFast SYBR Green RT-PCR kit (Qiagen) and QuantiTect primer assays (Qiagen) on a Step One Plus real-time thermal cycler (Applied Biosystems). Gene expression was calculated using the ΔΔCT method applying glyceraldehyde-3-phosphate dehydrogenase (GAPDH) as the housekeeping reference gene (Pfaffl, 2001). Each sample was analyzed in duplicate. The PCR primers for MCP-1 (Hs_CCL2_1_SG), IL-6 (Hs_IL6_1_SG), GROα (Hs_CXCL1_2_SG), and GAPDH (Hs_GAPDH_2_SG) were purchased from

Qiagen.

Western blotting

The cells were lysed in SDS sample buffer containing Halt™ phosphatase and protease inhibitor cocktails (Thermo Scientific, Sigma-Aldrich, respectively). Samples were prepared for gel electrophoresis as previously described (Svensson et al., 2014). Proteins were loaded at an amount of 30 μg per lane on Criterion TXG any kD precast gels (Bio-Rad) and separated by SDS-PAGE after which they were transferred to 0.2 μm nitrocellulose membranes by a Trans-Blot Turbo transfer system (Bio-Rad). The membranes were blocked using 1% casein in TBS (Bio-Rad) and incubated with primary antibodies against MCP-1 (Abcam, Cat No. ab9669, 0.6 μg/ml dilution), GAPDH (Merck Millipore, clone 6C5, Cat No. MAB374, 1:5000 dilution), phospho-NF-κB p65 (Cell Signaling, phospho S536, Cat No. 3031S, 1:1000 dilution), phospho-NF-κB p105/p50 (Cell Signaling, phospho S933 (18E6), Cat No. 4806S, 1:1000 dilution), IκBα (Cell Signaling, Cat No. 9242S, 1:1000 dilution). The membranes were washed repeatedly in TBS-T and the immunoreactive bands were visualized by chemiluminescence using HRP-conjugated secondary anti-rabbit or anti-mouse antibodies followed by SuperSignal West Femto chemiluminescence reagent (Thermo Fisher Scientific). The immunospecific bands were analyzed by photo-densitometric scanning and normalized to GAPDH. Images were acquired using a LI-COR Odyssey Fc instrument (LI-COR Biosciences).

Statistics

For the HPLC method the approximate limits of detection and quantification where calculated using the following equations: LOD = 3.3 × (S_A/b) and LOQ = 10 × (S_A/b); where S_A is the standard deviation of the y-intercept and b is the slope from the linear regression statistics (Boca et al., 2005). Summarized data are presented as means ± SEM. Statistical significance was calculated using ANOVA for unpaired comparisons with Tukey´s Multiple Comparison test for *post hoc* analysis. p values < 0.05 were considered significant.

Results

HPLC analysis and quantification

Calibration curves

The external standard calibration curves for coronopilin and damsin were done considering four concentration points (75, 150, 225 and 300 μg/ml), measured in triplicate, and the average peak areas were used for least squares linear regression. The linearity for both compounds was confirmed (coronopilin: R^2 = 0.9925; and damsin: R^2 = 0.9965). The coronopilin method had a LOD value of 41.7 μg/ml and a LOQ value of 126.5 μg/ml, damsin method had a LOD value of 28.3 μg/ml and a LOQ value of 85.8 μg/ml.

Analysis of coronopilin and damsin contents in A. arborescens samples

The contents of coronopilin and damsin in EtOAc extracts from dry leaves of *A. arborescens* (500 mg), were quantified in triplicate using the developed HPLC-DAD methods (Fig. 1C). The concentration of coronopilin in the extract was 246.3 ± 5.2 μg/ml, corresponding to a content of 12.3 ± 0.3 mg/g of the compound in the dry leaves (C.V. = 2.12%). The extract had a concentration of damsin of 268.6 ± 0.5 μg/ml that corresponds to a content of 13.4 ± 0.02 mg/g in the dry leaves (C.V. = 0.18%).

Effects of coronopilin and damsin on LPS induced cytokine expression

Coronopilin and damsin attenuate LPS-induced IL-6 and MCP-1 gene expression in HDFa cells

Stimulation with LPS (0.5 μg/ml) for 24 h up-regulated the HDFa cell IL-6 cytokine mRNA expression by about 25 times compared to control cells (Fig. 2A and B). Treatment with either coronopilin or

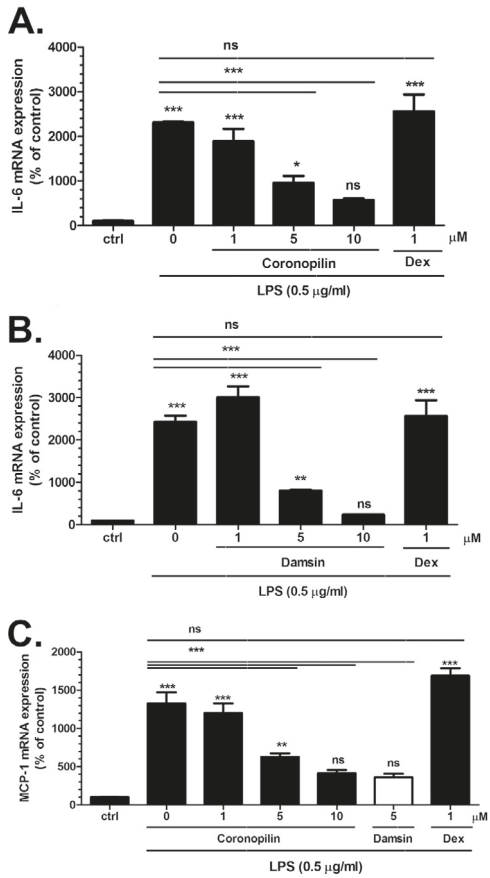

Fig. 2. Treatment with either (A) coronopilin or (B) damsin for 24 h attenuates LPS-induced mRNA expression of IL-6 in human dermal fibroblast HDFa cells. (C) Treatment with either coronopilin or damsin for 24 h reduces LPS-induced mRNA expression of MCP-1 in HDFa cells. Treatment with dexamethasone (Dex, 1 μM) had no effect on the LPS-induced expression of either MCP-1 or IL-6 mRNA (A–C). Values are presented as means ± SEM of 3 observations in each group. *p < 0.05, **p < 0.01 and ***p < 0.001. ns = not significant.

damsin, at 5 and 10 μM for both agents, for 24 h, prevented the LPS-induced IL-6 expression. A lower concentration (1 μM) of either coronopilin or damsin had no effect on LPS-induced IL-6 expression (Fig. 2A and B). The glucocorticoid dexamethasone (1 μM) did not reduce LPS-induced IL-6 mRNA (Fig. 2A and B). Damsin (5 and 10 μM) had a slightly stronger inhibitory effect than coronopilin (5 and 10 μM) on LPS-stimulated IL-6 expression (Fig. 2A and B).

Treatment with LPS (0.5 μg/ml) for 24 h stimulated MCP-1 gene expression by about 13 times, and, importantly, 10 μM coronopilin and 5 μM damsin completely inhibited the LPS-induced MCP-1 mRNA (Fig. 2C). In line with the results for IL-6, the LPS-stimulated MCP-1 gene expression was unaffected by treatment with 1 μM dexamethasone (Fig. 2C). We used LPS-stimulated THP-1 human monocytes as a positive control, to confirm the anti-inflammatory effect of dexamethasone in our experimental system. In the THP-1 cells, 1 μM dexamethasone,

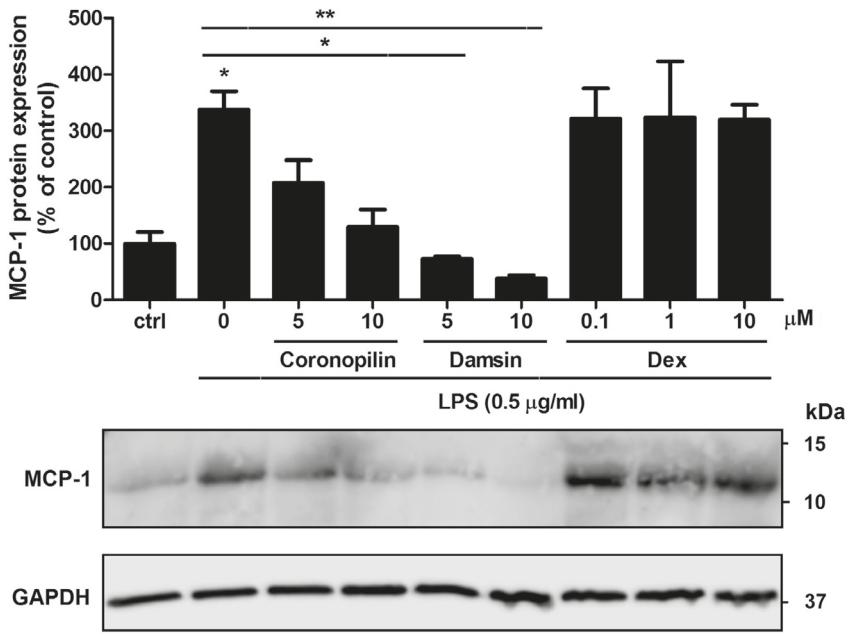

Fig. 3. Damsin inhibits the LPS-induced increase in MCP-1 protein in HDFa cells. The MCP-1 protein was assessed by western blotting in cells stimulated with LPS (0.5 μg/ml) for 24 h in the presence or absence of coronopilin, damsin or dexamethasone (Dex). The immunoreactive MCP-1 band appeared at the correct molecular weight (12–13 kDa) and was normalized by densitometric scanning to GAPDH serving as internal control. Ctrl = controls. Values are presented as means ± SEM of 3 observations in each group. * and ** represent $p < 0.05$ and $p < 0.01$, respectively.

just as 10 μM of either coronopilin or damsin, completely reversed the LPS-induced MCP-1 mRNA expression (Fig. S1).

Coronopilin and damsin attenuate LPS-induced MCP-1 protein expression in HDFa cells

The anti-inflammatory effect of the SLs in the HDFa cells was confirmed on the protein level. Stimulation with LPS (0.5 μg/ml) for 24 h up-regulated the HDFa MCP-1 protein expression by 3.5 times (Fig. 3). The LPS-evoked MCP-1 expression was effectively blocked by both 5 and 10 μM of damsin. Coronopilin tended to antagonize LPS-induced MCP-1 protein expression, but these results were not statistically significant (Fig. 3). Dexamethasone (0.1, 1 and 10 μM) had no effect on the LPS-induced MCP-1 protein levels (Fig. 3).

Coronopilin and damsin have no effects on HDFa cell viability and morphology at concentrations relevant for their inhibition of cytokine expression

Next, we investigated whether the anti-inflammatory effect of coronopilin and damsin is specific and not secondary to reduced cell viability. Treatment with 10 μM of either coronopilin or damsin for 24 h had no effect on HDFa cell morphology (Fig. 4A). Treatment with either coronopilin or damsin for 24 h, at concentrations (1–10 μM) relevant for their attenuation of LPS-induced IL-6 and MCP-1 expression, had no effect on HDFa cell viability assessed by the MTT assay (Fig. 4B and C). However, both coronopilin and damsin reduced cell viability when they were administered at a high concentration (100 μM) (Fig. 4B and C). Damsin (100 μM) reduced cell viability more strongly ($p < 0.01$) than an identical concentration (100 μM) of coronopilin (Fig. 4B and C).

Damsin attenuates mRNA expression of MCP-1 and promotes cell proliferation in human skin HaCaT keratinocytes

Next, we investigated the effects of damsin on HaCaT cell MCP-1 transcript expression and cell viability. The HaCaT cells did not respond to 24 h of LPS stimulation (0.5 μg/ml), but treatment with damsin 1–10 μM inhibited MCP-1 expression in the presence of LPS, showing that damsin reduces basal expression of MCP-1 in these cells (Fig. 5A). Treatment with 1–10 μM damsin for 24 h had no effect on HaCaT cell viability assessed by the MTT assay, while 100 μM damsin had a clear cytotoxic effect (Fig. 5B). Thus, the HaCaT cell data, showing no effect at 1–10 μM but reduced cell viability in response to 100 μM damsin, resemble those observed in HDFa cells. Treatment with 5 and 10 μM damsin for 24 h had a slight, but not statistically significant pro-proliferative effect in the HaCaT cells (Fig. 5B). To further investigate this trend, we treated the HaCaT cells with 10 μM damsin for a longer time point (48 h). Cell viability measurements by the MTT assay showed that incubation with 10 μM damsin for 48 h increased HaCaT cell viability by 12% (112 ± 2% in damsin treated cells *vs*. 100 ± 2% in control cells, $n = 20$, $p < 0.001$).

Damsin attenuates mRNA expression of the chemokine GROα in both HDFa and HaCaT cells

We also analyzed the expression levels of the pro-inflammatory chemokine GROα (CXCL1) in HDFa and HaCaT cells treated with LPS (0.5 μg/ml) in the presence or absence of damsin (10 μM). In HDFa cells, GROα expression increased 240-fold upon LPS-stimulation (Fig. 6A). This effect was completely reversed by damsin (Fig. 6A). In HaCaT cells, LPS had no effect on GROα mRNA, but damsin reduced the basal expression of GROα by about 60% (Fig. 6B).

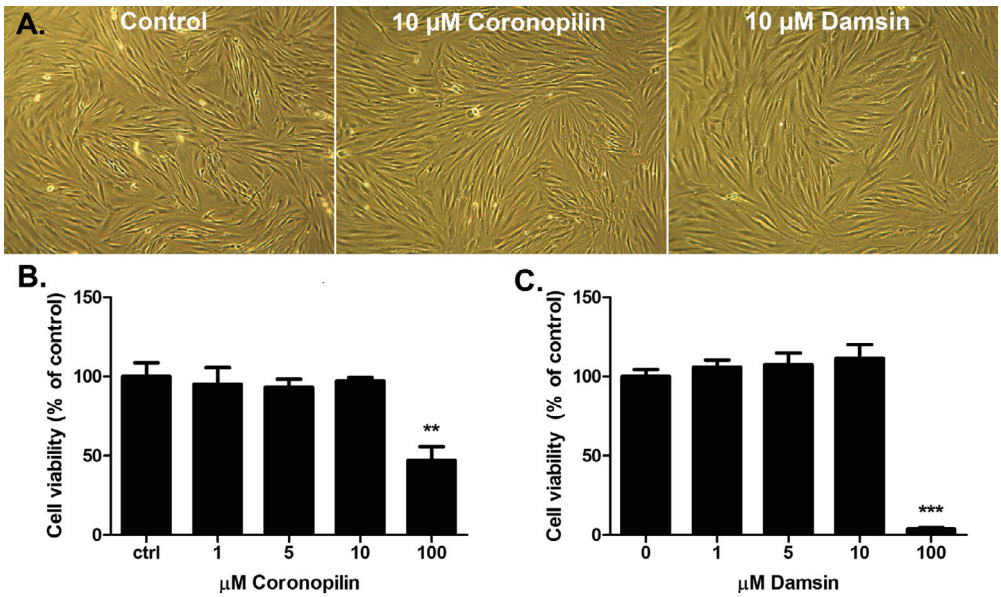

Fig. 4. (A) Photographs obtained by phase-contrast microscopy showing that treatment with either coronopilin (10 µM) or damsin (10 µM) for 24 h has no effect on HDFa cell morphology. Control cells were treated with vehicle (0.1% DMSO). (B, C) Cell viability, assessed by the MTT assay, was not affected by treatment for 24 h with either coronopilin or damsin at 1–10 µM, while a high concentration (100 µM) of either coronopilin or damsin reduced cell viability. Values are presented as means ± SEM of 4–5 observations in each group. ** and *** represent $p < 0.01$ and $p < 0.001$, respectively.

Damsin down-regulates phosphorylated NF-κB subunits p65 and p105 and up-regulates IκBα

To examine whether coronopilin and damsin inhibit some activation steps of NF-κB, HDFa cells were treated with LPS (0.5 µg/ml) in the presence or absence of SLs or dexamethasone for either 30 min or 24 h. The proteins involved in NF-κB signaling were then analyzed by western blotting. LPS (0.5 µg/ml) alone increased p-p65 at 30 min but not at 24 h. Treatment with damsin (10 µM) decreased LPS-induced p-p65 at 30 min while coronopilin (10 µM) had no effect (Fig. 7A and E). Treatment with 10 µM damsin for 24 h reduced basal p-p65 expression (Fig. 7A and E). LPS had no effect on the IκBα protein expression (Fig. 7B and E). Treatment with 10 µM damsin for 24 h increased IκBα protein compared to cells treated with LPS alone (Fig. 7B and E), but no effect was observed during the first 30 min after stimulation with LPS. Coronopilin had no effect on IκBα protein expression (Fig. 7B and E). LPS enhanced the expression of the p-p105 subunit of NF-κB by about 4

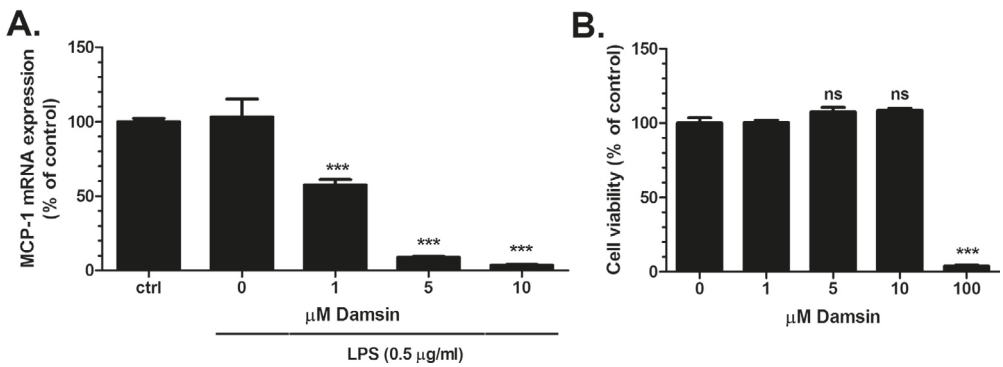

Fig. 5. (A) Damsin (1–10 µM) decreases the basal expression-level of MCP-1 mRNA in human HaCaT skin keratinocytes treated with LPS (0.5 µg/ml) for 24 h. LPS had no effect on MCP-1 expression in HaCaT cells. (B) Damsin (1–10 µM) has no effect on HaCaT cell viability assessed by MTT assay, while a higher concentration (100 µM) of damsin strongly attenuates cell viability. Values are presented as means ± SEM of 3 observations in each group. *$p < 0.05$, **$p < 0.01$ and ***$p < 0.001$.

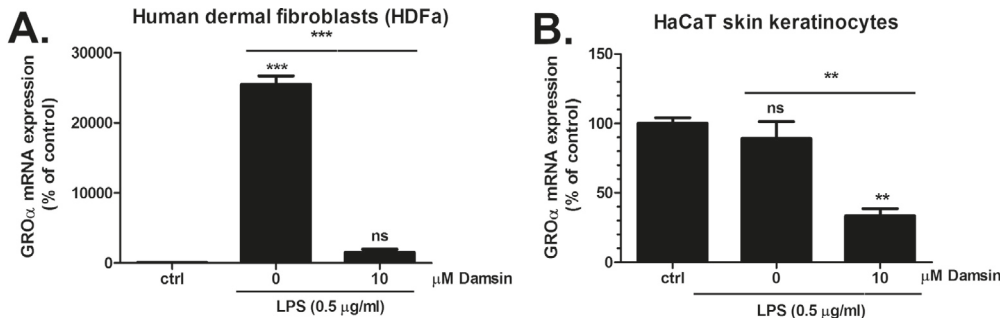

Fig. 6. (A) Damsin inhibits the LPS-induced GROα (CXCL1) chemokine expression in HDFa cells. (B) Damsin reduces basal expression of GROα in HaCaT cells. LPS had no effect on GROα expression in HaCaT cells. The cells were stimulated with LPS (0.5 μg/ml) for 24 h. Values are presented as means ± SEM of 3 observations in each group. ns = not significant. ** and *** represent $p < 0.01$ and $p < 0.001$, respectively.

times at 30 min but not 24 h (Fig. 7C and E). The LPS-induced p-p105 was antagonized by 10 μM damsin at 30 min, and at 24 h damsin (10 μM) reduced basal expression of p-p105 (Fig. 7C and E). In accordance with the previous results for p-p65 and IκBα, coronopilin (10 μM) had no effect. Treatment with LPS for 30 min and 24 h increased p-p50 between 3 and 4 times (Fig. 7D and E). Neither damsin (10 μM) nor coronopilin (10 μM) affected the LPS-stimulated p-p50 (Fig. 7D and E). Treatment with dexamethasone (1 μM) enhanced the expression of p-p65 at 24 h of stimulation with LPS but had no effect on LPS-induced p-p65 at 30 min (Fig. 7A). Dexamethasone (1 μM) had no effect on IκBα expression (Fig. 7B). Moreover, dexamethasone (1 μM) had no effect on the LPS-induced increase in phosphorylated p50 and p105 NF-κB subunits (Fig. 7D and E).

Discussion

We demonstrate that SLs, but not the glucocorticoid dexamethasone, down-regulates pro-inflammatory cytokine production in HDFa cells. Dexamethasone, however, attenuates MCP-1 expression in human THP-1 monocytes, acting as positive control. In the THP-1 cells both SLs and dexamethasone completely prevented the LPS-induced MCP-1 expression. Thus, these SLs show a more consistent action on LPS-induced cytokine expression in different cell types than the common steroidal drug dexamethasone. Indeed, there is a great need in the clinic for the development of new non-steroidal anti-inflammatory drugs (Barnes et al., 2015; McCarberg and Gibofsky, 2012), and our data suggest that coronopilin and damsin may be used as a complement to glucocorticoids to combat skin inflammation.

A. arborescens is a SL-rich medicinal plant from the Andean region which has a history of being used both topically and orally to treat inflammatory conditions. Our data shows that the dry aerial parts (the most commonly used part of the plant for medicinal purposes) contain 12.3 mg/g and 13.4 mg/g of coronopilin and damsin, respectively, corresponding to a concentration of 46.6 and 50.8 mmol/kg, respectively. This is about 10,000 times higher than the active concentrations of the components, and therefore it is reasonable to assume that topical application of dried leaves or galenicals thereof result in pharmacologically active concentration of both SLs (higher than 1 μM) in the proximity of the skin keratinocytes and dermal fibroblasts. Thus, the SL-evoked down-regulation of LPS-induced IL-6 and MCP-1 expression in cultured human HaCaT keratinocytes and HDFa dermal fibroblast observed in the present study seems to be representative for the human *in vivo* situation. Here, we show that both coronopilin and damsin decrease cell viability at high concentration (100 μM) in human skin cells, suggesting that these SLs should be applied on the skin in low μM concentrations, whereas over-dosage may antagonize their anti-inflammatory effect via reduction of cell viability. The observed dose-dependent attenuation of MCP-1 expression has previously been reported for other SLs, indicating that inhibition of MCP-1 expression is a common mechanism of action for anti-inflammatory SLs (Gao et al., 2017; Grassl et al., 2005; Qin et al., 2016). We used LPS to enhance the expression of the pro-inflammatory cytokines IL-6, MCP-1 and GROα. In HDFa cells, LPS enhances IL-6, MCP-1 and GROα expression by 25, 13 and 240 times, respectively, but no effect of LPS on cytokine expression was observed in HaCaT cells, suggesting a cell type specific effect of LPS that may reflect different level of expression of toll-like receptors (TLRs) in these two cell types.

We demonstrate that damsin interacts with NF-κB signaling at multiple steps, attenuating the levels of the phosphorylated forms of NF-κB p65 (S536) and p105 (S933) subunits and up-regulating IκBα. Thus, damsin may down-regulate LPS-induced cytokine expression via this mechanism. Additionally, the effects of damsin lasted for 24 h, while the LPS-evoked stimulation of NF-κB signaling in control cells returned to the basal state in the same period of time. On the other hand, we show that coronopilin-induced attenuation of LPS-stimulated cytokine expression is not associated with changes in phosphorylated NF-κB subunit and IκBα expression, suggesting that other mechanisms are involved in the coronopilin-evoked down-regulation of cytokine expression. In fact, coronopilin may act down-stream and directly interfere with NF-κB-induced transcription of cytokine genes. Interestingly, dexamethasone did not reduce the LPS-induced increase in phosphorylated p50 and p105 subunits and had no effect on the IκBα expression in the HDFa cells. In fact, dexamethasone even up-regulated the LPS-induced stimulation of phosphorylated p65 subunit at 24 h. These results provide a plausible mechanism to why dexamethasone did not antagonize the LPS-induced expression of IL-6 and MCP-1 in these cells.

The most studied mechanism for the SLs-induced inhibition of NF-κB signaling considers the hindering of p65 interaction with DNA κB binding sites by direct alkylation of Cys38 (Garcia-Pineres et al., 2001), and previously we reported that damsin indeed has this activity (Villagomez et al., 2015). However, the results obtained in this study, showed that the inhibitory mechanism of damsin is more complex, affecting the phosphorylation of critical sites for the activation, nuclear translocation and transcription capacity of NF-κB. Possibly this occurs after inhibition of specific kinases as IKK (Heissmeyer et al., 1999; Sakurai et al., 2003) or inhibition of the ubiquitination systems that regulate IκBα degradation, as was reported for SLs, such as parthenolide (Hehner et al., 1998). However, contradictory data were reported more recently for SLs, including parthenolide, which suggests that SL-induced inhibition of IκBα degradation is not strong enough to explain the overall NF-κB inhibition (Garcia-Pineres et al., 2001; Jae Youl,

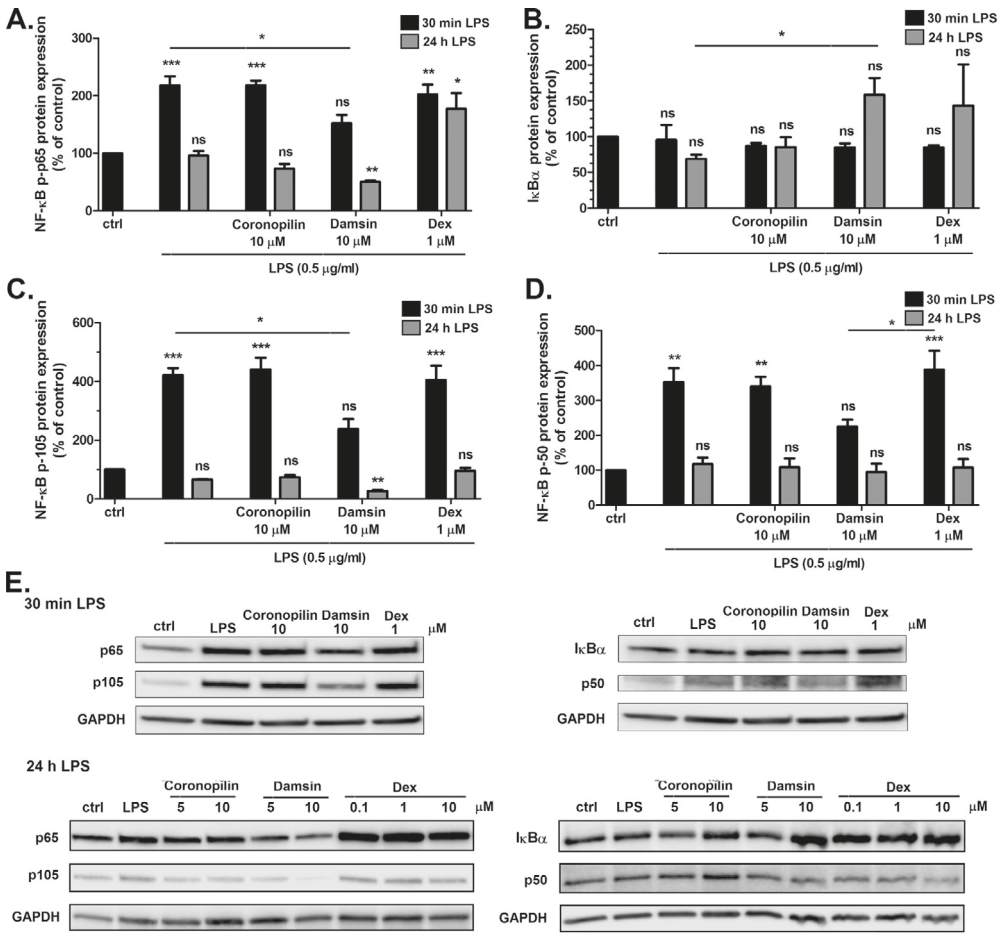

Fig. 7. (A, C) Treatment with damsin (10 μM) for either 30 min or 24 h decreases the level of phosphorylated p65 and p105 NF-κB subunits in human HDFa cells. LPS (0.5 μg/ml) increased p-p65 and p-p105 at 30 min but not 24 h. (B) Treatment with damsin (10 μM) for 24 h increases IκBα. (D) Neither coronopilin nor damsin show significant effect on LPS-induced p-p50 NF-κB subunit. The immunoreactive bands for the respective NF-κB subunit were normalized to GAPDH by densitometric scanning. (E) Western blot analysis of HDFa cells, using specific antibodies against p-p65, p-p105/p-p50, IκBα and GAPDH. Values are presented as means ± SEM of 3 observations in each group. $^{*}p < 0.05$, $^{**}p < 0.01$ and $^{***}p < 0.001$.

2006), even though further investigation is required to confirm these statements.

Conclusions

In the present study, we demonstrate that coronopilin and damsin, two SLs isolated from *A. arborescens,* attenuate the expression of the pro-inflammatory cytokines IL-6, MCP-1 and GROα in both human skin fibroblasts and keratinocytes, providing evidence that they antagonize inflammation in the skin through this mechanism. The down-regulation of pro-inflammatory cytokines by damsin, which is the most potent SL in our hands, is associated with down-regulation of the phosphorylated NF-κB subunits p65 and p105 and up-regulation of IκBα, providing a plausible mechanism of action. Interestingly, damsin promotes keratinocyte proliferation within the same concentration range where the compound reduces pro-inflammatory cytokine expression, suggesting that damsin both antagonizes inflammation and enhances cell proliferation. Additionally, both SLs were quantified in the aerial parts of *A. arborescens*, demonstrating that they are present in high concentrations in the plant, which could easily reach μM concentrations on the skin by topical application of the herbal medicine or in galenical preparations. Taken together, our results show that these SLs, and very likely the aerial parts of the plant, inhibit pro-inflammatory cytokine expression in human skin cells and that this effect is associated with modulation of the NF-κB signaling pathway. Thus, we propose that these SLs, as well as herbal medicines or galenicals containing them as active principles, may be used to antagonize inflammatory conditions of the human skin. However, future studies are urgently needed to assess

the anti-inflammatory properties of the SLs on *in vivo* models of human skin inflammation.

Acknowledgments

The authors are grateful to the Greta and Johan Kock Foundation, the Southern Region within the Swedish Dental Association and the Swedish International Development Agency (SIDA) for the support of this study which is part of the project "Research on Anti-cancer biomolecules" developed between the University of San Andres (UMSA, La Paz, Bolivia) and Lund University, Lund, Sweden.

Conflict of interest

The present paper does not present any conflict of interest.

Supplementary materials

Supplementary material associated with this article can be found, in the online version, at doi:10.1016/j.phymed.2018.04.011.

References

Abad, M.J., Bermejo, P., Gonzales, E., Iglesias, I., Irurzun, A., Carrasco, L., 1999. Antiviral activity of Bolivian plant extracts. Gen. Pharmacol. Vasc. Syst. 32, 499–503.
Barnes, L., Kaya, G., Rollason, V., 2015. Topical corticosteroid-induced skin atrophy: a comprehensive review. Drug Saf. 38, 493–509.
Boca, M.B., Apostolides, Z., Pretorius, E., 2005. A validated HPLC method for determining residues of a dual active ingredient anti-malarial drug on manufacturing equipment surfaces. J. Pharm. Biomed. Anal. 37, 461–468.
Calixto, J.B., 2005. Twenty-five years of research on medicinal plants in Latin America: a personal view. J. Ethnopharmacol. 100, 131–134.
Cavender, A.P., Albán, M., 2009. The use of magical plants by curanderos in the Ecuador highlands. J. Ethnobiol. Ethnomed. 5, 3.
Clark, A.R., 2007. Anti-inflammatory functions of glucocorticoid-induced genes. Mol. Cell. Endocrinol. 275, 79–97.
De-la-Cruz, H., Vilcapoma, G., Zevallos, P.A., 2007. Ethnobotanical study of medicinal plants used by the Andean people of Canta, Lima, Peru. J. Ethnopharmacol. 111, 284–294.
Ekenas, C., Zebrowska, A., Schuler, B., Vrede, T., Andreasen, K., Backlund, A., Merfort, I., Bohlin, L., 2008. Screening for anti-inflammatory activity of 12 Arnica (Asteraceae) species assessed by inhibition of NF-κB and release of human neutrophil elastase. Planta Med. 74, 1789–1794.
Emami, S.A., Taghizadeh Rabe, S.Z., Iranshahi, M., Ahi, A., Mahmoudi, M., 2010. Sesquiterpene lactone fraction from *Artemisia khorassanica* inhibits inducible nitric oxide synthase and cyclooxygenase-2 expression through the inactivation of NF-κB. Immunopharmacol. Immunotoxicol. 32, 688–695.
Farnsworth, N.R., Akerele, O., Bingel, A.S., Soejarto, D.D., Guo, Z., 1985. Medicinal plants in therapy. Bull. World Health Org. 63, 965–981.
Fernandez, E.C., Sandi, Y.E., Kokoska, L., 2003. Ethnobotanical inventory of medicinal plants used in the Bustillo Province of the Potosi Department, Bolivia. Fitoterapia 74, 407–416.
Gao, S., Wang, Q., Tian, X.-H., Li, H.-L., Shen, Y.-H., Xu, X.-K., Wu, G.-Z., Hu, Z.-L., Zhang, W.-D., 2017. Total sesquiterpene lactones prepared from *Inula helenium* L. has potentials in prevention and therapy of rheumatoid arthritis. J. Ethnopharmacol. 196, 39–46.
Garcia-Pineres, A.J., Castro, V., Mora, G., Schmidt, T.J., Strunck, E., Pahl, H.L., Merfort, I., 2001. Cysteine 38 in p65/NF-κB plays a crucial role in DNA binding inhibition by sesquiterpene lactones. J. Biol. Chem. 276, 39713–39720.
Gonzales de la Cruz, M., Baldeón Malpartida, S., Beltrán Santiago, H., Jullian, V., Bourdy, G., 2014. Hot and cold: medicinal plant uses in Quechua speaking communities in the high Andes (Callejón de Huaylas, Ancash, Perú). J. Ethnopharmacol. 155, 1093–1117.
Grassl, G.A., Fessele, S., Merfort, I., Lindenmeyer, M.T., Castro, V., Murillo, R., Nelson, P.J., Autenrieth, I.B., 2005. Sesquiterpene lactones inhibit *Yersinia invasin* protein-induced IL-8 and MCP-1 production in epithelial cells. Int. J. Med. Microbiol. 295, 531–538.
Hehner, S.P., Heinrich, M., Bork, P.M., Vogt, M., Ratter, F., Lehmann, V., Schulze-Osthoff, K., Droge, W., Schmitz, M.L., 1998. Sesquiterpene lactones specifically inhibit activation of NF-κB by preventing the degradation of IκB-alpha and IκB-beta. J. Biol. Chem. 273, 1288–1297.
Heissmeyer, V., Krappmann, D., Wulczyn, F.G., Scheidereit, C., 1999. NF-κB p105 is a target of IκB kinases and controls signal induction of Bcl-3-p50 complexes. EMBO J. 18, 4766–4778.
Jae Youl, C., 2006. Sesquiterpene lactones as a potent class of NF-κB activation inhibitors. Curr. Enzym. Inhib. 2, 329–341.
Jerves-Andrade, L., León-Tamariz, F., Peñaherrera, E., Cuzco, N., Tobar, V., Ansaloni, R., Maes, L., Wilches, I., 2014. Medicinal plants used in South Ecuador for gastrointestinal problems: an evaluation of their antibacterial potential. J. Med. Plants Res. 8, 1310–1320.
Kreuger, M.R., Grootjans, S., Biavatti, M.W., Vandenabeele, P., D'Herde, K., 2012. Sesquiterpene lactones as drugs with multiple targets in cancer treatment: focus on parthenolide. Anti-Cancer Drugs 23, 883–896.
Kumar, D., Kumar, A., Prakash, O., 2012. Potential antifertility agents from plants: a comprehensive review. J. Ethnopharmacol. 140, 1–32.
Lagos-López, M.I., 2007. Estudio etnobotánico de especies vegetales con propiedades medicinales en seis minicipios de Boyacá. Colombia. Actual Biol. 29, 87–96.
Libermann, T.A., Baltimore, D., 1990. Activation of interleukin-6 gene expression through the NF-κB transcription factor. Mol. Cell. Biol. 10, 2327–2334.
Macía, M.J., García, E., Vidaurre, P.J., 2005. An ethnobotanical survey of medicinal plants commercialized in the markets of La Paz and El Alto, Bolivia. J. Ethnopharmacol. 97, 337–350.
McCarberg, B., Gibofsky, A., 2012. Need to develop new nonsteroidal anti-inflammatory drug formulations. Clin. Ther. 34, 1954–1963.
Payne, W.W., 1964. A re-evaluation of the genus Ambrosia (compositae). J. Arnold. Arbor. 45, 401–438.
Pedersen, D., Baruffati, V., 1985. Special issue: health and social science in Latin America health and traditional medicine cultures in Latin America and the Caribbean. Soc. Sci. Med. 21, 5–12.
Pfaffl, M.W., 2001. A new mathematical model for relative quantification in real-time RT-PCR. Nucleic Acids Res 29, e45.
Qin, X., Jiang, X., Jiang, X., Wang, Y., Miao, Z., He, W., Yang, G., Lv, Z., Yu, Y., Zheng, Y., 2016. Michefiolide inhibits LPS-induced inflammatory response and protects mice from LPS challenge. Sci. Rep. 6, 23240.
Rehecho, S., Uriarte-Pueyo, I., Calvo, J., Vivas, L.A., Calvo, M.I., 2011. Ethnopharmacological survey of medicinal plants in Nor-Yauyos, a part of the Landscape Reserve Nor-Yauyos-Cochas, Peru. J. Ethnopharmacol. 133, 75–85.
Rojas, R., Bustamante, B., Bauer, J., Fernández, I., Albán, J., Lock, O., 2003. Antimicrobial activity of selected Peruvian medicinal plants. J. Ethnopharmacol. 88, 199–204.
Rosen, J., Miner, J.N., 2005. The search for safer glucocorticoid receptor ligands. Endocr. Rev. 26, 452–464.
Rovin, B.H., Dickerson, J.A., Tan, L.C., Hebert, C.A., 1995. Activation of nuclear factor-κB correlates with MCP-1 expression by human mesangial cells. Kidney Int. 48, 1263–1271.
Sakurai, H., Suzuki, S., Kawasaki, N., Nakano, H., Okazaki, T., Chino, A., Doi, T., Saiki, I., 2003. TNF-a-induced IKK phosphorylation of NF-kB p65 on serine 536 is mediated through TRAF2, TRAF5 and TAK1 signaling pathway. J. Biol. Chem 278, 36916–36923.
Schenone, M., Dancik, V., Wagner, B.K., Clemons, P.A., 2013. Target identification and mechanism of action in chemical biology and drug discovery. Nat. Chem. Biol. 9, 232–240.
Svensson, D., Gidlof, O., Turczynska, K.M., Erlinge, D., Albinsson, S., Nilsson, B.O., 2014. Inhibition of microRNA-125a promotes human endothelial cell proliferation and viability through an antiapoptotic mechanism. J. Vasc. Res. 51, 239–245.
Svensson, D., Wilk, L., Mörgelin, M., Herwald, H., Nilsson, B.-O., 2016. LL-37-induced host cell cytotoxicity depends on cellular expression of the globular C1q receptor (p33). Biochem. J. 473, 87–98.
Tene, V., Malagón, O., Finzi, P.V., Vidari, G., Armijos, C., Zaragoza, T., 2007. An ethnobotanical survey of medicinal plants used in Loja and Zamora-Chinchipe, Ecuador. J. Ethnopharmacol. 111, 63–81.
Valerio, D.A., Cunha, T.M., Arakawa, N.S., Lemos, H.P., Da Costa, F.B., Parada, C.A., Ferreira, S.H., Cunha, F.Q., Verri Jr., W.A., 2007. Anti-inflammatory and analgesic effects of the sesquiterpene lactone budlein A in mice: inhibition of cytokine production-dependent mechanism. Eur. J. Pharmacol. 562, 155–163.
Villagomez, R., Hatti-Kaul, R., Sterner, O., Almanza, G., Linares-Pastén, J.A., 2015. Effect of natural and semisynthetic pseudoguianolides on the stability of NF-κB:DNA complex studied by agarose gel electrophoresis. PLoS One 10, e0115819.
Villagomez, R., Rodrigo, G.C., Collado, I.G., Calzado, M.A., Munoz, E., Akesson, B., Sterner, O., Almanza, G.R., Duan, R.D., 2013. Multiple anticancer effects of damsin and coronopilin isolated from Ambrosia arborescens on cell cultures. Anticancer Res. 33, 3799–3805.

Paper II

OPEN ACCESS
Freely Available Online

JOURNAL OF ADVANCED PHARMACEUTICAL SCIENCE AND TECHNOLOGY
ISSN NO: 2328-0182

Research Article **DOI: 10.14302/issn.2328-0182.japst-19-2759**

Selective Cytotoxicity of Damsin Derivatives in Breast Cancer Cells

Maribel Lozano[1,3], Wendy Soria[2,4], Giovanna R. Almanza[3], Sophie Manner[1], Stina Oredsson[2], Rodrigo Villagomez[3], Olov Sterner[1,*]

[1]Centre for Analysis and Synthesis, Lund University, P.O.Box 124, 22100 Lund, Sweden

[2]Department of Biology, Lund University, Lund, Sweden

[3]Instituto de Investigaciones Químicas, Universidad Mayor de San Andrés, La Paz, Bolivia

[4]Instituto de Biología Molecular y Biotecnología, Universidad Mayor de San Andrés, La Paz, Bolivia

Abstract

Cancer is the leading cause of death worldwide, and there is a constant need for new treatment strategies. Sesquiterpene lactones containing a 3-methylenedihydrofuran-2(3*H*)-one (or α-methylene-γ-lactone) moiety, for example damsin (1), are Michael acceptors that affect biological processes such as cell proliferation, death/apoptosis, and cell migration, by interfering with cell signalling pathways. Although the reactivity of the α-methylene-γ-lactone moiety is important for these effects, the Michael addition is reversible and it can be assumed that also other parts of the molecules will moderate any given biological activity. In this investigation, the cytotoxicity of 23 α-methylene-γ-lactone towards normal breast epithelial MCF-10A cells as well as breast cancer JIMT-1 cells is compared. Most of the investigated compounds are semisynthetic derivatives prepared by the condensation of the natural product damsin (1) with aldehydes. The two cell lines were treated with various concentrations of the compounds in dose response assays, and the 50 % inhibitory concentration (IC_{50}) was determined from dose response curves. The IC_{50} values were found to depend strongly on the overall structure. The ratio between the IC_{50} values for MCF-10A and JIMT-1 cells, as a measure for the selectivity of a compound to kill cancer cells, was calculated, and found to vary between just over 1 to more than 10. The most potent derivatives formed from the condensation of 1 with aromatic aldehydes towards JIMT-1 cells are 3a and 3i, both with ratios between the IC_{50} values for MCF-10A and JIMT-1 cells close to 5. Also some aldol condensation products with acyclic aldehydes, i.e. 3r and 3u, were equally potent, and the latter showed the highest selectivity (ratio > 10). Structure-activity relationships that may explain the observed differences in potency and selectivity are discussed.

Corresponding author: Olov Sterner, Centre for Analysis and Synthesis, Lund University, P.O.Box 124, 22100 Lund, Sweden, Email: Olov.Sterner@chem.lu.se

Keywords: MCF-10A; JIMT-1; semisynthesis; α-methylene-γ-lactone; Michael acceptors; SAR:s

Received: Apr 02, 2019 **Accepted:** Apr 18, 2019 **Published:** Apr 19, 2019

Editor: Sahar Ahmed, University of Alberta, Canada.

Introduction

The incidence of cancer is increasing, and different strategies for controlling the disease are developed. The pool of secondary plant metabolites has always been an important provider of low-molecular anti-cancer drugs, and is expected to be so also in the future. As our understanding about the molecular mechanisms of cancer development and progression, as well as the development of treatment resistance, has increased, our ability to design new anti-cancer drugs has improved.[1,2] One of the cellular molecular pathways that is important for chemoresistance and metastasis in many cancer cells is the NF-κB pathway, where constitutive activation, or over-expression, is part of the tumour aggressiveness.[3] Terpenes containing an α-methylene-γ-lactone moiety are natural products that have been shown to possess promising anti-cancer effects, interfering with biological processes such as cell signalling, proliferation, death/apoptosis, and migration.[4,5] The significant cytotoxic activity of such terpenes is linked to the α-methylene-β-lactone moiety, which via a Michael addition can alkylate nucleophilic residues (primarily free thiols of cysteines) in proteins. A target suggested for such an interaction is the protein p65 in the NF-κB pathway.[6]

In general, electrophilic compounds are considered potentially toxic and have been rejected by the pharmaceutical industry in their search for novel drug candidates.[7,8] However, 39 electrophilic drugs, mainly used in oncological therapies, have been approved by the US Food and Drug Administration.[8] These will display more or less off-target toxicity, including immunogenic responses.[8] The efficiency and selectivity of an electrophilic compound will besides the reactivity of the electrophilic moiety depend on the affinity to the target through non-covalent interactions. Michael acceptors will react with nucleophiles via an addition reaction, not a substitution, in a reaction that is reversible, and will bind tighter to nucleophiles that present a more favourable molecular environment. However, the identification of specific targets and structural features of non-covalent interactions of Michael acceptors has been elusive and complex to study.

Several studies of structure-activity relationships (SARs) of natural terpenoid Michael acceptors have shown that guaianolide and pseudoguaianolide sesquiterpenes with a α-methylene-γ-lactone moiety possess the most potent anti-cancer and cytotoxic activities.[9,10] Although such sesquiterpenoids are considered to interact with multiple targets in cancer cells, they have been shown to inhibit transcription factors such as NF-κB, STAT3, and AP-1, up- or downregulate the protein kinases MAPK and JNK, and increase the expression of the p53 protein.[11] Besides that, they have been shown to disrupt the redox balance and induce an oxidative stress in cancer cells.[12]

In the present study we compare the cytotoxicity of 23 α-methylene-γ-lactones based on the natural product damsin (1) (see Figure 1), in normal breast epithelial MCF-10A cells and breast cancer JIMT-1 cells. 1 is a pseudoguainolide sesquiterpene with a moderate inhibitory activity on NF-κB,[13] available from the plant Ambrosia arborescens together with the 1-hydroxy derivative coronopilin (2). Compound 1 was used as the starting material for the semi-synthetic preparation of 21 novel analogues.

Experimental Procedure

General Chemical Procedures

Chemicals (analytical grade) were purchased from different commercial suppliers and used without further purification. Damsin (1) and coronopilin (2) (Figure 1) were isolated from A. arborescens as previously described.[13] IR spectra were recorded with a Brucker Alpha FT-IR Spectrometer, and the optical rotations was measured with a Perkin-Elmer 141 polarimeter. HRMS spectra were recorded with a Waters XEVO-G2 QTOF instrument, while NMR spectra were recorded in $CDCl_3$ using a Bruker DRX spectrometer operating at 400 MHz for ^{1}H and at 100 MHz for ^{13}C. Chemical shifts are given in ppm relative to the solvent signals (7.26 ppm for ^{1}H and 77.00 ppm for ^{13}C). All compounds described here were completely analysed by 2D NMR (COSY, HMQC, HMBC and NOESY), and as the syntheses start with the pure enantiomer damsin (1) all compounds are given with the absolute configuration in Figures 1 and 2. Chromatography was performed with 60 Å 30-75 µm silica gel, while TLC analyses were made on Silica Gel 60 F_{254} (Merck) plates.

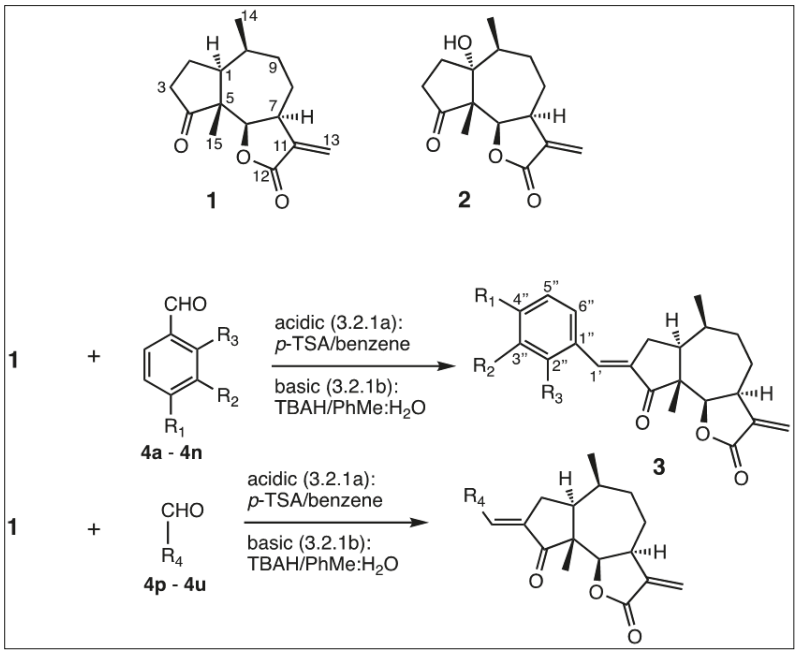

Compound	R_1	R_2	R_3	Compound	R_1	R_2	R_3
3a	H	H	H	**3k**	H	H	OCH_3
3b	CH_3	H	H	**3l**[a]	OH	H	H
3c	H	CH_3	H	**3m**[a]	H	OH	H
3d	H	H	CH_3	**3n**[a]	H	H	OH
3e	CH_3	H	CH_3	**3p**	R_4 = (*E*)-cyclohexyl		
3f	CF_3	H	H	**3q**	R_4 = (*Z*)-cyclohexyl		
3g	H	CF_3	H	**3r**	R_4 = ethyl		
3h	H	H	CF_3	**3s**	R_4 = propyl		
3i	OCH_3	H	H	**3t**	R_4 = 2-methyl propyl		
3j	H	OCH_3	H	**3u**	R_4 = 3-butenyl		

Figure 1. [a]The condensations to eventually give 3l, 3m, and 3n were carried out with the MOM-protected hydroxybenzaldehydes, prepared according to Figure 2 and the Experimental section. As damsin (1) was isolated as a pure enantiomer, the absolute configuration for all compounds is as shown in Figure 1.

1. Synthetic Procedures

1a. General Procedure for Claisen-Schmidt/aldol Condensations Under Acidic Conditions

A mixture of 1 (1 eq., 0.4027 mmol), aldehyde (1.3 eq., 0.5235 mmol), and p-TsOH (1.5 eq., 0.6040 mmol) in benzene (10 ml) was prepared in a sealed tube, and stirred at 80 °C for 19 to 66 h until the reaction was completed (monitored by TLC). The reaction was quenched by adding 2 ml of 5 % $NaHCO_3$ followed by 15 ml brine, and the mixture was extracted with DCM (3 x 15 ml). The combined organic layers were dried with $MgSO_4$ and concentrated in vacuo. The crude product was purified by silica gel chromatography (EtOAc:petroleum ether 1:1).

1b. General Procedure for Claisen-Schmidt/aldol Condensations Under Basic Conditions

A mixture of aldehyde (3 eq., 1.2081 mmol) and 1 (1 eq., 0.4027 mmol) in 50 % PhMe:H_2O 1:1 (3 ml) was cooled in an ice-bath, and TBAH (1.2 eq., 0.4832 mmol, 1.5 M in H_2O) was added dropwise. The ice-bath was removed after 10 min and the reaction was left to reach room temperature. The reaction was monitored by TLC, and after 3 to 24 h the reaction was quenched by addition of 2 ml of 5 % HCl and stirred for 15 min at r.t. The reaction mixture was diluted with 15 ml brine, and extracted with DCM (3 x 10 ml), and the combined organic layers were dried with $MgSO_4$ and concentrated in vacuo. The crude condensation product was purified by silica gel chromatography (EtOAc:petroleum ether 1:1).

1c. General Procedure for the MOM-Protection of the Hydroxybenzaldehydes.

To a solution of hydroxybenzaldehydes 4l – 4n (284.9 mg, 2.3333 mmol) in 6 ml dry DCM was added $EtN(i\text{-}Pr)_2$ (2 ml, 11.6665 mmol), followed by MOMBr (400 µl, 4.8999 mmol) dropwise under N_2 at 0 °C, whereafter the mixture was stirred at room temperature for 6 h. The reaction was quenched with 10 ml of a saturated solution of $NaHCO_3$ by stirring for 15 min at r.t., and the mixture was extracted with DCM (2 x 15 ml). The combined organic layers were dried with $MgSO_4$ and concentrated in vacuo. The product was purified by chromatography on silica gel (n-heptane:DCM 1:1).

1d. General Procedure for the Deprotection of the Claisen-Schmidt Adducts with MOM-Protected Hydroxyl Groups.

To a solution of a MOM protected Claisen-Schmidt adduct (50 mg, 0.1261 mmol) in MeOH (2.6 ml), HCl conc. (22.5 µl, 0.2695 mmol, 37 %) was added slowly. The reaction mixture was heated to 40 °C for 5 h and then cooled to room temperature, whereafter the organic solvent was evaporated in vacuo. The residue was dissolved in DCM (15 ml), washed with brine (10 ml), dried with $MgSO_4$, and concentrated in vacuo. The product was purified by chromatography on silica gel (EtOAc:petroleum ether 1:1).

2. Biological Assays

2a. Cell Lines

The normal-like epithelial MCF-10A cell line was purchased from American Type Culture Collection (Manassas, VA, USA) (CRL-10781) and was used as a representative for normal breast epithelial cells. The cell line retains many normal traits, including lack of tumorigenicity in nude mice, anchorage-dependent growth, and dependence on growth factors and hormones for proliferation and survival.[19,20] The MCF-10A cells were cultured in RPMI 1640 medium supplemented with 10 % heat-inactivated fetal calf serum (FCS), non-essential amino acids (1 mM), insulin (10 µg/ml), epidermal growth factor (20 ng/ml), cholera toxin (50 ng/ml), hydrocortisol (250 ng/ml), penicillin (100 U/ml), and streptomycin (100 µg/ml).

The JIMT-1 human breast carcinoma cell line (ACC589) was purchased from the German Collection of Microorganisms and Cell Cultures (Braunschweig, Germany). It carries an amplified HER-2 oncogene and is insensitive to HER-2 inhibiting drugs and belongs to the HER2 sub-type of breast cancer.[21,22] The JIMT-1 cells were routinely cultured in DMEM/Ham's F-12 medium supplemented with 10 % FCS, non-essential amino acids (1 mM), insulin (10 µg/ml), penicillin (100 U/ml) and streptomycin (100 µg/ml).

Both cell lines were kept at 37 °C in a humidified incubator with 5 % CO_2 in air. For the experiments, cells were seeded at the following densities: MCF-10A: 104 cells/cm2, and JIMT-1: 1.5×104 cells/cm2, in tissue culture vessels of the appropriate size to obtain the desired cell number for the different assays. The volume

of medium used was 0.2–0.3 ml per cm2. The cells were allowed to attach for 24 hours before the addition of the compounds.[23]

2b. Compound Solutions

The sample compounds were dissolved in DMSO to 100 mM stock solutions that were kept at -20 °C. Working solutions were diluted in PBS and all had a DMSO concentration of 0.2 %. In the assay, the cells were exposed to PBS with 0.02 % DMSO, or with the respective compounds at 0.1, 0.25, 0.5, 1, 2.5, 5, 10, and 20 µM concentrations.

2c. Dose Response Assay

The dose response to treatment with the compounds was evaluated using an MTT assay, which is based on reduction of MTT in the mitochondria of live cells. The amount of formazan produced is proportional to the number of living cells.[22, 23]

For the assay, cells were trypsinized and counted in a hemocytometer. Aliquots of 180 µl cell suspension containing 3000 cells (MCF-10A) or 5000 cells (JIMT-1) were seeded in 96-well plates. Compounds were added 24 h later to the final concentrations described above. At 72 h of drug treatment, 20 µl of MTT solution (5 mg/ml in PBS) was added to each well and the 96-well plates were returned to the CO_2 incubator for 1 h. The medium was then removed and the blue formazan crystals were dissolved by adding of 100 µl of 100 % DMSO per well. The plates were swirled gently at room temperature for 10 minutes to dissolve the crystals in the cells. Absorbance was monitored at 540 nm in a Multiskan™ FC Microplate Photometer (Thermo Fisher Scientific, Lund, Sweden) using the software SkanIt 3.1. For each compound, three dose response experiments were performed with six replicates for each one of them. GraphPad Prism version 6.01 for Windows (GraphPad Software, La Jolla, CA, USA), was used for drawing dose response curves and calculating the IC_{50} values, i.e. the dose giving 50 % reduction in cell number.[23]

Materials and Methods

3. The Preparation of the Assayed Compounds 3a - 3u.

3a. (E)-3-(Benzyliden)Damsin (3a)

3a was obtained as a colourless oil in 72 % yield after chromatographic purification of the product obtained after the Claisen-Schmidt condensation of 4a with 1 under acidic conditions as described in Experimental Procedure (EP) section 1a. $[\alpha]_D^{20}$ +8.1 (c 1.00, CH_2Cl_2); IR spectrum (film, ν, cm^{-1}): 3366, 3059, 2926, 2870, 1755, 1714, 1623, 1573, 1449, 1271, 1232, 1186, 1158, 1111, 983, 768, 733, 714, 693, 646; TOFMS: $[M+H^+]$, found 337.1832, $C_{22}H_{25}O_3$ requires 337.1804. See Tables 2 and 3 for ^1H and ^{13}C NMR shifts.

3b. (E)-3-(4-Methylbenzyliden)Damsin (3b)

3b was obtained as a colourless oil in 70 % yield after chromatographic purification of the product obtained after the Claisen-Schmidt condensation of 4b with 1 under acidic conditions as described in EP section 1a. $[\alpha]_D^{20}$ +29 (c 1.00, CH_2Cl_2); IR spectrum (film, ν, cm^{-1}): 2921, 2862, 1752, 1712, 1625, 1603, 1271, 1253, 1179, 1159, 1117, 119, 814, 743, 521; TOFMS: $[M+H^+]$, found 351.1922, $C_{23}H_{27}O_3$ requires 351.1915. See Tables 2 and 3 for ^1H and ^{13}C NMR shifts.

3c. (E)-3-(3-Methylbenzyliden)Damsin (3c)

3c was obtained as a colourless oil in 90 % yield after chromatographic purification of the product obtained after the Claisen-Schmidt condensation of 4c with 1 under acidic conditions as described in EP section 1a. $[\alpha]_D^{20}$ +3.0 (c 1.00, CH_2Cl_2); IR spectrum (film, ν, cm^{-1}): 2922, 1758, 1714, 1625, 1271, 1157, 1118, 993, 693; TOFMS: $[M+H^+]$, found 351.1933, $C_{23}H_{27}O_3$ requires 351.1915. See Tables 2 and 3 for ^1H and ^{13}C NMR shifts.

3d. (E)-3-(2-Methylbenzyliden)Damsin (3d)

3d was obtained as a colourless oil in 90 % yield after chromatographic purification of the product obtained after the Claisen-Schmidt condensation of 4d with 1 under acidic conditions as described in EP section 1a. $[\alpha]_D^{20}$ +62.6 (c 1.00, CH_2Cl_2); IR spectrum (film, ν, cm^{-1}): 2922, 2862, 1757, 1714, 1623, 1597, 1270, 1251, 1161, 1119, 982, 949, 759, 735; TOFMS: $[M+H^+]$, found 351.1934, $C_{23}H_{27}O_3$ requires 351.1915. See Tables 2 and 3 for ^1H and ^{13}C NMR shifts.

3e. (E)-3-(2,4-Dimethylbenzyliden)Damsin (3e)

3e was obtained as a colourless oil in 46 % yield after chromatographic purification of the product obtained after the Claisen-Schmidt condensation of 4e with 1 under acidic conditions as described in EP section 1a. $[\alpha]_D^{20}$ +12.2 (c 1.00, CH_2Cl_2); IR spectrum (film, ν,

Table 1. The cytotoxicity of compounds 1, 2, and 3a – 3u (see Figure 1), given as IC_{50} values (mM) calculated from experiments with six concentrations up to 20 mM. Standard deviations were obtained from [1]three dose-response curves or [2]four dose-response curves. na, not applicable.

Compound	MCF-10A (μM)	JIMT-1 (μM)	Ratio MCF-10A:JIMT-1
1	8.1 ± 0.4[2]	3.3 ± 0.6[2]	2.5
2	15.3 ± 0.9[2]	5.6 ± 0.8 [2]	2.7
3a	8.2 ± 1.6 [2]	1.7 ± 0.4 [1]	4.8
3b	3.7 ± 0.4[2]	2.1 ± 0.3[2]	1.8
3c	12.6 ± 1.6[2]	4.8 ± 0.3[2]	2.6
3d	11.1 ± 1.8[2]	4.7 ± 0.1[1]	2.4
3e	5.2 ± 1.5[2]	3.5 ± 0.7[2]	1.5
3f	3.1 ± 0.3[2]	1.8 ± 0.2[2]	1.7
3g	11.9 ± 0.4[1]	4.4 ± 0.7[1]	2.7
3h	13.0 ± 0.8[1]	8.1 ± 0.6[1]	1.6
3i	7.9 ± 1.2[2]	1.6 ± 0.1[2]	4.9
3j	> 20[1]	9.0 ± 1.0[1]	na
3k	> 20[1]	7.1 ± 0.2[1]	na
3l	13.6 ± 0.6[2]	2.9 ± 0.2[1]	4.7
3m	10.6 ± 1.3[2]	2.4 ± 0.1[2]	4.4
3n	6.7 ± 0.9[2]	2.1 ± 0.2[1]	3.2
3o	7.1 ± 0.6[2]	2.0 ± 0.6[2]	3.6
3p	11.7 ± 1.9[2]	8.1 ± 3.1[2]	1.4
3q	> 20[2]	12.3 ± 1.3[2]	na
3r	5.5 ± 1.1[1]	1.4 ± 0.1[1]	3.9
3s	12.6 ± 0.8[1]	3.7 ± 0.1[2]	3.4
3t	20.3 ± 0.3[1]	8.1 ± 0.1[1]	2.5
3u	17.5 ± 5.1[1]	1.7 ± 0.0[1]	10.3

Table 2. ^{1}H NMR chemical shifts (δ) for the assayed compounds 3a – 3u, determined at 400 MHz in $CDCl_3$.

	1-H	2-H_2	6-H	7-H	8-H_2	9-H_2	10-H	13-H_2	14-H_3	15-H_3	1′-H	2″-H	3″-H	4″-H	5″-H	6″-H
3a	2.07	2.87/2.97	4.65	3.28	1.80/2.06	1.74/1.89	2.28	5.57/6.28	1.17	1.16	7.44	7.41	7.54	7.37	7.54	7.41
3b[a]	2.06	2.84/2.94	4.63	3.38	1.80/2.07	1.74/1.88	2.27	5.56/6.27	1.17	1.14	7.4	7.43	7.21	-	7.21	7.43
3c[b]	2.05	2.84/2.94	4.63	3.28	1.80/2.06	1.73/1.87	2.28	5.56/6.26	1.17	1.14	7.38	7.32	-	7.17	7.3	7.32
3d[c]	2.03	2.74/2.94	4.64	3.28	1.81/2.06	1.70/1.86	2.24	5.57/6.28	1.16	1.18	7.65	-	7.23	7.26	7.24	7.46
3e[d]	2.03	2.75/2.94	4.65	3.28	1.82/2.09	1.70/1.86	2.24	5.57/6.29	1.19	1.16	7.66	-	7.07	-	7.07	7.38
3f	2.1	2.86/2.99	4.66	3.31	1.84/2.07	1.74/1.91	2.3	5.58/6.29	1.19	1.17	7.43	7.65	7.66	-	7.66	7.65
3g	2.1	2.85/2.98	4.65	3.3	1.84/2.08	1.75/1.91	2.31	5.58/6.29	1.19	1.17	7.43	7.76	-	7.62	7.55	7.71
3h	2.05	2.65/2.90	4.64	3.29	1.81/2.03	1.72/1.85	2.22	5.56/6.27	1.14	1.18	7.71	-	7.58	7.58	7.45	7.71
3i[e]	2.06	2.82/2.92	4.63	3.27	1.79/2.04	1.74/1.86	2.27	5.56/6.26	1.16	1.13	7.37	7.5	9.93	-	6.93	7.5
3j[f]	2.06	2.86/2.95	4.64	3.28	1.80/2.03	1.72/1.86	2.27	5.57/6.27	1.16	1.15	7.38	7.05	-	6.92	7.33	7.14
3k[g]	2.01	2.73/2.91	4.59	3.25	1.77/2.04	1.72/1.84	2.22	5.55/6.24	1.14	1.14	7.82	-	6.89	7.32	6.96	7.47
3l	2.07	2.81/2.91	4.67	3.3	1.81/2.04	1.72/1.90	2.27	5.59/6.29	1.16	1.14	7.36	7.43	6.93	-	6.93	7.43
3m	2.01	2.80/2.90	4.71	3.34	1.84/2.04	1.74/1.90	2.24	5.59/6.29	1.14	1.12	7.48	7.08	-	6.91	7.25	7.25
3n	2.04	2.79/2.94	4.64	3.29	1.82/2.06	1.73/1.87	2.24	5.58/6.29	1.16	1.17	7.92	-	6.94	7.22	6.9	7.45
3o[h]	1.99	1.71/1.87	4.5	3.31	1.79/2.02	1.69/1.81	2.16	5.53/6.29	1	0.91	2.66/3.19	7.17	7.28	7.21	7.28	7.17
3p[i]	2	2.51/2.59	4.59	3.26	1.78/2.03	1.71/1.84	2.23	5.54/6.26	1.1	1.08	6.47	1.23/1.66	1.26/1.75	1.77 br	1.26/1.75	1.23/1.66
3q[j]	2.01	1.82/2.55	4.47	3.28	1.82/2.03	1.72/1.80	2.21	5.52/6.26	1.05	1.03	5.43	1.59/2.08	1.65/1.97	1.71 br	1.65/1.97	1.59/2.08
3r[k]	2	2.50/2.58	4.6	3.26	1.79/2.02	1.71/1.86	2.23	5.55/6.26	1.11	1.09	6.61	2.16	1.06	-	-	-
3s[l]	1.98	2.47/2.53	4.56	3.24	1.76/2.00	1.68/1.79	2.19	5.52/6.20	1.06	1.04	6.57	2.09	1.44	0.88	-	-
3t[m]	1.96	2.50/2.54	4.59	3.25	1.74/1.86	1.70/1.84	2.19	5.53/6.23	1.07	1.05	6.62	2.02	1.76	0.89	0.89	-
3u[n]	2	2.47/2.55	4.6	3.26	1.78/2.02	1.73/1.85	2.24	5.51/6.26	1.09	1.08	6.61	2.25	2.22	5.78	5	-

[a]Aromatic methyl group at 2.37. [b]Aromatic methyl group at 2.37. [c]Aromatic methyl group at 2.39. [d]Aromatic methyl groups at 2.34 and 2.38. [e]Aromatic methoxy group at 3.83. [f]Aromatic methoxy group at 3.83. [g]Aromatic methoxy group at 3.83. [h]A signal for 3-H at 2.56. [i]A signal for 1"-H at 2.21. [j]A signal for 1"-H at 2.54. [k]Signals for the ethyl group at 2.16 and 1.06. [l]Signals for the propyl group at 2.09, 1.44 and 0.88. [m]Signals for the 2-methyl propyl group at 2.02, 1.76 and 0.89. [n]Signals for the 3-butenyl group at 5.78, 5.00, 2.25 and 2.22.

Table 3. ^{13}C NMR chemical shifts (δ) for the assayed compounds 3a – 3u, determined at 100 MHz in $CDCl_3$.

	C-1	C-2	C-3	C-4	C-5	C-6	C-7	C-8	C-9	C-10	C-11	C-12	C-13	C-14	C-15	C-1′	C-1″	C-2″	C-3″	C-4″	C-5″	C-6″
3a	43.6	31.4	133.3	207.9	54.8	81.8	44.8	26.5	34.2	34.1	140.1	170.2	121.2	15.7	14.5	133.9	129	130.6	128.8	135.4	128.8	130.6
3b[a]	43.6	31.4	132.4	208.1	54.8	81.9	44.8	26.5	34.3	34.1	140.1	170.3	121.3	15.8	14.5	133.9	132.6	130.6	129.6	140	129.6	130.6
3c[b]	43.6	31.4	133.2	208.1	54.8	81.9	44.8	26.5	34.2	34	140.1	170.3	121.3	15.8	14.5	134	135.3	131.4	138.4	130.4	128.7	127.6
3d[c]	43.9	31.3	134.1	207.9	54.9	81.9	44.8	26.4	34.1	34	140.1	170.3	121.2	15.8	14.5	131.5	134.1	139	130.7	129.4	125.9	128.7
3e[d]	44	31.5	133.3	208	55	82	45	26.5	34.3	34.2	140.2	170.4	121.2	15.9	14.6	131.7	131.4	139.3	131.6	139.8	126.7	128.8
3f[e]	43.6	31.4	135.8	207.6	55	81.7	44.8	26.4	34.1	34	139.9	170.2	121.5	15.7	14.4	132	138.9	130.6	125.7	130.8	125.7	130.6
3g[f]	43.7	31.2	135.2	207.7	54.9	81.8	44.8	26.4	34.2	34	140	170.3	121.4	15.7	14.5	132	131.4	126.8	136.2	125.9	129.4	133.5
3h[g]	43.7	31.1	137	207	55	81.7	44.7	26.3	34	34	139.9	170.3	121.3	15.7	14.4	129.4	129.8	134.1	130.1	131.7	128.8	126.3
3i[h]	43.6	31.4	130.9	208	54.7	81.9	44.9	26.6	34.3	34.1	140.2	170.3	121.2	15.8	14.6	133.7	128.1	132.4	114.3	160.7	114.3	132.4
3j[i]	43.6	31.4	133.7	208	54.8	81.8	44.8	26.5	34.2	34	140.1	170.3	121.3	15.7	14.5	133.8	136.7	116.1	159.7	115	129.8	123.1
3k[j]	43.6	31.4	133.2	207.9	54.7	81.9	44.8	25.4	34.1	34	140.1	170.4	121.1	15.8	14.5	128.5	124.3	158.8	110.8	131.1	120.2	129.6
3l	43.8	31.4	130.3	208.7	54.8	82.3	44.8	26.5	34.3	34.1	140.1	170.9	121.7	15.8	14.6	134.7	127.5	132.8	116.1	158.2	116.1	132.8
3m	43.6	31.5	133.3	208.8	54.9	82.4	44.5	26.3	34.1	34	139.9	171.1	121.9	15.7	14.5	134.8	136.8	122	156.7	117.3	129.8	118.5
3n	43.8	31.4	132	209.1	55	82.1	44.8	26.5	34.2	34.1	140.1	170.7	121.5	15.8	14.6	129.8	122.5	156.8	116.4	131.5	120	129.6
3o	44.1	30.6	50.3	218.6	55.3	81.9	44.5	25.6	33.1	34.2	139.6	170.3	120.8	14.6	14	36.3	139.4	129.2	128.5	126.4	128.5	129.2
3p	43.2	28.6	132.8	207.6	55.4	81.9	44.9	26.5	34.2	34.2	140.2	170.4	121.1	15.8	14.4	143.1	39.1	31.7	25.6	25.1	25.6	31.7
3q	44.1	28.3	135.4	219.9	55.3	82	44.6	25.3	33.3	34.3	139.6	170.3	120.8	16.2	14.3	122.9	39.5	31.6	25.8	25.5	25.8	31.6
3r	43.1	28.5	134.1	207.2	55.5	81.9	44.9	26.5	34.2	34.2	140.1	170.3	121.2	15.8	14.4	139.7	23.2	12.9	-	-	-	-
3s	43	28.6	134.8	207	55.3	81.8	44.7	26.3	34	34	140	170.3	121.1	15.7	14.2	138.1	31.7	21.6	13.9	-	-	-
3t	43	28.8	135.3	207	55.4	81.9	44.7	26.4	34.1	34.1	140.1	170.4	121.2	15.7	14.3	137.4	38.9	28.2	22.6	22.6	-	-
3u	43.1	28.7	135.1	206.9	55.5	81.8	44.8	26.4	34.2	34.2	140.1	170.3	121.2	15.7	14.4	137.3	29.2	34.3	137.3	115.6	-	-

[a]Aromatic methyl group at 21.5. [b]Aromatic methyl group at 21.5. [c]Aromatic methyl group at 20.0. [d]Aromatic methyl groups at 21.4 and 20.0. [e]A signal for an aromatic -CF_3 group at 122.7. [f]A signal for an aromatic -CF_3 group at 122.5. [g]A signal for an aromatic -CF_3 group at 122.5. [h]Aromatic methoxy group at 55.4. [i]Aromatic methoxy group at 55.4. [j]Aromatic methoxy group at 55.5.

cm^{-1}); 2922, 2857, 1758, 1713, 1625, 1606, 1448, 1384, 1336, 1271, 1241, 1190, 1162, 1119, 1068, 984, 816. TOFMS: [M+H$^+$], found 365.2109, $C_{24}H_{29}O_3$ requires 365.2117. See Tables 2 and 3 for ^{1}H and ^{13}C NMR shifts.

3f. (E)-3-((4-Trifluoromethylbenzyliden)Damsin (3f)

3f was obtained as a colourless oil in 88 % yield after chromatographic purification of the product obtained after the Claisen-Schmidt condensation of 4-(trifluoromethyl)benzaldehyde with 1 under acidic conditions as described in EP section 1a. $[\alpha]_D^{20}$ +0.9 (c 1.00, CH_2Cl_2); IR spectrum (film, γ, cm^{-1}): 2925, 2863, 1758, 1717, 1630, 1322, 1163, 1116, 1068, 1014, 984; TOFMS: [M+H$^+$], found 405.1657, $C_{23}H_{24}F_3O_3$ requires 405.1633. See Tables 2 and 3 for ^{1}H and ^{13}C NMR shifts.

3g. (E)-3-((3-Trifluoromethylbenzyliden)Damsin (3g)

3g was obtained as a colourless oil in 56 % yield after chromatographic purification of the product obtained after the Claisen-Schmidt condensation of 4g with 1 under basic conditions as described in EP section 1b. $[\alpha]_D^{20}$ -6.7 (c 1.00, CH_2Cl_2); IR spectrum (film, γ, cm^{-1}): 2924, 2864, 1758, 1716, 1630, 1327, 1271, 1160, 1073, 1119, 1000, 986, 808, 696, 736; TOFMS: [M+H$^+$], found 405.1655 $C_{23}H_{24}F_3O_3$ requires 405.1633. See Tables 2 and 3 for ^{1}H and ^{13}C NMR shifts.

3h. (E)-3-((2-Trifluoromethylbenzyliden)Damsin (3h)

3h was obtained as a colourless oil in 88 % yield after chromatographic purification of the product obtained after the Claisen-Schmidt condensation of 4h with 1 under acidic conditions as described in EP section 1a. $[\alpha]_D^{20}$ +36.8 (c 1.00, CH_2Cl_2); IR spectrum (film, γ, cm^{-1}): 2925, 1758, 1719, 1631, 1486, 1452, 1387, 1335, 1313, 1286, 1271, 1252, 1154, 1116, 1059, 1034, 985, 814, 799, 769, 735, 666; TOFMS: [M+H$^+$], found 405.1634 $C_{23}H_{24}F_3O_3$ requires 405.1633. See Tables 2 and 3 for ^{1}H and ^{13}C NMR shifts.

3i. (E)-3-(4-Methoxybenzyliden)Damsin (3i)

3i was obtained as a colourless oil in 87 % yield after chromatographic purification of the product obtained after the Claisen-Schmidt condensation of 4i with 1 under acidic conditions as described in EP section 1a. $[\alpha]_D^{20}$ +54.4 (c 1.00, CH_2Cl_2); IR spectrum (film, γ, cm^{-1}): 2942, 2902, 2869, 2846, 1752, 1709, 1623, 1592, 1510, 1272, 1254, 1179, 1148, 1122, 1027, 979, 940, 835, 814; TOFMS: [M+H$^+$], found 367.1891 $C_{23}H_{27}O_4$ requires 367.1865. See Tables 2 and 3 for ^{1}H and ^{13}C NMR shifts.

3j. (E)-3-(3-Methoxybenzyliden)Damsin (3j)

3j was obtained as a colourless oil in 73 % yield after chromatographic purification of the product obtained after the Claisen-Schmidt condensation of 4j with 1 under acidic conditions as described in EP section 1a. $[\alpha]_D^{20}$ +2.4 (c 1.00, CH_2Cl_2); IR spectrum (film, γ, cm^{-1}): 2958, 2862, 1752, 1709, 1623, 1592, 1510, 1272, 1254, 1179, 1148, 1122, 1027, 979, 940, 835; TOFMS: [M+H$^+$], found 367.1856 $C_{23}H_{27}O_4$ requires 367.1865. See Tables 2 and 3 for ^{1}H and ^{13}C NMR shifts.

3k. (E)-3-(2-Methoxybenzyliden)Damsin (3k)

3k was obtained as a colourless oil as the single product obtained after the Claisen-Schmidt condensation of 4k with 1 under acidic conditions as described in EP section 1a. $[\alpha]_D^{20}$ +58.2 (c 1.00, CH_2Cl_2); IR spectrum (film, γ, cm^{-1}): 2928, 2859, 1757, 1712, 1619, 1596, 1486, 1463, 1437, 1270, 1247, 1188, 1161, 1119, 984, 814, 754, 743; TOFMS: [M+H$^+$], found 367.1849 $C_{23}H_{27}O_4$ requires 367.1865. See Tables 2 and 3 for ^{1}H and ^{13}C NMR shifts.

3l (E)-3-(4-Hydroxybenzyliden)Damsin (3l)

4l was protected to 4x according to EP section 1c, 4x was condensed with 1 under basic conditions as described in EP section 1b to form 3x. 3x was subsequently deprotected to 3l according to EP section 1d, 3l was obtained as a colourless oil in 23 % overall yield (from 1) after chromatographic purification of the crude product. $[\alpha]_D^{20}$: +33.0 (c 1.00, CH_2Cl_2); IR spectrum; 3319, 2923, 2853, 1755, 1737, 1706, 1595, 1578, 1511, 1469, 1443, 1272, 1254, 1168, 1157, 1120,1104, 984, 833, 816; TOFMS: [M+H$^+$], found 353.1722 $C_{22}H_{25}O_4$ requires 353.1708. See Tables 2 and 3 for ^{1}H and ^{13}C NMR shifts.

3m (E)-3-(3-Hydroxybenzyliden)Damsin (3m)

4m was protected to 4y according to EP section 1c, 4y was condensed with 1 under basic conditions as described in EP section 1b to form 3y. 3y was subsequently deprotected to 3m according to EP section 1d, 3l was obtained as a colourless oil in 43 % overall yield (from 1) after chromatographic purification of the crude product. $[\alpha]_D^{20}$ -11.7 (c 1.00, CH_2Cl_2); IR spectrum

(film, γ, cm^{-1}); 3353, 2927, 2864, 1735, 1712, 1621, 1591, 1578, 1490, 1471, 1449, 1272, 1228, 1158, 1112, 1119, 992, 785, 687; TOFMS: [M+H$^+$], found 353.1733 $C_{22}H_{25}O_4$ requires 353.1708. See Tables 2 and 3 for ^{1}H and ^{13}C NMR shifts.

3n (E)-3-(2-Hydroxybenzyliden)Damsin (3n)

4n was protected to 4z according to EP section 1c, 4z was condensed with 1 under basic conditions as described in EP section 1b to form 3z. 3z was subsequently deprotected to 3n according to EP section 1d, 3n was obtained as a colourless oil in 27 % overall yield (from 1) after chromatographic purification of the crude product. $[\alpha]_D^{20}$ +29.5 (c 1.00, CH_2Cl_2); IR spectrum (film, γ, cm-1): 3353, 2927, 2864, 1735, 1712, 1621, 1591, 1578, 1490, 1471, 1449, 1272, 1228, 1158, 1112, 1119, 992, 785, 687; TOFMS: [M+H$^+$], found 353.1704 $C_{22}H_{25}O_4$ requires 353.1708. See Tables 2 and 3 for ^{1}H and ^{13}C NMR shifts.

3o. (E)-3-Benzyldamsin (3o)

The procedure for preparing 3o is shown in Figure 2. The Michael acceptor functionality of 1 was protected by adding 1 in EtOH (6 ml) to a solution of PhSNa (3.7 eq., 7.4499 mmol) in EtOH (10 ml). The reaction mixture was stirred under N_2 atmosphere at room temperature for 3h until completion, quenched with concentrated AcOH (2.5 ml) and H_2O (4 ml) at 0 ° C. After stirring for an additional 5 minutes, the aqueous phase was extracted with DCM (3 x 10 ml) and the organic layers were dried with Na_2SO_4, concentrated in vacuo and purified by chromatography on silica gel (EtOAc:petroleum ether 1:1) to yield the protected product 5. This was condensed with benzaldehyde as described above, to give 6. A vial with Pd/C (100 mg) was purged with vacuum/H_2 for two cycles to remove air from the reaction tube, whereafter EtOH (2 ml) and a solution of the protected 6 (100 mg, 0.2790 mmol) in DCM (1 ml) and EtOH (1 ml) was added then the mixture of reaction was hydrogenated at ambient pressure and temperature (20 °C) for 29 h. The progress of reaction was followed with TLC. The reaction mixture was filtered in vacuo through a short path of Celite and washed with ethyl acetate (3 ml). The organic layers were concentrated in vacuo to obtain the protected compound 7. For the deprotection, $NaIO_4$ (2.1 eq., 0.0515 mmol) was added to a stirred solution of compound 7 (1 eq., 0.0468 mmol) in MeOH:H_2O (1:9, 3 ml) and the reaction mixture was stirred at room temperature for 33 h. When completed it was diluted with DCM (20 ml) and the organic layer was washed with 15 ml of water, whereafter the organic layer were dried with Na_2SO_4 and concentrated in vacuo to give the elimination product. This mixture of reaction was warmed in PhMe (4 ml) at 120 °C in order to complete the elimination of PhSOH. The crude extract was purified by silica gel chromatography with EtOAc:n-heptane 1:1, to yield 3o with the overall yield 18 % (starting from 1). $[\alpha]_D^{20}$ +36.1 (c 1.00, CH_2Cl_2); IR spectrum (film, γ, cm^{-1}): 2924, 2870, 1758, 1739, 1625, 1451, 1385, 1338, 1271, 1160, 1118, 1046, 1025, 1002, 981, 949, 815, 753, 699 TOFMS [M+H$^+$], found 339.1960 $C_{22}H_{27}O_3$ requires 339.1960. See Tables 2 and 3 for ^{1}H and ^{13}C NMR shifts.

3p. (E)-3-(Cyclohexylmethylene)Damsin (3p)

3p was obtained as a colourless oil in 42 % yield after chromatographic purification of the product obtained after the Claisen-Schmidt condensation of 4p with 1 under acidic conditions as described in EP section 1a. $[\alpha]_D^{20}$ -33.6 (c 1.00, CH_2Cl_2); IR spectrum (film, γ, cm^{-1}): 2923, 2851, 1757, 1720, 1649, 1448, 1384, 1346, 1270, 1250, 1190, 1156, 1101, 993, 953, 802. TOFMS [M+H$^+$], found 343. 2261, $C_{22}H_{31}O_3$ requires 343. 2273. See Tables 2 and 3 for ^{1}H and ^{13}C NMR shifts.

3q. (Z)-3-(Cyclohexylmethylene)Damsin (3q)

3q was obtained as a colourless oil in 20 % yield after chromatographic purification of the product obtained after the Claisen-Schmidt condensation of 4q with 1 under acidic conditions as described in EP section 1a. $[\alpha]_D^{20}$ +34.4 (c 1.00, CH_2Cl_2); IR spectrum (film, γ, cm^{-1}): 2924, 2870, 1738, 1660, 1449, 1384, 1341, 1271, 1162, 1119, 1002, 977, 949. TOFMS [M+H$^+$], found 343. 2279 $C_{22}H_{31}O_3$ requires 343. 2273. See Tables 2 and 3 for ^{1}H and ^{13}C NMR shifts.

3r. (E)-3-Propylidenedamsin (3r)

3r was obtained as a colourless oil in 20 % yield after chromatographic purification of the product obtained after the Claisen-Schmidt condensation of 4r with 1 under acidic conditions as described in EP section 1a. $[\alpha]_D^{20}$ -53.7 (c 1.00, CH_2Cl_2); IR spectrum (film, γ, cm^{-1}): 2927, 1757, 1649, 1271, 979; TOFMS: [M+H$^+$],

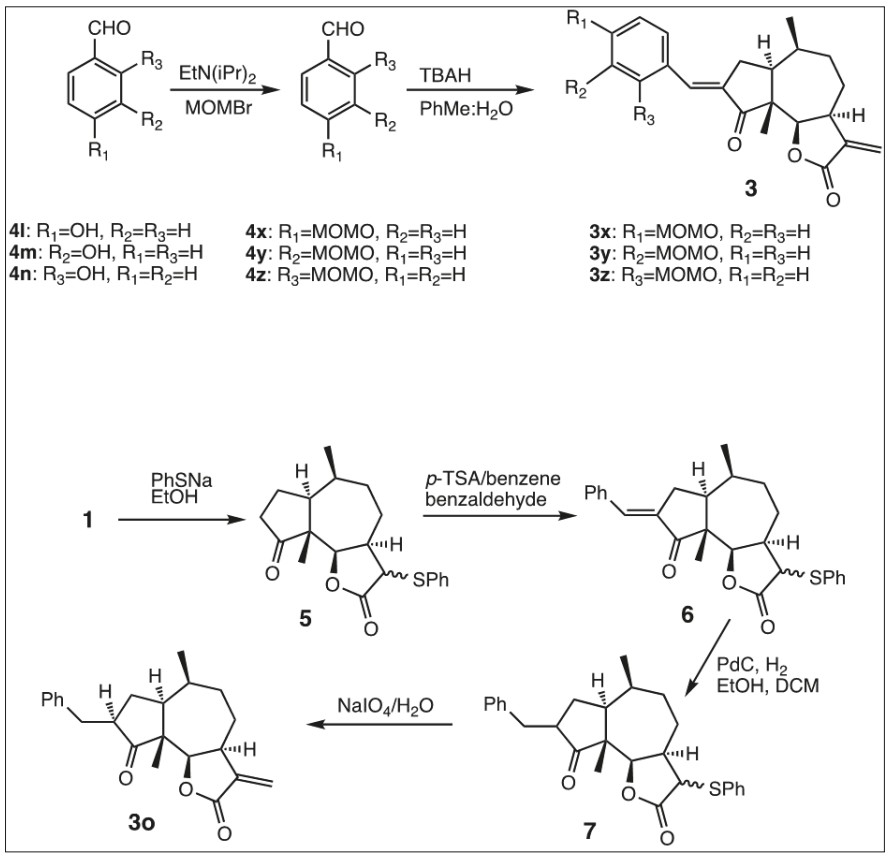

Figure 2. The hydroxybenzaldehydes 4l – 4n were protected using MOMBr and EtN(*i*Pr)$_2$, and the condensations of the protected hydroxybenzaldehydes 4x - 4z with 1 were carried out under basic conditions (3.2.1b). The reduced derivative 3o was prepared by protection of C-13 of 1 as a phenyl thiol ether (5), the condensation of 5 with benzaldehyde under acidic conditions (3.2.1a) to give 6, which was hydrogenated to 7 and deprotected to yield 3o.

found 289.1786, $C_{18}H_{25}O_3$ requires 289.1759. See Tables 2 and 3 for ^1H and ^{13}C NMR shifts.

3s. (E)-3-ButylideneDamsin (3s)

3s was obtained as a colourless oil in 42 % yield after chromatographic purification of the product obtained after the Claisen-Schmidt condensation of 4s with 1 under basic conditions as described in EP section 1b. $[\alpha]_D^{20}$ -44.0 (c 1.00, CH_2Cl_2); IR spectrum (film, γ, cm^{-1}): 2929, 1758, 1719, 1649, 1269, 1111, 954, 814, 731; TOFMS: $[M+H^+]$, found 303.1864, $C_{19}H_{27}O_3$ requires 302.1882. See Tables 2 and 3 for ^1H and ^{13}C NMR shifts.

3t. (E)-3-(3-Methylbutylidene)Damsin (3t)

3t was obtained as a colourless oil in 42 % yield after chromatographic purification of the product obtained after the Claisen-Schmidt condensation of 4t with 1 under basic conditions as described in EP section 1b. $[\alpha]_D^{20}$ -63.0 (c 1.00, CH_2Cl_2); IR spectrum (film, γ, cm^{-1}): 2955, 1757, 1649, 1271, 967; TOFMS: $[M+H^+]$, found 317.2100, $C_{20}H_{29}O_3$ requires 317.2072. See Tables 2 and 3 for ^1H and ^{13}C NMR shifts.

3u. (E)-3-(Pent-4-en-1-ylidene)Damsin (3u)

3u was obtained as a colourless oil in 36 % yield after chromatographic purification of the product obtained after the Claisen-Schmidt condensation of 4u with 1 under basic conditions as described in EP section 1b. $[\alpha]_D^{20}$ -50.6 (c 1.00, CH_2Cl_2); IR spectrum (film, γ, cm^{-1}): 2921, 1757, 1719, 1850, 1271, 1112, 994; TOFMS: $[M+H^+]$, found 315.1926 $C_{20}H_{27}O_3$ requires 315.1915. See Tables 2 and 3 for ^1H and ^{13}C NMR shifts.

Results

Damsin (1) and coronopilin (2) were isolated from the plant Ambrosia arborescens as previously described.[14] Since 1 can be obtained in good amounts from the plant, we investigated the possibility to modify the structure of 1 while retaining the α-methylene-γ-lactone moiety intact. The latter is important as procedures that require that this functionality is protected/deprotected would waist too much starting material. The Claisen-Schmidt condensation of 1 with aromatic aldehydes, under either acidic or basic conditions, was found to work reasonably well and without affecting the α-methylene-γ-lactone moiety of 1. The condensation between 1 and benzaldehyde yielded (E)-3-benzylidendamsin (3a), and when the cytotoxicity of 3a towards the two cell lines was compared to that of 1, 3a was found to be more potent in JIMT-1 cells than in MCF-10A cells and thereby more selective for cancer cells than normal cells (see Table 1). Apparently an (E)-3-benzyliden substituent has a favourable effect, either on the reactivity of the α-methylene-γ-lactone moiety, or on the association of 3a with critical cellular components such as proteins. To investigate this further, we decided to expand the investigation and study 3-benzyliden derivatives formed by the Claisen-Schmidt condensation of 1 with the aromatic aldehydes 4a – 4n. The 13 derivatives 3b – 3n (see Figure 1) substituted with methyl , triflouro-, methoxy- and hydroxyl groups were prepared, and assayed for cytotoxicity (see Table 1). In general, the condensations proceeded well, and often, but not always, best under acidic conditions (the yields are given in Materials and Methods). However, it was not possible to use the hydoxybenzaldehydes 4l – 4n directly (to produce 3l – 3n), instead the hydroxyl groups had to be protected as MOMO substituents to form 4x – 4z (see Figure 2) prior to the condensation with 1, to form compounds 3x – 3z (see Figure 2). These were subsequently deprotected as described in the Experimental section, to yield 3l – 3n. The condensations with aromatic aldehydes were highly stereoselective, only the E-alkenes were obtained. To investigate the influence of the double bond resulting from the condensation, the reduced derivative 3o was prepared. As direct hydrogenation of 3a also reduced the C-11/C-13 double bond in the α-methylene-γ-lactone moiety, it was necessary to first protect the C-11/C-13 double bond of 1 as the 13-phenylthio ether to give compound 5 (see Figure 2). 5 was then condensed with benzaldehyde to give 6 which subsequently was reduced to 7 and deprotected to obtain the desired product 3o (see Figure 2 and Materials and Methods). In order to investigate if the 3-substituent needs to be aromatic, the condensation was also carried out with cyclohexanecarbaldehyde. In this aldol condensation both the E (3p) and the Z (3q) isomers were obtained, which gave us an opportunity to investigate the influence of this double bond's configuration on the activity. Finally, aldol condensations were also

performed with a few alkyl- and alkenyl aldehydes, producing the derivatives 3r – 3u for comparison.

Discussion

The structures of all compounds prepared in this investigation was carefully determined by 1- and 2D NMR experiments (including COSY, NOESY, HMQC and HMBC experiments), in combination with the IR and HRMS data reported in the Experimental section. The configuration of the C-3/C-1' double bond was determined by NOESY NMR experiments. For the E isomers correlations were observed between 2-H_2 and 2''-H/6''-H (for 3a - 3n) or 1''-H_2 (for 3p - 3u), and between 1'-H and 2-H_2 for the Z-isomer 3q. The absolute configuration of C-3 in derivative 3o was suggested by the observed NOESY correlation between 1-H and 3-H, as well as the lack of NOESY correlations between both 14-H_3 and 15-H_3, and 3-H. This configuration is also supported by the ^{1}H-^{1}H coupling constants observed, 8.4 and 12.1 Hz between 3-H and 2-H_2 as well as 3.9 and 8.8 Hz between 3-H and 1'-H_2.

The chemical shifts for all proton and carbon signals observed in $CDCl_3$ are presented in Tables 2 and 3. In all cases, the NMR couplings observed between protons are those that we expected from our previous experience from this type of compounds, and are for reasons of space not reported here. The comparison of the proton and carbon shifts in Tables 2 and 3 gives some interesting information. Firstly, in all the prepared and assayed compounds except for 3o, a second Michael acceptor functionality (C-1'/C-3/C-4/4-O) is created by the condensation, and one may ask if this also is involved in the chemical reactivity of the compounds. The NMR chemical shifts, as well as the reactivity of the compounds, are strongly influenced by the electronic properties of the chemical bonds close to a specific nucleus or involved in a reactive functionality. Michael acceptors are more reactive if they are perfectly conjugated and situated in a plane, which is reflected in the chemical shifts of the atoms involved. If this new Michael acceptor functionality is well conjugated and thereby reactive, one would expect the carbon shift of the keto functionality (C-4) to be below 200, not close to 210. The exceptions are 3o which has no double bond for conjugation (carbon shift of C-4 218.6), and the Z-isomer 3q in which this Michael acceptor functionality for steric reasons can not be in a plane. The conclusion is therefore that only a weak conjugation is present, and that the reactivity of the C-1'/C-3/C-4/4-O Michael acceptor is small. Secondly, assuming that the α-methylene-β-lactone moiety is critical for the cytotoxicity of all compounds assayed, it is interesting to compare the chemical shifts of 6-H, 7-H, 13-H_2, C-6, C-7, C-11, C-12 and C-13 of the assayed compounds, in search for any indication that the substituent at C-3 affect the electronic properties of this lactone ring. 6-H are all between 4.6 and 4.7 ppm, except in 3o and 3q in which the shift is slightly lower (due to the lack of conjugation discussed above). 7-H are all between 3.2 and 3.3 ppm, 13-Ha are between 5.5 and 5.6 ppm, while 13-Hb are between 6.2 and 6.3 ppm. All C-6 values are close to 82 ppm, C-7 between 44.5 and 45.0 ppm, C-11 between 139.6 and 140.2 ppm, C-12 between 170.2 and 171.1 ppm, and C-13 between 120.8 and 121.9. So, the electronic properties of the α-methylene-β-lactone moiety remains essentially intact, and independent of the C-3 substituent. The conclusion is therefore that the differences in cytotoxic activities shown in Table 1 and discussed below, depend on the molecular interaction that the C-3 substituent can provide with a protein at the site where a Michael addition can take place.

Conclusion

The MCF-10A cell line used in this study is a non-tumorigenic breast epithelial cell line[15] while the JIMT-1 cells are breast cancer-derived tumorigenic.[16] Table 1 shows the experimental cytotoxicity IC_{50} values in μM obtained with the two cell lines, calculated from the dose response curves. In addition, the ratios between the IC_{50} MCF-10A and IC_{50} JIMT-1 were calculated, and are presented in Table 1 as a measure for the selectivity of each compound. As indicated above, (E)-3-benzylidendamsin (3a) possessing a phenylmethylene group in position 3, has a similar cytotoxicity as 1 in MCF-10A cells although it is more potent in JIMT-1 cells, and this simple improvement of potency and selectivity was the starting point for this investigation. The IC_{50} values show consistently that the JIMT-1 cells are more sensitive to the compounds assayed compared to the MCF-10A cells. It is interesting to compare the toxicity with the population doubling time of the two cell lines. For MCF-10A cells this is

approximately 17 h, while for JIMT-1 cells it is 24 h. Consequently, the MCF-10A cells have had a longer exposure time since they have had the possibility to go through more population doublings, suggesting that the toxicity is not related to the rate of cell proliferation but to some other intrinsic property in the cells. One such property could be the intracellular glutathione level. Glutathione has been shown to reduce the toxicity of sesquiterpene lactones[17] and MCF-10A cells have been shown to have a slightly higher glutathione level than JIMT-1 cells.[18]

The cytotoxicity of the reduced derivative 3o is similar to that of 3a, indicating that the double bond created at C-3 by the condensation is unimportant. Replacing the phenyl group of 3a with a cyclohexyl (in 3p) decreases both potency and selectivity, and when comparing 3p with 3q it is obvious that an E configuration of the C-3 double bond is preferable. None of the methylated derivatives 3b – 3e is more potent compared to 3a, although the p-substituted derivative 3b has a similar potency, and they are all less selective. Methyl substituents in the benzene ring are therefore not beneficial. For the trifluoromethyl derivatives 3f – 3h there is a strong tendency that p-substitution is better for the potency than m-substitution, and m is better than o, but all three suffer from lower selectivity. For the methoxylated derivatives 3i – 3k, it is obvious that the p-methoxy derivative 3i not only retains the potency of 3a but also the selectivity. However, the m- and o-methoxy derivatives 3j and 3k are considerably less cytotoxic. Furthermore, the p-hydroxy derivative 3l retains much of the potency and selectivity of 3a, although the m- and o-hydroxyl derivatives 3m and 3n are even more potent than 3l. The differences in the trends observed may be explained by the ability of the hydroxyl group to both give and accept hydrogen bonds, which is not the case for the other substituents used here. Also, the size of a hydroxyl group is smaller than a trifluoromethyl or methoxy group, so there may be a steric component. For the alkenyl derivatives 3r – 3u, the results are quite interesting. The smallest, 3r, is as potent and selective as 3a, indicating that a short alkyl group influences the molecular interaction as much as a phenyl group. An extra methyl group (as in 3s) is less advantageous, while two extra methyl groups (as in 3t) is even worse for both potency and selectivity. Remarkably, by keeping the same number of carbons in the chain but without branching and with a double bond in the end (as in 3u), the potency is the same as that of 3a while the selectivity is high. With a ratio of IC_{50} MCF-10A cells and IC_{50} JIMT-1 cells greater than 10, 3u is the most selective derivative prepared in this investigation, and will be a future starting point for the development of this class of compounds.

Acknowledgments

The authors thank the Swedish International Development Agency (SIDA) for the financial support of this study, which is part of the project "Biomolecules of medicinal and industrial interest" developed between the Universidad Mayor de San Andrés (UMSA La Paz – Bolivia) and Lund University (Sweden).

Conflict of Interest

No author has any associations that may represent a potential conflict of interest.

References

1. Cragg GM, Newman DJ (2013) Natural products: a continuing source of novel drug leads. Biochimica et biophysica acta. 1830 (6), 3670-3695.
2. Atanasov AG, Waltenberger B, Pferschy-Wenzig EM, Linder T, WawroschC et al. (2015) Discovery and resupply of pharmacologically active plant-derived natural products: A review. Biotechnology advances. 33 (8), 1582-1614.
3. Weldon CB, Burow ME, Rolfe KW, Clayton JL, Jaffe BM et al. (2001) NF-κB–mediated chemoresistance in breast cancer cells. Surgery. 130 (2), 143-150.
4. Zhang S, Won YK, Ong CN, Shen HM (2005) Anti-cancer potential of sesquiterpene lactones: bioactivity and molecular mechanisms. Current medicinal chemistry. Anti-cancer agents. 5,(3), 239-249.
5. Ghantous A, Gali-Muhtasib H, Vuorela H, Saliba NA, Darwiche N (2010) What made sesquiterpene lactones reach cancer clinical trials? Drug discovery today. 15 (15-16), 668-678.
6. García-Piñeres AJ, Castro VC, Mora G, Schmidt,TJ, Strunck E (2001) Cysteine 38 in p65/NF-κB plays a crucial role in DNA binding inhibition by

sesquiterpene lactones. Journal of Biological Chemistry. 276 (43), 39713-39720.

7. Wilson AJ, Kerns JK, Callahan JF, Moody CJ (2013) Keap calm, and carry on covalently. Journal of Medicinal Chemistry. 56 (19), 7463-76.
8. Gonzalez-Bello C (2016) Designing Irreversible Inhibitors--Worth the Effort? ChemMedChem. 11 (1), 22-30.
9. Scotti MT, Fernandes MB, Ferreira MJP, Emerenciano VP (2007) Quantitative structure–activity relationship of sesquiterpene lactones with cytotoxic activity. Bioorganic and Medicinal Chemistry. 15 (8), 2927-2934.
10. Fernandes MB, Scotti MT, Ferreira MJP,Emerenciano VP (2008) Use of self-organizing maps and molecular descriptors to predict the cytotoxic activity of sesquiterpene lactones. European Journal of Medicinal Chemistry. 43 (10), 2197-2205.
11. Kreuger,MR, Grootjans S, Biavatti MW, Vandenabeele P, D'Herde K (2012) Sesquiterpene lactones as drugs with multiple targets in cancer treatment: focus on parthenolide. Anti-cancer Drugs. 23 (9), 883-896.
12. Gach K, Dlugosz A, Janecka A (2015) The role of oxidative stress in anticancer activity of sesquiterpene lactones. Naunyn-Schmiedeberg's archives of pharmacology. 388 (5), 477-486.
13. Villagomez, R, Rodrigo, G. C, Collado, I. G, Calzado, M. A, Munoz, E et al. (2013) Multiple anticancer effects of damsin and coronopilin isolated from Ambrosia arborescens on cell cultures. Anticancer Research. 33 (9), 3799-3805.
14. Herz W, Anderson G, Gibaja S, Raulais D (1969) Sesquiterpene lactones of some Ambrosia species. Phytochemistry. 8 (5), 877-881.
15. Soule HD, Maloney TM, Wolman SR, Peterson WD,Jr, Brenz R et al. (1990) Isolation and characterization of a spontaneously immortalized human breast epithelial cell line, MCF-10. Cancer Research. 50 (18), 6075-6086.
16. Tanner M, Kapanen AI, Junttila T, Raheem O, Grenman S et al. (2004) Characterization of a novel cell line established from a patient with Herceptin-resistant breast cancer. Molecular Cancer Therapeutics. 3 (12), 1585-1592.
17. Itoh T, Ohguchi K, Nozawa Y, Akao Y (2009) Intracellular glutathione regulates sesquiterpene lactone-induced conversion of autophagy to apoptosis in human leukemia HL60 cells. Anticancer Research. 29 (4), 1449-1457.
18. Silva TM, Fiuza SM, Marques MPM, Persson L, Oredsson S (2014) Increased breast cancer cell toxicity by palladination of the polyamine analogue N(1),N(11)-bis(ethyl)norspermine. Amino Acids. 46 (2), 339-352.
19. Debnath J, Muthuswamy SK, Brugge J. S (2003) Morphogenesis and oncogenesis of MCF-10A mammary epithelial acini grown in three-dimensional basement membrane cultures. Methods. 30 (3), 256-268.
20. Underwood JM, Imbalzano KM, Weaver VM, Fischer AH, Imbalzano AN et al. (2006) The ultrastructure of MCF-10A acini. Journal of Cellular Physiology. 208 (1), 141-148.
21. Berridge MV, Tan AS (1993) Characterization of the cellular reduction of 3-(4,5-dimethylthiazol-2-yl)-2, 5-diphenyltetrazolium bromide (MTT): Subcellular Localization, Substrate Dependence, and Involvement of Mitochondrial electron transport in MTT reduction. Archives of Biochemistry and Biophysics. 303 (2), 474-482.
22. Holst CM, Oredsson SM (2005) Comparison of three cytotoxicity tests in the evaluation of the cytotoxicity of a spermine analogue on human breast cancer cell lines. Toxicology in vitro. 19 (3), 379-387.
23. Sotillo W, Villagomez R, Smiljanic S, Huang X, Malakpour A et al. (2017) Anti-cancer stem cellactivity of a sesquiterpene lactone isolated from Ambrosia arborescens and of a synthetic derivative. PLoS ONE 12 (9): e0184304.

Paper III

Volume 1 • Issue 2 • 2019

Research Article

Journal of Pharmacy and Drug Development

Cytotoxicity of New Damsin Derivatives in Breast Cancer Cells

Maribel Lozano[1,3], Wendy Soria[2,4], Giovanna R. Almanza[3], Sophie Manner[1], Stina Oredsson[2], Rodrigo Villagomez[3] and Olov Sterner[1]*

[1]*Centre for Analysis and Synthesis, Lund University, P.O.Box 124, 22100 Lund, Sweden*

[2]*Department of Biology, Lund University, Lund, Sweden*

[3]*Instituto de Investigaciones Químicas, Universidad Mayor de San Andrés, La Paz, Bolivia*

[4]*Instituto de Biología Molecular y Biotecnología, Universidad Mayor de San Andrés, La Paz, Bolivia*

***Corresponding Author:** Olov Sterner, Centre for Analysis and Synthesis, Lund University, P.O.Box 124, 22100 Lund, Sweden.

Received: August 19, 2019; **Published:** August 27, 2019

Abstract

As a follow-up of a previous investigation in which semisynthetic damsin derivatives were shown to possess up to 10 times higher cytotoxicity in JIMT-1 breast cancer cells compared to normal breast epithelial MCF-10A cells, a range of new derivatives were prepared and assayed toward the same cells. Damsin, a natural plant metabolite containing a α-methylene-γ-lactone (or 3-methylenedihydrofuran-2(3H)-one) moiety, was modified in position 3 by Claisen-Schmidt condensations with aromatic aldehydes, mainly mono- or disubstituted benzaldehydes, without affecting the α-methylene-γ-lactone function. This lactone ring is a Michael acceptor that is known to affect biological processes such as cell proliferation, death/apoptosis, and cell migration, by interfering with nucleophilic sites in cell signalling pathways. However, although Michael acceptors are reactive, the Michael addition is reversible and it can be assumed that also other parts of the molecules will moderate the binding to and the release from any given nucleophilic site in a protein, and thereby moderate a specific biological activity. In this investigation, the cytotoxicity of 20 α-methylene-γ-lactones towards normal breast epithelial MCF-10A cells as well as breast cancer JIMT-1 cells is compared, by determining the inhibitory concentration 50 (IC_{50}) from dose response curves. The IC_{50} values in the two cell lines were found to depend on the overall structure of the assayed compounds, although less in this subset of compounds compared to a previous investigation. Structure-activity relationships that may explain the observed differences in potency and selectivity are discussed.

Key words: *MCF-10A; JIMT-1; Semisynthesis; α-methylene-γ-lactones; Michael acceptors; SAR:*

Introduction

Breast cancer is one of the most common forms of cancer and established as a principal cause of death for women. In 2016, more than 500 000 women in the world died from this disease, which is expected to increase over the coming years. [1] At least 20% of all breast cancer cells show overexpression of human epidermal growth factor receptor 2 (HER2) protein, and HER2 overexpression has repeatedly been identified as a factor indicating poor prognosis. [2] Other proteins also involved in breast cancers are transcription factors as well as proteins involved in the cellular signalling pathways. Although there are traditional methods for the treatment of breast cancer such as surgery, chemotherapy and radiotherapy, these are not efficient enough. Novel and effective treatments or

more potent drugs with less side effects specifically targeting breast cancer are urgently needed. [3]

Secondary plant metabolites have always been an important provider of low-molecular anti-cancer drugs, and are expected to be so also in the future. [4,5,6] Our understanding of how cancer cells are formed and tumours develop and progress, as well as how treatment resistance may develop, has increased, not the least on a molecular level. This should enable us to design new and better drugs. [7] A cellular molecular pathway important for the development of chemoresistance and metastasis in many cancer cells is the NF-κB pathway, which the activation or the over-expression of is a harmful property of tumour cells. [7] Terpenoids with an α-methylene-γ-lactone moiety have been shown to possess promising anti-cancer effects, interfering with biological processes such as cell signalling, proliferation, death/apoptosis, and migration. [8,9] Such terpeniods are most commonly sesquiterpens, and sesquiterpene lactones (SLs) is a large group of natural products that have been isolated from numerous genera of Asteraceae family. [10] Modern pharmacological studies have revealed their diverse biological activities, including anti-tumoral, anti-inflammatory, anti-feedant, anti-microbial and anti-protozoal. [11,12] The significant cytotoxic activity of such terpenes is linked to the α-methylene-β-lactone moiety, which via a Michael addition can alkylate nucleophilic residues (primarily free thiols of cysteines) in proteins. A target suggested for such an interaction is the protein p65 in the heterodimeric transcription factor NF-κB pathway. [13] p65 is one of the key regulator of genes involved in a broad range of biological activities such as immune responses, development, survival, proliferation, angiogenesis, invasion and metastasis. [14] A well-known SL is thapsigargin, which has undergone phase I clinical trials for breast, kidney and prostate cancer treatments.9

Electrophilic compounds are considered potentially toxic and have been rejected by the pharmaceutical industry in their search for novel drug candidates. However, 39 electrophilic drugs, mainly used in oncological therapies, have been approved by the US Food and Drug Administration. [1,16] These may display off-target toxicity, [8] but the efficiency and selectivity of an electrophilic compound will besides the reactivity of the electrophilic moiety depend on the affinity to the target through non-covalent interactions. Michael acceptors will react with nucleophiles via an addition reaction, not a substitution, in a reaction that is reversible, and will in principle bind tighter to nucleophiles that present a more favourable molecular environment.

Damsin (1a) and coronopilin (1b) are pseudoguaianolide SLs, present in the plant Ambrosia arborescens. A spectrum of biological activities of damsin have been reported, e.g. an inhibitory effect on colon cancer cell lines (Caco-2 cell), as well as an influence on DNA biosynthesis and expression of NF-κB and STAT3 patways. [17,18] In the present study we compare the cytotoxicity of 20 α-methylene-γ-lactones based on the natural product damsin (1a) (see Figure 1), in normal breast epithelial MCF-10A cells and breast cancer JIMT-1 cells. The compounds were prepared by Claisen-Schmidt condensations of 1a with aromatic aldehydes, as well as derivatives of 3-hydroxyldamsin (3c) prepared by oxidation of 1a. In addition, the two thioether adducts 5a and 5b in which cystein methyl ester by a Michael addition was added to C-13 in the α-methylene-γ-lactone moiety, were prepared and assayed.

Experimental Procedures

General chemical procedures

Chemicals (analytical grade) were purchased from different commercial suppliers and used without further purification. Damsin (1a) and coronopilin (1b) (Figure 1) were isolated from A. arborescens as previously described. [13] IR spectra were recorded with a Bruker Alpha FT-IR Spectrometer, and the optical rotations were measured with a Perkin-Elmer 141 polarimeter. HRMS spectra were recorded with a Waters XEVO-G2 QTOF instrument, while NMR spectra were recorded in $CDCl_3$ using a Bruker DRX spectrometer operating at 400 MHz for 1H and at 100 MHz for ^{13}C. Chemical shifts are given in ppm relative to the solvent signals (7.26 ppm for 1H and 77.00 ppm for ^{13}C). All compounds described here were completely analysed by 2D NMR (COSY, HMQC, HMBC and NOESY), and as the syntheses start with the pure enantiomer damsin (1a) all compounds are given with the absolute configuration in Figures 1 and 2. Chromatography was performed with 60 Å 30-75 μm silica gel, while TLC analyses were made on Silica Gel 60 F254 (Merck) plates.

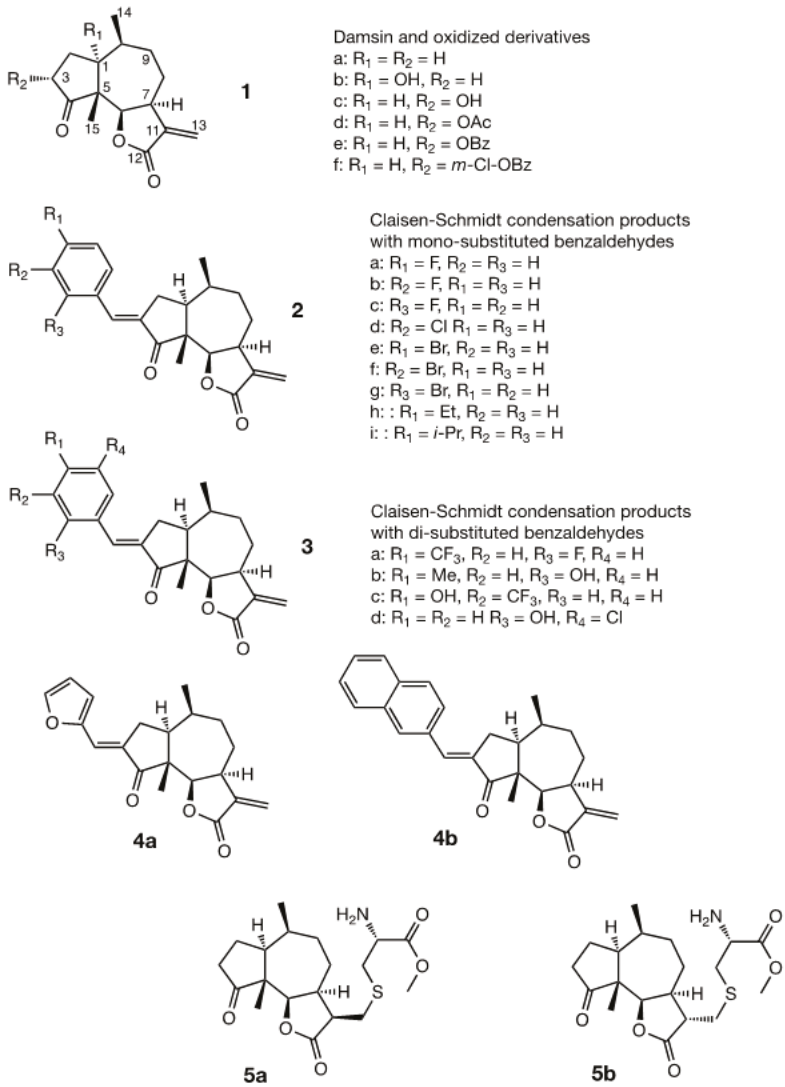

Figure 1: *The structures of the 23 derivatives assayed in this study.*

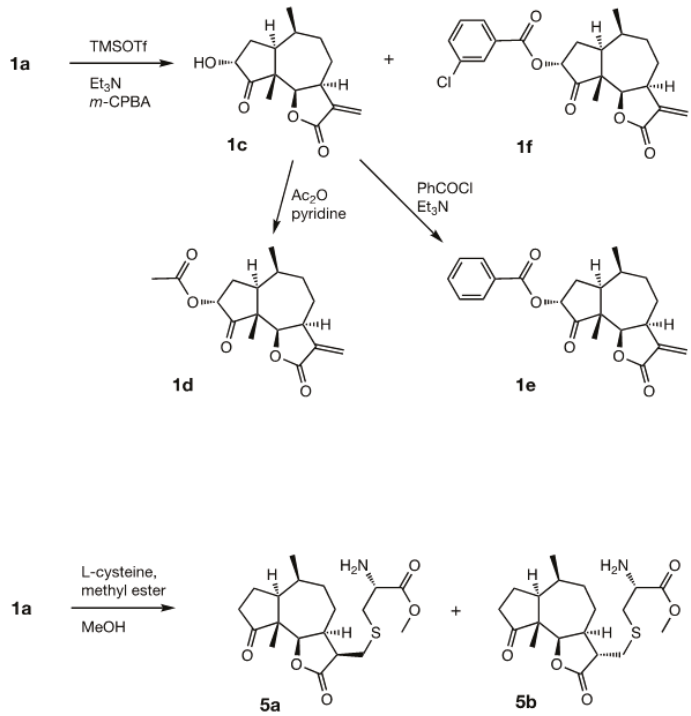

Figure 2: *The preparation of 1c, 1d, 1e, 1f, 5a, 5b.*

Synthetic Procedures

Preparation of 3α-hydroxydamsin (1c), 3α-acetoxydamsin (1d), 3α-benzoyloxydamsin (1e) and 3α-(m-chlorobenzoyloxy) damsin (1f).

The procedures are summarized in Figure 2. To a mixture of 1a (200 mg, 0.8054 mmol) and Et_3N (550 µl, 3.2216 mmol) in dry DCM (6 ml) at 0°C, TMSOTf (440 µl, 2.4162 mmol) was added slowly. The reaction was stirred at 0°C for 2h and then quenched by adding an excess of solid Na_2CO_3 whereafter the suspension was dried in vacuo. The dry remaining solid was extracted with hexane under stirring (3 x 20 ml x 30 min each extraction), the combined organic extracts were concentrated in vacuo to give the crude enol silane intermediate that was used in the next step without further purification. To a suspension of m-CPBA (218.4 mg, 0.8860 mmol) in n-hexane (6 ml) at -20°C, a solution of this crude enol silane intermediate in n-hexane (6.8 ml) was added dropwise. The reaction mixture was stirred for 5.5 h. The reaction was quenched with a saturated solution of $Na_2S_2O_3$ (1 ml) and brine (20 ml). The aqueous mixture was extracted with DCM (3 x 20 ml), the combined organic layers were dried over Na_2SO_4, and concentrated in vacuo. The products were purified by silica gel flash chromatography (EtOAc: $Pet.Et._{40\text{-}60}$) to yield the products 1f (62 mg, 19%) and 1c (70 mg, 33%). To a solution of 1c (60 mg, 0, 2270 mmol) in DCM (4.6 ml) at 0°C, PhCOCl (56 µl, 0.4824 mmol) was added followed by Et_3N (95 µl, 0.6834 mmol). The reaction was stirred for 23h, quenched with 5% HCl and brine (10 ml). The aqueous mixture was extracted with DCM (2 x 10 ml), the combined organic layers were dried over Na_2SO_4 and concentrated in vacuo. The product was purified by silica gel flash chromatography (EtOAc: n-hexane) to yield 1e (52 mg, 62%). 1d was prepared from 1c as reported previously. [19]

General procedure for Claisen-Schmidt/aldol condensations under acidic conditions (2e-2i and 4b)

A mixture of 1a (1 eq., 0.4027 mmol), aldehyde (1.3 eq., 0.5235 mmol), and p-TsOH (1.5 eq., 0.6040 mmol) in benzene (10 ml) was prepared in a sealed tube, and stirred at 80°C for 19 to 66 h until the reaction was completed (monitored by TLC). The reaction was quenched by adding 2 ml of 5% $NaHCO_3$ followed by 15 ml brine, and the mixture was extracted with DCM (3 x 15 ml). The combined organic layers were dried with $MgSO_4$ and concentrated in vacuo. The crude product was purified by silica gel chromatography (EtOAc:petroleum ether 1:1) to produce the condensation products 2e (14.1 mg, 8%), 2f (58.3 mg, 35%), 2g (84.5 mg, 50%), 2h (45 mg, 30%), 2i (44.6 mg, 29%) and 4b (17.1 mg, 11%).

General procedure for Claisen-Schmidt/aldol condensations under basic conditions (2a-2d, 3a-3d and 4a)

A mixture of aldehyde (3 eq., 1.2081 mmol) and 1a (1 eq., 0.4027 mmol) in 50% PhMe: H2O 1:1 (3 ml) was cooled in an ice-bath, and TBAH (1.2 eq., 0.4832 mmol, 1.5 M in H_2O) was added dropwise. The ice-bath was removed after 10 min and the reaction was left to reach room temperature. The reaction was monitored by TLC, and after 3 to 24h, the reaction was quenched by addition of 2 ml of 5% HCl and stirred for 15 min at r.t. The reaction mixture was diluted with 15 ml brine, and extracted with DCM (3 x 10 ml), and the combined organic layers were dried with $MgSO_4$ and concentrated in vacuo. The crude condensation product was purified by silica gel chromatography (EtOAc:petroleum ether 1:1) to produce the condensation products 2a (22.4 mg, 39%), 2b (84.5 mg, 59%), 2c (101.5 mg, 71%), 2d (62.2 mg, 41%), 3a (100 mg, 59%), 3b (44.6 mg, 27%), 3c (61.2 mg, 32%), 3d (247 mg, 94%) and 4b (96.7 mg, 73%).

General procedure for the MOM-protection of the hydroxybenzaldehydes.

To a solution of the hydroxybenzaldehydes corresponding to derivatives 3b-3d (2.3333 mmol) in 6 ml dry DCM was added $EtN(i\text{-}Pr)_2$ (2 ml, 11.6665 mmol), followed by MOMBr (400 µl, 4.8999 mmol) dropwise under N2 at 0°C, whereafter the mixture was stirred at room temperature for 6 h. The reaction was quenched with 10 ml of a saturated solution of $NaHCO_3$ by stirring for 15 min at r.t., and the mixture was extracted with DCM (2 x 15 ml). The combined organic layers were dried with $MgSO_4$ and concentrated in vacuo. The product was purified by chromatography on silica gel (n-heptane:DCM 1:1) to yield the MOM-protected hydroxybenzaldehydes corresponding to derivatives 3b-3d.

General procedure for the deprotection of the Claisen-Schmidt adducts with MOM-protected hydroxyl groups.

To a solution of a MOM protected Claisen-Schmidt adduct, formed either by procedure 1b or 1c, (50 mg, 0.1261 mmol) in MeOH (2.6 ml), HCl conc. (22.5 µl, 0.2695 mmol, 37%) was added slowly. The reaction mixture was heated to 40°C for 5 h and then cooled to room temperature, whereafter the organic solvent was evaporated in vacuo. The residue was dissolved in DCM (15 ml), washed with brine (10 ml), dried with $MgSO_4$, and concentrated in vacuo. The product was purified by chromatography on silica gel (EtOAc:petroleum ether 1:1) to yield the products 3b-3d that were assayed.

Procedure for the preparation of the thioether adducts 5a and 5b from 1a

To a mixture of 1a (1 eq., 1.2081 mmol), L-cysteine methyl ester hydrochloride (1 eq., 1.2081 mmol) in methanol (6 ml) was added TEA (100 µl), the mixture of reaction was stirred at room temperature for 20 h until the reaction was completed (analysed by TLC). The reaction mixture was concentrated in vacuo, and the product was purified by silica gel chromatography (MeOH;DCM;TEA) to yield 45% of adduct 5a and 22.4% of adduct 5b.

Biological assays

Cell lines

The normal-like epithelial MCF–10A cell line was purchased from American Type Culture Collection (Manassas, VA, USA) (CRL-10781) and was used as a representative for normal breast epithelial cells. The cell line retains many normal traits, including lack of tumorigenicity in nude mice, anchorage-dependent growth, and dependence on growth factors and hormones for proliferation and survival. [18,19] The MCF-10A cells were cultured in RPMI 1640 medium supplemented with 10% heat-inactivated fetal bovine serum (FBS), non-essential amino acids (1 mM), insulin (10 µg/ml), epidermal growth factor (20 ng/ml), cholera toxin (50 ng/ml), hydrocortisol (250 ng/ml), penicillin (100 U/ml), and streptomycin (100 µg/ml).

The JIMT–1 human breast carcinoma cell line (ACC589) was purchased from the German Collection of Microorganisms and Cell Cultures (Braunschweig, Germany). It carries an amplified HER2 oncogene and is insensitive to HER2 inhibiting drugs and belongs to the HER2 sub-type of breast cancer. [20,21] The JIMT-1 cells were routinely cultured in DMEM/Ham's F-12 medium supplemented with 10% FBS, non-essential amino acids (1 mM), insulin (10 µg/ml), penicillin (100 U/ml) and streptomycin (100 µg/ml). Both cell lines were kept at 37°C in a humidified incubator with 5% CO_2 in air.

Compound solutions

The sample compounds were dissolved in DMSO to 100 mM stock solutions that were kept at -20°C. Working solutions were diluted in PBS and all had a DMSO concentration of 0.2%. In the assay, the cells were exposed to PBS with 0.02% DMSO, or with the respective compounds at 0.1, 0.25, 0.5, 1, 2.5, 5, 10, and 20 μM concentrations.

Dose response assay

The dose response to treatment with the compounds was evaluated using an MTT assay, which is based on reduction of MTT in the mitochondria of live cells. The amount of formazan produced is proportional to the number of living cells. [21,22] For the assay, cells were trypsinized and counted in a hemocytometer. Aliquots of 180 μl cell suspension containing 3000 cells (MCF-10A) or 5000 cells (JIMT-1) were seeded in 96-well plates. Compounds were added 24 h later to the final concentrations described above. At 72 h of drug treatment, 20 μl of MTT solution (5 mg/ml in PBS) was added to each well and the 96-well plates were returned to the CO_2 incubator for 1 h. The medium was then removed and the blue formazan crystals were dissolved by adding of 100 μl of 100% DMSO per well. The plates were swirled gently at room temperature for 10 minutes to dissolve the crystals. Absorbance was monitored at 540 nm in a Multiskan™ FC Microplate Photometer (Thermo Fisher Scientific, Lund, Sweden) using the software SkanIt 3.1. For each compound, three dose response experiments were performed with six replicates for each one of them. GraphPad Prism version 6.01 for Windows (GraphPad Software, La Jolla, CA, USA), was used for drawing dose response curves and calculating the IC_{50} values, i.e. the dose giving 50% reduction in cell number.

Determination of the cellular glutathione content

The cellular concentration of glutathione was determined using the GSH-Glo™ Glutathione Assay (Promega, Madison, WI, USA). The instructions of the manufacturer were followed. In short, MCF-10A cells and JIMT-1 cells were seeded at different densities (MCF-10A: 5000, 10000, and 20000. JIMT-1: 10000, 20000, and 40000) in 96-well plates in 150 μl medium and incubated for 24 hours to allow attachment of the cells. Then the glutathione assay was performed on the attached cell and in the same plate, the standard curve was generated. The glutathione content of cells seeded at different densities was obtained from the standard curve according to the instructions of the manufacturer. This data was used to calculate the intracellular concentration using cell volumes. [23] MCF-10A cells were found to have a mean volume of 998 μm^3 and MCF-7 breast cancer cells a mean volume of 10124 μm^3. Since we have not found any data of the volume of JIMT-1 cells but have cultured both JIMT-1 and MCF-7 cells and compared their size in the phase contrast microscope, we assume they have a similar volume. Thus, using the data from the GSH-Glo™ Glutathione Assay together with cell volume data, we have determined the glutathione concentration to be 588 ± 173 μM and 47 ± 18 μM in MCF-10A and JIMT-1 cells, respectively.

Results and Discussion

The two natural products damsin (1a) and coronopilin (1b) were isolated from the plant A. arborescens as previously described, [20] and 1a was used as the starting material for semisynthesis of new derivatives retaining the α-methylene-γ-lactone moiety intact. The present study is based on a previous study [21] in which Claisen-Schmidt condensation products of 1a with aromatic aldehydes forming (E)-3-benzylidendamsin derivatives were found to be more potent in the JIMT-1 cancer cells compared to the MCF-10A normal-like cells. The selectivity for the JIMT-1 cancer cells was measured as the ratio of the IC_{50} values for MCF-10A and JIMT-1 cells, see Table 1). Our focus in this study was therefore to prepare new condensation products between 1a and aromatic aldehydes. In general, the condensations proceeded well, and worked both under acidic and basic conditions (see Experimental procedures for more information). As noted during the previous study, it was not possible to use hydoxybenzaldehydes directly, the hydroxyl groups had to be protected as MOMO substituents prior to the condensation with 1, to eventually form compounds 3b – 3d after subsequent deprotection (as described in the Experimental procedures). As observed previously, the condensations with between 1a and aromatic aldehydes were highly stereoselective, only the E-alkenes were obtained. [21] This additional double bond, although it forms a second Michael acceptor fuctionality that theoretically could influence the biological activity, was previously shown to have no significant effect on either the potency or the selectivity. [22] In order to demonstrate the necessity of a α-methylene-γ-lactone moiety for cytotoxicity of the compounds, we prepared the adducts 5a and 5b in which cysteine methyl ester was added to the the α-methylene-β-lactone moiety of damsin. This reaction proceede smoothly in methanol at room temperature, and the product could be purified by chromatography.

Compound	MCF-10A (μM)	JIMT-1 (μM)	Ratio MCF-10-A:JIMT-1
1a (damsin)	8.1 ± 0.4[2]	3.3 ± 0.6[2]	2.5
1b (coronopolin)	15.3 ± 0.9	5.6 ± 0.8	2.7
1c	12.8 ± 1.1[2]	6.3 ± 0.2[2]	2.0
1d	> 20[1]	> 20[1]	na
1e	> 20[1]	> 20[1]	na
1f	> 20[1]	> 20[1]	na
2a	4.4 ± 1.6[2]	2.3 ± 0.4[3]	1.9
2b	2.5 ± 0.3[2]	1.1 ± 0.1[3]	2.3
2c	2.2 ± 0.4[2]	1.1 ± 0.3[3]	2.0
2d	3.8 ± 0.6[2]	1.4 ± 0.3[2]	2.6
2e	6.2 ± 1.3[3]	1.8 ± 0.7[3]	3.5
2f	6.1 ± 0.4[3]	1.8 ± 0.9[3]	3.4
2g	2.0 ± 0.4[3]	1.2 ± 0.3[3]	1.6
2h	2.5 ± 0.4[2]	1.9 ± 0.8[2]	1.3
2i	6.2 ± 1.4[2]	3.8 ± 1.0[2]	1.6
3a	2.3 ± 0.9[2]	1.2 ± 0.1[3]	2.0
3b	4.7 ± 0.7[2]	1.9 ± 0.1[3]	2.4
3c	5.4 ± 1.4[3]	1.8 ± 0.2[3]	3.0
3d	2.1 ± 0.7[2]	0.7 ± 0.1[2]	2.6
4a	7.7 ± 2.8[2]	2.3 ± 0.9[2]	3.3
4b	3.2 ± 1.6[3]	2.1 ± 1.0[3]	1.5
5a	16.0 ± 3.5[3]	8.8 ± 1.7[3]	1.7
5b	> 20	15.9 ± 1.4[3]	na

Table 1: *The cytotoxicity of compounds 2 – 8, given as IC_{50} values (μM) calculated from experiments with six concentrations up to 20 μM. Standard deviations were obtained from [1]two dose-response curves, [2]three dose-response curves, or [3]four dose-response curves.*

The structures of all compounds prepared in this investigation was carefully determined by 1- and 2D NMR experiments (including COSY, NOESY, HMQC and HMBC experiments), in combination with the IR and HRMS data reported in the Supporting Information. The configuration of the C-3/C-1' double bond was determined by NOESY NMR experiments. [22] The chemical shifts for all proton and carbon signals observed in $CDCl_3$ are presented in Tables 2 and 3. In all cases, the NMR couplings observed between protons are those that we expected from our previous experience from this type of compounds, and are for reasons of space not reported here but found in the Supporting Information. The comparison of the proton and carbon shifts in Tables 2 and 3 gives some interesting information. The NMR chemical shifts, and thereby the properties including the reactivity of the compounds are influenced by the electronic properties of the chemical bonds close to a specific nucleus or involved in a reactive functionality. Assuming that the α-methylene-γ-lactone moiety is critical for the cytotoxicity of the compounds assayed, it is interesting to compare the chemical shifts of 6-H, 7-H, 13-H_2, C-6, C-7, C-11, C-12 and C-13 of the assayed compounds, in search for any indication that the substituent at C-3 affect the electronic properties of this lactone ring. 6-H are all close to 4.7 ppm, except in 5a and 5b which no longer possess a α-methylene-β-lactone moiety. 7-H are all close to 3.3 ppm, 13-Ha are close to 5.6 ppm, while 13-Hb are close to 6.3 ppm. The C-6 values are close to 82 ppm, C-7 close to 45 ppm, C-11 close 140 ppm, C-12 close to 170 ppm, and C-13 close to 121 ppm. So, the electronic properties of the α-methylene-β-lactone moiety remains essentially intact, and appears to be essentially independent of the C-3 substituent. The conclusion is therefore that the differences in cytotoxic activities shown in Table 1 and discussed below, depend on the molecular interaction that the C-3 substituent can provide with a protein at the site where a Michael addition can take place.

	1-H	2-H_2	6-H	7-H	8-H2	9-H_2	10-H	13-H_2	14-H_3	15-H_3	1'-H	2''-H	3''-H	4''-H	5''-H	6''-H
1a	2.01	1.79/ 2.00	4.44	3.24	1.79/ 1.85	1.81/ 1.81	2.15	5.46/ 6.13	1.01	1.00	-	-	-	-	-	-
1b	2.47	2.47/ 2.47	4.92	3.34	1.71/ 2.08	1.60/ 2.40	2.19	5.58/ 6.26	1.20	1.15	-	-	-	-	-	-
1c	2.27	1.81/ 2.34	4.69	3.33	1.91/ 1.94	1.68/ 1.86	2.15	5.54/ 6.25	1.07	1.09	-	-	-	-	-	-
1d	2.35	1.81/ 2.48	4.70	3.31	1.86/ 1.99	1.70/ 1.87	2.14	5.55/ 6.26	1.07	1.12	-	-	-	-	-	-
1e	2.49	1.98/ 2.59 4.79	3.34	1.86/ 2.10	1.73/ 1.87	2.16	5.57/ 6.28	1.10	1.18	-	8.00	7.42	7.56	7.42	8.00	

1f 2.46	1.96/ 2.59 4.78	3.35	1.88/ 1.99	1.74/ 1.91	2.17	5.56/ 6.27	1.10	1.17	-	7.65	-	7.53	7.36	7.88		
2a 2.07	2.86/ 2.96	4.65	3.29	1.78/ 2.08	1.72/ 1.87	2.28	5.58/ 6.29	1.17	1.16	7.40	7.11	7.54	-	7.54	7.11	
2b	2.10	2.85/ 2.95	4.64	3.30	1.81/ 2.07	1.72/ 1.90	2.28	5.57/ 6.28	1.18	1.15	7.37	7.30	-	7.06	7.39	7.23
2c	2.06	2.76/ 2.94	4.64	3.29	1.82/ 2.07	1.73/ 1.86	2.26	5.57/ 6.27	1.17	1.16	7.62	-	7.09	7.35	7.18	7.53
2d	2.08	2.84/ 2.95	4.64	3.30	1.82/ 2.06	1.73/ 1.91	2.29	5.57/ 6.28	1.18	1.15	7.33	7.50	-	7.35	7.34	7.40
2e	2.08	2.81/ 2.93	4.65	3.29	1.83/ 2.09	1.75/ 1.90	2.22	5.56/ 6.28	1.18	1.16	7.36	7.40	7.55	-	7.55	7.40
2f	2.08	2.83/ 2.94	4.63	3.29	1.83/ 2.07	1.74/ 1.89	2.29	5.57/ 6.27	1.17	1.14	7.31	7.64	-	7.48	7.28	7.44
2g	2.04	2.69/ 2.90	4.61	3.29	1.81/ 2.06	1.72/ 1.85	2.21	5.56/ 6.26	1.14	1.16	7.67	-	7.61	7.19	7.50	7.25
2h	2.07	2.79/ 2.94	4.65	3.28	1.81/ 2.08	1.74/ 1.88	2.28	5.57/ 6.28	1.18	1.16	7.42	7.47	7.25	-	7.25	7.47
2i	2.07	2.87/ 2.96	4.65	3.28	1.81/ 2.09	1.73/ 1.88	2.28	5.57/ 6.28	1.18	1.16	7.43	7.49	7.28	-	7.28	7.49
3a	2.09	2.75/ 2.95	4.64	3.31	1.85/ 2.07	1.75/ 1.89	2.26	5.57/ 6.28	1.16	1.16	7.55	-	7.36	-	7.45	7.65
3b	2.06	2.80/ 2.93	4.65	3.28	1.78/ 2.07	1.74/ 1.87	2.26	5.58/ 6.30	1.17	1.18	8.0	-	6.8	-	6.73	7.36
3c	2.06	2.80/ 2.91	4.63	3.28	1.84/ 2.07	1.73/ 1.89	2.27	5.57/ 6.27	1.16	1.13	7.34	7.70	-	-	6.96	7.52
3d	2.03	2.74/ 2.88	4.60	3.26	1.79/ 2.04	1.69/ 1.84	2.25	5.56/ 6.25	1.14	1.12	7.71	-	6.77	7.12	-	7.34
4a	2.05	2.82/ 2.94	4.59	3.26	1.78/ 2.01	1.68/ 1.82	2.23	5.51/ 6.20	1.10	1.06	7.12	-	7,53	6,47	6,63	-
4b	2.10	2.97/ 3.08	4.67	3.29	1.82/ 2.11	1.76/ 1.91	2.32	5.58/ 6.30	1.22	1.20	7.60	-	-	-	-	-
5a	2.08	1.81/ 2.03	4.45	2.59	1.52/ 1.52	1.60/ 1.85	2.21	2.59/ 3.00	1.06	1.11	-	-	-	-	-	-
5b	2.05	1.83/ 1.98	4.41	2.79	1.78/ 1,87	1.66/ 1.74	2.18	2.96/ 2.87	1.07	1.08	-	-	-	-	-	-

Table 2: *^{1}H NMR chemical shifts (in ppm) for the assayed compounds 1a-f, 2a-i, 3a-d, 4a-b and 5a-b determined at 400 MHz in $CDCl_3$.*

In 1d, the acetyl signal appears at 2.08 ppm.

In 4b, the naphthyl signals appear at 7.51, 7.53, 7.83, 7.86, 7.89, 7.66 and 8.01 ppm.

In 5a, the cysteine signals appear at 2.78, 3.65 and 3.70 ppm, while the 11-H signal appears at 2.93 ppm.

In 5b, the cysteine signals appear at 2.98, 3.74 and 3.73 ppm, while the 11-H signal appears at 2.64 ppm.

	C-1	C-2	C-3	C-4	C-5	C-6	C-7	C-8	C-9	C-10	C-11	C-12	C-13	C-14	C-15	C-1'	C-1''	C-2''	C-3''	C-4''	C-5''	C-6''
1a	45.8	25.5	36.0	218.9	54.7	81.6	44.2	23.8	33.2	34.1	139.5	170.1	120.6	15.7	13.6	-	-	-	-	-	-	-
1b	84.2	32.3	31.0	216.4	57.9	78.4	43.9	26.8	29.4	42.1	140.0	169.4	120.7	16.5	13.9	-	-	-	-	-	-	-
1c	42.3	31.2	70.1	216.9	54.8	81.7	43.7	25.4	33.4	33.9	139.6	170.1	121.1	14.9	13.7	-	-	-	-	-	-	-
1d[a]	42.6	30.1	71.5	211.8	55.2	81.3	44.0	25.9	34.0	33.7	139.7	170.0	121.3	15.0	14.1	-	-	-	-	-	-	-
1e	42.8	30.3	72.2	211.8	55.4	81.5	44.1	26.0	34.0	33.8	139.8	170.1	121.4	15.2	14.3	165.7	129.3	129.9	128.5	133.5	128.5	129.9
1f	42.7	30.0	72.3	211.3	55.3	81.3	44.0	25.9	33.9	33.7	139.6	170.0	121.3	15.0	14.1	164.4	130.1	129.8	134.5	133.4	129.7	128.0
2a	43.8	31.3	132.5	207.3	54.9	81.9	44.8	26.5	34.3	34.1	139.9	170.8	121.5	15.8	14.6	132.9	161.9	116.1	132.6	164.2	132.6	115.9
2b	43.6	31.3	134.7	207.8	54.9	81.8	44.8	26.5	34.2	34.0	140.0	170.3	121.4	15.7	14.5	132.5	137.6	126.7	162.8	116.4	130.4	116.7
2c	43.6	31.4	135.5	207.5	54.9	81.8	44.8	26.5	34.3	34.1	140.1	170.3	121.3	15.8	14.5	125.7	123.6	160.4	115.9	131.3	124.2	130.1
2d	43.6	31.3	134.7	207.7	54.9	81.8	44.8	26.5	34.2	34.0	140.0	170.3	121.4	15.7	14.5	129.5	134.8	130.0	137.2	130.1	132.2	128.8
2e	43.7	31.4	134.1	207.8	54.9	81.8	44.8	26.5	34.2	34.1	140.0	170.3	121.4	15.8	14.5	132.6	134.1	131.9	132.1	124.0	132.1	131.9
2f	43.6	31.2	134.8	207.7	54.8	81.7	44.7	26.4	34.2	34.0	140.0	170.2	121.3	15.7	14.4	132.1	137.5	132.9	122.9	132.4	130.3	129.1
2g	43.7	31.0	135.8	207.4	54.9	81.8	44.7	26.3	34.0	34.0	140.0	170.3	121.2	15.7	14.4	132.2	135.2	126.2	133.4	130.5	127.3	130.1
2h	43.7	31.5	132.9	208.1	54.8	81.9	44.9	26.6	34.3	34.2	140.2	170.3	121.2	15.8	14.6	134.0	132.4	130.8	128.4	146.3	128.4	130.8
2i	43.7	31.5	132.5	208.1	54.8	81.9	44.9	26.6	34.3	34.2	140.2	170.3	121.3	15.8	14.6	134.0	133.1	130.8	127.0	150.9	127.0	130.8
3a	43.5	31.3	137.9	207.1	55.0	81.7	44.7	26.3	34.0	34.0	139.9	170.3	121.4	15.7	14.4	124.0	124.4	159.7	162.3	132.7	121.1	138.8
3b	43.8	31.6	131.6	209.8	54.9	82.1	45.0	26.7	34.2	34.3	140.2	170.7	121.5	15.9	14.7	129.9	119.9	156.7	117.1	142.6	121.3	129.5
3c	43.8	31.1	131.6	208.4	54.8	82.1	44.8	26.4	34.0	34.2	139.9	170.8	121.7	15.8	14.5	133.1	117.6	129.2	126.7	156.6	117.6	135.9
3d	43.8	31.1	133.5	208.5	54.9	82.1	44.7	26.4	34.1	34.0	139.9	170.7	121.6	15.7	14.4	128.0	124.2	155.9	117.3	130.7	124.0	128.8
4a	43.1	30.0	130.7	207.7	54.9	81.8	44.7	26.4	34.1	33.9	140.0	170.2	121.1	15.6	14.4	119.9	152.1	-	145.1	112.5	116.4	-
4b	43.8	31.5	133.6	208.0	54.9	81.9	44.9	26.6	34.3	34.2	140.2	170.3	121.3	15.9	14.2	134.1	-	-	-	-	-	-
5a	46.2	24.6	35.3	221.7	55.0	82.3	45.9	18.4	37.4	35.4	45.8	174.8	28.6	16.9	16.1	-	-	-	-	-	-	-
5b	46.8	24.3	36.9	219.3	55.1	83.1	45.2	25.3	33.5	34.8	47.2	177.6	33.3	16.2	14.3	-	-	-	-	-	-	-

Table 3: *^{13}C NMR chemical shifts (in ppm) for the assayed compounds 1a-1f, 2a-2i, 3a-3d, 4a-4b and 5a-5b determined at 100 MHz in $CDCl_3$.*

Citation: Maribel Lozano, Wendy Soria, Giovanna R. Almanza, Sophie Manner, Stina Oredsson, Rodrigo Villagomez and Olov Sterner. (2019). Cytotoxicity of New Damsin Derivatives in Breast Cancer Cells. *Journal of Pharmacy and Drug Development* 1(2).

In 1d, the acetyl signals appear at 20.7 and 170.0 ppm.
In 4b, the naphthyl signals appear at 126.8, 127.0, 127.4, 127.8, 128.5, 128.7, 131.4, 133.0, 133.3 and 133.6 ppm.
In 5a, the cysteine signals appear at 38.3, 54.8, 174.2 and 52.5 ppm.
In 5b, the cysteine signals appear at 38.2, 54.8, 176.4 and 52.7 ppm.

The MCF-10A cell line used in this study is a non-tumorigenic breast epithelial cell line [23] while the JIMT-1 cells are breast cancer-derived tumorigenic. [24] Table 1 shows the experimental cytotoxicity IC_{50} values in μM obtained with the two cell lines, calculated from the dose response curves. In addition, the ratios between the IC_{50} MCF-10A and IC_{50} JIMT-1 were calculated, and are presented in Table 1 as a measure for the selectivity of each compound. The IC50 values show consistently that the JIMT-1 cells are more sensitive to the compounds assayed compared to the MCF-10A cells, which is consistent with our previous observation. [21] A cellular component that has been recognized to be able to neutralize SLs is glutathione. [25] Glutathione can react spontaneously with various electrophilic substrates, e.g. Michael acceptors, but it is also conjugated to xenobiotics in a reaction catalyzed by glutathione S-transferase. [26] It has been shown that the reaction of glutathione with SLs is reversible. [27] When measuring glutathione levels in MCF-10A and JIMT-1 cells, we found that the former have a 10 times higher concentration than the latter. In addition, the JIMT-1 cells have low expression of the glutathione S-transferase M1 gene. [24] Our notion that the difference in sensitivity between the normal-like MCF-10A and the JIMT-1 breast cancer cells is due to the lower glutathione concentration and low expression of the glutathione S-transferase gene in the latter needs further experimental clarification.

It is interesting that the oxidized derivatives (1b-1f) of 1a are less potent, especially the 3-acylated derivatives (1d-1f). Compared to the 3-bezylidenes, carbon 3 of 1c-1f is chiral and the substituent is directed in a certain direction. This may be disadvantageous for the ability of 1c-1f to react with certain critical nucleophilic sites in the target proteins. Besides this observation, it can be noted that the benzylidene derivatives 2a-2i and 3a-3d show the expected potency in the JIMT-1 cells, but do not show a promising selectivity. The derivatives 5a and 5b, which formally lack the α-methylene-β-lactone moiety, are still cytotoxic. Presumably this is due to the reversibility of the Michael reaction, which would cause the derivatives 5a and 5b to regenerate damsin (1a) during the experiment. It would consequently be of interest to measure the reversibility of this reaction during relevant conditions. Another biological explanation to the difference in toxicity between 5a and 5b could be that the toxicity of SLs is not only dependent on the presence of an α-methylene-γ-lactone group but that there may be other toxic mechanisms independent of binding to p65/NF-κB [28,29] and this notion needs investigation as well. The stereoisomers 5a and 5b show slightly different toxicities (see Table 1) which may be related to different binding affinities to possible targets in the cell and/or differences in chemical stability.

In conclusion, with this paper and our previous paper [21], we demonstrate the synthesis of 43 unique damsin derivatives, many of which that show toxicity with a lower IC_{50} than that found for damsin itself. Most important is the increase in selective toxicity i.e. a lower IC_{50} in the JIMT-1 cancer cell line compared to the MCF-10A cell line. Further studies are needed to unravel the role of different chemical and biological entities that define toxicity with the goal to increase the selectivity towards cancer cells.

Supporting Information

Compound 1a (damsin)

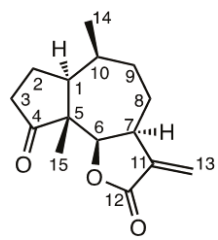

^{1}H NMR data (400 MHz, $CDCl_3$): 6.13 (1H, s, H-13b), 5.46 (1H, s, H-13b), 4.44 (1H, d, J 6.9 Hz, H-6), 3.24 (1H, m, H-7), 2.38 (2H, m, H-3), 2,15 (1H, m, H-10), 2,01 (1H, m, H-1) 1,95 (1H, m, H-8b), 1,81 (2H, m, H-9a,b), 1,79 (1h, m, H-8a), 1,69 (2H, m, H-2), 1,01 (3H, d, J 7.5 Hz, H-14), 1,0 (3H, m, H-15). ^{13}C NMR data (100 MHz, $CDCl_3$): 218.9 (C-4), 170.1 (C-12), 139.5 (C-11), 120.6 (C-13), 81.6 (C-6), 54.7 (C-5), 45.8 (C-1), 44.2 (C-7), 36.0 (C-3), 34.1 (C-10), 33.2 (C-9), 25.5 (C-2), 23.8 (C-8), 15.7 (C-14), 13.6 (C-15).

Compound 1b (coronopilin)

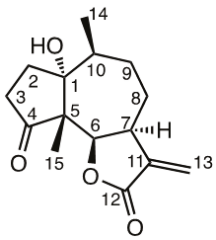

^{1}H NMR data (400 MHz, $CDCl_3$): 6.26 (1H, s, H-13b), 5.58 (1H,s, H-13a), 4.92 (1H,d, J 8.2 Hz, H-6), 3.34 (1H, m, H-7), 2.65 (1H, dd, J 23.2, 10.5 Hz, H-3b), 2.47 (2H, m, H-2), 2,40 (1H, m, H-9b), 2,19 (1H, m, H-10), 2,08 (1H, m, H-8b), 1,71(1H, m, H-8a), 1,61 (1H, m, H-3a), 1,60 (1H, m, H-9a), 1.20 (3H, d, J 7.5 Hz, H-14), 1.15 (3H, s, H-15). ^{13}C NMR data (100 MHz, $CDCl_3$): 216.4 (C-4), 169.4 (C-12), 140.0 (C-11), 120.7 (C-13), 84.2 (C-1), 78.4 (C-6), 57.9 (C-5), 43.9 (C-7), 42.1 (C-10), 32.3 (C-2), 31.0 (C-3), 29.4 (C-9), 26.8 (C-8), 16.5 (C-14), 13.9 (C-15).

Compound 1c (3α-hydroxydamsin)

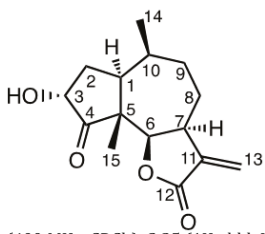

^{1}H NMR data (400 MHz, $CDCl_3$): 2.35 (1H, ddd, J 12.3; 7.6; 4.5 Hz, H-1), 1.81 (1H, m, H-2a), 2.48 (1H, ddd, J 14.4; 12.6; 9.7 Hz, H-2b), 5.19 (1H, dd, J 9.6; 2.4 Hz, H-3a), 4.70 (1H, d, J 8.9, H-6), 3.31 (1H, m, H-7), 1.86 (1H, m, H-8a), 1.99 (1H, m, H-8b), 1.70 (1H, m, H-9a), 1.87 (1H, m, H-9b), 2.14 (1H, m, H-10), 5.55 (1H, d, J 2.8Hz, H13a), 6.26 (1H, d, J 3.1Hz, H-13b), 1.07 (3H, d, J 7.5 Hz, CH_3-14), 1.12 (3H, s, CH_3-15), 2.08 (3H, s, CH3-17). ^{13}C NMR data (100 MHz, $CDCl_3$): 42.6 (C-1), 30.1 (C-2), 71.5 (C3), 211.8 (C-4), 55.2 (C-5), 81.3 (C-6), 44.0 (C-7), 25.9 (C-8), 34.0 (C-9), 33.7 (C-10), 139.7 (C-11), 170.0 (C-12), 121.3 (C-13), 15.0 (C-14), 14.1 (C15), 170.0 (C-16), 20.7 (C-17). [α]D20 -5 (c 1.00, CH_2Cl_2). IR spectrum (film, ν, cm-1): 2928, 2870, 1753, 1736, 1659, 1451, 1372, 1337, 1271, 1223, 1164, 1113, 1059, 1006, 977, 948, 882, 815, 733, 700, 627, 529, 460. HRMS-ESI (m/z, %) 265.1451 (100) $[M+H]^+$ (calculated for $C_{15}H_21O_4$ 265.1440).

Compound 1d (3α-acetoxydamsin)

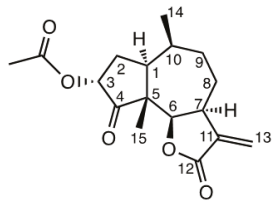

^{1}H NMR data (400 MHz, $CDCl_3$): 2.35 (1H, ddd, J 12.3; 7.6; 4.5 Hz, H-1), 1.81 (1H, m, H-2a), 2.48 (1H, ddd, 3 J 14.4; 12.6; 9.7 Hz, H-2b), 5.19 (1H, dd, J 9.6; 2.4 Hz, H-3a), 4.70 (1H, d, J 8.9 Hz, H-6), 3.31 (1H, m, H-7), 1.86 (1H, m, H-8a), 1.99 (1H, m, H-8b), 1.70 (1H, m, H-9a), 1.87 (1H, m, H-9b), 2.14 (1H, m, H-10), 5.55 (1H, d, J 2.8 Hz, H-13a), 6.26 (1H, d, J 3.1Hz, H-13b), 1.07 (3H, d, J 7.5, CH3-14), 1.12 (3H, s, CH3-15), 2.08 (3H, s, CH3-17). ^{13}C NMR data (100 MHz, $CDCl_3$): 42.6 (C-1), 30.1 (C-2), 71.5 (C3), 211.8 (C-4), 55.2 (C-5), 81.3 (C-6), 44.0 (C-7), 25.9 (C-8), 34.0 (C-9), 33.7 (C-10), 139.7 (C-11), 170.0 (C-12), 121.3 (C-13), 15.0 (C-14), 14.1 (C15), 170.0 (C-16), 20.7 (C-17). [α] D20 -20.5 (c 1.00, CH_2Cl_2). IR spectrum (film, ν, cm-1): 2928, 2870, 1753, 1736, 1659, 1451, 1372, 1337, 1271, 1223, 1164, 1113, 1059, 1006, 977, 948, 882, 815, 733, 700, 627, 529, 460. HRMS-ESI (m/z, %) 307.1549 (100) $[M+H]^+$ (calculated for $C_{17}H_{23}O_5$ (307.1546).

Compound 1e (3α-benzoyloxydamsin)

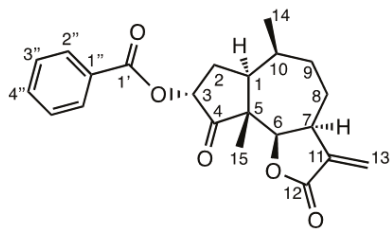

^{1}H NMR data (400 MHz, $CDCl_3$): 8.00 (2H, dd, J 8.4; 1.3 Hz, H-2´´/6´´), 7.56 (1H, m, H-4´), 7.42 (2H, m, 3´´/5´´), 6.28 (1H, d, J 3.2 Hz, H-13b), 5.57 (1H, d, J 2.8 Hz, H-13a), 5.39 (1H, dd, J 9.5, 2.4 Hz, H-3), 4.79 (1H, d, J 8.8 Hz, H-6), 3.34 (1H, m, H-7), 2.59 (1H, m, H-2b), 2.49 (1H, m, H-1), 2.16 (1H, m, H-10), 1.86 (2H, m, H-8a), 1.73 (1H, m, H-9a), 1.18 (3H, s, CH3-15), δ 1.10 (3H, d, J 7.5 Hz, CH3-14); 13C NMR data (100 MHz, $CDCl_3$): 211.8 (C-4), 170.1 (C-12), 165.7 (C-1´), 133.5 (C-4´´), 129.9 (C-2´´/6´´), 129.3 (C-1´´), 128.5 (C-3´´/5´´), 121.4 (C-13), 81.5 (C-6), 72.2 (C-3), 55.4 (C-5), 44.1 (C-7), 42.8 (C-1), 34.0 (C-9), 33.8

(C-10), 30.3 (C-2), 26.0 (C-8), 15.2 (C-14), 14.3 (C-15); [α]D20 -29.5 (c 1.00, CH_2Cl_2); IR spectrum (film, γ, cm-1): 2963, 1755, 1719, 1601, 1473, 1450, 1389, 1343, 1314, 1262, 1231, 1196, 1175, 1152, 1111, 1068, 1021, 975, 935, 892, 801, 708, 687, 642, 584, 534; TOF-MS: 369.1701 [M+H⁺] (calculated for $C_{22}H_{25}O_5$ 369.1702).

Compound 1f (3α-(m-chlorobenzoyloxy) damsin)

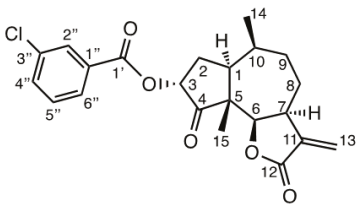

^{1}H NMR data (400 MHz, $CDCl_3$): 7.96 (1H, t, J 1.7; 1.7 Hz, H-2´´), 7.88 (1H, dt, J 7.8; 1.2; 1.2 Hz, H-6´´), 7.53 (1H, dq, J 7.9; 1.1;1.1; 1.1 Hz, H-4´´), 7.36 (1H, t, J 7.9; 7.9 Hz, H-5´´), 6.27 (1H, d, J 3.1 Hz, H-13b), 5.56 (1H, d, J 2.8 Hz, H-13a), 5.42 (1H, dd, J 9.8; 2.4 Hz, H-3a), 4.78 (1H, d, J 8.9 Hz, H-6), 3.35 (1H, m, H-7), 2.59 (1H, ddd, J 14.5; 12.6; 9.9 Hz, H-2b), 2.46 (1H, ddd, J 12.3; 7.7; 4.4 Hz, H-1), 2.17 (1H, m, H-10), 1.99 (1H, m, H-8b), 1.96 (1H, m, H-2a), 1.88 (1H, m, H-8a), 1.87 (1H, m, H-9b), 1.72 (1H, m, H-9a), 1.17 (3H, s, CH3-15), 1.10 (3H, d, J 7.5 Hz, CH3-14); ^{13}C NMR data (100 MHz, $CDCl_3$): 211.3 (C-4), 170.0 (C-12), 164.4 (C-1´), 139.6 (C-11), 134.5 (C-3´´), 133.4 (C-4´´), 130.1 (C-1´´), 129.8 (C-2´´), 129.7 (C-5´´), 128.0 (C-6´´), 121.3 (C-13), 81.3 (C-6), 72.3 (C-3), 55.3 (C-5), 44.0 (C-7), 42.7 (C-1), 33.9 (C-9), 33.7 (C-10), 30.0 (C-2), 25.9 (C-8), 15.0 (C-14), 14.1 (C-15). [α]D20 -40.0 (c 1.00, CH_2Cl_2). IR spectrum (film, γ, cm-1): 3071, 2960, 2936, 2873, 1756, 1722, 1661, 1574, 1473, 1451, 1426, 1388, 1364, 1336, 1277, 1254, 1164, 1126, 1087, 1073, 1009, 978, 903, 812, 747, 736, 700, 674, 632; TOFMS: 403.1325 [M+H+] (calculated for $C_{22}H_{24}ClO_5$ 403.1312).

Compound 2a [(E)-3-(p-(fluorophenyl) methylene) damsin]

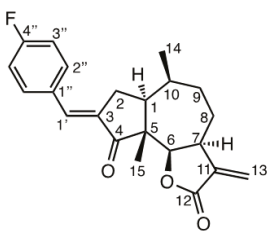

^{1}H NMR data (400 MHz, $CDCl_3$): 7.54 (2H, m, H-5´´/3´´), 7.40 (1H, m, H-1´), 7.11 (2H, m, H-2´´/6´´), 6.29 (1H, d, J 3.0 Hz, H-13b), 5.58 (1H, d, J 2.7 Hz, H-13a), 4.65 (1 H, d, J 8.5 Hz, H-6), 3.29 (1H, m, H-7), 2.94 (1H, ddd, J 15.7; 12,3; 3.1 Hz, H-2b), 2.83 (1H, ddd, J 16.8; 7.3; 1.9 Hz, H-2a), 2.28 (1H, m, H-10), 2.08 (1H, m, H-8b), 2.07 (1H, m, H-1), 1.87 (1H, m, H-9b), 1.78 (1H, m, H-8a), 1.74 (1H, m, H-9a), 1.17 (3H, d, J 7.5 Hz, CH3-14), 1.16 (3H, s, CH3-15); ^{13}C NMR data (100 MHz, $CDCl_3$): 207.3 (C-4), 170.8 (C-12), 164.2 (C-4´´), 161.9 (C-1´´), 139.9 (C-11), 132.9 (C-1´), 132.6 (C-3´´/5´´), 132.5 (C-3), 121.5 (C-13), 116.1 (C-2´´), 115.9 (C-6´´), 81.9 (C-6), 54.9 (C-5), 44.8 (C-7), 43.8 (C-1), 34.3 (C-9), 34.1 (C-10), 31.3 (C-2), 26.5 (C-8), 15.8 (C-14), 14.6 (C-15). [α]D20 -9.5 (c 1.00, CH_2Cl_2); IR spectrum (film, γ, cm-1). HRMS-ESI (m/z) 355.1702 [M+H]⁺ (calculated for $C_{22}H_{24}FO_3$ 355.1710).

Compound 2b [(E)-3-(m-(fluorophenyl) methylene) damsin]

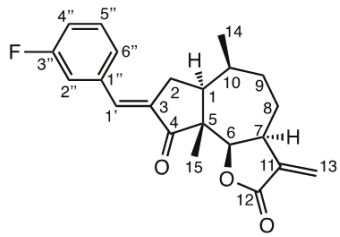

^{1}H NMR data (400 MHz, $CDCl_3$): 7.39 (1H, m, H-5´´), 7.37 (1H, m, H-1´), 7.30 (1 H, d, J 7.8 Hz, H-2´´), 7.23 (1H, dd, J 9.9; 2.0 Hz, H-6´´), 7.06 (1H, m, H-4´´), 6.28 (1H, d, J 3.0 Hz, H-13b), 5.57 (1H, d, J 2.7 Hz, H-13b), 4.64 (1H, d, J 8.5 Hz, H-6), 3.30 (1H, tdd, J 11.3; 5.4; 2.9 Hz, H-7), 2.95 (1H, ddd, J 16.1; 12.6; 3.2 Hz, H-2b), 2.85 (1H, ddd, J 17.0; 7.4; 2.0 Hz, H-2a), 2.28 (1H, m, H-10), 2.10 (1H, m, H-1), 2.07 (1H, m, H-8b), 1.90 (1H, m, H-9b), 1.81 (1H, m, H-8a) 1.72 (1H, m, H-9a), 1.18 (3H, d, J 7.5 Hz, CH3-14), 1.15 (3H, s, CH3-15); ^{13}C NMR data (100 MHz, $CDCl_3$): 207.8 (C-4), 170.3 (C-12), 162.8 (C-3´´), 140.0 (C-11), 137.6 (C-1´´), 134.7 (C-3), 132.5 (C-1´), 130.4 (C-5´´) 126.7 (C-2´´), 121.4 (C-13), 116.7 (C-6´´), 116.4 (C-4´´), 81.8 (C-6), 54.9 (C-5), 44.8 (C-7), 43.6 (C-1), 34.2 (C-9), 34.0 (C-10), 31.3 (C-2), 26.5 (C-8), 15.7 (C-14), 14.5 (C-15); [α]D20 +4.5 (c 1.00, CH_2Cl_2); IR spectrum (film, γ, cm-1): 2926, 2869, 1757, 1716, 1629, 1580, 1485, 1444, 1385, 1336, 1272, 1230, 1210, 1189, 1160, 1118, 1079, 1058, 1003, 990, 952, 884, 865, 814, 788, 735, 682. HRMS-ESI (m/z) 355.1723 [M+H]⁺ (calculated for $C_{22}H_{24}FO_3$ 355.1710).

Compound 2c [(E)-3-(o-(fluorophenyl) methylene) damsin]

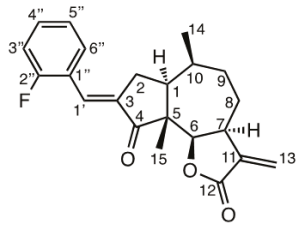

^{1}H NMR data (400 MHz, $CDCl_3$): 7.62 (1 H, s, H-1′), 7.53 (1H, td, J 7.7; 1.6 Hz, H-6′′), 7.35 (1H, m, H-4′′), 7.18 (1H, td, J 7.6; 0.8 Hz, H-5′′), 7.09 (1H, m, H-3′′), 6.27 (1H, d, J 3.0 Hz, H-13b), 5.57 (1H, d, J 2.7 Hz, H-13a), 4.64 (1H, d, J 8.5 Hz, H-6), 3.29 (1H, m, H-7), 2.94 (1H, ddd, J 16.2; 12.6; 3.3 Hz, H-2b), 2.76 (1H, ddd, J 16.9; 7.1; 1.8 Hz, H-2a), 2.26 (1H, m, H-10), 2.07 (1H, m, H-8b), 2.06 (1H, m, H-1), 1.86 (1H, m, H-9b), 1.82 (1H, m, H-8a), 1.73 (1H, m, H-9a), 1.17 (3H, d, J 7.5 Hz, CH3-14), 1.16 (3H, s, CH3-15); ^{13}C NMR data (100 MHz, $CDCl_3$): 207.6 (C-4), 170.3 (C-12), 162.9-160.4 (C-2′′), 140.1 (C-11), 135.5 (C-3), 131.3 (C-4′′), 130.1 (C-6′′), 125.7 (C-1′), 124.2 (C-5′′), 123.6 (C-1′′), 121.3 (C-13), 116.17 (s), 115.9 (C-3′′), 81.8 (C-6), 54.9 (C-5), 44.8 (C-7), 43.6 (C-1), 34.1 (C-10), 31.4 (C-2), 26.5 (C-8), 15.8 (C-14), 14.5 (C-15) ; [α]D20 +9.8 (c 1.00, CH_2Cl_2); IR spectrum (film, γ, cm-1): 2925, 2857, 1757, 1716, 1627, 1610, 1484, 1453, 1385, 1336, 1271, 1254, 1229, 1211, 1194, 1162, 1118, 1058, 985, 951, 913, 884, 838, 814, 799, 760. HRMS-ESI (m/z) 355.1716 [M+H]+ (calculated for $C_{22}H_{24}FO_3$ 355.1710).

Compound 2d [(E)-3-(m-(chlorophenyl) methylene)damsin]

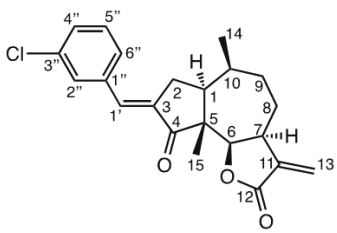

^{1}H NMR data (400 MHz, $CDCl_3$): 7.50 (1 H, s, H-2′′), 7.40 (1H, m, H-6′′), 7.35 (1H, m, H-4′′), 7.34 (1H, m, H-5′′), 7.33 (1H, m, H-1′), 6.28 (1H, d, J 3.0 Hz, H-13b) 5.57 (1H, d, J 2.7 Hz, H-13a), 4.64 (1H, d, J 8.5 Hz, H-6), 3.30 (1H, m, H-7), 2.95 (1H, ddd, J 16.6; 12.3; 3.2 Hz, H-2b), 2.84 (1H, ddd, J 17.0; 7.3; 2.0 Hz, H-2a), 2.29 (1H, m, H-10), 2.08 (1H, m, H-1), 2.06 (1H, m, H-8b), 1.91 (1H, m, H-9b), 1.82 (1H, m, H-8a), 1.73 (1H, m, H-9a), 1.18 (3H, d, J 7.5 Hz, CH3-14), 1.15 (3H, s, CH3-15); 13C NMR data (100 MHz, $CDCl_3$): 207.7 (C-4), 170.3 (C-12), 140.0 (C-11), 137.2 (C-3′′), 134.8 (C-1′′) 134.7 (C-3), 132.2 (C-5′′), 130.1 (C-4′′), 130.0 (C-2′′), 129.5 (C-1′), 128.8 (C-6′′), 121.4 (C-13), 81.8 (C-6) 54.9 (C-5), 44.8 (C-7), 43.6 (C-1), 34.2 (C-9), 34.0 (C-10), 31.3 (C-2), 26.5 (C-8), 15.7 (C-14), 14.5 (C-15); [α]D20 -8.2 (c 1.00, CH_2Cl_2); IR spectrum (film, γ, cm-1): 2925, 2866, 1758, 1716, 1628, 1562, 1473, 1449, 1420, 1385, 1337, 1271, 1250, 1206, 1186, 1160, 1118, 1058, 987, 952, 886, 815, 787, 734, 683. HRMS-ESI (m/z) 371.1425 [M+H]+ (calculated for $C_{22}H_{24}ClO_3$ 371.1414).

Compound 2e [(E)-3-(p-bromophenylmethylene) damsin]

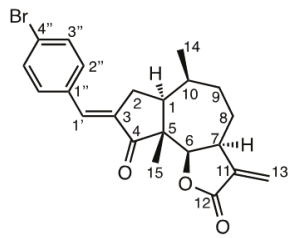

1H NMR data (400 MHz, $CDCl_3$): 7.55 (2H, m, H-3′′/5′′), 7.4 (2H, d, J 6.8 Hz, H-2′′/6′′), 7.36 (1H, m, H-1′), 6.28 (1H, dd, J 6.7, 3.1 Hz, H-13b), 5.56 (1H, dd, J 8.5; 2.7 Hz, H-13a), 4.65 (1H, m, H-6), 3.29 (1H, m, H-7), 2.93 (1H, ddd, J 16.8, 12.3, 3.2 Hz, H-2b), 2.81 (1H, ddd, J 16.9; 7.3; 2.0 Hz, H-2a), 2.28 (1H, m, H-10), 2.09 (1H, m, H-8b), 2.08 (1H, m, H-1), 1.90 (1H, m, H-9b), 1.83 (1H, m, H-8a), 1.75 (1H, m, H-9a), 1.18 (3H, d, J 7.5 Hz, CH3-14), 1.16 (3H, s, CH3-15); 13C NMR data (100 MHz, $CDCl_3$): 207.8 (C-4), 170.3 (C-12), 140.0 (C-11), 134.4 (C-3), 134.1 (C-1′′), 132.6 (C-1′), 132.1 (C-3′′/5′′), 131.9 (C-2′′/6′′), 124.0 (C-4′′), 121.4 (C-13), 81.8 (C-6), 54.9 (C-5), 44.8 (C-7), 43.7 (C-1), 34.2 (C-9), 34.1 (C-10), 31.4 (C-2), 26.5 (C-8), 15.8 (C-14), 14.5 (C-15) ; [α]D20 +24.5 (c 1.00, CH_2Cl_2); IR spectrum (film, γ, cm-1): 2925, 2861, 1757, 1714, 1624, 1583, 1487, 1448, 1403, 1337, 1306, 1271, 1252, 1238, 1161, 1119, 1073, 1006, 984, 951, 815, 733. HRMS-ESI (m/z) 415.0917 [M+H]+ (calculated for $C_{22}H_{24}BrO_3$ 415.0909).

Compound 2f [(E)-3-(m-bromophenylmethylene) damsin]

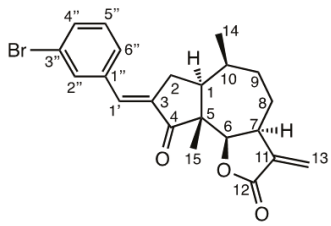

^{1}H NMR data (400 MHz, $CDCl_3$): 7.64 (1H, s, H-2´´), 7.48 (1H, d, J 8.0 Hz, H-4´´), 7.44 (1H, d, J 7.9 Hz, H-6´´), 7.31 (1H, m, H-1´), 7.28 (1H, t, J 7.9 Hz, H-5´´), 6.27 (1H, d, J 3.0 Hz, H-13b), 5.57 (1H, d, J 2.6 Hz, H-13a), 4.63 (1H, d, J 8.6 Hz, H-6), 3.29 (1H, m, H-7), 2.94 (1H, ddd, J 16.6; 12.3; 3.1 Hz, H-2b), 2.83 (1H, ddd, J 17.0; 7.3; 1.9 Hz, H-2a), 2.29 (1H, m, H-10), 2.08 (1 H, m, H-1), 2.07 (1H, m, H-8b), 1.89 (1H, m, H-9b), 1.83 (1H, m, H-8a), 1.74 (1H, m, H-9a), 1.17 (3H, d, J 7.5 Hz, CH3-14), 1.14 (3H, s, CH3-15); ^{13}C NMR data (100 MHz, $CDCl_3$): 207.7 (C-4), 170.2 (C-12), 140.0 (C-11), 137.5 (C1´´), 134.8 (C-3), 132.9 (C-2´´), 132.4 (C-4´´), 132.1 (C-1´), 130.3 (C-5´´), 129.1 (C-6´´), 122.9 (C-3´), 121.3 (C-13), 81.7 (C-6), 54.8 (C-5), 44.7 (C-7), 43.6 (C-1), 34.2 (C-9), 34.0 (C-10), 31.2 (C-2), 26.4 (C-8), 15.7 (C-14), 14.4 (C-15) ; [α]D20 -2.6 (c 1.00, CH_2Cl_2); IR spectrum (film, γ, cm-1): 2923, 2860, 1757, 1716, 1627, 1557, 1473, 1449, 1415, 1337, 1270, 1160, 1118, 986, 785, 682. . HRMS-ESI (m/z) 415.0919 $[M+H]^+$ (calculated for $C_{22}H_{24}BrO_3$ 415.0909).

Compound 2g [(E)-3-(o-bromophenylmethylene) damsin]

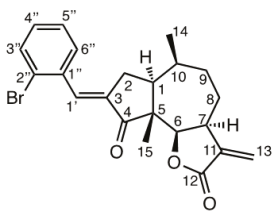

^{1}H NMR data (400 MHz, CDCl3): 7.67 (1H, dd, J 2.9; 1.9 Hz, H-1), 7.61 (1H, dd, J 8.0, 1.1 Hz, H-3´´), 7.50 (1H, dd, J 7.8; 1.4 Hz, H-6´´), 7.34 (1H, m, H-5´´), 7.19 (1H, td, J 7.8, 1.6 Hz, H-4´´), 6.26 (1H, d, J 3.0 Hz, H-13b), 5.56 (1H, d, J 2.7 Hz, H-13a), 4.61 (1H, d, J 8.5 Hz, H-6), 3.29 (1H, ddd, J 10.4; 7.6; 3.2 Hz, H-7), 2.90 (1H, ddd, J 16.3; 12.7; 3.4 Hz, H-2b), 2.69 (1H, ddd, J 16.7; 6.9; 1.8 Hz, H-2a), 2.21 (1H, ddd, J 11.7; 7.7; 4.3 Hz, H-10), 2.06 (1H, m, H-8b), δ 2.04 (1H, m, H-1), 1.85 (1H, m, H-9b), 1.81 (1H, m, H-8a), 1.72 (1H, m, H-9a), 1.16 (3H, s, CH3-15), 1.14 (3H, d, 7.5 Hz, CH3-14); ^{13}C NMR data (100 MHz, $CDCl_3$): 207.4 (C-4), 170.3 (C-12), 140.0 (C-11), 135.8 (C-3), 135.2 (C-1´´), 133.4 (C-3´´), 132.2 (C-1´), 130.5 (C-4´´), 130.1 (C-6´´), 127.3 (C-5´´), 126.2 (C-2´´), 121.2 (C-13), 81.8 (C-6), 54.9 (C-5), 44.7 (C-7), 43.7 (C-1), 34.0 (C-9), 34.0 (C-10), 31.0 (C-2), 26.3 (C-8), 15.7 (C-14), 14.4 (C-15); $[\alpha]_D^{20}$ +9.1 (c 1.00, CH_2Cl_2); IR spectrum (film, γ, cm-1): 2924, 2865, 1758, 1717, 1625, 1465, 1432, 1385, 1336, 1271, 1251, 1227, 1188, 1161, 1113, 1046, 1023, 985, 950, 815, 761, 740, 664. HRMS-ESI (m/z) 415.0912 $[M+H]^+$ (calculated for $C_{22}H_{24}BrO_3$ 415.0909).

Compound 2h [(E)-3-(p-ethylphenylmethylene) damsin]

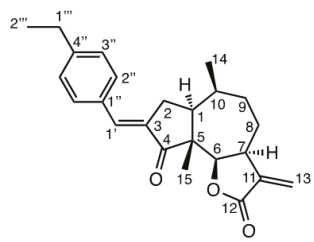

^{1}H NMR data (400 MHz, $CDCl_3$): 7.47 (2H, d, J 8.2 Hz, H-2´´/6´´), 7.42 (1H, m, H-1´), 7.25 (2H, d, J 7.9 Hz, H-3´´/5´´), 6.28 (1H, d, J 2.9 Hz, H-13b), 5.57 (1H, d, J 2.6 Hz, H-13a), 4.65 (1H, d, J 8.5 Hz, H-6), 3.28 (1H, m, H-7), 2.96 (1H, ddd, J 16.8; 7.4, 1.9 Hz, H-2b), 2.86 (1H, ddd, J 16.8; 7.4; 1.9 Hz, H-2a), 2.68 (2H, q, J 7.6 Hz, H-1´´´), 2.28 (1H, m, H-10), 2.08 (1H, m, H-8b), 2.07 (1H, m, H-1), 1.88 (1H, m, H-9b), 1.81 (1H, m, H-8a), 1.74 (1H, m, H-9a), 1.25 (3H, t, J 7.6 Hz, H-2´´´), 1.18 (3H, d, J 7.5 Hz, CH3-14), 1.16 (3H, s, CH3-15); ^{13}C NMR data (100 MHz, $CDCl_3$): 208.1 (C-4), 170.3 (C-12), 146.3 (C-4´´), 140.2 (C-11), 134.0 (C-1´), 132.9 (C-3), 132.4 (C-1´´), 130.8 (C-2´´/6´´), 128.4 (C-5´´/3´´), 121.2 (C-13), 81.9 (C-6), 54.8 (C-5), 44.9 (C-7), 43.7 (C-1), 34.3 (C-9), 34.2 (C-10), 31.5 (C-2), 28.9 (C-1´´´), 26.6 (C-8), 15.8 (C-14), 15.4 (C-2´´´), 14.6 (C-15); [α]D20 +38.3 (c 1.00, CH_2Cl_2); IR spectrum (film, γ, cm-1): 2963, 2928, 2869, 1757, 1713, 1624, 1605, 1510, 1451, 1385, 1335, 1271, 1254, 1159, 1117, 1058, 985, 915, 826. HRMS-ESI (m/z) 365.2109 [M+H]+ (calculated for $C_{24}H_{29}O_3$ 365.2117).

Compound 2i [(E)-3-(p-isopropylphenylmethylene) damsin]

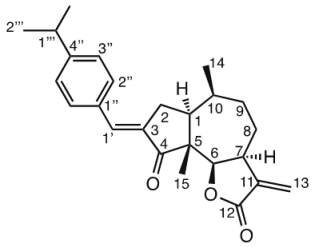

^{1}H NMR data (400 MHz, $CDCl_3$): 7.49 (2H, d, J 8.3 Hz, H-2´´/6´´), δ 7.43 (1H, m, H-1´), δ 7.28 (2H, d, J 8.2 Hz, H-3´´/5´´), δ 6.28 (1H, d, J 3.0 Hz, H-13b), δ 5.57 (1H, d, J 2.6 Hz, H-13a), δ 4.65 (1H, d, J 8.5 Hz, H-6), δ 3.28 (1H, m, H-7), δ 2.96 (1H, ddd, J 16.3; 9.5; 3.6 Hz, H-2b), δ 2.93 (1H, m, $(H_3C)_2$HC-Ar), δ 2.87 (1H, ddd, J 16.8; 7.5; 2.0 Hz, H-2a), δ 2.28 (1H, m, H-10), δ 2.09 (1H, m, H-8b), δ 2.07 (1H, m, H-1), δ 1.88 (1 H, m, H-9b), δ 1.81 (1H, m, H-8a), δ 1.73 (1H, m, H-9a), δ 1.26 (6H, d, J 6.9 Hz, $(H_3C)_2$HC-Ar), δ 1.18 (3H, d, J 7.5 Hz, CH_3-14), δ 1.16 (3H, s, CH3-15); ^{13}C NMR data (100 MHz, $CDCl_3$): 208.1 (C-4), 170.3 (C-12), 150.9 (C-4´´), 140.2 (C-11), 134.0 (C-1´), 133.1 (C-1´´), 132.5 (C-3), 130.8 (C-2´´/6´´), 127.0 (C-3´´/5´´), 121.3 (C-13), 81.9 (C-6), 54.8 (C-5), 44.9 (C-7), 43.7 (C-1), 34.3 (C-9), 34.2 (C-10), 34.1 ($(H_3C)_2$HC-Ar), 31.5 (C-2), 26.6 (C-8), 23.88 ($(H_3C)_2$HC-Ar), 15.8 (C-14), 14.6 (C-15); [α]D20 +40.2 (c 1.00, CH_2Cl_2); IR spectrum (film, γ, cm-1): 2959, 2926, 2868, 1759, 1714, 1624, 1605, 1458, 1417, 1384, 1362, 1336, 1309, 1271, 1254, 1160, 1118, 1055, 985, 825. HRMS-ESI (m/z) 379.2285 [M+H]+ (calculated for $C_{25}H_{31}O_3$ 379.2273).

Compound 3a [(E)-3-(o-(p-trifluoromethylfluorophenyl) methylene) damsin]

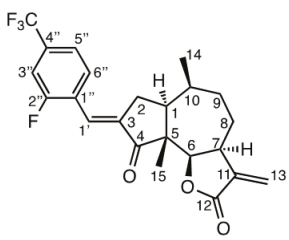

^{1}H NMR data (400 MHz, $CDCl_3$): 7.65 (1H, t, J 7.6 Hz, H-6´´), 7.55 (1H, s, H-1´), 7.45 (1H, d, J 8.2 Hz, H-5´´), 7.36 (1H, dd, J 9.4; 1.15 Hz, H-3´´),6.28 (1H, d, J 3.0 Hz, H-13b), 5.57 (1H, d, J 2.7 Hz, H-13a), 4.64 (1H, d, J 8.6 Hz, H-6), 3.31 (1H, m, H-7), 2.95 (1H, ddd, J 16.4; 12.7; 3.4 Hz, H-2b), 2.75 (1H, ddd, J 17.1; 7.0; 1.7 Hz, H-2a), 2.26 (1H, m, H-10), δ 2.09 (1H, m, H-1), 2.07 (1H, m, H-8b), 1.89 (1H, m, H-9b), 1.85 (1H, m, H-8a), 1.75 (1H, m, H-9a), 1.16 (3H, d, J 7.5 Hz, CH3-14), 1.16 (3H, s, CH3-15); ^{13}C NMR data (100 MHz, $CDCl_3$): 207.1 (C-4), 170.3 (C-12), 162.3 159.7 (C-2´´), 139.9 (C-11), 137.9 (C-3), 132.7 (C-4´´), 130.8 (C-6´´), 127.3 (C-1´´´), 124.4 (C-1´´), 124.0 (C-1´), 121.4 (C-13), 121.1 (C-5´´), 113.6 (C-3´´), 81.7 (C-6), 55.0 (C-5), 44.7 (C-7), 43.5 (C-1), 34.0 (C-9, 10), 31.3 (C-2), 26.3 (C-8), 15.7 (C-14), 14.4 (C-15); [α]D20 -18.6 (c 1.00, CH_2Cl_2); IR spectrum (film, γ, cm-1): 2928, 2868, 1758, 1720, 1636, 1574, 1507, 1426, 1329, 1272, 1210, 1195, 1167, 1122, 1066, 986, 949, 909, 880, 832, 815, 743, 659. HRMS-ESI (m/z) 423.1594 [M+H]+ (calculated for $C_{23}H_{23}F_4O_3$ 423.1583).

Compound 3b [(E)-3-(o-(p-methylhydroxyphenyl) methylene) damsin]

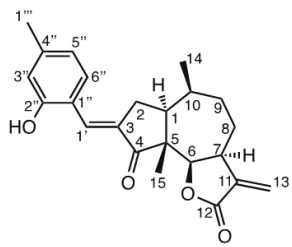

^{1}H NMR data (400 MHz, $CDCl_3$): 8.0 (1H, s, H-1´), 7.36 (1 H, d, H-6´´), 6.73 (1H, d, H-5´´), 6.8 (1H, s, H-3´´), 6.3 (1H, d, J 3.0 Hz, H-13b), 5.58 (1H, d, J 2.7 Hz, H-13a), 4.65 (1H, d, J 8.4 Hz, H-6), 3.28 (1H, m, H-7), 2.93 (1H, ddd, J 16.7; 12.3; 3.1 Hz, H-2b), 2.8 (1H, ddd, J 16.6; 7.2; 1.7 Hz, H-2a), 2.32 (3H, s, H3C-Ar), 2.26 (1H, m, H-10), 2.07 (1H, m, H-8b), 2.06 (1H, m, H-1), 1.87 (1H, m, H-9b), 1.78 (1H, m, H-8a), 1.74 (1H, m, H-9a), 1.18 (3H, d, J 7.5 Hz, CH3-14), 1.17 (3H, s, CH3-14); ^{13}C NMR data (100 MHz, $CDCl_3$): 209.6 (C-4), 170.7 (C-12), 156.7 (C-2´´), 142.6 (C-4´´), 140.2 (C-11), 131.6 (C-3), 129.9 (C-1´), 129.5 (C-6´´), 121.5 (C-13), 121.3 (C-5´´), 119.9 (C-1´´), 117.1 (C-3´´), 82.1 (C-6), 54.9 (C-5), 45.0(C-7), 43.8 (C-1), 34.3 (C-10), 34.2 (C-9), 31.6 (C-2), 26.7 (C-8), 21.7(H_3C-Ar), 15.9 (C-14), 14.7 (C-15); [α]D20 +45.6 (c 1.00, CH_2Cl_2); IR spectrum (film, γ, cm-1): 3349, 2924, 2858, 1742, 1710, 1658, 1605, 1450, 1419, 1384, 1342, 1305, 1261, 1187, 1162, 1107, 1058, 985, 884, 866, 814, 733, 643. HRMS-ESI (m/z) 367.1900 [M+H]+ (calculated for $C_{23}H_{27}O_4$ 367.1909).

Compound 3c [(E)-3-(p-(m-trifluoromethylhydroxyphenyl) methylene) damsin]

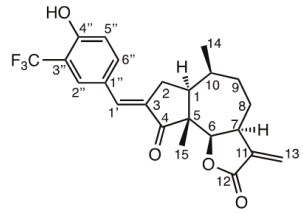

^{1}H NMR data (400 MHz, $CDCl_3$): 7.7 (1H, s, H-2´´), 7.52 (1H, d, H-6´´), 7.34 (1H, s, H-1´), 6.96 (1H, d, H-5´´), 6.27 (1H, d, J 3.0 Hz, H-13b), 5.57 (1H, d, J 2.7 Hz, H-13a), 4.63 (1H, d, J 8.5 Hz, H-6), 3.28 (1H, m, H-7), 2.91 (1H, ddd, J 15.5; 12.2; 3.1Hz, H-2b), 2.8 (1H, ddd, J 16.7; 7.4; 1.9 Hz, H-2a), 2.27 (1H, m, H-10), 2.07(1H, m, H-8b), 2.06 (1H, m, H-1), 1.89 (1H, m, H-9b), 1.84 (1H, m, H-8a), 1.73 (1H, m, H-9a), 1.16 (3H, d, J 7.5 Hz, CH_3-14), 1.13 (3H, s, CH_3-15); ^{13}C NMR data (100 MHz, $CDCl_3$): 208.4 (C-4), 170.8 (C-12), 156.6 (C-4´´), 139.9 (C-11), 135.9 (C-6´´), 133.1 (C-1´), 131.6 (C-3), 129.2 (C-2´´), 126.7 (C-3´´), 121.7 (C-13/ F3C-Ar), 117.6 (C-1´´/C-5´´), 82.1 (C-6), 54.8 (C-5), 44.8 (C-7), 43.8 (C-1), 34.2 (C-10), 34.0 (C-9), 31.1 (C-2), 26.4 (C-8), 15.8 (C-14), 14.5 (C-15); $[\alpha]D^{20}$ +16.4 (c 1.00, CH_2Cl_2); IR spectrum (film, γ, cm-1): 3273, 2925, 2856, 1737, 1713, 1606, 1509, 1435, 1365, 1327, 1297, 1274, 1252, 1207, 1185, 1159, 1123, 1052, 989, 952, 883, 832, 816, 756, 664. HRMS-ESI (m/z) 421.1632 [M+H]+ (calculated for $C_{23}H_{24}F_3O_4$ 421.1627).

Compound 3d [(E)-3-(o-(m-chlorohydroxyphenyl) methylene) damsin]

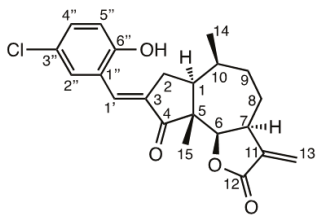

^{1}H NMR data (400 MHz, $CDCl_3$): 7.71 (1H, m, H-1´), 7.34 (1H, d, J 2.5 Hz, H-2´´), 7.12 (1H, dd, J 8.7; 2.5 Hz, H-4´´), 6.77 (1H, d, J 8.7 Hz, H-5´´), 6.25 (1H, d, J 3.0 Hz, H-13b), 5.56 (1H, d, J 2.6 Hz, H-13a), 4.60 (1H, d, J 8.6 Hz, H-6), 3.26 (1H, m, H-7), 2.88 (1H, m, H-2b), 2.88 (1H, ddd, J 18.8; 7.1; 1.7 Hz, H-2a), 2.25 (1H, m, H-10), 2.04 (1H, m, H-8b), 2.03 (1H, m, H-1), 1.84 (1H, m, H-9b), 1.79 (1H, m, H-8a), 1.69 (1H, m, H-9a), 1.14 (3H, d, J 7.5 Hz, CH3-14), 1.12 (3H, s, CH_3-15); ^{13}C NMR data (100 MHz, $CDCl_3$): 208.5 (C-4), 170.7 (C-12), 155.9 (C-6´´), 139.9 (C-11), 133.5 (C-3), 130.7 (C-4´´), 128.8 (C-2´´), 128.0 (C-1´), 124.2 (C-1´´), 124.0 (C-3´´), 121.6 (C-13), 117.3 (C-5´´), 82.1 (C-6), 54.9 (C-5) 44.7 (C-7) 43.8 (C-1), 34.1 (C-9), 34.0 (C-10), 31.1 (C-2), 26.4 (C-8), 15.7 (C-14), 14.4 (C-15); $[\alpha]_D^{20}$ -7.0 (c 1.00, CH_2Cl_2); IR spectrum (film, γ, cm-1): 3343, 2924, 2856, 1738, 1713, 1656, 1615, 1490, 1474, 1447, 1417, 1385, 1342, 1274, 1255, 1192, 1159, 1115, 1058, 988, 951, 915, 896, 881, 816, 753, 665, 644. HRMS-ESI (m/z) 387.1370 $[M+H]^+$ (calculated for $C_{22}H_{24}ClO_4$ 387.1363).

Compound 4a [(E)-3-(furanylmethylene) damsin]

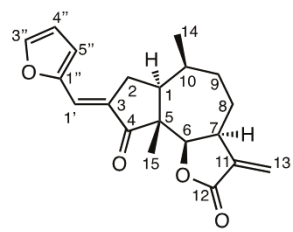

^{1}H NMR data (400 MHz, $CDCl_3$): 7.53 (1H, d, J 1.4 Hz, H-3´´), 7.12 (1H, m, H-1´´), 6.63 (1H, d, J 3.5 Hz, .H-5´´), 6.47 (1 H, dd, J 3.4; 1.8 Hz, H-4´´) 6.20 (1H, d, J 3.0 Hz, H-13b), 5.51 (1H, d, J 2.7 Hz, H-13a), 4.59 (1H, d, J 8.5 Hz, H-6), 3.26 (1H, m, H-7), 2.94 (1H, ddd, J 17.8; 7.5; 1.8 Hz, H-2b), 2.82 (1H, m, H-2a), 2.23 (1H, m, H-10), 2.05 (1H, m, H-1), 2.01 (1H, m, H-8b), 1.82 (1H, m, H-9b), 1.78 (1H, m, H-8a), 1.68 (1H, m, H-9a), 1.10 (3H, d, J 7.5 Hz, CH_3-14), 1.06 (3H, s, CH3-15); ^{13}C NMR data (100 MHz, $CDCl_3$): 207.7 (C-4), 170.2 (C-12), 152.1 (C-1´´), 145.1 (C-3´´), 140.0 (C-11), 130.7 (C-3), 121.1 (C-13), 119.9 (C-1´), 116.4 (C-5´´), 112.5 (C-4´´), 81.8 (C-6), 54.9 (C-5), 44.7 (C-7), 43.1 (C-1), 34.1 (C-9), 33.9 (C-10), 30.8 (C-2), 26.4 (C-8), 15.6 (C-14), 14.4 (C-15) ; $[\alpha]D^{20}$ -71.9 (c 1.00, CH_2Cl_2); IR spectrum (film, γ, cm-1): 2923, 2863, 1757, 1709, 1622, 1474, 1389, 1338, 1271, 1253, 1232, 1161, 1117, 1069, 1021, 982, 950, 882, 815, 752, 633. HRMS-ESI (m/z) 327.1584 [M+H]+ (calculated for $C_{20}H_{23}O_4$ 327.1596).

Compound 4b [(E)-3-(naphtylmethylene) damsin]

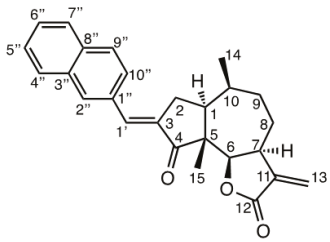

^{1}H NMR data (400 MHz, $CDCl_3$): 8.01 (1H, s, H-2´´), 7.89 (1H, m, H-4´´), 7.86 (1H, m, H-9´´), 7.83 (1H, m, H-7´´), 7.66 (1H, m, H-10´´), 7.60 (1H, m, H-1´), 7.53 (1H, m, H-6´´), 7.51 (1H, m, H-5´´), 6.30 (1H, J 3.0 Hz, H-13b), 5.58 (1H, J 2.6 Hz, H-13a). 4.67 (1H, J 8.5 Hz, H-6), 3.29 (1H, m, H-7), 3.08 (1H, ddd, J 16.2; 12.1; 3.2 Hz, H-2b), 2.97 (1H, ddd, J 16.8; 7.4; 1.9 Hz, H-2a), 2.32 (1H, m, H-10), 2.11 (1H, m, H-8b), 2.10 (1H, m, H-1), 1.91 (1H, m, H-9b), 1.82 (1H, m, H-8a), 1.76 (1H, m, H-9a), 1.22 (3H, d, J 7.5 Hz, CH_3-14), 1.20 (3H, m, CH_3-15); ^{13}C NMR data (100 MHz, $CDCl_3$): 208.0 (C-4), 170.3 (C-12), 140.2 (C-11), 134.1 (C-1´) 133.6 (C-3´´), 133.6 (C-3), 133.3 (C-8´´), 133.0 (C-1´´), 131.4 (C-2´´), 128.7 (C-9´´), 128.5 (C-4´´), 127.8 (C-7´´), 127.4 (C-6´´), 127.0 (C-10´´), 126.8 (C-5´´), 121.3 (C-13), 81.9 (C-6) 54.9 (C-5), 44.9 (C-7), 43.8 (C-1), 34.3 (C-9), 34.2 (C-10) 31.5 (C-2), 26.6 (C-8), 15.9 (C-14) 14.2 (C-15) ; $[\alpha]D^{20}$ +23.8 (c 1.00, CH_2Cl_2); IR spectrum (film, γ, cm-1): 2924, 2857, 1756, 1713, 1617, 1472, 1447, 1385, 1335, 1271, 1231, 1191, 1161, 1117, 1057, 988, 955, 882, 859, 816, 735, 640. HRMS-ESI (m/z) 387.1955 [M+H]+ (calculated for $C_{26}H_{27}O_3$ 387.1960).

Compound 5a

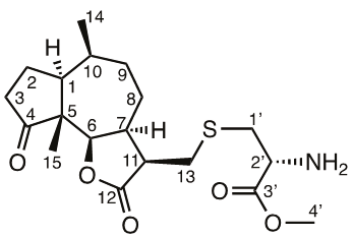

^{1}H NMR data (400 MHz, $CDCl_3$): 4.41 (1H, dd, J, 8.8; 2.8 Hz, H-6), 3.74 (1H, m, H-2´), 3.73 (3H, s, H-4´), 2.98 (1H, td, J 13.3; 4.8 Hz, H-1´b), 2.96 (1H, m, H-13b), 2.87 (1H, ddd, J 13.6; 6.6; 3.8 Hz, H-13a), 2.86 (1H, m, H-1b), 2.79 (1H, m, H-7), 2.78 (1H, ddd, J 18.7; 9.3; 4.5 Hz, H-7), 2.64 (1H, ddd, J 9.3; 6.3; 4.6 Hz, H-11), 2.40 (1H, m, H-3b), 2.22 (1H, m, H-3a), 2.18 (1H, m, H-10), 2.05 (1H, m, H-1), 1.98 (1H, m, H-2b), 1.87 (1H, m, H-8b), 1.83 (1H, m, H-2a), 1.78 (1H, m, H-8a), 1.74 (1H, m, H-9b), 1.66 (1H, m, H-9a), 1.08 (3H, m, CH_3-15), 1.07 (3H, d, J 7.5 Hz, CH3-14); ^{13}C NMR data (100 MHz, CD2-Cl2): 219.3 (C-4), 177.6 (C-12), 174.2 (C-3´), 83.1 (C-6), 55.1 (C-5), 54.8 (C-2´), 52.7 (C-4´), 47.2 (C-11), 46.8 (C-1), 45.2 (C-7), 38.2 (C-1´), 36.9 (C-3), 34.8 (C-10), 33.5 (C-9), 33.3 (C-13), 25.3 (C-8), 24.3 (C-2), 16.2 (C-14), 14.3 (C-15) ; $[\alpha]D^{20}$ 7.6 (c 1.00, CH_2Cl_2); IR spectrum (film, γ, cm-1): 2922, 1736, 1438, 1408, 1385, 1359, 1176, 1053, 1000, 910. TOFMS: 384.1844 [M+H]+ (calculated for $C_{19}H_{30}NO_5S$ 384.1845).

Compound 5b

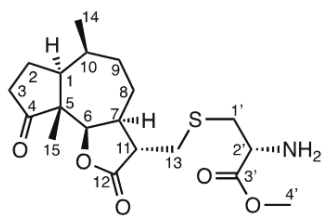

^{1}H NMR data (400 MHz, $CDCl_3$): 4.45 (1H, d, J 5.5 Hz, H-6), δ 3.70 (3H, s, H-4´), δ 3.65 (1H, dd, J 7.1; 4.9 Hz, H-2´), δ 3.00 (1H, dd, J 13.0; 4.5 Hz, H-13b), δ 2.93 (2H, m, H-11/1´), δ 2.78 (1H, ddd, J 13.5; 7.2; 0.7 Hz, H-1´), δ 2.59 (2H, m, H-7/13a), δ 2.43 (1H, dd, J 19.2; 8.6 Hz, H-3), δ 2.21 (1H, m, H-10), δ 2.16 (1H, m, H-3a), δ 2.08 (1H, m, H-1), δ 2.03 (1H, m, H-2), δ 1.85 (1H, m, H-9b), δ 1.81 (1H, m, H-2a), δ 1.60 (1H, tdd, J 13.3; 8.7; 4.8 Hz, H-9a), δ 1.52 (2H, dd, J 9.5; 5.8 Hz, H8-a/8b), δ 1.11 (3H, s, CH3-15), 1.06 (3H, d, J 7.6 Hz, CH3-14); ^{13}C NMR data (100 MHz, CD_2Cl_2): 221.7 (C-4), 176.4 (C-3´), 174.8 (C-12), 82.3 (C-6), 55.0 (C-5), 54.8 (C-2´), 52.5 (C-4´), 46.2 (C-1), 45.9(C-7), 45.8 (C-11), 38.3 (C-1´), 37.4 (C-9), 35.4 (C-10), 35.3 (C-3), 28.6 (C-13b), 24.6 (C-2), 18.4 (C-8), 16.9 (C-14), 16.1 (C-15); $[\alpha]D^{20}$ -17.5 (c 1.00, CH_2Cl_2); IR spectrum (film, γ, cm-1): 2921, 1831, 1732, 1620, 1435, 1408, 1385, 1340, 1176, 1053, 1000, 931, 840. TOFMS: 384.1843 [M+H]+ (calculated for $C_{19}H_{30}NO_5S$ 384.1845).

Acknowledgments

The authors thank the Swedish International Development Agency (SIDA) for the financial support of this study, which is part of the project "Biomolecules of medicinal and industrial interest" developed between the Universidad Mayor de San Andrés (UMSA La Paz – Bolivia) and Lund University (Sweden).

Conflict of interest

No author has any associations that may represent a potential conflict of interest.

References

1. Suter MB, Pagani O. (2018). Should age impact breast cancer management in young women? Fine tuning of treatment guidelines. Therapeutic advances in medical oncology 10: 1758835918776923.
2. Mukohara T. (2011). Mechanisms of resistance to anti-human epidermal growth factor receptor 2 agents in breast cancer. Cancer Science 102: 1-8.
3. Zhu L, Chen Y, Wei C, Yang X, Cheng J, Yang Z, Chen C, Ji Z. (2018). Anti-proliferative and pro-apoptotic effects of cinobufagin on human breast cancer MCF-7 cells and its molecular mechanism. Natural product research 32: 493-497.
4. Cragg GM, Newman DJ (2013) Natural products: a continuing source of novel drug leads. Biochimica et biophysica acta 2013; 1830: 3670-3695.
5. Atanasov AG, Waltenberger B, Pferschy-Wenzig EM, Linder T, Wawrosch C et al. (2015) Discovery and resupply of pharmacologically active plant-derived natural products: A review. Biotechnology advances 2015; 33: 1582-1614.
6. Panda AK, Chakraborty D, Sarkar I, Khan T, Sa G. (2017). New insights into therapeutic activity and anticancer properties of curcumin. Journal of experimental pharmacology 9: 31-45.
7. Weldon CB, Burow ME, Rolfe KW, Clayton JL, Jaffe BM et al. (2001). NF-κB–mediated chemoresistance in breast cancer cells. Surgery 130: 143-150.
8. Zhang S, Won YK, Ong CN, Shen HM. (2005). Anti-cancer potential of sesquiterpene lactones: bioactivity and molecular mechanisms. Current medicinal chemistry. Anti-cancer agents 5: 239-249.
9. Ghantous A, Gali-Muhtasib H, Vuorela H, Saliba NA, Darwiche N. (2010). What made sesquiterpene lactones reach cancer clinical trials? Drug discovery today 15: 668-678.
10. Scotti MT, Fernandes MB, Ferreira MJP, Emerenciano VP. (2007). Quantitative structure–activity relationship of sesquiterpene lactones with cytotoxic activity. Bioorganic and Medicinal Chemistry 15: 2927-2934.
11. Rüngeler P, Castro V, Mora G, Gören N, Vishnewski W, Pahl HL, Schmidt TJ. (1999). Inhibition of transcription factor NF-κB by sesquiterpene lactones: a proposed molecular mechanism of action. Bioorganic and Medicinal Chemistry 7: 2343-2352.
12. Chen H, Chen B-Y, Liu C-T, et al. (2014). Synthesis and structure–activity relationships of guaiane-type sesquiterpene lactone derivatives with respect to inhibiting NO production in lipopolysaccharide-induced RAW 264.7 macrophages. European Journal of Medicinal Chemistry 83: 307-316.
13. García-Piñeres AJ, Castro VC, Mora G, Schmidt TJ, Strunck E. (2001). Cysteine 38 in p65/NF-κB plays a crucial role in DNA binding inhibition by sesquiterpene lactones. Journal of Biological Chemistry 276: 39713-39720.
14. Hehner SP, Heinrich M, Bork PM, et al. (1998). Sesquiterpene lactones specifically inhibit activation of NF-κB by preventing the degradation of IκB-α and IκB-β. Journal of Biological Chemistry 273: 1288-1297.
15. Wilson AJ, Kerns JK, Callahan JF, Moody CJ. (2013). Keap calm, and carry on covalently. Journal of Medicinal Chemistry 56: 7463-7476.
16. Gonzalez-Bello C. (2016). Designing Irreversible Inhibitors--Worth the Effort? ChemMedChem 11: 22-30.
17. Villagomez R, Rodrigo GC, Collado IG, Calzado M, Munoz E, Åkesson B, Sterner O, Almanza G, Duan R. (2013). Multiple anticancer effects of damsin and coronopilin isolated from Ambrosia arborescens on cell cultures. Anticancer Research 33: 3799-3805.
18. Villagomez R, Collado JA, Muñoz E, Almanza G, Sterner O. (2014). Natural and semi-synthetic pseudoguaianolides as inhibitors of NF-κB. Journal of Biomedical Science and Engineering 7: 833-847.
19. Villagomez, R.; Quiroz, M.; Tito, A.; Sterner, O.; Almanza, G. (2015). Natural Pseudoguaianolides prepared from damsin. Chemistry of Natural Compounds 51: 675-680
20. Herz W, Anderson G, Gibaja S, Raulais D. (1969). Sesquiterpene lactones of some Ambrosia species. Phytochemistry 8: 877-881.
21. Lozano M, Soria W, Almanza GR, Manner S, Oredsson S, Villagomez R, Sterner O. (2019). Selective cytotoxicity of damsin derivatives in breast cancer cells. Journal of Advanced Pharmaceutical Science and Technology 2: 22-36.
22. Soule HD, Maloney TM, Wolman SR, Peterson WD, Brenz R, McGrath CM, Russo J, Pauley RJ, Jones RF, Brooks SC. (1990). Isolation and characterization of a spontaneously immortalized human breast epithelial cell line, MCF-10. Cancer Research 50: 6075-6086.

Citation: Maribel Lozano, Wendy Soria, Giovanna R. Almanza, Sophie Manner, Stina Oredsson, Rodrigo Villagomez and Olov Sterner. (2019). Cytotoxicity of New Damsin Derivatives in Breast Cancer Cells. *Journal of Pharmacy and Drug Development* 1(2).

23. Geltmeier A, Rinner B, Bade D, Meditz K, Witt R, Bicker U, Bludszuweit C, Maier P. (2015). Characterization of dynamic behaviour of MCF7 and MCF10A cells in ultrasonic field using modal and harmonic analyses. PLoS ONE 10: e0134999. doi:10.1371/journal.pone.0134999.
24. Tanner M, Kapanen AI, Junttila T, Raheem O, Grenman S, Elo J, Elenius K, Isola J. (2004). Characterization of a novel cell line established from a patient with Herceptin-resistant breast cancer. Molecular Cancer Therapeutics 3: 1585-1592.
25. Schwöbel JAH, Wondrousch D, Koleva YK, Madden JC, Cronin MTD, Schüürmann G. (2010). Prediction of Michael-type acceptor reactivity toward glutathione. Chemical Research and Toxicology 23: 1576–1585.
26. Lushchak VL. (2012). Glutathione homeostasis and functions: potential targets for medical interventions. Journal of Amino Acids doi:10.1155/2012/736837.
27. Schmidt TJ. (2000). Glutathione adducts of helenalin and 11α, 13-dihydrohelenalin acetate inhibit glutathione S-transferase from horse liver. Planta Medica 66: 106-109.
28. Whipple RA, Vitolo MI, Boggs AE, Charpentier MS, Thompson K, Martin SS. (2013). Parthenolide and costunolide reduce microtentacles and tumor cell attachment by selectively targeting detyrosinated tubulin independent from NF-κB inhibition. Breast Cancer Research 15: R83.
29. Fonrose X, Ausseil F, Soleilhac E, Masson V, David B, Pouny I, Cintrat J-C, Bernard Rousseau B, Barette C, Massiot G, and Lafanechère L. (2007) Parthenolide inhibits tubulin carboxypeptidase activity. Cancer Research 67: 2271-3378.

Manuscript I

Molecular mechanisms of breast cancer cell active chemically synthesized damsin derivatives

Soria-Sotillo W [1,2], Lozano M [3,4], Huang X [1], Malakpour A [1], Almanza GR [4], Sterner O [2], and Oredsson S. [1]*

[1] Department of Biology, Lund University, Lund, Sweden.
[2] Molecular Biology and Biotechnology Institute, University Major of San Andrés, La Paz, Bolivia.
[3] Centre for Analysis and Synthesis, Department of Chemistry, Lund University, Lund, Sweden.
[4] Chemical Research Institute, University Major of San Andres, La Paz, Bolivia.

* Corresponding author
E-mail: stina.oredsson@biol.lu.se

Abstract

Sesquiterpene lactones (SLs) are a group of secondary plant metabolites that have been shown to have anti-proliferative capacity. The chemical reactivity of SLs is due to the presence of an α-methylene-γ-lactone moiety, which via a Michael addition can alkylate free thiols of the amino acid cysteine in proteins. Evidence suggests that the cysteine 38 in the p65 subunit of the transcription factor NF−κB is the target for the inhibitory action of SLs. Based on previous results showing cancer cell and cancer stem cell (CSC) activity of damsin, we synthesized damsin derivatives. Here we investigate the toxicity and molecular mechanisms of 12 damsin derivatives. The JIMT-1 breast cancer cell line was treated with an IC_{50} concentration (single digit μM range) of the respective damsin derivative. When cells are treated with tumour necrosis factor-α (TNF-α), NF-κB is rapidly translocated to the nucleus to initiate transcription. Pre-treatment with damsin derivatives for only 60 minutes inhibited TNF-α–induced translocation of NF-kB to the nucleus. These data implicate that alkylation of p65/NF-kB probably inhibits the binding of NF−κB nuclear transport proteins. Treatment with a damsin derivative for 24 hours resulted in activation of Wnt and MAPK/ERK pathways while the NF-kB, Myc/Max, and MAPK/JNK were inhibited. An inhibitory effect on cell proliferation was found at 24 hours after seeding with concentrations lower than IC_{50} however there was a degree of reversibility of the inhibitory effect observed between 48 and 72 hours of treatment. Treatment with the damsin derivatives for 72 hours decreased the CSC population. This may be related to observed changes in signal transduction pathways and related protein such as the decreased level of human telomerase reverse transcriptase. This gene is transactivated by the ΣTAT3/NΦ−κB complex. Altogether our data point to inhibition of NF-kB being the molecular initiating event in the adverse outcome pathway of treating with damsin derivatives.

Key words

Breast cancer, cancer stem cells, sesquiterpene lactones, NF-κB, STAT3.

Introduction

Sesquiterpene lactones (SLs), a group of at least 5000 secondary plant metabolites, have achieved immense interest due to their presence in medicinal plants and their various pharmaceutical activities e.g. in inflammation and cancer [1]. The molecular mechanism by which SLs impair cancer cell proliferation and viability are not clear although a majority of studies have focused on the transcription factor NF-kB [2,3]. Other molecular mechanisms have been suggested and it is obvious that the response to SL exposure is complex. Part of the complexity lies in the multitude of SLs with different structures that allow the participation of different steric interactions with the varied reported molecular targets resulting in effect on cell proliferation and cell death [4] [5]. Important for the reactivity towards at least NF-κB is the α-methylene-γ-lactone moiety in SLs, which via a Michael addition can alkylate free thiols of the amino acid cysteine in proteins. Evidence suggests that the cysteine 38 sulfhydryl groups in the p65 subunit of NF−κB is the targets for inhibitory action of SLs.

We have previously shown that the pseudoguaianolides damsin and ambrosin inhibit breast cancer cells as well as target breast cancer stem cells (CSCs) [6]. These compounds inhibit tumor necrosis factor-α (TNF-α)-induced translocation of p65/NF-κB to the cell nucleus thus implying covalent binding of damsin and ambrosin to the p65 unit preventing the NF−κB complex to be released from its cytoplasmic binding protein IκB [6]. The NF-κB signaling pathway has been shown to be constitutively activated in CSCs [7] and one means of eradicating this subpopulation of aggressive cancer cells could be through inhibition of p65/NF-κB.

One goal of medicinal chemistry is to design and chemically modify natural compounds to increase their efficiency. We have recently presented the synthesis of and structure-activity relationship of 23 semisynthetic damsin derivatives [8]. Their cytotoxicity was evaluated in MTT-based dose-response assays and all proved to be more cytotoxic in the JIMT-1 breast cancer cell line compared to the normal-like MCF-10A cell line. Here, we investigate further the mechanisms affected resulting in impairment of JIMT-1 cancer cell proliferation by treatment with a selected group of damsin derivatives at their respective IC_{50} concentrations.

We show that the investigated damsin derivatives inhibit TNF-α-induced translocation of p65/NF-κB to the cell nucleus in JIMT-1 breast cancer cells when used at the IC_{50} concentration, thus the compounds are active in a context of potent activation of NF−κB. In growth curve experiments, we show that an IC_{50} concentration inhibits cell proliferation within 24 hours of addition of a damsin derivative. NF-κB is known to interact closely with many pathways of which STAT3 is one [9]. STAT3 is important for the expression of human telomerase reverse transcriptase (hTERT), an enzyme which is important for promotion of the

CSC phenotype in breast cancer [10,11] hTERT expression is linked to most of cancer malignancies and it is been suggested as a strategic target for cancer therapy. Here we show that treatment with damsin derivatives decreases hTERT expression and there is also a decrease in the CSC population. Although we found a decrease in the expression of the cell migration promoting protein vimentin, there was no marked effect on JIMT-1 cell migration in a wound healing assay. The readout of a signal transduction reporter assay shows the complexity in the response to treatment with SLs, and, thus possible mechanism for the anti-proliferative activity of the tested SLs may be their ability to simultaneously target several molecular pathways as reported for other SLs although inhibition of the NF-κB pathway may be one of the earliest molecular events after the start of treatment [12].

Material and Methods

Cell lines and culture conditions

The JIMT-1 human breast carcinoma cell line (ACC589) was purchased from the German Collection of Microorganisms and Cell Cultures (DSMZ, Braunschweig, Germany). The cells were cultured in DMEM/F-12 medium supplemented with 10 % fetal calf serum (FCS), 1 mM non-essential amino acids (VWR, Lund, Sweden), 10 µg/ml insulin (Sigma-Aldrich, Stockholm, Sweden), and 100 U/ml penicillin/100 µg/ml streptomycin (VWR). The cells were routine-passaged twice a week and were kept at 37 °C in a humidified incubator with 5 % CO_2 in air.

For the experiments, the cells were detached with Accutase™ (Sigma-Aldrich) and seeded at a density of 1.5×10^4 cells/cm^2 in appropriate size tissue culture vessels to obtain the suitable cell number for the different assays.

Compounds and stock solutions

Twelve sesquiterpene lactones (SL) synthetized from damsin were used in the present study (Fig. 1) [8]. All compounds were dissolved in 100 % DMSO to a 100 mM stock solution which was stored at -20°C. Before use, the compounds were diluted in phosphate-buffered saline (PBS: 8 g/l NaCl, 0.2 g/L KCl, 1.15 g/l Na_2HPO_4, 0.2 g/l KH_2PO_4, pH 7.3). Controls were supplemented with PBS containing DMSO at the same concentrations as the working solutions of the compounds. The final DMSO concentration was equal to or less than 0.1 % in all assays. All compounds were used at their IC_{50} concentration [8].

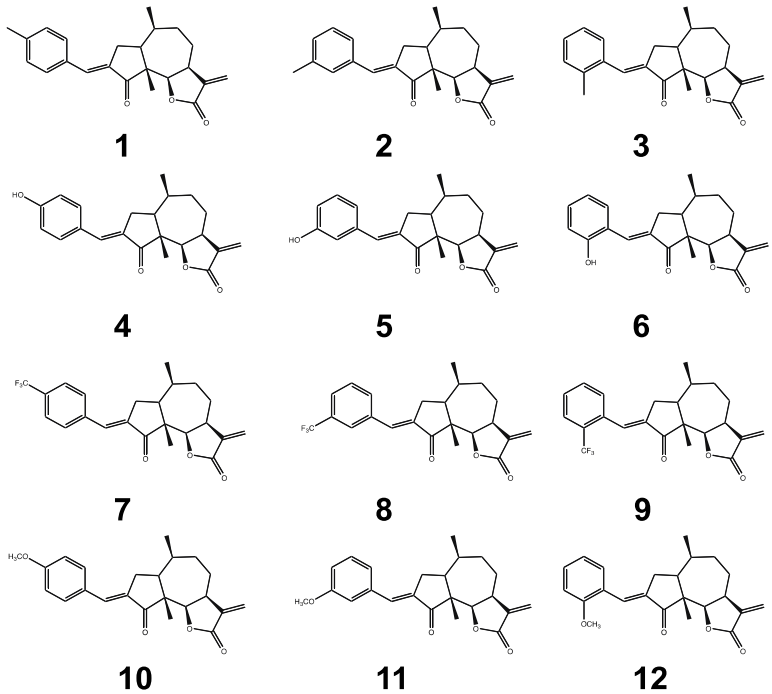

1	(E)-3-(4-Methylbenzyliden)damsin	[a] IC_{50} = 2.1±0.3 μM
2	(E)-3-(3-Methylbenzyliden)damsin	IC_{50} = 4.8±0.3 μM
3	(E)-3-(2-Methylbenzyliden)damsin	IC_{50} = 4.7±0.1 μM
4	(E)-3-(4-Hydroxybenzyliden)damsin.	IC_{50} = 2.9±0.2 μM
5	(E)-3-(3-Hydroxybenzyliden)damsin.	IC_{50} = 2.4±0.1 μM
6	(E)-3-(2-Hydroxybenzyliden)damsin	IC_{50} = 2.1±0.1 μM
7	(E)-3-((4-Trifluoromethylbenzyliden)damsin	IC_{50} = 1.8±0.2 μM
8	(E)-3-((3-Trifluoromethylbenzyliden)damsin	IC_{50} = 4.4±0.7 μM
9	(E)-3-((2-Trifluoromethylbenzyliden)damsin	IC_{50} = 8.1±0.6 μM
10	(E)-3-(4-Methoxybenzyliden)damsin	IC_{50} = 1.6±0.1 μM
11	(E)-3-(3-Methoxybenzyliden)damsin	IC_{50} = 9.0±1.0 μM
12	(E)-3-(2-Methoxybenzyliden)damsin	IC_{50} = 7.1±0.2 μM

Figure 1. Chemical structures of the 12 damsin derivatives with benzene addition used in the present study. [a] IC_{50} concentrations from [8].

TNF-α-induced translocation of p65/NF-κB to the cell nucleus

The effect of the 12 compounds on TNF-α induced translocation of NF-κB to the cell nucleus was performed as described previously [6]. In brief, 24 hours after seeding, the cells were treated with compound at IC_{50} for 60 min and then TNF-α (25 ng/ml) was added to the medium and incubation was continued for another 40 minutes. The cells were fixed in 4 % formaldehyde in PBS for 15 min at 4 °C. The cellular localization of NF-kB was visualized by immunofluorescene microscopy (Olympus epifluorescence microscope Olympus OpticalCo.Ltd.,Japan equipped with a Olympus DP74 digital camera) after labelling with rabbit anti-p65/NF-κB (Abcam,Cambridge,MA,USA) and Alexa 488 anti-rabbit-conjugated secondary antibody (MolecularProbes,Inc.,Eugene,USA).

Western blot analysis

Cells were seeded at a density of 1.5×10^4 cells/cm^2 in Petri dishes with 5 cm diameter in 5 ml of medium and incubated for 24 hours to let them to attach. Twenty-four hours later, the compounds were added at corresponding IC_{50} concentration. After 72 hours of treatment, the cells were detached with Accutase™ (Sigma-Aldrich), counted in a hemocytometer and pelleted. The dry pellets were stored at -80˚C. The pellets were diluted in sample buffer (62.5 mM Tris-HCl (pH 6.8), 20 % glycerol, 2 % sodium dodecyl sulfate, 5 % β-mercaptoethanol, 1% NP-40; 100,000 cells/15 µl). The samples were sonicated twice for 20 seconds each, boiled for 7 minutes and stored at -20˚C until further application. Pre-cast polyacrylamide Mini-PROTEAN®TGX™ Precast Gels (4–20 % acrylamide Bis-Tris) were loaded with 10 µl of prepared samples per lane. Western blot and electrophoresis were performed in a Bio-Rad electrophoresis and blotting system (Bio-Rad, Hercules, California, USA). Electrophoresis was performed at 150 V for 5 minutes and at 300 V for 15 min in a Tris-glycine buffer. Then, the gels were blotted onto nitrocellulose membranes using a semi-dry Trans-Blot® Turbo™ Transfer System (Bio-Rad, Hercules, California, USA). The membranes were blocked in 5 % bovine serum albumin (BSA) (Sigma-Aldrich, Copenhagen, Denmark) and 1 % Tween 20 (Sigma-Aldrich) in PBS and incubated with the following primary antibodies: β-catenin (1:500) (BD Transduction laboratories™, CA, USA, 610154), p53 (1:500) (BD Biosciences, Stockholm, Sweden, 554294), p65/NF-κB (1:1000) (ab76311), IκBα (1:2000) (ab7217), pIκBα (1:500) (ab12135), hTERT (1:1000) (ab32020), STAT3 (1:1000) (ab 68153), pSTAT3 (1:2000) (ab 76315), vimentin (1:1000) (ab 8069), or β-actin (1:500) from Abcam, Cambridge, UK. All antibodies were diluted in PBS containing 5 % BSA and 0.1 % Tween 20. After incubation with horseradish peroxidase (HRP)-conjugated swine antirabbit or HRP-conjugated goat anti-mouse secondary antibodies (Dako, Glostrup, Denmark) at room temperature, the membranes were exposed to enhanced chemiluminescent solution (GE Healthcare, Buckinghamshire, UK) to detect the

protein bands. Data were collected and analyzed using Quantity One software (Bio-Rad, Hercules, California, USA). The intensities of the bands were determined by densitometric scanning.

Scrape wound healing

The wound-healing assay was performed as described by Huang *et al*. [13].

CD24/CD44 and ALDH analysis

The identification of the cell surface markers CD24 and CD44 and the analysis of ALDH positive cells was performed as described previously [6,13].

Colony formation assay in soft agar

The identification of CSCs in a colony forming efficiency assay was performed as described previously [6].

Reporter assay for analysis of 10 signaling pathways

The Cignal Finder Cancer 10-Pathway Reporter Array (Qiagen, Hilden, Germany) was used to simultaneously analyze the effect of treatment with compound **6** on 10 signaling pathways. JIMT-1 cells (2 x 10^4 cells) were seeded in 100 µL of Opti-MEM® containing 10 % FBS per well in the provided 96 well white assay plate containing reporters. After 24 hours, the cells were transfected overnight using Attractene. Cells were then treated for 24 hours with compound 6 at the IC_{50} concentration. Firefly and Renilla signals were detected using Dual-Glo luciferase detection reagents (Promega, Wisc., USA) according to the manufacturer's instructions. Renilla luciferase was used as the internal transfection control. Firefly luciferase levels were normalized to Renilla luciferase levels to generate a measurement of relative luciferase units. The results are presented as percentage luciferase activities normalized to control JIMT-1 cells according to the manufactures instructions. The experiment was performed two times with three independent samples in each experiment.

Growth curve

Cells were seeded at a density of 300 000 cells in Petri dishes with 5 cm diameter in 5 ml of medium and incubated for 24 hours to let them to attach before addition of compound **6**. The compound was added to the final concentrations of 0.5, 1, 1.5, 2, and 2.5 µM. Cells were sampled every 24 hours for 96 hours for cell counting using a hemocytometer.

Statistical analysis

A one-way ANOVA was used to determine if there was a significant difference between means and a Dunnet post-test was used to compare the difference between

groups and control for the Western blot analysis. For the CSC analysis a student´s t-test with a Holm-Sidak post-test was applied for grouped data. GraphPad Prism 6 software was used to run all statistical analyses. Treatment groups were considered significantly different if the p value was <0.05.

Results

Growth curve experiment to compare with dose response data

We have previously deduced IC_{50} values for the damsin derivatives from dose response curves obtained using an MTT assay [8]. This assay is only an indirect means to determine the cell number. Thus, we decided to treat JIMT-1 cells with one of the damsin derivatives ((E)-3-(2-hydroxybenzyliden) damsin (**6**)) at different concentrations and count the cells at 24, 48, and 72 hours of treatment to get a true evaluation of the effect on cell proliferation (Fig. 2A).

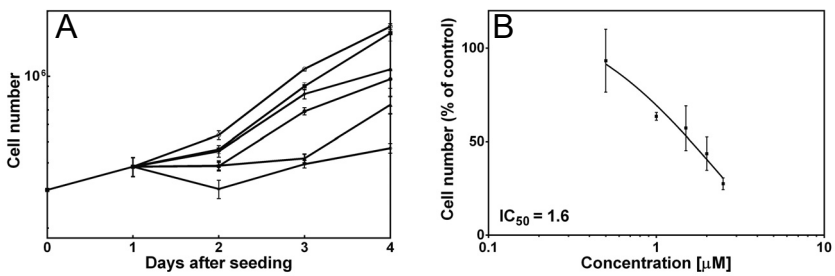

Figure 2. (E)-3-(2-Hydroxybenzyliden)damsin (**6**) treatment inhibits proliferation of JIMT-1 breast cancer cells in a time- and dose-dependent manner. (A) Growth curves. Cells were seeded day 0, and the compound was added 1 day after seeding at different concentrations. o: control. ■, 0.5 μM. ♦, 1 μM. •, 1.5 μM. ▲, 2 μM. ×, 2.5 μM. The cell number was determined by counting in a hemocytometer after cell detachment at 1-4 days after seeding. Data are presented as the mean of 6 independent cultures and bars show ±SD. (B) Cell number-derived dose response curve. The cell number at 72 hours of treatment in B expressed in % of control. The mean of 6 values is shown in each point.

Figure 2A shows the effect of treating JIMT-1 cells with different concentrations of compound **6**. The cells were clearly affected after 24 hours of treatment with **6** at different concentrations (i.e. 2 days after seeding, Fig. 2A). Thus, while the cell number increased in control between 1 and 2 days after seeding, the cell number did not increase to the same extent or was totally halted in cultures treated with the different concentrations of **6**, even the lowest concentration 0.5 μM. Between 48 and 72 hours of treatment (i.e. days 2 to 4 after seeding), the cell number increased in treated cultures, implying a partial recovery from the initial inhibition. Figure 2B shows a dose response curve drawn from the cell number data after 72 hours of

treatment where the cell number of treated is expressed in % of control. The IC_{50} for compound **6** is 1.6 µM derived from the cell number-based dose response curve.

Treatment with SLs at IC_{50} inhibits TNF-α-induced translocation of p65/NF-κB to the cell nucleus

Treatment with damsin inhibited TNF-α-induced NF-κB translocation into the nucleus [9]. Here we investigated if the 12 damsin derivatives had the same effects when treating JIMT-1 cells at IC_{50} for 60 minutes before TNF-α stimulation. TNF-α is a potent activator of NF−κB and analysis by immune fluorescence microscopy is an efficient means of investigating inhibition of this activation [14]. In control, p65/NF-κB is found in the cytoplasm and after treatment with TNF-α, p65/NF-κB is found mainly in the nuclei (Fig. 3). In cells pre-treated with the damsin derivatives, the TNF-α-induced nuclear translocation of NF-κB was inhibited (Fig. 3, **1-12**).

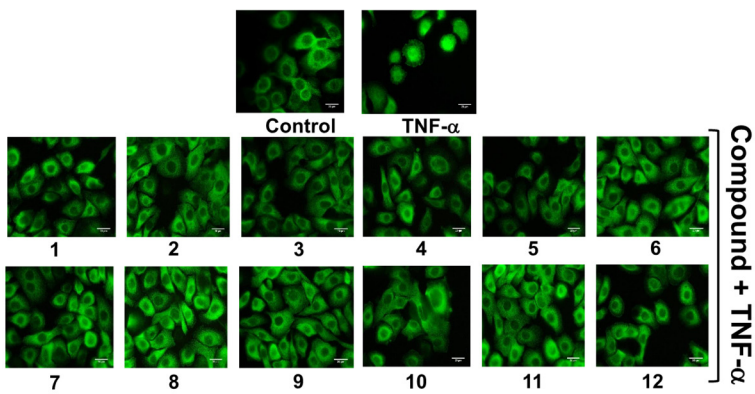

Figure 3. Treatment of JIMT-1 cells with 12 damsin derivatives inhibited TNF-α-induced p65/NF-κB nuclear translocation. JIMT-1 cells were pre-treated for 60 minutes with 12 damsin derivatives at their respective IC_{50} concentration. Then cells were stimulated with 25 ng/ml TNF-α for 40 minutes. Control: cells incubated with compound vehicle and TNF-α vehicle. TNF-α: cells incubated with control vehicle for 60 minutes and then TNF-α for 40 minutes. **1-12**: cells incubated with compound for 60 minutes and then TNF-α for 40 minutes. The cells were fixed and stained to visualize p65/NF-κB expression (green). Images were taken with a 100x oil immersion objective using an Olympus epifluorescence microscope. The scale bars denote 20 µm. Representative images from three independent experiments are shown.

Activity against cancer stem cells

We then decided to work with a selected number of the 12 analogues and choose compounds **1**, **6**, **7**, and **10** since they had the lowest IC_{50} values and belong to groups with different additives (Fig. 1) [8]. We used three different assays to evaluate the effect of SLs on CSCs: a colony forming efficiency assay in serum free medium containing soft agar, a flow cytometric assay to determine cell surface expression of CD44 and CD24, and a flow cytometric assay to determine the ALDH activity. Breast CSCs have the phenotype $CD44^+/CD24^-$ [15], express ALDH activity [16,17], and form colonies in serum free conditions [18]. Figure 4 shows that treatment with damsin derivatives decreases the CSC population, with the most obvious results obtained with the colony forming efficiency assay in serum free soft agar (Fig. 4C).

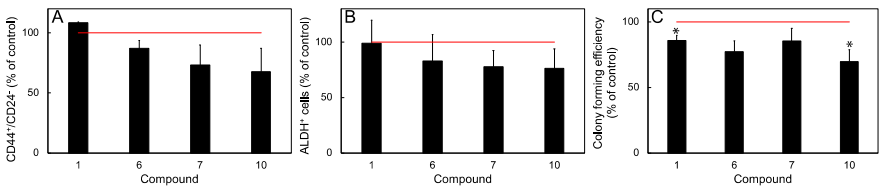

Figure 4. Treatment with damsin derivatives decreases the CSC population. The cells were treated with **1** (E)-3-(4-methylbenzyliden)damsin, **6** (E)-3-(2-hydroxybenzyliden)damsin, **7** (E)-3-((4-trifluoromethylbenzyliden)damsin, or **10** (E)-3-(4-methoxybenzyliden)damsin at IC_{50} for 72 hours. (A) The $CD44^+/CD24^-$ and (B) the $ALDH^+$ populations were evaluated by flow cytometry. (C) Colony forming efficiency was evaluated using a serum-free soft agar assay. JIMT-1 cells were treated for 72 hours and then reseeded at cloning density. The colonies were counted after two weeks of incubation. Data are presented as the mean ± SE for n = 3.

Wound healing assay

We have previously shown that damsin treatment inhibited migration of JIMT-1 cells in a wound healing assay [6]. Here we investigate the effect of treating with damsin derivatives on wound healing (Fig. 5). The damsin derivatives did not affect the wound healing process of directed cell migration.

Vimentin is an intermediate cytoskeletal filamentous protein that is important for cell migration [19]. Vimentin is a NF-kB target gene [20] and vimentin has also been shown to be involved in NF-kB signaling [21,22]. Here we show that the protein expression of vimentin is decreased by all for damsin derivatives tested.

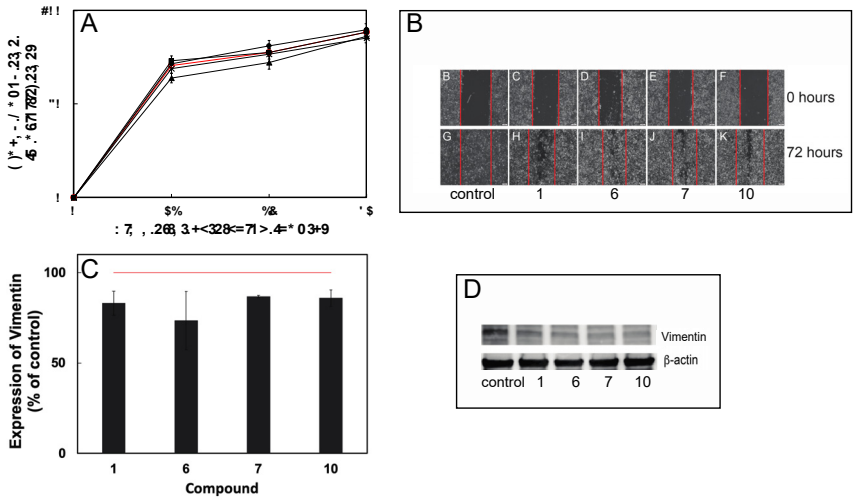

Figure 5. Treatment with damsin derivatives at IC_{50} concentrations does not inhibit directed cell migration although the level of the intermediary filament protein vimentin is lowered. (A) Evaluation of wound closure. Control: ○. **1** (E)-3-(4-methylbenzyliden)damsin, ●. **6** (E)-3-(2-hydroxybenzyliden)damsin, ■. **7** (E)-3-((4-trifluoromethylbenzyliden)damsin, ▲. **10** (E)-3-(4-methoxybenzyliden)damsin, ×. Data in A is presented as the mean ± SE for n = 6. (B) Representative phase-contrast microscopy images 72 hours after wounding. The bars denote 100 µm. The red lines encompass the 0-hour wound area. (C) Data obtained from densitometric evaluation of Western blots of vimentin. The data in C are expressed in % of control and presented as the mean ± SE for n = 3. (D) Representative blots used for densitometric scanning. Representative blots used for densitometric scanning to obtain the data D.

Proteins in the NF-κB pathway

We then investigating the levels of three key proteins in the NF-κB pathway: p65/NF-κB, IκBα, and pIκBα. When the NF-κB complex containing p65 (Rel A) and p50 is not active, it is kept in the cytoplasm by the protein IκBα [20]. When IκBα is phosphorylated by different signals, the NF-κB complex is released and translocates into the nucleus. Our notion was that the levels of these proteins might be affected after 72 hours of treatment. However, Western blot analysis shows, that treatment with damsin derivatives for 72 hours did not have any major impact on the protein levels of IκBα (Fig. 5A), pIκBα (Fig. 5B), or p65/NF-κB (Fig. 5C). Compound **10** showed a tendency to decrease the IκBα protein level (Fig. 5A) but without affecting pIκBα (Fig. 5B). Thus, although the compounds inhibit the TNF-□-induced translocation of p65/NF-κB to the cell nucleus, the levels of the key players in the NF-κB pathway are not affected at 72 hours of treatment.

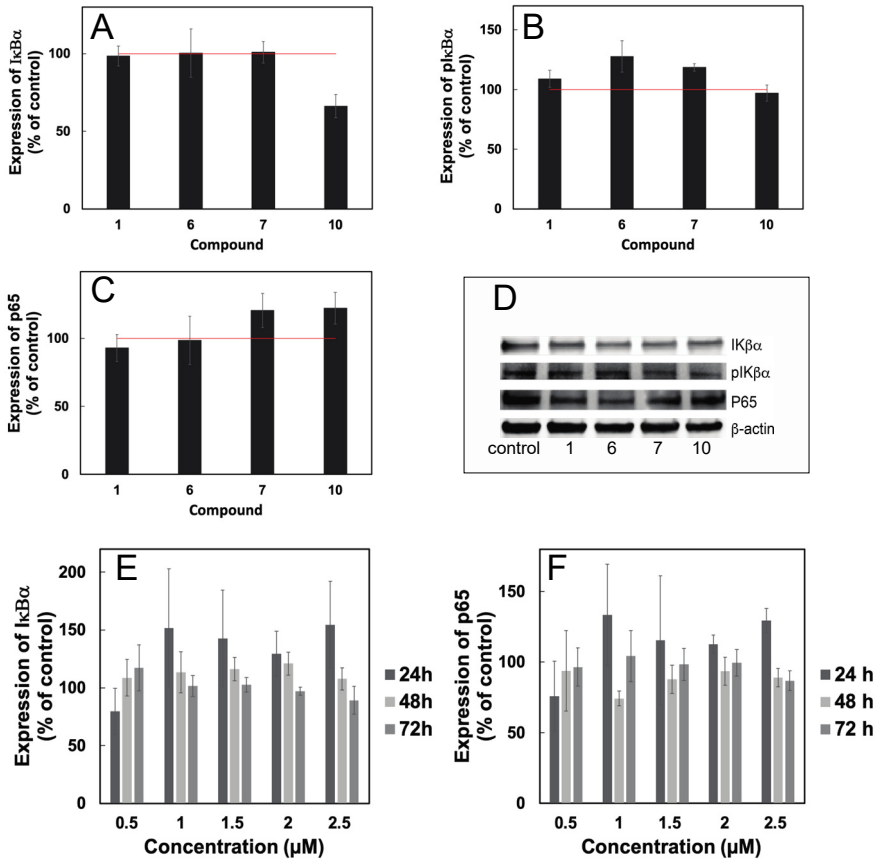

Figure 5. Effect of treating JIMT-1 cells with SLs on proteins in the NF-κB pathway. (A) IκBα expression. (B) pIκBα expression. (C) p65/NF-κB expression. The cells were treated with **1** (E)-3-(4-methylbenzyliden)damsin, **6** (E)-3-(2-hydroxybenzyliden)damsin, **7** (E)-3-((4-trifluoromethylbenzyliden)damsin, or **10** (E)-3-(4-methoxybenzyliden)damsin at IC_{50} for 72 hours before sampling for Western blot. (D) Representative blots used for densitometric scanning of A-C. The data in A-C are expressed in % of control and presented as the mean ± SE for n = 4. (E) and (F) Expression of IκBα and p65/NF-κB, respectively, at 24, 48, and 72 hours of treatment of JIMT-1 cells with different concentrations of compound **6**. The data in E and F are expressed in % of control and presented as the mean ± SE for n = 3.

We then investigated the IκBα and NF-κB/p65 protein levels in JIMT-1 cells treated with different concentrations of compound **6** for 24, 48, and 72 hours of treatment (Figs. 3E and 3F). Figures 3E and 3F show that there is a dynamic in the levels of IκBα and p65/NF-κB at different times of treatment and that the largest deviation from control is 24 hours after treatment where the protein levels were increased in cells treated with 1-2.5 μM concentrations of compound **6**.

Proteins in the STAT3 pathway

Since the NF-κB and STAT3 pathways are activated in cancer and engaged in excessive crosstalk important for cancer progression [9], we decided to investigate if proteins involved in the STAT3 pathway might be affected in SL-treated JIMT-1 cells. Also, SLs have been shown to inhibit the STAT3 pathway [23,24]. Figures 4A and 4B show that treatment with compounds **1**, **6**, **7**, or **10** either do not affect the level of STAT3 or pSTAT3 or lowers the level of the proteins. The level of hTERT was decreased by treatment with damsin derivatives **7** and **10** (Fig. 4C). hTERT gene expression is activated by STAT3 as well as STAT3 in a complex with NF-κB [11].

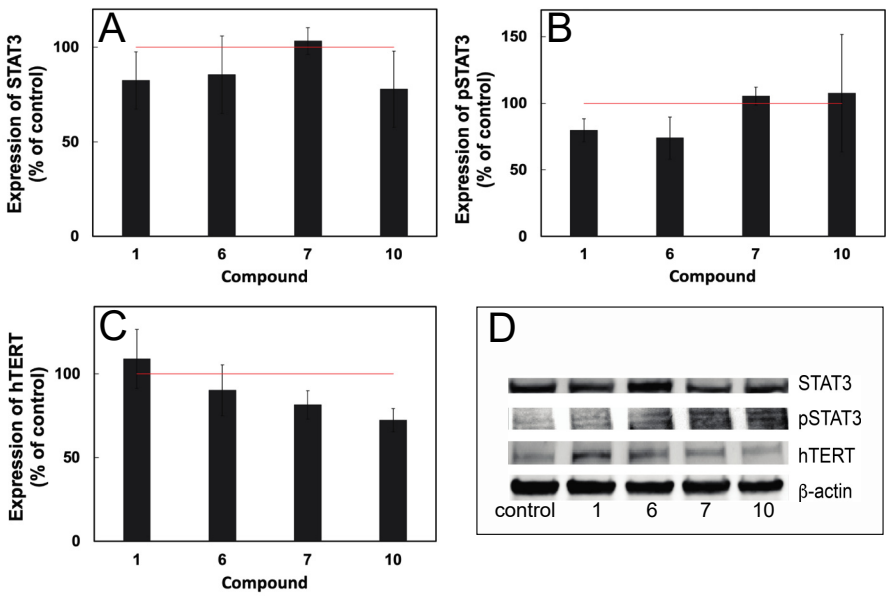

Figure 6. Effect of treating JIMT-1 cells with SLs on proteins in the STAT3 pathway. (A) STAT3 expression. (B) pSTAT3 expression. (C) hTERT expression. The cells were treated with **1** (E)-3-(4-methylbenzyliden)damsin, **6** (E)-3-(2-hydroxybenzyliden)damsin, **7** (E)-3-((4-trifluoromethylbenzyliden)damsin, or **10** (E)-3-(4-methoxybenzyliden)damsin at IC_{50} for 72 hours before sampling for Western blot. (D) Representative blots used for densitometric scanning to obtain the data in A-C. The data in A-C are expressed in % of control and presented as the mean ± SE for n = 3.

Signaling pathways affected by SL treatment

To get an overview of the cellular reaction to treatment with the damsin derivatives, we choose to evaluate compound **6** in a reporter assay for signal transduction pathways (Fig. 6). In this assay, the cells were treated for 24 hours. The Wnt and MAPK/ERK pathways were activated while the NF-kB, Myc/Max, and MAPK/JNK were inhibited.

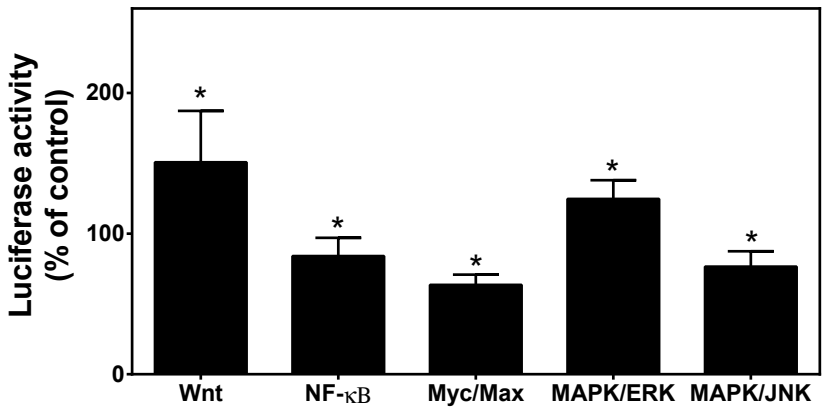

Figure 6. Signal transduction pathways affected by treatment with (E)-3-(2-hydroxybenzyliden)damsin (**6**) for 24 hours. A reporter assay was used to investigate the effect of treatment with 2 μM of compound **6** after 24 hours of treatment. The data show the mean of two experiments compared to control with three independent samples in each ± SEM. *, $p < 0.05$, significantly different compared to control.

Discussion

Cancer is a disease with no boundaries affecting all humans on the earth. The global cancer burden is estimated to increase due to factors such as population growth and an increasing ageing population. Despite this, cancer deaths are decreasing due to early detection and improved treatments. To further decrease the number of cancer deaths, much research is aimed at finding new compounds for treatment, aiming at a variety of targets that are important for cancer cell and CSC survival. Among numerous groups of compounds tested for anti-cancer activity are the plant-derived SLs. Still much research is needed around the molecular mechanisms of these compounds and also research into chemically modified structures. We did an initial

study on the toxicity of the SL damsin [6] and then opted to synthesize damsin derivatives [8] some of which we have investigated here.

The general notion is that the chemical reactivity of SLs is concentrated to the α-methylene-γ-lactone group which has a high reactivity towards sulfhydryl groups in proteins [25]. The cystein 38 of p65/NF-κB has been shown to be a specifically vulnerable target for SL alkylation [26]. This cysteine is located in the DNA binding pocket of NF-kB and when an SL is bound to it, NF-kB is prevented from binding to DNA [27]. Here we show that TNF−α-induced translocation of NF-κB is blocked by treatment with an SL, with the obvious result that there can be no DNA binding and gene activation. Thus, the blocking of DNA binding of NF−κB in the cells is inhibited already in the cytoplasm, implying that actually it is the transport into the nucleus that is blocked. NF-kB is transported into the nucleus by importins α3 and α4 [28]. The binding of importins is also in the DNA binding pocket of NF-κB [29,30]. Thus, alkylation of cystein 38 of p65/NF-κB may affect the binding of NF-kB to serval proteins besides binding to DNA. Other proteins that bind to NF-kB in the DNA binding pocket region are co-activator coactivator ribosomal protein S3 [31], and the cAMP-responsive element-binding protein-binding protein [32].

Several observations show an interaction between NF−κB and STAT3 being required for gene transcription [10,33–35]. It has been shown that STAT3 binds to the p65/NF-kB transactivation domain and that STAT3 is present in the DNA binding complex [35]. This may also imply that alkylation of cysteine 38 in p65/NF-κB blocks the binding of STAT3 there by inhibiting transcription that is dependent on STAT3/NF-κB complexes. STAT3/NF-κB has been shown to regulate hTERT expression [10]. Here we found a decreased expression of the hTERT protein level after treatment of JIMT-1 cells for 72 hours with SLs.

The NF-κB and STAT3 pathways are important in the regulation of the CSC phenotype and inhibiting these pathways has been suggested therapeutic targets [7] [36]. Here we show that treatment with SLs reduces the CSC population of the JIMT-1 breast cancer cell line. It has previously been shown that inhibition of NF-kB signaling with a synthetic inhibitor reduces the stemness characteristics in lung cancer cell lines [37], which is in line with our results. In another study it was shown that inhibition of NF-kB signaling reduced the proliferative capacity of bladder CSCs [38]. Inhibition of hTERT by a synthetic inhibitor was shown to decrease the CSC population of breast and pancreatic cell lines [39]. From our data we cannot draw the conclusion that it is a direct effect of SLs on STAT3 that reduces the level of hTERT. In fact, the promoter for hTERT also contains promoters for NF-κB and c-Myc [11] and here we demonstrate an inhibiting effect of compound **6** on the Myc/Mac signaling pathway.

We have previously shown that SLs inhibit directed cell migration in a scrath wound assay in concentrations close to IC_{50} [6]. Here we did not find a similar inhibiting effect when treating JIMT-1 cells with IC_{50} concentration of the compounds **1**, **6**, **7**, and **10**. This finding suggests that the damsin derivatives are not as efficient as damsin in inhibiting JIMT-1 breast cancer cells at IC_{50} concentrations. However, we did find a decrease in the expression of the intermediate filament protein vimentin compared to control. Vimentin is important for cell migration by integrating mechanical input from the environment and modulating the dynamics of microtubules and the actomyosin network [19].

The rapid initial inhibition of cell proliferation after addition of compound **6** and the slight recovery is compelling. The TNF-α-induced translocation of p65/NF-kB to the cell nucleus assay shows that only 60 min preincubation with the SLs is needed to inhibit the translocation. Obviously, the SLs pass the cell membrane readily to achieve an inhibitory concentration. JIMT-1 is a HER2 over-expressing trastuzumab resistant estrogen receptor negative breast cancer cell line, and it has been suggested that NF-kB is constitutively activated in this context contributing to the resistance [40]. Thus, treatment with SLs may inhibit this constitutive signalling and this need further investigation to exploit its utility in a clinical setting. We also need to investigate the mechanisms behind the partly reversible effect of the initial inhibition of cell proliferation.

Conclusion

Our data suggest that the molecular initiating event of treating cells with an SL is the binding to NF-κB that occurs within 1 hour after addition of the compound, which then leads to down-stream effects in the adverse outcome pathway. The down stream effect involves molecular pathways that are affected in parallel or in series. Our data implicate that Wnt, MAPK/ERK, NF-kB, Myc/Max, and MAPK/JNK pathways are affected 24 hours after treatment. At 72 hours of treatment, we found effects on protein levels as well as cell functions and phenotypes that are down-stream consequences of early effects on the signal transduction pathways. However, a cell has a multitude of sulfhydryl groups prone to alkylation by an SL. Thus, we cannot rule out alkylation of other proteins. Important to remember is that the outcome is a question of dose. There may be intracellular concentrations where SLs actually selectively alkylate cysteine 38 of p65/NF-κB because of the formation of more favorable entropy and enthalpy.

References

1. Fridlender M, Kapulnik Y, Koltai H. Plant derived substances with anti-cancer activity: From folklore to practice. Front Plant Sci. 2015;6: 1–9. doi:10.3389/fpls.2015.00799
2. Rüngeler P, Castro V, Mora G, Gören N, Vichnewski W, Pahl HL, et al. Inhibition of transcription factor NF-κB by sesquiterpene lactones: A proposed molecular mechanism of action. Bioorganic Med Chem. 1999;7: 2343–2352. doi:10.1016/S0968-0896(99)00195-9
3. Chadwick M, Trewin H, Gawthrop F, Wagstaff C. Sesquiterpenoids lactones: Benefits to plants and people. Int J Mol Sci. 2013;14: 12780–12805. doi:10.3390/ijms140612780
4. Sülsen VP, Martino VS. Sesquiterpene lactones. Sülsen VP, Martino VS, editors. CONICET University of Buenos Aires. Springer; 2018. doi:10.1007/978-3-319-78274
5. Orofino Kreuger MR, Grootjans S, Biavatti MW, Vandenabeele P, D'Herde K. Sesquiterpene lactones as drugs with multiple targets in cancer treatment: focus on parthenolide. Anticancer Drugs. 2012;00: 1–14. doi:10.1097/CAD.0b013e328356cad9
6. Soria-Sotillo W, Villagomez R, Smiljanic S, Huang X, Malakpour A, Kempengren S, et al. Anti-cancer stem cell activity of a sesquiterpene lactone isolated from Ambrosia arborescens and of a synthetic derivative. PLoS One. 2017; 1–16. doi:doi.org/10.1371/journal.pone.0184304
7. Vazquez-Santillan K, Melendez-Zajgla J, Jimenez-Hernandez L, Martinez-Ruiz G, Maldonado V, Martínez-Ruiz G, et al. NF-kB signaling in cancer stem cells: a promising therapeutic target? Cell Oncol. Cellular Oncology; 2015;38: 327–339. doi:10.1007/s13402-015-0236-6
8. Lozano M, Soria-Sotillo W, Almanza GR, Manner S, Oredsson S, Villagomez R, et al. Selective Cytotoxicity of Damsin Derivatives in Breast Cancer Cells. J Adv Pharm Sci Technol. 2019;2: 22. doi:10.14302/issn.2328
9. Grivennikov S, Karin M. Dangerous liaisons: STAT3 and NF-κB collaboration and crosstalk in cancer Sergei. 2011;21: 11–19. doi:10.1016/j.cytogfr.2009.11.005.
10. Chung SS, Aroh C, Vadgama J V. Constitutive activation of STAT3 signaling regulates hTERT and promotes stem cell-like traits in human breast cancer cells. PLoS One. 2013;8: 10. doi:10.1371/journal.pone.0083971
11. Ramlee MK, Wang J, Toh WX, Li S. Transcription regulation of the human telomerase reverse transcriptase (hTERT) gene. Genes (Basel). 2016;7. doi:10.3390/genes7080050
12. Dey A, Tergaonkar V, Lane DP. Double-edged swords as cancer therapeutics : simultaneously targeting p53 and NF- κ B pathways. Nat Rev Drug Discov. 2008;7: 1031–1040. doi:10.1038/nrd2759
13. Huang X, Borgström B, Kempengren S, Persson L, Hegardt C, Strand D, et al. Breast cancer stem cell selectivity of synthetic nanomolar-active salinomycin analogs. BMC Cancer. BMC Cancer; 2016;16: 145. doi:10.1186/s12885-016-2142-3

14. Noursadeghi M, Tsang J, Haustein T, Miller RF, Chain BM, Katz DR. Quantitative imaging assay for NF-κB nuclear translocation in primary human macrophages. J Immunol Methods. Elsevier B.V.; 2008;329: 194–200. doi:10.1016/j.jim.2007.10.015
15. Al-Hajj M, Wicha MS, Benito-Hernandez A, Morrison SJ, Clarke MF. Prospective identification of tumorigenic breast cancer cells. Proc Natl Acad Sci U S A. 2003;100: 3983–8. doi:10.1073/pnas.0530291100
16. Huang X, Borgström B, Månsson L, Persson L, Oredsson S, Hegardt C, et al. Semisynthesis of SY-1 for investigation of breast cancer stem cell selectivity of C-ring-modified salinomycin analogues. ACS Chem Biol. 2014;9: 1587–1594. doi:10.1021/cb5002153
17. Vasillou V, Pappa A, Estey T. Role of human aldehyde dehydrogenases in endobiotic and xenobiotic metabolism. Drug Metabolism Reviews. 2004. pp. 279–299. doi:10.1081/DMR-120034001
18. Papaccio F, Paino F, Regad T, Papaccio G, Desiderio V, Tirino V. Concise review: Cancer cells, cancer stem cells, and mesenchymal stem cells: Influence in cancer development. Stem Cells Transl Med. 2017;6: 2115–2125. doi:10.1002/sctm.17-0138
19. Battaglia RA, Delic S, Herrmann H, Snider NT. Vimentin on the move: new developments in cell migration. F1000Research. 2018;7: 1796. doi:10.12688/f1000research.15967.1
20. Hl P. Activators and target genes of Rel/NF-kappaB transcription factors. Oncogene. 1999;18: 6853–66.
21. Huang SH, Chi F, Peng L, Bo T, Zhang B, Liu LQ, et al. Vimentin, a Novel NF-κB regulator, is required for meningitic Escherichia coli K1 - Induced pathogen invasion and PMN transmigration across the blood-brain barrier. PLoS One. 2016;11: 1–20. doi:10.1371/journal.pone.0162641
22. Li Y, Hu Y, Dong C, Lu H, Zhang C, Hu Q, et al. Vimentin-mediated steroidogenesis induced by phthalate esters: Involvement of DNA demethylation and nuclear factor κB. PLoS One. 2016;11: 1–14. doi:10.1371/journal.pone.0146138
23. Villagomez R, Rodrigo G, Collado I, Calzado M, Muñoz E, Åkesso B, et al. Multiple anticancer effects of damsin and coronopilin isolated from Ambrosia arborescens on cell cultures. Anticancer Res. 2014;34: 503–507.
24. Mehmood T, Maryam A, Tian X, Khan M, Ma T. Santamarine inhibits NF-κB and STAT3 activation and induces apoptosis in HepG2 liver cancer cells via oxidative stress. J Cancer. 2017;8: 3707–3717. doi:10.7150/jca.20239
25. Janecka A, Wyrebska A, Gach K, Fichna J, Janecki T. Natural and synthetic alpha-methylenelactones and alpha- methylenelactams with anticancer potential. Drug Discov Today. 2012;17: 561–572. doi:10.1016/j.drudis.2012.01.013
26. Perkins ND. Cysteine 38 holds the key to NF-κB activation. Mol Cell. 2012;45: 1–3. doi:10.1016/j.molcel.2011.12.023
27. Gupta SC, Sundaram C, Reuter S, Aggarwal BB. Inhibiting NF-κB activation by small molecules as a therapeutic strategy. Biochim Biophys Acta - Gene Regul Mech. Elsevier B.V.; 2010;1799: 775–787. doi:10.1016/j.bbagrm.2010.05.004
28. Fagerlund R, Kinnunen L, Köhler M, Julkunen I, Melén K. NF-κB is transported into the nucleus by importin α3 and importin α4. J Biol Chem. 2005;280: 15942–15951. doi:10.1074/jbc.M500814200

29. Cavey M, Lecuit T. Molecular bases of cell–cell junctions stability and dynamics. Cold Spring Harb Perspect Biol. 2009;1: 1–18. doi:10.1101/cshperspect.a002998
30. Aleksandrov R, Dotchev A, Poser I, Krastev D, Georgiev G, Panova G, et al. Protein dynamics in complex DNA lesions. Mol Cell. Elsevier Inc.; 2018;69: 1046-1061.e5. doi:10.1016/j.molcel.2018.02.016
31. Sen N, Paul BD, Gadalla MM, Mustafa AK, Sen T, Xu R, et al. Hydrogen sulfide-linked sulfhydration of NF-κB mediates its antiapoptotic actions. Mol Cell. Elsevier Inc.; 2012;45: 13–24. doi:10.1016/j.molcel.2011.10.021
32. Vanden Berghe W, De Bosscher K, Boone E, Plaisance S, Haegeman G. The Nuclear Factor- κB engages CBP / p300 and histone acetyltransferase activity for transcriptional activation of the interleukin-6 gene promoter. J Biol Chem. 1999;274: 32091–32098. doi:10.1074/jbc.274.45.32091
33. Yang J, Liao X, Agarwal MK, Barnes L, Auron PE, Stark GR. Unphosphorylated STAT3 accumulates in response to IL-6 and activates transcription by binding to NFκB. Genes Dev. 2007;21: 1396–1408. doi:10.1101/gad.1553707
34. Fan Y, Mao R, Yang J. NF-κB and STAT3 signaling pathways collaboratively link inflammation to cancer. Protein Cell. 2013;4: 176–185. doi:10.1007/s13238-013-2084-3
35. Kesanakurti D, Chetty C, Maddirela DR, Gujrati M, Rao J. Essential Role of Cooperative NF-κB and Stat3 Recruitment to ICAM-1 Intronic Consensus Elements in the Regulation of Radiation-induced Invasion and Migration in Glioma. Oncogene. 2013;32: 1–23. doi:10.1038/onc.2012.546.
36. Galoczova M, Coates P, Vojtesek B. STAT3, stem cells, cancer stem cells and p63. Cell Mol Biol Lett. Cellular & Molecular Biology Letters; 2018;23: 1–20. doi:10.1186/s11658-018-0078-0
37. Zakaria N, Mohd Yusoff N, Zakaria Z, Widera D, Yahaya BH. Inhibition of NF-κB Signaling Reduces the Stemness Characteristics of Lung Cancer Stem Cells. Front Oncol. 2018;8: 1–12. doi:10.3389/fonc.2018.00166
38. Zhu Y, Zhou Y, Zhou X, Guo Y, Huang D, Zhang J, et al. S100A4 suppresses cancer stem cell proliferation via interaction with the IKK/NF-KB signaling pathway. BMC Cancer. BMC Cancer; 2018;18: 1–7. doi:10.1186/s12885-018-4563-7
39. Kowalski S, Hac S, Wyrzykowski D, Zauszkiewicz-Pawlak AZ, Inkielewicz-Stepniak I. Selective cytotoxicity of vanadium complexes on human pancreatic ductal adenocarcinoma cell line by inducing necroptosis, apoptosis and mitotic catastrophe process. Oncotarget. 2017;8: 60324–60341. doi:10.18632/oncotarget.19454
40. Kanzaki H, Mukhopadhya NK, Cui X, Ramanujan VK, Murali R. Trastuzumab-resistant luminal B breast cancer cells show basal-like cell growth features through NF-κB-activation. Monoclon Antib Immunodiagn Immunother. 2016;35: 1–11. doi:10.1089/mab.2015.0056

Paper IV

REVISTA BOLIVIANA DE QUÍMICA
ISSN 0250-5460 Rev. Bol. Quim. *Paper edition*
ISSN 2078-3949 Rev. boliv. quim. *Electronic edition*
Lozano et al. RBQ Vol. 34, No.1, pp. 28-32, 2017

HIGH CONTENTS OF OLEANOLIC ACID IN HIGHLAND BOLIVIAN PLANTS

ALTO CONTENIDO DE ACIDO OLEANOLICO EN PLANTAS BOLIVIANAS DE ALTITUD

Received 01 30 2017
Accepted 04 17 2017
Published 04 30 2017

Vol. 34, No.1, pp. 28-32, Ene./Abr. 2017
34(1), 28-32, Jan./Apr. 2017
Bolivian Journal of Chemistry

Full original article

Maribel Lozano, Yonny R. Flores, Giovanna R. Almanza*

Laboratorio de Química Bioorgánica, Instituto de Investigaciones Químicas IIQ, Ciencias Químicas, Facultad de Ciencias Puras y Naturales FCPN, Universidad Mayor de San Andrés UMSA, P.O. Box 303, Calle Andrés Bello s/n, Ciudad Universitaria Cota Cota, phone +59122795878, La Paz, Bolivia, gralmanza@umsa.bo, yrflores@umsa.bo

Keywords: Oleanolic acid, HPLC quantification, Bolivian highland plants, *Junellia seriphioides*, *Lampaya castellani*, *Baccharis tola*, *Polylepis besseri*

ABSTRACT

Oleanolic acid is a pentacyclic triterpenoid widely distributed in the plant kingdom, it has several pharmacological properties and it has been marketed in China as hepatoprotective drug since decades. The plants are the main source of this interesting compound, in this sense; during this study we quantified this metabolite in several Bolivian highland plants (*Tetraglochin cristatum*, *Lampaya castellani*, *Junellia seriphioides*, *Baccharis tola*, *Polylepis tomentella*, *P. hieronyni*, *P. besseri* and *Satureja boliviana*) by a high-performance liquid chromatography (HPLC) method. The amount determined (2,87 to 22,69 mg/g) was higher than the concentration reported for the olive fruit (0,17-0,56 mg/g) and similar than the reported for olive leaf (31,0 mg/g) which is the main source of commercial oleanolic acid. So native species, such as *Junellia seriphioides* (22,69 mg/g), *Lampaya castellani* (13,87 mg/g), *Baccharis tola* (11,93 mg/g) and *Polylepis besseri* bark (11,06 mg/g) are an interesting potential natural source of oleanolic acid in the region.

*Corresponding author: giovyalmanza@gmail.com; gralmanza@umsa.bo

RESUMEN

***Spanish title**: Alto contenido de ácido oleanólico en plantas bolivianas de altitud*. El ácido oleanólico es un triterpeno pentaciclico ampliamente distribuido en el reino vegetal, posee diversas propiedades farmacológicas y ha sido comercializado en China como droga hepatoprotectora desde hace décadas. Las plantas son la principal fuente de este interesante compuesto, en este sentido, durante este estudio cuantificamos este metabolito en varias plantas bolivianas de altura (*Tetraglochin cristatum*, *Lampaya castellani*, *Junellia seriphioides*, *Baccharis tola*, *Polylepis tomentella*, *P. hieronyni*, *P. besseri* y *Satureja boliviana*) por un método de cromatografía líquida de alta resolución (HPLC). La cantidad determinada (2,87 a 22,69 mg/g) fue mayor que la concentración reportada en frutos de oliva (0,17-0,56 mg/g) y similar a la reportada para hojas de oliva (31,00 mg/g) la fuente más importante de ácido oleanolico comercial. Por lo que especies nativas, como *Junellia seriphioides (*22,69 mg/g), *Lampaya castellani* (13,87 mg/g), *Baccharis tola* (11,93 mg/g) y *Polylepis besseri* corteza (11,06 mg/g) son una interesante potencial fuente natural de ácido oleanolico en la región.

INTRODUCTION

The natural product oleanolic acid (3β-hydroxyolean-12-en-28-oic acid) (Figure Nº 1) is a bioactive pentacyclic triterpenoid compound that has been isolated from more than 1620 plant species, including many food and medicinal plants where it exists as free acid or as an aglycone of saponins [1, 2]

This metabolite is relatively non-toxic and possesses several promising pharmacological activities. Among them, the hepatoprotective effects were widely studied [1] and are the bases of a drug against liver disorders commercialized in China [3]. On the other hand, the antioxidant, anti-inflammatory, anti-HIV, and anticancer activities, among others, motivated a large number of studies, reviews and publications of this compound and its derivatives [1,2,3,4,5], giving as one of the main results, the possible commercialization of the first oleanolic acid-derived drug [5].

The compound is especially prevalent in the Oleaceae family, among which olive (*Olea europaea*) still serves as the main source of commercial oleanolic acid where it is found in a concentration from 0,17 (in fruits) to 31,0 mg/g (in leaves) [6,7,8]. Nevertheless, in our previous studies, we found oleanolic acid as one of the major secondary metabolites in several studied plants of Bolivian highlands (3500 to 4200 m.a.s.l.) [9]. Even plants that biosynthesize few secondary metabolites use part of their energy for the production of this compound, because it seems to play an important role during the periods of frost [9]. However, in our previous report, the measure amount of this metabolite was done by semi-quantitative classic methods, as thin layer chromatography (TLC), isolation by chromatography and recrystallization. In this study, we developed a protocol to quantify this important metabolite in plants by HPLC, because this technique is fast, reproducible, and reliable. Also, it only requires small amounts of sample, compared to classical techniques [10].

The plants are the main source of this metabolite [5,8,11]. So, for this study we selected eight plants from Bolivian highlands: *Tetraglochin cristatum*, *Lampaya castellani*, *Junellia seriphioides*, *Baccharis tola*, *Polylepis tomentella*, *P. hieronyni*, *P. besseri* and *Satureja boliviana* based on the analysis done by TLC in our previous report [9], where all of them showed a majority presence of this metabolite in the EtOH extract, in order to determine new potential natural sources of this interesting metabolite.

RESULTS AND DISCUSSION

In agreement of our previous studies [8], eight plants from Bolivian highlands (*Tetraglochin cristatum*, *Lampaya castellani*, *Junellia seriphioides*, *Baccharis tola*, *Polylepis tomentella*, *P. hieronyni*, *P. besseri* and *Satureja boliviana*) were considered for this study. The plant material was submitted to an EtOH extraction by maceration for 48 h and the content of oleanolic acid in the extracts was quantified by triplicate using the HPLC-DAD developed method.

The HPLC developed method was based in three previously reported methods for triterpenic acids [12, 13, 14] and the calibration curve was done using the oleanolic acid isolated from *Chenopodium quinoa* residues after an acid hydrolysis of its saponins [13,15]. Figure Nº1 shows the HPLC-DAD chromatogram of oleanolic acid using a mixture of Acetonitrile/ 0,15 % Formic acid (93:7) as a mobile phase, an EclipsePlus C-18 column at a flow rate 1.0 ml/min, and detecting the analyte at 210 nm where the oleanolic acid appears at retention time $t_{R=}$ 8,2 min. Figure Nº2 shows the calibration curve, which was obtained using the peak areas of the standard whit different concentration. The area for every point was the average of three runs. The calibration curve was constructed in the range of 400-2500 ug/ml. The linear correlation equations and coefficient (r) was: 12,957x + 735,69 (r=0,9983.) showing a good linearity.

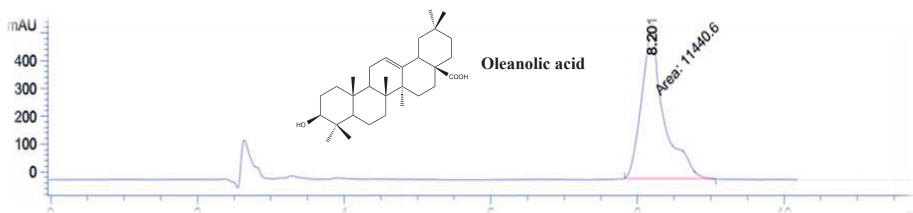

***Figure Nº1**. HPLC chromatogram of oleanolic acid (t_R= 8,2); EclipsePlus C-18, wavelenght 210 nm and flow rate 1.0ml/min*

The limit of detection (LOD) was obtained as the sample concentration that caused a peak with a height three times the baseline noise level and the limit of quantification (LOQ) was calculated as 10 times the base noise level. Thus, the LOD and LOQ calculated were 138.96 µg/ml and 421,11 µg/ml respectively.

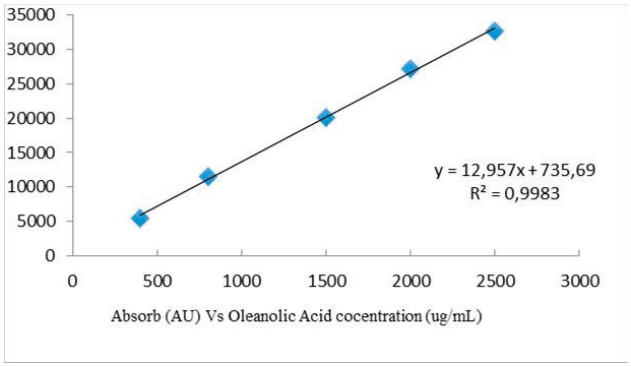

Figure Nº2. *Calibration curve of oleanolic acid*

Then, the concentration of oleanolic acid was measured (Table Nº1), showing that the species with high content of oleanolic acid are *Junellia seriphioides*, *Lampaya castellani*, *Baccharis tola* and *Polylepis besseri* bark. Nevertheless, it is important to note that all the plants evaluated showed a higher content of oleanolic acid than those found in the olive fruit (0,17-0,56 mg/g) and similar than the reported for olive leaf (31,0 mg/g) which is still used as main source of commercial oleanolic acid [7, 1]. In addition, one of these plants, *Baccharis tola* commonly known as "tola", is widely distributed in the Bolivian Highlands, so it could be used as new natural source of this compound. It is also interesting to note that the bark of *Polylepis besseri* has a good content of oleanolic acid, because the shredding bark of *Polylepis* is constantly peeling. Table Nº 1 and Figure Nº 3 show the high amounts of oleanolic acid in all the collected plants.

Table Nº1. *Content of oleanolic acid (mg/g) in highland Bolivian plants (n=3)*

Code	Plants	(Mean ± SD) (mg/g)	CV (%)
JUNE	*Junellia seriphioide*	22,69 ±0,41	1,8
TETRA	*Tetraglochin cristatum*	4,19 ±0,04	1,2
LAMP	*Lampaya castellani*	13,87 ±0,08	0,6
BTHO	*Baccharis tola*	11,93 ±0,32	2,7
PTOM **	*Polylepis tomentella leaves*	4,49 ±0,15	3,5
SATB	*Satureja boliviana*	8,73 ±0,08	1,0
PTOM *	*Polylepis tomentella bark*	2,87 ±0,04	1,4
PHIE	*Polylepis hieronyni*	3,62 ±0,04	1,1
PBESS *	*Polylepis besseri bark*	11,06 ±0,03	0,3
PBESS **	*Polylepis besseri leaves*	2,88 ±0,16	5,8

*Bark; **Leaves

In conclusion, we developed a new HPLC-DAD protocol for the quantification of oleanolic acid in plant extracts. The method was used to quantify this compound in selected Bolivian highland plants determining high amounts in all of them, in particular in *Junellia seriphioides*, *Lampaya castellani*, *Baccharis tola* and *Polylepis besseri* bark which could be used as new natural source of this important metabolite.

EXPERIMENTAL

Plant material

Tetraglochin cristatum, *Baccharis tola* and *Lampaya castellani* were collected in Orinoca at Oruro department, Bolivia (3768 m.a.s.l); *Junellia seriphioides* was collected near to the Sajama mountain (3940 m.a.s.l) and finally *Satureja boliviana* and *Polylepis* species were collected at the Botanical Garden of the University of San Andres (UMSA), located in Cota Cota town of La Paz City (3600 m.a.s.l.). Voucher specimens of all plants where deposited in the Bolivian National Herbarium where were identified by the staff.

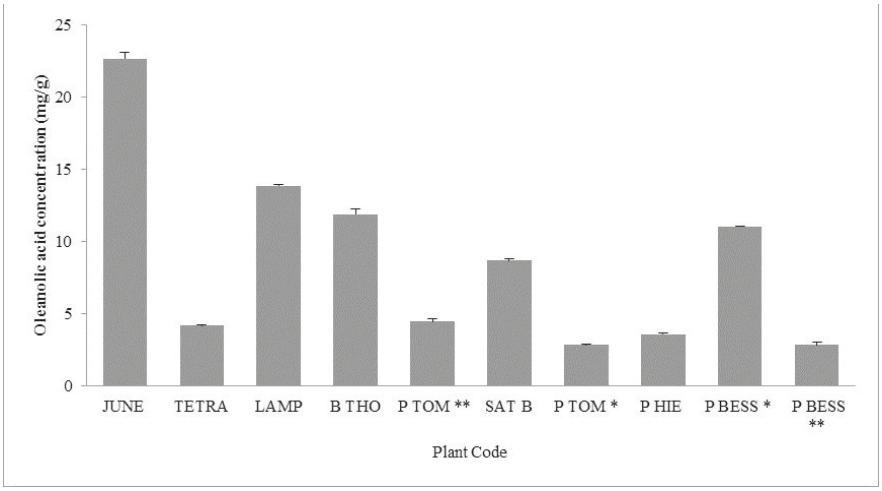

Figure Nº 3 *Oleanolic acid contents in plants of Bolivian highland.*

Oleanolic acid

The oleanolic acid, used as standard, was obtained of the industrial residue of *Chenopodium quinoa* Willd called "mojuelo" rich in saponins [15, 13]. That residue was extracted with EtOH/H_2O (75/25) for 72 h at room temperature. The concentrated EtOH/H_2O extract was submitted to an acid hydrolysis adding HCl 2N under reflux for 3 h, giving the sapogenin extract. The oleanolic acid was isolated out of that extract after a VLC chromatography on Silicagel G-60 and recrystallization, comparing the TLC and NMR data with those of the previous oleanolic acid isolated in our lab [13, 15].

Sample preparation

Aerial parts of *Tetraglochin cristatum*, *Junellia seriphioides* and *Satureja boliviana*; leaves of *Lampaya castellani* and *Baccharis tola*; bark and leaves of *Polylepis tomentella*, *P. hieronyni*, and *P. besseri* were dried in the bioorganic laboratory at room temperature for 2 or 3 days. 500 mg of the dried and ground plant material were extracted in 25 ml of EtOH 96 GL for 48 h. The extract was filtered through filter paper Whatman #4 and the residue was washed with 5 ml of EtOH, then the liquid extract was concentrated *in vacuo*. Before the analysis by HPLC the samples were dissolved and set, with MeOH (HPLC grade), to 5 ml volumetric flasks.

HPLC analysis

The HPLC data were recorded on Agilent Technologies HPLC 1100 series instrument consisting of a quaternary pump, continuous vacuum degasser, manual injection and column compartment coupled to a variable wavelength diode-array detector (DAD). The column was an Agilent Technologies EclipsePlus RP-C18 (4.6×250mm×5µm) with a 0.5 µm pre-column filter (Agilent Technologies), and the column compartment was heated at 35 ºC. The acetonitrile (HPLC grade, Sigma-Aldrich), formic acid >98% (Merck) and Ultrapure water at 18.3 MΩ resistance were used for

HPLC mobile phase. Water solvent was filtered through a 0.45 µm filtration system (Sartorius Stedim Biotech) before use.

Calibration curve

A series of oleanolic acid solutions were prepared in MeOH HPLC at five different concentrations (400, 800, 1500, 2000 and 2500 µg/ml). The analyte was detected at 210 nm (DAD) and the area in the chromatogram at retention time 8,2 was recorder by triplicate. The analyte showed a linear relationship between 400 and 2500 µg/ml yielded the following calibration curve y=12,957x+735,69 (R^2= 0,9983).

Sample quantification

The samples were injected manually; the volume of standards and samples was 25 µl. Chromatographic separation was done with an isocratic solvent of 93 % ACN as solvent D and 7% of 0.15 % (v) formic acid in water as a solvent C, at a flow rate of 1.0 ml/min. The solvent C was filtered with a Whatman 0.45 µm PTFE/cellulose filter prior to use. Then, the area of the compound at retention time T_R–8,2 min. was recorded by triplicate and the average was used for the calculation of the amount of oleanolic acid in the EtOH extract of every plant.

Statistics

The limit of quantification (LOQ) and the limit of detection (LOD) were calculated on the base of standard deviation of the response and the slope obtained from linear equation following equations: LOD = 3.3×(SD/slope "b") and LOQ = 10×(SD/ slope "b"); where SD is the standard deviation of the *y*-intercept.

ACKNOWLEDGEMENT

We are indebted to SIDA Swedish Agency for the financial support of the project "Biomolecules of industrial and medicinal interest. Anticancer". We also would like to thank to National Bolivian Herbarium for the identification of plant material.

REFERENCES

1. Pollier, J., Goossens A. **2012**, Oleanolic acid, *Phytochemistry*, *77*, 10–15.
2. Ovesná, Z., Vachalkova, A., Horvathova, K., Tothova, D. **2004**, Pentacyclic triterpenoic acids: new chemoprotective compounds, *Neoplasma*, *51*(5), 327-333.
3. Liu, J., **1995**, Pharmacology of oleanolic acid and ursolic acid, *J. Ethnopharmacol*., *49*, 57-68.
4. Liu, J., **2005**, Oleanolic acid and ursolic acid: Research perspectives, *J. Ethnopharmacol*., *100*, 92-94.
5. Sultana, N., Ata, A., **2008**, Oleanolic acid and related derivatives as medicinally important compounds, *Journal of enzyme inhibition and medicinal chemistry*, *23*(6), 739-756.
6. Sporn, M. B., Liby, K. T., Yore, M. M., Fu L., Lopchuk J. M., Gribble G. W., **2011**, New synthetic triterpenoids: Potent agents for prevention and treatment of tisuue injury caused by inflammatory and oxidative stress, *Journal of Natural Products*, *74*, 537-545.
7. Romero, C., García, A., Medina, E., Ruiz-Mendez, M. V., De Castro, A., Brenes, M., **2010**, Triterpenic acids in table olives, *Food Chemistry*, *118*, 670-674.
8. Jager, S., Trijan, H., Kopp, T., Laszczyk, M.N., Scheffler, A., **2009**, Pentacyclic triterpene distribution in various plants – Rich sources for a new group of multi-potent plant extracts, *Molecules*, *14*, 2016-231.
9. Flores, Y., Sterner, O., Almanza, G. R., **2004**, Oleanolic acid. Presence and importance in Highland Bolivian Plants, *Revista Boliviana de Química*., *21*(1), 31-34.
10. Skoog, D.A., Holle,r F.J., Crouch, S.R., Principios de análisis instrumental, **2008** Cengage Learning, México.
11. Kowalski, R., **2007**, Studies of selected plant raw materials as alternative sources of triterpenes of Oleanolic and Ursolic Acid types, *J. Agruc. Food Chem,, 55*, 656-662.
12. Zacchigna, M.., Cateni, F., Faudale, M., Sosa, S., Della Logia, R. **2009**, Rapid HPLC Analysis for Quantitative Determination of the Two Isomeric Triterpenic Acids, Oleanolic acid and Ursolic acid, in *Plantago Major*; *Sci Pharm*., *77*, 79–86.
13. Lozano, M., Gonzales, E., Flores, Y., Almanza, G.R., **2013**, Effect in acute inflammation of sapogenin extract and Isolated sapogenins from quinoa waste (*Chenopodium quinoa* Willd), *Revista Boliviana de Química*, *30*(2), 115-121.
14. Gbaguidi, F., Accrombessi, G., Moudachirou, M., Quetin-Leclercq, J., **2005**, HPLC quantification of two isomeric triterpenic acids isolated from *Mitracarpus scaber* and antimicrobial activity on *Dermatophilus congolensis*, *Journal of Pharmaceutical and Biomedical Analysis*, *39*, 990-995.
15. Flores, Y., Díaz, C., Garay, F., Colque, O., Sterner, O. and Almanza, G.R., **2005** "Oleanane-type triterpenes and derivatives from seed coat of Bolivian *Chenopodium quinoa* genotype salar", *Revista Boliviana de Química*, *22*(1), 71-77.

Paper V

REVISTA BOLIVIANA DE QUÍMICA
ISSN 0250-5460 Rev. Bol. Quim. *Paper edition*
ISSN 2078-3949 Rev. boliv. quim. *Electronic edition*
Suxo et al. RBQ Vol. 35, No.3, pp. 98-107, 2018

SAPOGENINS FROM THE HUSK OF *CHENOPODIUM QUINOA*, THE OBTAINING OF THEIR DERIVATIVES, AND THE EVALUATION OF THEIR CYTOTOXIC ACTIVITY

SAPOGENINAS DE CÁSCARAS DE *CHENOPODIUM QUINOA*, OBTENCIÓN DE SUS DERIVADOS, Y EVALUACIÓN DE SU ACTIVIDAD CITOTÓXICA

Received 08 15 2018
Accepted 08 26 2018
Published 08 30 2018

Vol. 35, No.3, pp. 98-107, Jul./Ago. 2018
35(3), 98-107, Jul./Aug. 2018
Bolivian Journal of Chemistry

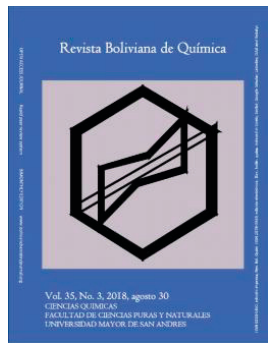

Full original article *Peer-reviewed*

Yaquelin Suxo[1], Maribel Lozano[1,2], Wendy Soria[3,4], Stina Oredsson[4], Giovanna R. Almanza[1,*]

[1]Bioorganic Laboratory, Instituto de Investigaciones Químicas, Universidad Mayor de San Andrés, La Paz, Bolivia, CP 303, Calle 27, Cota-Cota, La Paz – Bolivia, www.umsa.bo

[2]Centre for Analysis and Synthesis, Lund University, Lund, Sweden, SE-221 00, Naturvetarvägen 14 (former Getingevägen 60) /Sölvegatan 39 A-C, Lund –Sweden

[3]Institute of Molecular Biology and Biotechnology, Universidad Mayor de San Andrés, La Paz, Bolivia, Calle 27, Cota-Cota, La Paz – Bolivia, www.umsa.bo

[4]Department of Biology, Lund University, Sweden, SE-223 62, Sölvegatan 35, Lund-Sweden

Keywords: *Quinoa, Sapogenins, Acid hydrolysis, Oleanolic acid derivatives, Cytotoxic evaluation, JIMT-1, MCF-10A cells.*

ABSTRACT

In this paper, we present the evaluation of two types of methods for obtaining sapogenins by acid hydrolysis of a hydroalcoholic extract rich in saponins from quinoa husks. In the first method, called microwave method, the acid solution of saponins was pre-stirred for one minute in a microwave and then was heated and stirred at 100° C for 15 min. In the second one, called conventional method, the same acid solution was heated and stirred at 80 ºC for 4 h. The results show that the conventional method is better to obtain more quantity of sapogenins. Then four sapogenins were isolated: oleanolic acid (**1**), methyl oleanate (**2**), hederagenin (**3**), and phytolaccagenic acid (**4**). The cytotoxicity of the compounds was evaluated in human JIMT-1 breast cancer cells and human MCF-10A normal-like breast epithelial cells. The most active compound is hederagenin, which is more toxic in JIMT-1 cells (IC_{50} 27.3 μM) than in MCF-10A cells (IC_{50} 39.6 μM). Methyl oleanate is somewhat less toxic than hederagenin while oleanolic acid and phytolaccagenic acid needed treatment concentrations up to 100 μM to become cytotoxic. Finally, we obtained four new derivatives of oleanolic acid, the major sapogenin isolated, by oxidation of the OH group in C-3 to carbonyl (**5**) and subsequent reaction of aldol condensation, adding to carbon C-2 the follow aldehydes: benzaldehyde **6a**, *p*-

methylbenzaldehyde **6b**, *m*-methylbenzaldehyde **6c**, and *o*-methylbenzaldehyde **6d,** these synthesis were carried out in order to incorporate a Michael-acceptor into a molecular structure to enhance the biological activity, we obtained yields of around 50% for **6a** and **6b**, and of around 10% for **6c** and **6d**.

*Corresponding author: giovyalmanza@gmail.com, galmanza3@umsa.bo

RESUMEN

En este trabajo, presentamos la evaluación de dos tipos de métodos para la obtención sapogeninas por hidrólisis ácida de un extracto hidroalcohólico rico en saponinas de cáscaras de quinua. En el primer método, denominado método de microondas, la solución ácida de saponinas se agitó previamente durante un minuto en un microondas y luego se calentó y agitó a 100 °C durante 15 minutos. En el segundo, llamado método convencional, la misma solución ácida se calentó y agitó a 80ºC durante 4 h, nuestros resultados mostraron que el método convencional es mejor para obtener más cantidad de sapogeninas. Luego aislamos cuatro sapogeninas ácido oleanólico (**1**), metiloleanato (**2**), hederagenina (**3**) y ácido fitolaccagénico (**4**) evaluando su actividad citotóxica en células humanas de cáncer de mama JIMT-1 y células epiteliales de mama MCF-10A similares a células humanas normales, observando que todos ellos tienen citotoxicidad en ambas líneas celulares, pero el compuesto más activo es la hederagenina, que es más tóxica en las células JIMT-1 (IC_{50} 27.3 μM) que en las células MCF-10A (IC_{50} 39.6 μM). Finalmente, obtuvimos cuatro nuevos derivados de ácido oleanólico, la principal sapogenina aislada, por oxidación del grupo OH en C-3 a carbonilo (**5**) y reacción subsiguiente de condensación aldólica, añadiendo al carbono C-2 los siguientes aldehídos: benzaldehído **6a**, *p*-metilbenzaldehído **6b**, *m*-metilbenzaldehído **6c**, y *o*-metilbenzaldehído **6d**, estas síntesis se llevaron a cabo para incorporar un aceptor de Michael en la estructura molecular para potenciar la actividad biológica, obtuvimos rendimientos de alrededor del 50% para **6a** y **6b** y de alrededor del 10% para **6c** y **6d**.

INTRODUCTION

Quinoa (*Chenopodium quinoa* Willd) is the main export crop of the western zone of Bolivia, in particular from the Bolivian Southern Altiplano. It is a pseudo cereal determined as a strategic crop in the region, due to its high nutritive value. In addition, it can grow in under harsh environmental conditions, such as dry and saline soils, strong winds and frosts. Quinoa is a crop that has shown important growth in terms of production (92,312 t for the agricultural period 2017) [1]. In its natural state quinoa seeds have a bitter cover containing saponins, which cause an unpleasant taste and these the bitter components must be removed before cooking and export. Before export, the Bolivian food industries remove the seed coat by a mechanic process of scarification, where the dry grains are mixed causing friction to remove the cover which results in a residue called “mojuelo”. The quinoa husks, which are residues of scarification contain a high level of triterpenic oleanan-type saponins. In previous studies of quinoa husks, mainly bidesmosidic triterpenic saponins with a glucose linked in the position C-28 and one, two or three sugars linked in the carbon C-3, and four different aglycones (e.g., oleanolic acid, hederagenin, phytolaccagenic acid and serjanic acid) were investigated [2, 3].

One of the main sapogenins in quinoa husks is oleanolic acid (OA), and it is present in more than 1620 plant species [4]. In particular, it is one of the secondary metabolites found at a high concentration in high altitude plants [5], and it seems to play an important role in protecting the plant in the adverse environmental conditions found in the Altiplano region [6]. OA is one of the most popularly natural products studied, and from a pharmacological point of view, it has been suggested that this triterpene has activities such as anti-diabetic [7], anti-HIV [8], chemopreventive, hepatoprotective, tumor suppressant, anti-inflammatory, contraceptive, antioxidant, antineoplastic, and anti-cancer in different cell lines [9]. In addition, several chemical modifications were carried out using OA as a lead compound in order to improve the pharmacological activity as e.g. gastro protector [10], anti-liver cancer [11], and anti-HIV [12]. However, among the OA derivatives, there are no compounds with an α,β-unsaturated ketone, an important group that has the ability to react via Michael-type nucleophilic additions with soft electrophiles, giving an enhancement in the bioactivity of the molecules, particularly the cytotoxicity against cancer cell lines [13,14].

In this study, first we evaluate two types of methods for an acid hydrolysis reaction to obtain sapogenins from quinoa husks. Then, we isolated four sapogenins: oleanolic acid (**1**), methyl oleanate (**2**), hederagenin (**3**), and phytolaccagenic acid (**4**) evaluating their cytotoxic activity in human JIMT-1 breast cancer cells and human MCF-

10A normal-like breast epithelial cells. Finally, we synthesized four new derivatives of OA, by oxidation of the OH group in C-3 to carbonyl and a subsequent reaction of aldol condensation, adding to carbon C-2 the aldehydes benzaldehyde **6a**, *p*-methylbenzaldehyde **6b**, *m*- methylbenzaldehyde **6c**, or *o*-methylbenzaldehyde **6d**.

RESULTS AND DISCUSSION

Acid hydrolysis reaction

In agreement with previous reports [2], the saponins from quinoa husks are mainly bidesmosidics. When these saponins are submitted to acid hydrolysis, the sugars are removed leaving the sapogenins (Figure 1). Then, to obtain sapogenins, industrial residue of quinoa husks (100 g) was extracted with EtOH/H_2O (1:1) for 3 h under constant stirring (350 rpm) at room temperature giving a hydroalcoholic extract rich in saponins dried *in vacuo* at 55°C. The obtained extract was subjected to two types of acid hydrolysis methods giving sapogenin extracts. In the first method, called microwave method, an acid solution [1 g in 10 ml of 2 M HCl in ethanol (1:1)] was pre-stirred for one minute in a microwave and then was heated and stirred at 100°C for 15 min. In the second one, called conventional method, the same acidic solution was heated and stirred at 80ºC for 3 h. The sapogenin extracts obtained by both methods were chromatographed using VLC (Vacuum Liquid Chromatography) and Flash Chromatography over Silicagel giving the isolation of four sapogenins (Figure 1) in the proportions found in Table 1.

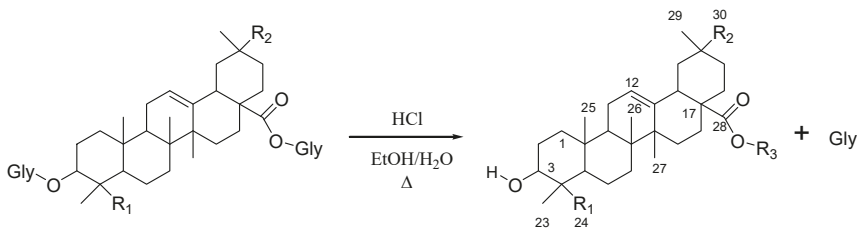

		R_1	R_2	R_3
1	Oleanolic acid	CH_3	CH_3	H
2	Methyl oleanate	CH_3	CH_3	CH_3
3	Hederagenine	CH_2OH	CH_3	H
4	Phytolaccagenic acid	CH_2OH	$COOCH_3$	H

Figure 1. *Acid hydrolysis of quinoa husks saponins to give four sapogenins*

Table 1. *Quantity of sapogenins isolated obtained by two acid hydrolysis methods*

Compound	Microwave method mg/g*	Conventional method mg/g*
1	98	317
2	21.2	66
3	21.6	279
4	116	104

*mg of sapogenin per g of hydro alcoholic extract.

Table 1 shows that the conventional method is more effective than the microwave method. But the conventional method was improved in several assays done in our lab and it is the first assay using the microwave method. So, the last one could be improved maybe using more time in the pre-stirring microwave process and/or more time in the stirring heated process. On the other hand, the quantification of obtained sapogenins should be done by HPLC methods, which are more exact and precise.

Cytotoxic evaluation

The cytotoxicity of the four isolated sapogenins was evaluated in one normal-like human breast epithelial cell line (MCF-10A) and in one breast cancer cell line (JIMT-1) using an MTT dose response assay, where the cells were

incubated with each compound for 72 h. Table 2 shows the IC_{50} values obtained from dose response curves. Hederagenin is the most toxic compound and it is more toxic in JIMT-1 cells than in MCF-10A cells. Methyl oleanate also shows toxicity in both cell lines, however, for this compound the MCF-10A cells were more sensitive than the JIMT-1 cells. Oleanolic acid itself and phytolaccagenic acid where less toxic than hederaginin and methyl oleanate. Although not very toxic, hederaginin may be a compound for further synthetic modification to increase the bioactivity preferentially towards cancer cells.

Table 2. *IC_{50} values of cytotoxicity of the isolated sapogenins in MCF-10A and JIMT-1 cells*

Compound	IC_{50} µM[a]	
	MCF-10A	JIMT-1
1	101.5 ± 11.4	90.9[b]
2	51.8 ± 19.5	80.3 ± 7.6
3	39.6 ± 0.4	27.3 ± 5.0
4	73.0 ± 0.4	105.1 ± 2.7

[a] Each value represents the mean of two independent experiments with 6 values in each ± gives the highest and lowest value.
[b] This result represents just one determination

Some of the compounds where previously evaluated against other cancer cell lines, like OA (**1**), which showed cytotoxicity against the following lines: prostate cancer PC3 cells (IC_{50} 6.5 µM), lung cancer A549 cells (IC_{50} 0.4 µM), breast cancer MCF-7 cells (IC_{50} 35.4 µM), and gastric cancer BGC823 cells (IC_{50} 2.6 µM) [7]. Compared with our data, we found a lower degree of toxicity. However, considering the activity of hederagenin (**3**) against the JIMT-1 breast cancer cell line, is still interesting to continue studies with hederagenin and synthetic derivatives of it investigating the activity in different cancer cell lines.

Synthesis of derivatives

The major sapogenin isolated from quinoa husks was OA (**1**). As mentioned in the introduction, it is one of the most popular natural product studied, because of chemical and pharmacological reasons [7-12] but the synthesis of analogs with an α,β-unsaturated ketone moiety are not still carried out. This synthesis was done to incorporate a Michael acceptor into the molecular structure because this type of compounds forms a major component of the natural products having anti-cancer activity [14], enhancing the biological activity of natural products [13].

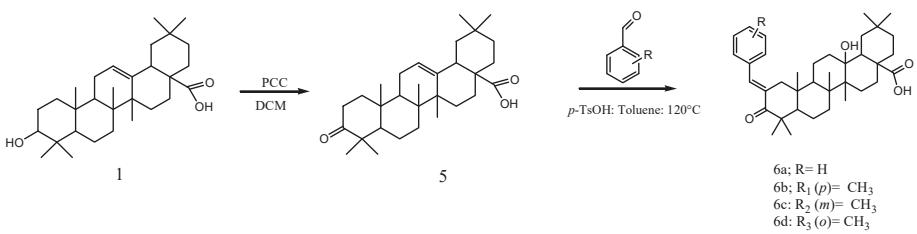

Figure 3. *Schematic procedure to obtain derivatives 5, 6a, 6b, 6c, and 6d*

The synthesis of new derivatives is showed in the Figure 3 where we can see that the reactions goes through the compound **5** which was prepared by oxidation of the OH group in C-3 using pyridium chlorochromate (PCC) in dichloromethane (DCM), yield 70.1%. Compound **5** is the target compound for carrying out aldol reactions of Claisen Schmidt adding to carbon C-2 different benzaldehydes. The first reaction was done with benzaldehyde to find the reaction conditions; the method was developed based on the method described by Karimi-Jaberi & Pooladian [15]. Thus, compound **5** was dissolved in different solvents founding toluene as the most suitable, then we added benzaldehyde (1 equiv) followed of *p*-TsOH (1 equiv) and the reaction was stirred at 120°C for different times founding that the reaction needs more than 24 hours to be completed.

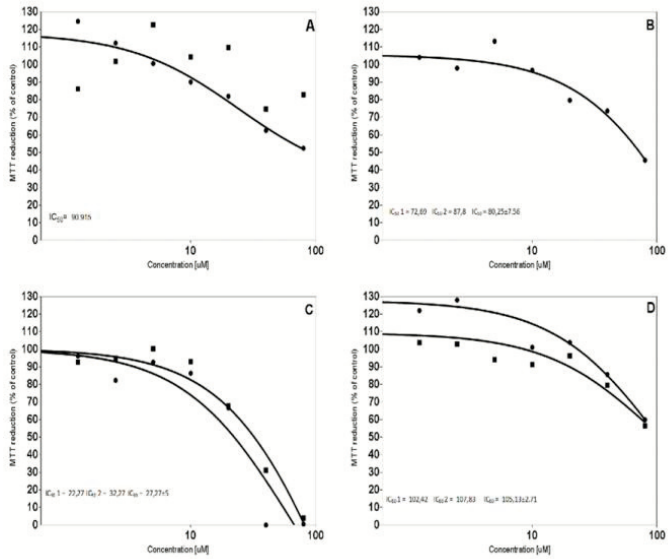

Figure 1. *Dose response curves and IC_{50} values of isolated sapogenins obtained by treatment of JIMT-1 breast cancer cells. The dose response was evaluated with a MTT assay after 72 hours of incubation with each compound. Each curve shows an independent experiment (n=6). A. (1) Oleanolic acid, B. (2) Methyl oleanate, C. (3) Hederagenine, D. (4) Phytolaccagenic acid*

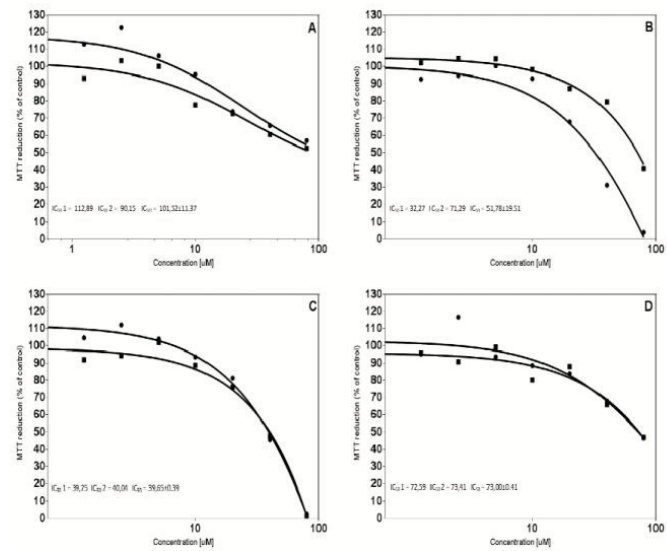

Figure 2. *Dose response curves and IC_{50} values of isolated sapogenins obtained by treatment of MCF-10A normal-like breast epithelial cells. The dose response was evaluated with a MTT assay after 72 hours of incubation with each compound. Each curve shows an independent experiment (n=6). A. (1) Oleanolic acid, B. (2) Methyl oleanate, C. (3) Hederagenine, D. (4) Phytolaccagenic acid*

After the reaction was completed and the formation of aldol product was observed by TLC evaluations, the reaction was quenched and the product was purified by Column Chromatography, giving the compound **6a** (yield 48,9 %) elucidated by NMR 1D and 2D. After founding the reaction conditions, we extended the substrate scope to different methylbenzaldehydes to give the compounds **6b** (yield 41.8%), **6c** (yield 9.3%), and **6d** (yield 10.3%), all of them were purified by Column Chromatography and elucidated by NMR 1D and 2D. We still do not evaluate the compounds against cancer cell lines, but we recommend their realization not only against breast cancer cell lines, but also against of lung, gastric and prostate cancer cell lines, among others. It is also recommended to synthesize similar derivatives from hederagenin, because, as we can see, it showed most activity against breast cancer cell lines than oleanolic acid.

EXPERIMENTAL

General

All chemicals and solvents were purchased from Sigma Aldrich. ^{1}H NMR and ^{13}C NMR spectra were recorded in a Bruker 250 MHz spectrometer using deuterated DMSO. Column chromatography was performed using Silica gel 60 (35-63μm) and TLC analysis was made on Silica Gel 60 F_{254} (Merck, Darmstadt, Germany) plates.

Plant material

The quinoa husk industrial residue was collected from the Andean Organic Food Company "Irupana" located in La Paz city at 3800 m.a.s.l. on June of 2016, then it was deposited in the laboratory of Bioorganic of Universidad Mayor de San Andres at La Paz Bolivia.

Extraction and isolation

100 g of quinoa husk were extracted with an aqueous solution of EtOH (1:1) for 3 h under constant stirring at room temperature. The hydro-alcoholic extract was concentrated *in vacuo*, to remove ethanol, the aqueous residue was dried at 55°C.

Acid hydrolysis method 1 (Microwave)

A solution of extract 1g in 2M HCl in methanol (1:1) (10 ml) was heated at 100°C for 15 min with 1 min of pre-stirring in a microwave. The mixture was neutralized with an aqueous solution of NaOH 5% (10 ml), followed by 10 ml of brine. The aqueous mixture was extracted with ethyl acetate (2x10 ml). The combined organics phases were dried over Na_2SO_4 and concentrated *in vacuo* to yield 0.416g of crude extract. The crude product was purified by flash chromatography over silica gel, eluting with EtOAc/n-heptane from 20% to 80%. Obtaining four pure compounds **1** (98 mg), **2** (21.2) mg, **3** (21.6) mg and **4** (116 mg).

Acid hydrolysis method 2 (Conventional)

A solution of 1 g of hydro alcoholic extract with 10 ml of HCl 2N (1:1 EtOH/H_2O) was stirred at 80°C for 3 h. The progress of reaction was monitored by TLC. After the reaction was completed, the precipitate obtained was filtered, washed with 5 ml of a solution of NaOH 2N and dried at room temperature for 72 h. The dried extract was diluted with 15 ml of DCM/MeOH (9:1), filtered and concentrated *in vacuo*. The crude product was purified by vacuum liquid chromatography (VLC) and Flash chromatography with a gradient of 10 to 100% of EtOAc/$PeEt_{20\text{-}60}$ and 100 to 95% of EtOAc/MeOH obtaining the four sapogenins: **1** (317 mg), **2** (66 mg), **3** (279 mg) and **4** (104 mg)

Compound 1; oleanolic acid

^{1}H NMR (300 MHz, DMSO) δ 12.05 (*s*, 1H, COOH), 5.16 (*bs*, 1H, H–12), 3.00 (*t*, *J*=5.39 Hz, 1H, H–3), 2.74 (*dd*, *J*=13.33, 3.63 Hz, 1H, H–18), 1.90 (*t*, *J*=11.51 Hz, 1H, H–16a), 1.81 (*m*, 4H, H–11, H–22), 1,65 (*bs*, 1H, 15a), 1,61 (*bs*, 1H, H–2a), 1.56 (*bs*, 1H, H–19a) 1.49 (*m*, 3H, H–15b, H–16b, H–9), 1.46 (*m*, 3H, H–1a, H–7), 1,41 (*m*, 1H, H–2b), 1,34, (*m*, 2H, H–6) 1,21 (*m*, 3H, H–5, H–21), 1,10 (*s*, 3H, H–27), 0,99 (*m*, 2H, H–19b, H–1b), 0.89 (*s*, 3H, H–23), 0.87 (*s*, 6H, H–24 , H–25) 0,85 (*s*, 3H, H–30), 0.71 (*s*, 3H, H–29), 0.67 (*s*, 3H, H–26) ^{13}C NMR (75 MHz,

DMSO) δ 179.0 (C–28), 144.3 (C–13), 122.0 (C–12), 77.3 (C–3), 55.2 (C–5), 47.5 (C–9), 46.1 (C–17), 45.9 (C–19), 41.8 (C–14), 41.3 (C–18), 39.3 (C–8), 38.8 (C–4), 38.5 (C–1), 37.1 (C–10), 33.8 (C–21), 33.3 (C–29), 32.9 (C–7), 32.6 (C–22), 30.9 (C–20), 28.7 (C–23), 27.7 (C–15), 27.4 (C–2), 26.1 (C–27), 23.8 (C–11), 23.4 (C–30), 23.1 (C–16), 18.5 (C–6), 17.3 (C–26), 16.5 (C–24), 15.6 (C–25).

Compound 2; methyl oleanate

^{1}H NMR (300 MHz, DMSO) δ 5.17 (*bs*, 1H, H–12), 3.62 (*s*, 3H, H–31), 3.00 (*t*, *J*=5,48 1H, H–3), 2.55 (*bs*, 1H, H–18), 1.94 (*t*, *J*=11.44, 1H, H–16a), 1.83 (*m*, 4H, H–22, H–11a, H–11b), 1.66 (*bs*, 1H, 15a), 1.62 (*bs*, 1H, H–2a), 1.57 (*bs* 1H, H–19a), 1.48 (*m*, 6H, H–16b, H–9, H–1a, H–7, H–15b, H–2b), 1.38 (*m*, 2H, H–6), 1.23 (*m,* 3H, H–5, H–21), 1.09 (*s*, 6H, H–27, H–23), 1.00 (*m*, 2H, H–19b, H–1b), 0.89 (*s*, 6H, H–24, H–25), 0.85 (*s*, 3H, H–30), 0.68 (*s*, 6H, H–29, H–26). ^{13}C NMR (75 MHz, DMSO) δ 176.8 (C–28), 144.1 (C–13), 122.4 (C–12), 77.3 (C–3), 55.2 (C–5), 52.1 (C–31), 47.5 (C–9), 43.7 (C–19), 42.5 (C–17), 42.1 (C–14), 41.7 (C–18), 39.3 (C–8), 38.8 (C–4), 38.5 (C–1), 37.1 (C–10), 33.7 (C–21), 32.9 (C–7), 30.1 (C–29), 28.7 (C–20), 28.3 (C–22), 27.7 (C–23), 27.4 (C–15), 26.0 (C–2), 23.3 (C–27), 23.2 (C–30), 21.2 (C–16), 18.5 (C–11), 17.3 (C–6), 16.5 (C–26), 15.6 (C–24), 14.5 (C–25).

Compound 3; hederagenin

^{1}H NMR (300 MHz, DMSO) δ 12.05 (*s*, 1H, COOH), 5.16 (*t*, *J*=3,19, 1H, H–12), 3.43 (*s*, 2H, H–24), 3.16 (*bs*, 1H, H–3), 3.07 (*dd*, *J*=10.6, 2.65 Hz, 1H, H–18), 1.91 (*t*, *J*=11,6 1H, H–16a), 1.81 (*d*, *J*=5.9 Hz, 2H, H–11), 1.65 (*m*, 1H, H–15a), 1.61 (*m*, 2H, H–22), 1.56 (*m*, 1H, H–2a), 1.53 (*d*, J=6,93 1H, H–19a), 1.45 (*m*, 5H, H–16b, H–9 H–1a, H–7, H–15b), 1,38 (*m*, 2H, H–6), 1.14 (*m*, 3H, H–5, H–21), 1.10 (*s*, 3H, H–27), 0.99 (*m*, 2H, H–19b, H–1b), 0.87 (*s*, 9H, H–23, H–25, H–30), 0.71 (*s*, 3H, H–29), 0.53 (*s*, 3H, H–26). ^{13}C NMR (75 MHz, DMSO) δ 179.1 (C–28), 144.3 (C–13), 122.0 (C–12), 70.7 (C–3), 64.8 (C–23), 49.1 (C–5), 47.5 (C–9), 46.8 (C–17), 46.1 (C–19), 45.9 (C–4), 42.3 (C–14), 41.8 (C–18), 41.3 (C–8), 39.3 (C–1), 38.4 (C–10), 36.8 (C–21), 33.8 (C–22), 33.3 (C–29), 32.4 (C–7), 30.9 (C–20), 27.7 (C–15), 27.0 (C–2), 26.1 (C–27), 23.8 (C–11), 23.4 (C–30), 23.1 (C–16), 18.0 (C–6), 17.4 (C–26), 16.0 (C–25), 13.1 (C–24).

Compound 4; phytolaccagenic acid

^{1}H NMR (300 MHz, DMSO) δ 12.02 (*m*, 1H, COOH), 5.18 (*t, J*=3.30, 1H, H–12), 3.62 (*s*, 3H, H–31), 3.30 (*s*, 2H, H–24), 3.07 (*dd*, *J*=10.3, 4.6 Hz, 1H, H–3), 2.57 (*m*, 1H, H–18), 1.95 (*t*, *J*=11.3, 1H, H–16a,), 1.81 (*d*, *J*=14.0 Hz, 2H, H–11,), 1.67 (*bs*, 1H, H–15a), 1.62 (*bs*, 2H H–22), 1.57 (*bs*, 1H, H–2a), 1.54 (*bs*, 1H, H–19a), 1.48 (*m*, 5H, H–16b, H–9, H–1a, H–7, H–15b), 1.38 (*m*, 2H, H–6), 1.22 (*m,* 3H, H–5, H–21), 1.11 (*s*, 3H, H–27), 1.09 (*s*, 3H, H–23), 1.00 (*m*, 2H, H–19b, H–1b), 0.87 (*s*, 3H, H–25), 0.70 (*s*, 3H, H–29), 0.53 (*s*, 3H, H–26). ^{13}C NMR (75 MHz, DMSO) δ 178.7 (C–28), 176.8 (C–30), 144.1 (C–13), 122.4 (C–12), 70.7 (C–3), 64.8 (C–23), 52.1 (C–31), 47.5 (C–5), 46.8 (C–9), 45.4 (C–17), 43.7 (C–20), 42.5 (C–18), 42.3 (C–4), 42.1 (C–14), 41.7 (C–19), 39.2 (C–8), 38.4 (C–1), 36.8 (C–10), 33.7 (C–22), 32.4 (C–7), 30.1 (C–21), 28.3 (C–15), 27.7 (C–29), 27.0 (C–2), 26.0 (C–27), 23.3 (C–11), 23.2 (C–16), 17.9 (C–6), 17.3 (C–26), 16.0 (C–25), 13.1 (C–24).

Synthesis of derivatives

Procedure to obtain compound 5, 3-oxoolean-12-en-28-oic acid

A solution of 1 (100 mg, 0.219 mmol) in DCM (5 ml) PCC (114 mg, 0.668 mmol) was added then the mixture of reaction was stirred at room temperature for 2 h. The progress of reaction was controlled by TLC. After the reaction was completed, the reaction was quenched by adding 10 ml of brine followed the extraction with DCM (4x15 ml). The organic phases were dried over $MgSO_4$, concentrated *in vacuo* and purified by flash chromatography with a mixture of $PeEt_{20\text{-}60}$/DCM/EtOAc (75:20:5) obtaining compound **5** (70.1 mg).

^{1}H NMR (300 MHz, $CDCl_3$). δ 5.31 (*t*, *J*=3.31, 1H, H–12), 2.85 (*dd*, *J*=13.6, 3.8 Hz, 1H, H–18), 2.56 (*ddd*, *J*=16.0, 11.1, 7.2 Hz, 1H, H–1a), 2.38 (*dd*, *J*=16.29, 6.88 Hz, 1H, H–18), 2.00 (*t*, *J*=3.75 Hz, 1H, H–16a), 1.94 (*dd*, *J*=6.3, 3.3 Hz, 2H, H–11), 1.88 (*m*, 1H, H–1a), 1.78 (*t*, *J*=5.5 Hz, 1H, H–22a), 1.72 (*t*, *J*=4.11 Hz, 1H, H–15a), 1.71–1.58 (*m*, 4H, H–9, H–19a, H–22b, H–16b), 1.49 (*m*, 3H, H–7a, H–6), 1.43 (*dd*, *J*=11.8, 3.9 Hz, 1H, H–1b), 1.39–1.30 (*m*, 3H, H–5, H–21a, H–7b), 1.25 (*m*, 1H, H–21b), 1.20 (*d*, *J*=4.5 Hz, 1H, H–19b), 1.16 (*s*, 4H, H–15b, H–27), 1.10 (*s*,

3H, H–23), 1.06 (*s*, 3H, H–25), 1.04 (*s*, 3H, H–24), 0.94 (*s*, 3H, H–30), 0.92 (*s*, 3H, H–29), 0.82 (*s*, 3H, H–26). ^{13}C NMR (75 MHz, $CDCl_3$) δ 217.7 (C–3), 184.1 (C–28), 143.6 (C–13), 122.4 (C–12), 55.3 (C–5), 47.4 (C–4), 46.9 (C–9), 46.6 (C–17), 45.8 (C–19), 41.7 (C–14), 41.0 (C–18), 39.3 (C–8), 39.1 (C–1), 36.8 (C–10), 34.1 (C–2), 33.8 (C–21), 33.0 (C–29), 32.4 (C–22), 32.2 (C–7), 30.7 (C–20), 27.7 (C–15), 26.4 (C–23), 25.8 (C–27), 23.5 (C–30), 23.5 (C–11), 22.9 (C–16), 21.4 (C–24), 19.5 (C–6), 17.0 (C–26), 15.0 (C–25).

Claisen Schmidt condensation products, from ***5***

Compounds ***6a, 6b, 6c,*** *and* ***6d***

A solution of **5** (80 mg, 0.176 mmol) in toluene (3 ml) benzaldehyde (36 µl, 0.352 mmol) was added followed of *p*-TsOH (68 mg, 0.352 mmol), then the reaction was stirred at 120°C for 24 hours to obtain compound **6a**, and 30 hours to obtain compounds **6b**, **6c** and **6d**. The progress of reaction was controlled by TLC. After the reaction was completed it was quenched by addition of 10 ml of brine, the aqueous was extracted with DCM (4x15 ml). The organic phases were dried with $MgSO_4$, concentrated *in vacuo* and purified by column chromatography with mixtures of $PeEt_{20\text{-}60}$:DCM between 97 to 65% of $PeEt_{20\text{-}60}$ obtaining compounds **6a** (39,1mg), **6b** (33,4 mg), **6c** (7,4 mg) and **6d** (8,2 mg).

Compound ***6a, 2-****phenylmethylene-3-oxo-13-hydroxy oleanolic acid.*

^{1}H NMR (300 MHz, $CDCl_3$) δ 7.55 (*s*, 1H, H–1´), 7.42–7.41 (*m*, 4H, H–2´´, H–6´´, H–3´´, H–5´´), 7.35 (*m*, 1H, H–4´´), 3.14 (*d*, *J*=16.1 Hz, 1H, H–1a), 2.31 (*t*, *J*=3,61, 1H, H–18), 2.29 (*d*, *J*=5.1 Hz, 1H, H–1b), 1.99–1.82 (*m*, 3H, H–22a, H–16a, H–15a), 1.69–1.62 (*d*, *J*=9.6 Hz, 4H, H–12, H–22b, H–6a), 1.56–1.51 (*dd*, *J*=10.7, 7.3 Hz, 5H, H–5, H–7a, H–11, H–6b), 1.44–1.41 (*m*, 3H, H–9, H–7b, H–16b), 1.27 (*m*, 2H, H–19a, H–15b), 1.24 (*s*, 4H, H–21a, H–26), 1.21 (*s*, 3H, H–27), 1.19 (*s*, 4H, H–21b, H–24), 1.16 (*s*, 3H, H–23), 0.95 (*s*, 1H, H–19b), 0.91 (*s*, 3H, H–29), 0.86 (*s*, 6H, H–30, H–25). ^{13}C NMR (75 MHz, $CDCl_3$) δ 207.8 (C–3), 179.1 (C–28), 137,5 (C–1´), 135,9 (C–2), 133.9 (C–1´´), 130.3 (C–2´´), 130.3 (C–6´´), 128.5 (C–4´´), 128.4 (C–3´´), 128.4 (C–5´´), 89.5 (C–13), 52.8 (C–5), 47.9 (C–9), 47.4 (C–4), 45.3 (C–14), 44.9 (C–18), 44.5 (C–1), 43.9 (C–17), 41.2 (C–8), 36.3 (C–10), 36.2 (C–19), 35.2 (C–21), 33.7 (C–7), 33.0 (C–29), 31.5 (C–12), 29.9 (C–20), 29.5(C–23), 28.0 (C–22), 26.5 (C–16), 26.0 (C–15), 23.1 (C–30), 22.5 (C–24), 19.8 (C–11), 19.2(C–27), 18.9 (C–6), 17.4 (C–26), 15.9 (C–25).

Compound ***6b,*** *2-(p-(methylphenyl) methylene)-3-oxo-13-hydroxy oleanolic acid*

^{1}H NMR (300 MHz, $CDCl_3$) δ 7.53 (*s*, 1H, H–1´), 7.34 (*d*, *J*=8.0 Hz, 2H, H–2´´, H–6´´), 7.22 (*d*, *J*=8.6 Hz, 2H, H–5´´, H–3´´), 3.13 (*d*, *J*=16.0 Hz, 1H, H–1a), 2.40 (*s*, 3H, H–1´´´), 2.34 (*m*, *J*=6.4 Hz, 2H, H–18, H–1b), 1.92 (*m*, 1H, H–22a), 1.88 (*m*, 2H, H–16a, H–15a), 1.66–1.65 (*m*, 4H, H–12, H–22b, H–6a), 1.56 (*bs*, 1H, H–7a), 1.50 (*m*, 3H, H–5, H–11), 1.47 (*m*, 1H, H–6b), 1.44–1,42 (*m*, 3H, H–9, H–7b, H–16b), 1.27 (*m,* 3H, H–19a, H–21a, H–15b), 1.24 (*s*, 3H, H–26), 1.21 (*s*, 3H, H–27), 1.18 (*s*, 3H, H–24), 1.15 (*s*, 3H, H–23), 1.09 (*bs*, 1H, H–19b), 0.91 (*s*, 3H, H–29), 0.86 (*s*, 6H, H–30, H–25). ^{13}C NMR (75 MHz, $CDCl_3$) δ 207.8 (C–3), 179.1 (C–28), 138.7 (C–4´´), 137.7 (C–1´), 133.1(C–1´´), 133.0 (C–2), 130.4 (C–2´´), 130.4 (C–6´´), 129.2 (C–3´´), 129.2 (C–5´´), 89.5 (C–13), 52.8 (C–5), 48.0 (C–9), 47.4 (C–4), 45.2 (C–14), 44.9 (C–18), 44.6 (C–1), 43.9 (C–17), 41.2 (C–8), 38.7 (C–10), 36.3 (C–19), 35.1 (C–21), 33.7 (C–7), 33.0 (C–29), 31.5 (C–12), 29.9 (C–20), 29.5 (C–23), 28.0 (C–22), 26.5 (C–16), 26.0(C–15), 23.1 (C–30), 22.4 (C–24), 21.4 (C–1´´´), 19.8 (C–11), 19.2 (C–27), 19.0 (C–6), 17.4 (C–26), 15.9 (C–25).

Compound ***6c,*** *2-(m-(methylphenyl) methylene)-3-oxo-13-hydroxy oleanolic acid*

^{1}H NMR (300 MHz, $CDCl_3$) δ 7.52 (*s*, 1H, H–1´), 7.24 (*m*, 2H, H–2´´, H–6´´), 7.17 (*d*, *J*=5.8 Hz, 2H, H–4´´, H–5´´), 3.14 (*d*, *J*=15.4 Hz, 1H, H–1a), 2.40 (*s*, 3H, H–1´´´), 2.30 (*bs*, 1H, H–18), 2.25 (*d*, *J*=5,15, 1H, H–1b), 1.90 (*m*, 1H, H–22a), 1.88 (*m*, 2H, H–16a, H–15a), 1.67–1.63 (*m*, 4H, H–12, H–22b, H–6a), 1.57 (*m*, 1H, H–7), 1.52–1.50 (*m*, 4H, H–5, H–11, H–6b), 1.44–1.41 (*m*, 3H, H–9, H–7b, H–16b), 1.27 (*m*, 1H, H–19a), 1.24 (*m*, 4H, H–21a, H–26), 1.21 (*s*, 3H, H–27), 1.18 (*s*, 4H, H–15b, H–24), 1.16 (*s*, 3H, H–23), 1.10 (*bs* 1H, H–21b), 0.95 (*m*, 1H, H–19b), 0.91 (*s*, 3H, H–29), 0.86 (*s*, 6H, H–25, H–30). ^{13}C NMR (75 MHz, $CDCl_3$) δ 207.8 (C–3), 179.1 (C–28), 138.1(C–3´´), 137.8 (C–1´), 135.9 (C–2), 133.7(C–1´´), 131.3 (C–2´´), 129.3 (C–4´´), 128.3 (C–5´´), 127.0 (C–6´´), 89.5 (C–13), 52.8 (C–5), 48.0 (C–9), 47.4 (C–4), 45.3 (C–14), 44.9 (C–18), 44.5 (C–1), 43.9 (C–17), 41.2 (C–8), 36.3 (C–10), 36.2 (C–19), 35.2 (C–21), 33.7 (C–7), 33.0 (C–29), 31.5 (C–12), 29.9 (C–20), 29.4 (C–23), 28.0 (C–22), 26.5 (C–

16), 26.0 (C–15), 23.1 (C–30), 22.5 (C–24), 21.5 (C–1′′′), 19.8 (C–11), 19.2 (C–27), 18.9 (C–6), 17.4 (C–26), 16.0 (C–25).

Compound ***6d,*** *2-(o-(methylphenyl) methylene)-3-oxo-13-hydroxy oleanolic acid*

^{1}H NMR (300 MHz, $CDCl_3$) δ 7.67 (*s*, 1H, H–1′), 7.24 (*bs*, 2H, H–3′′, H–4′′), 7.20 (*bs*, 2H, H–5′′, H–6′′), 2.96 (*d*, *J*=15.8 Hz, 1H, H–1a), 2.31 (*s*, 3H, H–1′′′), 2.26 (*t*, *J*=4.97 Hz, 1H, H–18), 2.05 (*d*, *J*=15.6 Hz, 1H, H–1b), 1.87–1.84 (*m,* 3H, H–22a, H–16a, H–15a), 1.65–1.64 (*m*, 3H, H–6a, H–12), 1.58 (*m*, 1H, H–22b), 1.55–1.54 (*m*, 2H, H–7a, H–6b), 1.51–1.49 (*m*, 3H, H–5, H–11), 1.42–1.39 (*m*, 3H, H–9, H–7b, H–16b), 1.27 (*m*, 2H, H–21a, H–15b), 1.22 (*s*, 3H, H–26), 1.20 (*s*, 4H, H–23, H–19a), 1.18 (*s*, 3H, H–27), 1.17 (*s*, 3H, H–24), 0.95 (*bs*, 1H, H–21b), 0.91 (*bs*, 1H, H–19b), 0.89 (*s*, 3H, H–29), 0.86 (*s*, 3H, H–25), 0.84 (*s*, 3H, H–30). ^{13}C NMR (75 MHz, $CDCl_3$) δ 207.6 (C–3), 179.1 (C–28), 137.8 (C–2′′), 137.0 (C–1′), 135.1 (C–1′′), 134.2 (C–2), 130.2(C–3′′), 128.5 (C–4′′), 128.3 (C–5′′), 125.4 (C–6′′), 89.5 (C–13), 53.3 (C–5), 47.8 (C–9), 47.4 (C–4), 45.6 (C–14), 44.9 (C–18), 43.9 (C–17), 43.5 (C–1), 41.2 (C–8), 36.5 (C–10), 36.2 (C–19), 35.1 (C–21), 33.8 (C–7), 33.0 (C–29), 31.5 (C–12), 29.9 (C–20), 29.1(C–23), 27.8 (C–22), 26.5 (C–16), 25.9 (C–15), 23.1 (C–30), 22.7 (C–24), 20.1 (C–1′′′), 19.7 (C–11), 19.2 (C–27), 18.8 (C–6), 17.5 (C–26), 15.7 (C–25).

Cytotoxicity

Sample preparation

The compounds were diluted in 100 % DMSO to a 10 mM stock solution, which was kept at -20º C. The compounds were diluted in PBS to give working solutions at appropriate concentrations. The controls were supplemented with PBS containing DMSO at the same concentration as in the working solution of the compounds. The final DMSO concentration was 0.1 % when using the compounds at 80, 40, 20, 10, 5, 2.5, 1.25 and 0.625 µM for MTT assays.

Cell lines

Two cell lines were selected for testing: the normal-like breast epithelial cell line MCF-10A and the breast cancer cell lines JIMT-1 assays.

MCF-10A is an immortalized, non-transformed epithelial cell line derived from the breast tissue of a 36-year-old patient with a fibrocystic change. It has retained many normal traits, including lack of tumorigenicity in nude mice, lack of anchorage-independent growth, and dependence on growth factors and hormones for proliferation and survival [16].

The MCF-10A cells were cultured in RPMI 1640 medium supplemented with 10% heat-inactivated fetal calf serum (FCS), non-essential amino acids (1 mmol/L), insulin (10 µg/ml), epidermal growth factor (20 ng/ml), cholera toxin toxin (50 ng/ml), hydrocortisol (250 ng/ml), penicillin (100 U/ml), and streptomycin (100 µg/ml).

JIMT-1 cells were established from the pleural effusion of a 62-year-old woman with ductal breast cancer (grade 3 invasive, T2N1M0) after postoperative radiation; cell line was described to carry an amplified HER-2 oncogene and to be insensitive to HER-2-inhibiting drugs, like trastuzumab (Herceptin) [17].

The human breast carcinoma cell line JIMT-1 (ACC589) was purchased from the German Collection of Microorganisms and Cell Cultures (Braunschweig, Germany) and routinely cultured in DMEM/F-12 medium supplemented with 10% FCS, nonessential amino acids (1 mmol/L), insulin (10 µg/mL), penicillin (100 U/mL), and streptomycin (100 mg/mL). All cell lines were kept at 37 °C in a humidified incubator with 5 % CO_2 in air.

For the experiments, cells were seeded at the following densities: MCF-10A: $1x10^4/cm^2$ and JIMT-1: $1.5x10^4/cm^2$ in tissue culture vessels of appropriate size to obtain the desired cell number. The volume of medium used was 0.2-0.3 per cm^2. The cells were allowed to attach for 24 h before addition of compound.

MTT assay

Cytotoxicity assays were performed to obtain dose response curves for compounds in JIMT-1 and MCF-10A cells. For the MTT assay, cells were trypsinized, counted in a hemocytometer, and resuspended in cell culture medium. Aliquots of 180 ul cell suspension containing 3000 (MCF-10A) and 5000 (JIMT-1) cells were seeded in 96-well plates. Twenty-four hours later, the compounds were added. At 72 h of drug treatment, 20 µl of MTT solution (5 mg/ml MTT in PBS) was added to each well and the 96 well plates were returned to the CO_2 incubator for 1 hour.

The blue formazan product formed by reduction in live attached cells was dissolved by adding 100 µl of 100% DMSO per well. The plates were swirled gently at room temperature for 10 minutes to dissolve the precipitate. Absorbance was monitored at 540 nm.

The data were processed in GraphPadPrism 6.

ACKNOWLEDGEMENTS

The authors would like to thank to the Swedish Agency SIDA for providing the financial support of this study involved in the project “Biomolecules of medicinal and industrial interest, anticancer” and the grant for Yaquelin Suxo.

REFERENCES

1. Barrientos, E., Carevic, F.; Delatorre, J. **2017**, La sustentabilidad del altiplano sur de Bolivia y su relación con la ampliación de superficies de cultivo de quinua. *Idesia*, *35*(2), 7-15.
2. Madl, T., Sterk, H., Mittelbach, M. **2006**, Tandem Mass Spectrometric Analysis of a Complex Triterpene Saponin Mixture of *Chenopodium quinoa*. *J Am Soc Mass Spectrom*, *17*, 795– 806.
3. Kuljanabhagavadad, T., Thongphasuk, P., Chamulitrat, W., Wink M. **2008**. Triterpene saponins from *Chenopodium quinoa* Willd. *Phytochemistry*, *69*(9), 1919-1926.
4. Pollier, J., Goossens, A. **2012**, Oleanolic acid, *Phytochemistry*, *77*, 10–15.
5. Lozano, M., Flores, Y. R., Almanza, G. R. **2017**, High contents of oleanolic acid in highland Bolivian plants, *Rev. Bol. Quim. 34* (1), 28-32.
6. Flores, Y., Sterner, O., Almanza, G. R. **2004**, Oleanolic acid. Presence and importance in highland Bolivian plants. *Rev. Bol. Quim.*, *21*, 31-35.
7. Hao, J., Liu, J., Wen, X., Sun, H. **2013**, Synthesis and cytotoxicity evaluation of oleanolic acid derivatives. *Bioorganic & Medicinal Chemistry Letters*, *23*(7), 2074-2077.
8. Rali, S., Oyedeji, O. O., Aremu, O. O., Oyedeji, A. O., Nkeh-Chungag, B. N. **2016**, Semisynthesis of derivatives of oleanolic acid from *Syzygium aromaticum* and their antinociceptive and anti-inflammatory properties. *Mediators of inflammation*, *16*, 1-9.
9. Kim, G. J., Jo, H. J., Chung, K. H., Lee, K. J., Choi, J.W., An, J. H. **2018**. Oleanolic Acid Induces p53 Dependent Apoptosis via the ERK/JNK/AKT Pathway in Cancer Cell Lines. *Oncotarget*, *9*(41), 26370–26386.
10. Astudillo, L., Rodriguez, J. A., Schmeda-Hirschmann, G. **2002**. Gastroprotective activity of oleanolic acid derivatives on experimentally induced gastric lesions in rats and mice. *Journal of Pharmacy and Pharmacology*, *54*(4), 583-588..
11. Chen, L., Zhang, Y., Kong, X., Lan, E., Huang, Z., Peng, S., Tian, J. **2008**. Design, synthesis, and antihepatocellular carcinoma activity of nitric oxide releasing derivatives of oleanolic acid, *Journal of Medicinal Chemistry*, *51*(15), 4834-4838.
12. Zhu, Y. M., Shen, J. K., Wang, H. K., Cosentino, L. M., & Lee, K. H. **2001**. Synthesis and anti-HIV activity of oleanolic acid derivatives. *Bioorganic & Medicinal Chemistry Letters*, *11*(24), 3115-3118.
13. Schultz, T.W., Yarbrough, J.W., Johnson, E.L. (2005). Structure–activity relationships for reactivity of carbonyl-containing compounds with glutathione*, SAR and QSAR in Environmental Research, 16*(4), 313-322.
14. Kumar, A., Qayum, A., Sharma, P. R., Kingh S. K., Shah, B. A. **2016**, Synthesis of β-boswellic acid derivatives as cytotoxic and apoptotic, *Bioorganic & Medicinal Chemistry Letters*, *26*, 76–81.
15. Karimi-Jaberi, Z., Pooladian, B. **2012**, A facile synthesis of α,α’-bis(substituted benzylidene) cycloalkanones catalyzed by p-TSA under solvent-free conditions, *Green Chemistry Letters and Reviews*, *5*(2), 187-193.
16. Debnath, J., Muthuswamy, S. K., Brugge, J. S. **2003**. Morphogenesis and oncogenesis of MCF-10A mammary epithelial acini grown in three-dimensional basement membrane cultures. *Methods*, *30*(3), 256-268.
17. Tanner, M., Kapanen, A. I., Junttila, T., Raheem, O., Grenman, S., Elo, J., Isola, J. **2004**. Characterization of a novel cell line established from a patient with Herceptin-resistant breast cancer. *Molecular cancer therapeutics*, *3*(12), 1585-1592.

Paper VI

REVISTA BOLIVIANA DE QUÍMICA
Bolivian Journal of Chemistry
Received 22 10 2013

Vol. 30, No.2, pp. 115-121, Sep./Dic. 2013
30(2) 115-121, Sep./Dec. 2013
Published 31 12 2013

EFFECT IN ACUTE INFLAMMATION OF SAPOGENIN EXTRACT AND ISOLATED SAPOGENINS FROM QUINOA WASTE (*CHENOPODIUM QUINOA* WILLD)

Maribel Lozano[a,b], Eduardo Gonzales[b], Yonny Flores[a], Giovanna R. Almanza[a,]*

[a] Laboratorio de Bioorgánica, Instituto de Investigaciones Químicas, Universidad Mayor de San Andrés, Calle 27 Cota Cota, P.O.Box. 303 La Paz-Bolivia; [b] Laboratorio de Farmacología, Instituto de Investigaciones Fármaco Bioquímicas, Universidad Mayor de San Andrés Av. Saavedra 1995, La Paz Bolivia

Keywords: Sapogenins, *Chenopodium quinoa*, acute anti-inflammatory activity, ear edema model, paw edema model.

ABSTRACT

A sapogenin extract was obtained from quinoa waste (*Chenopodium quinoa* Willd) and analyzed by HPLC, as well as other chromatographic and spectroscopic methods, determining four major constituents: Oleanolic acid **1**, methyl oleanate **2**, hederagenin **3** and phytolaccagenic acid **4**. The acute anti-inflammatory activity of both, isolated sapogenins and sapogenin extract, were evaluated in two animal models, carrageenan-induced paw edema and croton-induced ear edema, determining that the extract shows anti-inflammatory activity significant in ear edema model, greater than the compounds, suggesting a synergistic effect between the compounds, while in the paw edema model the isolated compounds show a significant anti-inflammatory activity while the extract shows only a moderate anti-inflammatory activity.

*Corresponding author: giovyalmanza@yahoo.com.ar

RESUMEN

A partir de residuos de quinua real (*Chenopodium quinoa* Willd) se obtuvo un extracto de sapogeninas el cual fue analizado por cromatografía HPLC, además de otros métodos cromatográficos y espectroscópicos, determinándose 4 constituyentes mayoritarios: ácido oleanólico **1**, oleanato de metilo **2**, hederagenina **3** y ácido fitolaccagenico **4**. La actividad antiinflamatoria aguda fue evaluada mediante dos modelos animales, modelo de edema de oreja de ratón inducido por aceite de croton y edema de pata inducido por carragenina, determinándose que el extracto muestra una actividad antiinflamatoria significativa en el modelo de edema de oreja, mayor que los compuestos, sugiriendo un efecto sinérgico entre ellos; mientras que en el modelo de edema de pata se observa una actividad antiinflamatoria significativa en los compuestos aislados y solo una actividad antiinflamatoria moderada en el extracto.

INTRODUCTION

Inflammatory diseases are currently treated with steroidal and non-steroidal anti-inflammatory drugs (NSAIDs). NSAIDs exert their effects by inhibiting the metabolism of arachidonic acid, by both cyclo-oxigenase and lipoxygenase enzyme pathways.[1] Despite their widespread use, NSAIDs are often associated with severe adverse effects; the most common being gastrointestinal bleeding.[2] For this reason, safer compounds with less side effects are needed.

Bolivia is the first exporter of quinoa generating tons of quinoa waste each year. This quinoa waste does not have application and contents around 20% of saponins [12]. The hydrolysis of those saponins can produce sapogenins as oleanolic acid which have several studies about its anti-inflammatory effects [5]. The anti- inflammatory effect of Oleanolic acid was first reported in 1960s [3] where the inhibition of carrageenan-induced rat paw edema was showed and later was confirmed by other studies [4]. The other sapogenins have similar structures and can have similar anti-inflammatory effects than Oleanolic acid. In view of those antecedents, in the present work we have studied the activity of sapogenin extract and pure sapogenins in different inflammatory tests to observe the best administration vie and possible synergy among the compounds.

Vol. 30, No.2, pp. 115-121, Sep./Dic. 2013
30(2) 115-121, Sep./Dec. 2013
Published 31 12 2013

RESULTS AND DISCUSSION

Isolated Compounds from quinoa waste

A sapogenin extract was obtained from an acid hydrolysis of saponin extract of quinoa waste. The sapogenin extract was subjected to diverse chromatographic separations giving four compounds. Compound **1** was identified as Oleanolic acid and isolated as white power of m.p 314 ^{o}C. The molecular formula $C_{30}H_{48}O_3$, 456,70 g/mol was consistent with the ^{13}C NMR data (table1) which showed 30 signals, seven for methyl carbons C23 (δ 28,7), C24 (δ 16,7), C25(δ 15,6), C26 (δ 17,3), C27 (δ 26,1), C29 (δ 32,9), C30 (δ 23,8); one for a carbon hydroxyl substituted C3 (δ 77,3), one for a carboxyl group substituent C28 (δ 179,0) and two for a double bound in C12 (δ 122,0) and C13 (δ 144,3), all of them characteristic of an oleanane ring. Based on those data and previous reports we proposed the oleanoic acid structure for compound **1** which was confirmed by comparison with bibliographic data.[5] Compound **2** was identified as methyl oleanate, it has the molecular formula $C_{31}H_{50}O_3$, 470.73 g/mol, m.p 314-316^{o}C and was isolated as amorphous power. The ^{13}C NMR data (table 1) showed 31 signals, similar chemical shifts to compound **1** were observed, the unique difference is the signal C31 (δ 51,8) which was identified as a methyl ester located at C17 (δ 46,2) by HMBC correlation ^{2}J of H31 (δ_H 3.71) with C28 (δ_C 177.0), as well as ^{3}J coupling of H22 (δ_H 1.31) and H16 (δ_H 2.06) with C28, proposing for **2** a methyl oleanate structure. Compound **3** was identified as hederagenin by comparison of the ^{13}C chemical shifts with literature data.[6] It was isolated as white power of m.p. 314-316^{o}C, the molecular formula $C_{30}H_{48}O_4$, 472.36 g/mol was consistent with the ^{13}C NMR data which present 30 signals, similar to oleanolic acid only exception in C-23 by the hydroxyl substitution. The hydroxyl group was located in C23 (δ 70.3) by a HMBC analysis which revealed ^{3}J and ^{2}J couplings of H-24 (δ_H 0.65) with the carbons C-23 (δ_C 70.3), C3 (δ_C 75.6) and C4 (δ_C 41.5) confirming a hydroxyl group in C23.

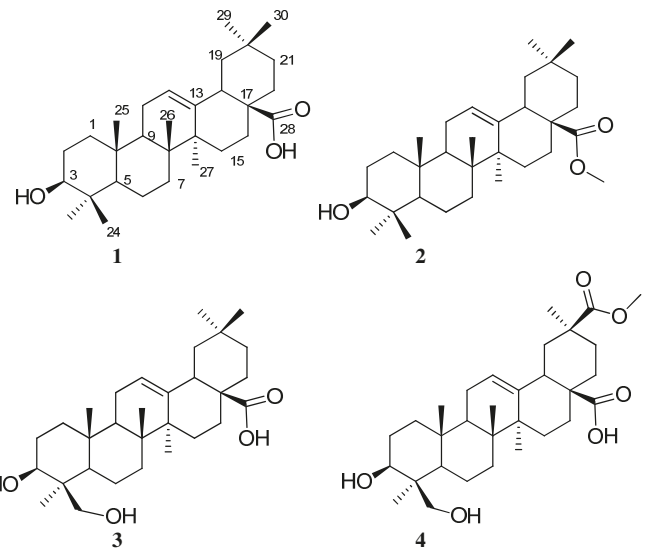

Figure 1. *Compounds isolated from quinoa waste*

Compound **4** was identified as phytolaccagenic acid; by comparison of experimental ^{13}C chemical shifts with literature data, it was also isolated as an amorphous white power, m.p 281 -284 ^{o}C, with a molecular formula, $C_{31}H_{48}O_6$, 516.36 g/mol. The ^{13}C NMR spectrum showed 31 carbon signals (table1) similar to oleanolic acid except by the presence of an ester group located in C-30 confirmed by analysis of the HMBC spectrum.[5]

Table 1. *^{13}C NMR experimental data for compounds 1-4*

	1[a]	**2**[a]	**3**[b]	**4**[b]
1	37,0	38,4	37,9	38,0
2	27,5	27,1	27,4	27,5
3	77,3	79,0	75,6	75,8
4	38,5	38,7	41,5	42,4
5	55,3	55,2	49,4	49,3
6	18,5	18,3	18,1	18,2
7	32,6	32,6	32,1	32,3
8	38,9	39,2	39,0	39,0
9	47,6	47,6	47,6	47,5
10	33,8	37,1	36,6	36,7
11	23,1	23,1	23,2	23,0
12	122,0	123,4	122,0	122,8
13	144,3	142,9	143,7	143,1
14	41,8	41,4	41,4	41,4
15	27,7	27,7	29,4	25,6
16	23,4	23,4	22,8	23,2
17	46,7	46,2	46,2	45,6
18	41,3	41,3	41,0	42,4
19	45,9	45,9	45,8	42,0
20	30,9	30,3	30,4	43,7
21	33,3	33,5	33,6	30,2
22	30,9	28,4	32,7	33,5
23	28,7	28,7	70,3	70,6
24	16,7	15,5	11,3	11,3
25	15,6	15,3	15,4	15,4
26	17,3	17,1	16,6	16,6
27	26,1	26,1	25,8	26,0
28	179,0	177,0	180,7	180,0
29	32,9	32,9	32,3	28,2
30	23,8	23,8	25,6	177,6
31		51,8		51,6

[a] ^{13}C NMR data for compound 1-2 measured in DMSO at 300 at 300MHz
[b] ^{13}C NMR data for compound 3-4 measured in $CDCl_3$ +CD_3OD at 300 MHz

Anti- inflammatory activity

Ear edema test

Compounds **1**-**4** and sapogenin extract were submitted to the croton oil ear test, at the dose of 2 and 56 mg/ear, to evaluate the topical anti-inflammatory effect. As showed in figure 2, all pure compounds **1**-**4** exerted some anti-inflammatory activity, while sapogenin extract showed strong active, inducing 68,2% edema inhibition at the highest administered dose (56 mg/ear). Consequently, the contribution to the activity of the extract could be very interesting for mew pharmaceutical formulations by topical application.

Paw edema test

The development of edema induced by carrageenan corresponded to the events in the acute phase of inflammation mediated by histamine, bradykinin and prostaglandins produced under an effect of cyclooxygenase.[7] Sapogenin extract and compounds **1**-**4** had an anti-inflammatory effect at 636mg/kg po and 100mg/po, respectively, observable to 3 ($p< 0,05$), 5($p< 0,01$) and 7($p<0,01$) hours, respectively (figure 3). In this test, the compounds **1**-**4** had higher anti-inflammatory between 5-7 hours after treatment, while the activity of the sapogenins extract was less respect to compounds. The strong activity of oleanolic acid and phytolaccagenic acid could be employed for anti-inflammatory drugs of oral administration

Vol. 30, No.2, pp. 115-121, Sep./Dic. 2013
30(2) 115-121, Sep./Dec. 2013
Published 31 12 2013

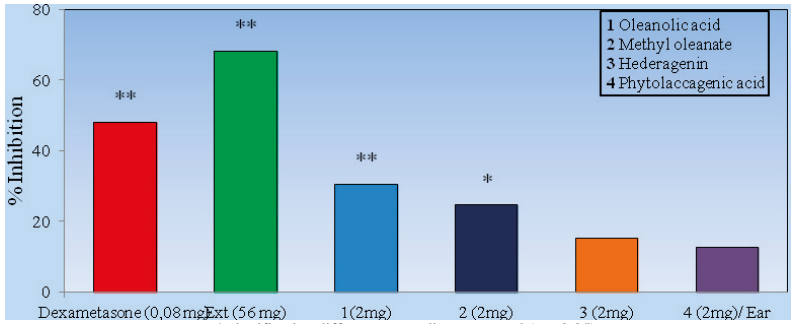

* significative difference regarding to control ($p < 0,05$)
**significative difference regarding to control ($p < 0,01$)

Figure 2. *Topical anti-inflammatory effect of compounds **1-4** and sapogenin extract versus croton oil-induced imflammation of the mouse ear. All values were significantly different from the negative control considered as 100% inflammation*

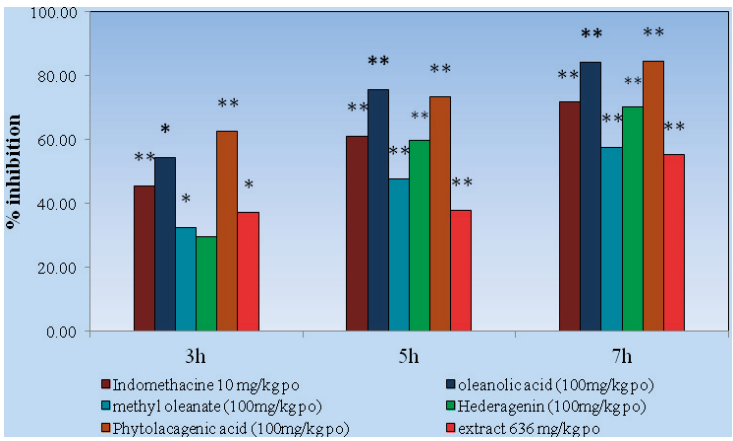

* Diferencia significativa frente al control ($p < 0,05$)
**Diferencia significativa frente al control ($p < 0,01$)

Figure 3 *Anti- inflammatory activity of isolated compounds **1-4** respect of negative control; Paw edema test using carrageenan as irritant agent.*

HPLC analysis of sapogenins

The HPLC analysis revealed the presence of four triterpenic compounds in quinoa waste identified by external standard and the purity peaks (purified compounds **1**-**4**) verified by UV (DAD, 210 nm) spectra (figure 4). Oleanolic acid (13,3 min), methyl oleanate (6,2 min) , hederagenin (5,4 min) and Phytolaccagenic acid (2,8 min). A subsequent HPLC quantification of sapogenin extract, give the follow yields for the pure compounds: 24% Oleanolic acid, 12% methyl oleanate, 28% hederagenin and 27% Phytolaccagenic acid. The extract contents 91% of sapogenins (Figure 5). This composition could be used for the analysis of the strong topical anti- inflammatory activity of the extract.

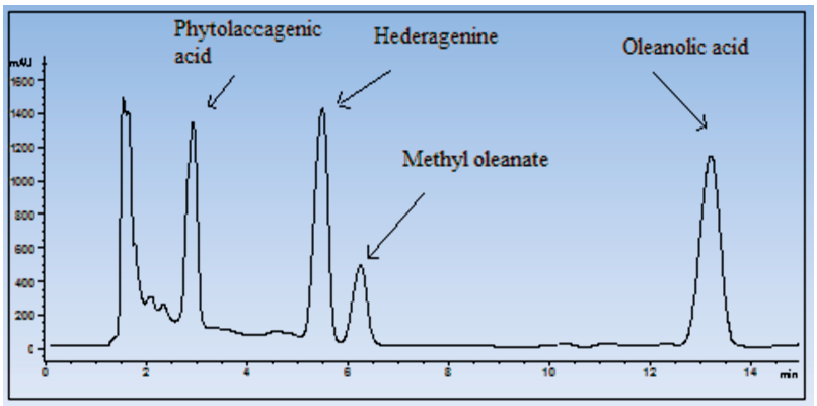

***Figure 4**.HPLC Chromatogram of sapogenins of quinoa waste at 210 nm*

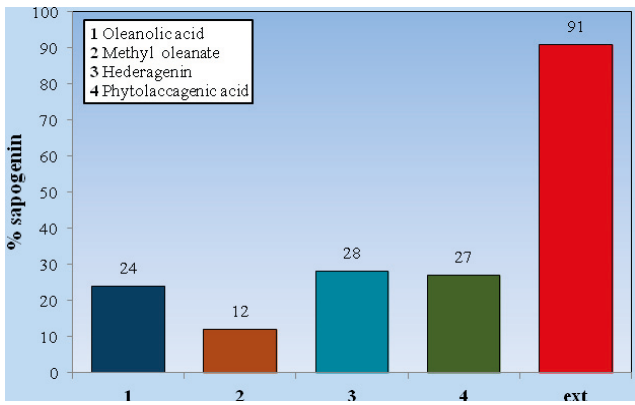

***Figure 5.** Quantitative HPLC analysis of pure compounds in the crude sapogenin extract from quinoa waste; HPLC analysis using external standards*

CONCLUSION

The quinoa waste is generally considered for its higher content in saponins while triterpenoid sapogenins are not equal considered. An interesting pharmacological activity was observed for the sapogenin extract and isolated sapogenins, which can be considered of therapeutical relevance for quinoa waste in pharmaceutical formulations against inflammatory disorders. The HPLC analytical method set up here was fit for the determination of sapogenins in the extract, as a mean to control the quality of bioactive extract which could be obtained in big quantities from quinoa waste. Furthermore, the quinoa waste could also be a cheap primary material to obtain sapogenins extract or individual sapogenins with anti-inflammatory propierties.

EXPERIMENTAL

Extraction and isolation

Vol. 30, No.2, pp. 115-121, Sep./Dic. 2013
30(2) 115-121, Sep./Dec. 2013
Published 31 12 2013

The modified method of San Martin and Briones [8] was used for saponins extractions; first 500 g of ground sample was extracted with an aqueous solution of ethanol 50% v/v (ratio 1:9) for 3 h under constant stirring at 200 rpm. The extract was then filtered and ethanol was removed using a rota-evaporator and the water residue was dried by frizzed. 20g of saponin extract was hydrolyzed with 200ml of 2N HCl in 50% aqueous ethanol under reflux for 3h at 85°C, and therefore sugars and aglicones were separated. The solid phase sapogenins were washed with H_2O and $NaHCO_3$ at 5% m/v, this residue was dried using high vacuum pump by 7h.[9], [10]

6,2g was subjected to Vacuum Liquid Chromatography (VLC) silica gel chromatography using mixtures of petroleum ether/EtOAc (EtOAc: 10, 20, 30, 40, 50, 70, 80, 100 %, v/v) and EtOAc/ MeOH (MeOH: 5% v/v) as a gradient solvent system to give ten fractions. The fraction 2 consist of pure compound oleanolic acid 1 and fraction 9 pure phytolaccagenic acid 4. The pure compounds 2 and 3 were obtained by further silica gel flash chromatography using ether/EtOAc 90% and40 % v/v.

HPLC chromatographic analysis of sapogenins

Quantification of oleanolic acid **1**, methyl oleanate **2**, hederagenin **3** and phytolaccgenic acid **4** were performed on an HPLC system (Agilent, 1100 series) equipped with quaternary pump, DAD detector and Eclipse Plus C_{18} column (125x4,6, 5µm). All these four compounds were detected at 210 nm at room temperature with an eluent flow rate of 1.0 mL/min. The mobile phase consisted of formic acid (0,1%) (A) and methanol (B) with a ratio of 15:85 (A:B, v/v) and isocratic elution.[11]

Animals

Experiments were performed on females *Swiss* mice (24 -26g), housed in controlled room temperature (20 ±2 °C) under a 12: 12h light-dark cycle (lights on 7 a.m.). Animals were kept in groups of 6 in light cages and had a free access to standard laboratory diet (pellets) and tap water in their cages.

Administration of extracts, fractions, isolated compound and drugs

Croton-induced ear edema

The topical anti-inflammatory activity was evaluated as inhibition of the croton oil-induced ear edema in mice (CYTED, 1995ref) at doses of 2 mg/ear for the pure compounds and 56 mg/ear for the sapogenin extract, to the right ear of each mouse was administered mean dose and after mean hour was administered the other mean dose. Inflammation was induced on the inner surface of the right ear of mice, by application of 20µL of Croton oil, suspended in the appropriated vehicle, In the left ear was only applied the vehicle. Control animals received only the irritant solution, whereas the other mice received both the irritant and the test substances: At the maximum of the edematous response, 4 h later, mice were sacrificed and a plug (6mm Ø) was removed from both the treated (right) and the untreated (left) ears. The edematous response was measured as the weight difference between the two plugs. The anti-inflammatory activity was expressed as percentage of the edema reduction in treated mice in comparison to control mice. As a reference, the non-steroidal anti-inflammatory drug (NSAID) Dexamethasone (0.04 mg/ear) was used.

Carrageenan-induced paw edema

Pure compounds and sapogenin extract in 100 mg/kg p.o. and 636 mg/kg p.o., indomethacin in 10 mg/kg p.o. doses were given to rats orally by feeding tube. One hour after of administration, 0,05 ml (1% w/v) carrageenan solution was subcutaneously injected into the plantar surface of the left hind paw. The paw volume was measured with bernier, at 1, 2, 3, 5 y 7 hours after carrageenan administration . The anti-inflammatory activity in animals of pure compounds and sapogenins extract were compared with that of indomethacin and control groups.

Statistical analysis

Values are presented as mean ± S.E.M. Independent samples *t*-test and analysis of variance (ANOVA, Dunnett method) were used for the evaluation of data and P005 was accepted as statistically significant

ACKNOWLEDGEMENTS

This work was supported by the "Development of natural phytotherapeutic products" project financed by FEMCIDI/OEA and "Research on plant biodiversity" project financed by the Swedish agency SIDA/UMSA.

REFERENCES

[1] INSEL, P.A.,
Analgesic, Antipyretic and Antiinflammatory Agents and Drugs Employed in the Treatment of Gout. McGraw-Hill, New York1996, pp. 617–657. In: J.G. Hardman, Limbird, L.E. (Eds.),
[2] FUNG, H.B., KIRSCHENBAUM, H.L.,
Clinical Therapeutics, 1999, 21, 1131–1157.
[3] GUPTA, M.B., BHALLA, T.N., GUPTA, G.P., MITRA, C.R., BHARGAVA K.P.
European Journal of Pharmacology, 1969, **6**, 67–70
[4] JIE L.
Journal of Ethnopharmacology, 1995, **49**; 57-68
[5] FLORES, Y., DÍAZ, C., GARAY, F., COLQUE, O., STERNER, O., ALMANZA. G.R.,
Revista Boliviana de química, 2005, **1**, 22
[6] MEHTA, B. K, MEHTA, D., AMRITA, I.,
Carbohydrate Research, 2004, 339; 2871–2874
[7] NSONDENTANDOU, G.F, BANZOUZI, J.T., MBATCHIA, B., ELION-ITOU, R.D.G., ETOU-OSSIBI, A.W., RAMOS, S., BENOIT-VICAL F., ABENA, A.A., OUAMBA, J.M.,
Journal of Ethnopharmacology 2010, 127; 108–111
[8] SAN MARTÍN, R., BRIONES, R.
Journal of the Science of Food and Agriculture, 2000, **80**: 2063- 2068.
[9] TIWATT, K., THONGPHASUK, P., CHAMULITRAT, W., WINK, M..
Phytochemistry 2008, **69**; 1919–1926
[10] DICK M.H., LIMBURG, H., GILLES, T., MARVIN H.J.P.
J Sci Food Agric, 2000, **80**:152-156
[11] CHUNHUA, Z., CHEN, K., SUN, C., CHEN, Q., ZHANG, W., LI, X.
Biomed.Chromatogr, 2007, **21**, 755–761.